Functional comparison of regulatory proteins expressed by different Herpes Viruses

Yongxu Lu

A thesis presented for the degree of Doctor of Philosophy in the

College of Medical, Veterinary and Life Sciences

University of Glasgow

MRC-University of Glasgow Centre for Virus Research

Garscube Campus

464 Bearsden Road

Glasgow

G61 1QH

2015

Abstract

The human body defends itself from pathogen infections through very complicated processes. They include host innate, adaptive and cellular intrinsic immunities. Host innate and adaptive immunities have been studied extensively in past decades, and more detail is being continuously revealed to us. Cellular intrinsic immunity has been recognised in more recent decades and has attracted great interest among researchers. Many cellular proteins have been identified to repress viral infections such as HIV, Influenza and Herpes Viruses. One aspect of intrinsic immunity, or intrinsic resistance, to herpes virus infections was demonstrated to involve nuclear structures known as ND10 (nuclear domain 10). With accumulating evidence about ND10, many components of ND10 that are involved in intrinsic immunity were identified. In the early stage of infection, HSV-1 and HCMV genomes become associated with ND10 components, which include PML, Sp100 and the hDaxx-ATRX complex. All these proteins were identified to repress HSV-1 and HCMV infection and replication. Viral proteins that have been identified to interact with PML, Sp100 and the hDaxx-ATRX complex and that counteract their anti-viral activities include ICP0 from HSV-1 and IE1 and pp71 from HCMV. Furthermore, recently studies on EBV proteins identified BNRF1 to interact with the hDaxx-ATRX complex, while EBNA1 appears to down regulate PML and EBNA-LP is involved in Sp100 dispersion from ND10. The evidence above raises the possibility that ND10 interacting proteins from different herpes viruses may be functionally interchangeable.

IE1 interacts with ND10 to de-sumoylate and disperse PML and Sp100. There is also evidence of interaction between IE1 and hDaxx complex. pp71 was demonstrated to interact with and promote the degradation of hDaxx, and to disrupt the hDaxx-ATRX complex to stimulate HCMV infection and replication. For HSV-1, ICP0 was identified to degrade PML and Sp100, and counteract the effects of the hDaxx-ATRX complex on viral infection repression. Therefore, IE1 and pp71 were analysed for their ability to complement ICP0 null HSV-1, and they were demonstrated to stimulate ICP0 null HSV-1 infection to a large extent. In this study, the reverse investigation was analysed. To extend the study, EBV proteins that interact with ND10 were also analysed in stimulating HSV-1 and HCMV mutant viruses.

The major findings in this thesis are summarised as follows:

1. IE1 and pp71 can separately and cooperatively stimulate ICP0 null HSV-1 infection in HepaRG cells and human fibroblasts.

2. The expression of IE1 and ICP0 in human fibroblasts can increase wt HCMV infection.

3. ICP0 can complement pp71 null HCMV infection but not IE1 null HCMV.

4. Two sequences that are essential for IE1 functions were identified and one IE1 sequence was identified to be HCMV specific on promoting viral infection and replication.

5. EBV proteins that interact with ND10 can stimulate ICP0 null HSV-1 and pp71 null HCMV infection.

The data in this thesis demonstrated that the combination of IE1 and pp71 is interchangeable with ICP0 in HSV-1 infection and EBV proteins that interact with ND10 partially complement ICP0 null HSV-1 infection. The results indicated that the integrity of ND10 is an important part of cellular intrinsic resistance to HSV-1 infection. The observation on ICP0 complementing IE1 deletion HCMV indicated the HCMV specific role of IE1. ICP0, BNRF1 and pp71 are all involved in counteracting the hDaxx-ATRX complex repression on viral infection and replication. These three proteins were demonstrated to complement ICP0 null HSV-1 and pp71 null HCMV infection, which indicates the importance of the hDaxx-ATRX complex on repressing herpes viruses infection. Even though solid data in this thesis has confirmed the ND10 repression on herpes virus infection and the herpes viruses from different subfamilies counteracting this repression through different viral proteins, more detail about this intrinsic resistance mechanisms still require extensive investigation.

Acknowledgements

First of all and most importantly, I would like to thank my supervisor Prof. Roger Everett for providing this precious opportunity to work in his group and for providing enormous help and guidance within the last three years. It is my honour to work with Prof. Roger Everett and it is also my personal honour for being one of the last two PhD students that Prof. Roger Everett supervised in CVR. Prof. Roger Everett's opening mind, innovation and rigorous attitudes of doing scientific research always inspired me during my PhD study and it will keeps inspiring me in my future scientific research career.

I am very thankful to China Scholarship Council and University of Glasgow for giving me the opportunity to join MRC-University of Glasgow Centre for Virus Research (CVR). I am also very thankful to Dr. Andrew Davison and Dr. Mandy Glass for being my advisors. I would also like to thank the CVR administrative staff for being efficient and helpful for dealing with my non-scientific issues.

I thank all the lab mates of Prof. Roger Everett's group for being so helpful and supportive and providing such a friendly and comfortable atmosphere: Delphine Cuchet (for her constant help on my experimental techniques and her sense of humour), Mandy Glass (for her advice about my technical issues and my background knowledge) and Elizabeth Sloan (for her helpful advice in lab meetings and tea breaks). My special thanks go to Anne Orr, who provided important help in my project, Steven McFarlane, who provided technique support in the yeast 2-hybrid experiments, Kathleen Pheasant, who shared my ups and downs during the course of my experiments and always encouraged me to be moving on, and Lily Tong, who gave me many helpful bits of advice about the life in Scotland and the research work in UK.

I am very grateful to all my friends in Glasgow, all my fellows in the PhD student office (especially Wan, James, Claire and Matt) and all fellows in the Real Badminton group who have provided me enormous fun to hang out with outside of work. I would also like to thank Allan and Seamus, who provided many help and advices on my research work and scientific career.

Finally, I would like to thank my Mum and Dad for their enormous love and always being supportive. I would also like to thank my girlfriend Jin Shen, who shared both

my happiness and difficulties even though we are thousands miles away from each other. I thank Glasgow for being such a friendly and beautiful city, and for its un-predictable weather which kept me inside the lab as much as possible.

Contents

List of Figures

List of Tables

List of Abbreviations

aa	amino acid
Amp	Ampicillin resistance
AMP	Adenosine monophosphate
APC	Antigen presenting cell
APOBEC	Apolipoprotein B mRNA-editing enzyme catalytic polypeptide
ATP	Adenosine triphosphate
ATRX	Alpha-thallasaemia mental retardation X-linked
BCR	B cell receptor
^{o}C	Degrees Celsius
CNS	Central Nervous System
cDNA	Complementary DNA
dH_2O	Distilled water
ddH_2O	Double distilled water
Daxx	Death domain associated protein
DMEM	Dulbecco's modified Eagle's medium
DMSO	Dimethyl sulphoxide
DNA	Deoxyribonucleic acid

E	Early
EBV	Epstein Barr virus
EBNA1	Epstein–Barr virus nuclear antigen 1
EBNA-LP	Epstein-Barr virus nuclear antigen leader protein
E. coli	Escherichia coli
EDTA	Ethylenediaminetetraacetic acid
EtBr	Ethidium bromide
EGFP	Enhanced green fluorescent protein
EYFP	Enhanced yellow florescent protein
FCS	Foetal calf serum
g	gram
h	hour
HCMV	Human cytomegalovirus
HCF	Host Cell Factor
HDAC	Histone deacetylase
HF	Human fibroblasts
HIV	Human immunodeficiency virus
HMG	High Mobility Group
hpi	Hours post infection

HSV	Herpes simplex virus
ICP	Infected cell protein
IE	Immediate-Early
IF	Immunofluorescence
IFN	Interferon
Ig	Immunoglobulin
IRES	Internal ribosome entry site
ISG	Interferon stimulated gene
K	Kilo (103)
Kbp	Kilobase pair
KSHV	Kaposi's sarcoma associated herpesvirus
l	Litre
L	Late
LANA	Latency associated nuclear antigen
LTR	Long terminal repeats
µ	micro (10-6)
m	milli (10-3)
M	Molar
mA	milliamps

MHC	major histocompatibility complex
MIEP	Major immediate-early promoter
min	Minute
m.o.i	multiplicity of infection
mRNA	messenger RNA
n	nano (10-9)
N-	amino (terminal region of a protein)
NaCl	Sodium chloride
ND	nuclear domain
NK	Natural killer
NLS	nuclear localisation signal
NP40	Nonidet-P 40
o/n	Over night
Orf	Open reading frame
Ori	Origin of replication
PAGE	Polyacrylamide gel electrophoresis
PBS	Phosphate buffered saline
PCR	Polymerase chain reaction
p.f.u.	Plaque-forming unit

PHD	Plant-homeodomain
PML	Promyelocytic leukaemia protein
PuroR	Puromycin resistance
RBCC	RING, B-box(es), coiled coil motif
RGB	Resolving gel buffer
RING	Really interesting new gene
RNA	Ribonucleic acid
RNAi	RNA interference
RNase	Ribonuclease
rpm	Revolutions per minute
RRE	Rev response element
SDS	Sodium dodecyl sulphate
SENP	Sentrin-specific protease
SGB	Stacking gel buffer
shRNA	Short hairpin RNA
siRNA	Small inhibitory RNA
SIM	SUMO-Interaction Motif
SUMO	Small ubiquitin-like modifier
SV40	Simian virus 40

TEMED	Tetramethylethylene diamine
TGF-β	Transforming Growth Factor beta
TNF-α	Tumour Necrosis Factor alpha
TRIM	tripartite motif
TRL	Terminal repeat long
TRS	Terminal repeat short
UL	Unique long
US	Unique short
USP	ubiquitin specific protease
UV	Ultraviolet
V	Volts
v/v	Volume to volume ratio
v/w	Volume to weight ratio
Vhs	virion host shut off
VP	virion protein
VSV	Vesicular stomatitis virus
VZV	Varicella Zoster virus
wt	wild-type
X-gal	5-bromo-4-chloro-3-indolyl-β-D-galactoside

1 Introduction

Viruses are small infectious agents that can only replicate inside the living cells of hosts. Virus can infect all kinds of organisms, from animals and plants to bacteria and archaea. Viruses cause many kinds of human diseases, from colds, chickenpox and influenza to AIDS, hepatitis, SARS and several forms of cancer. Within the evolution process, organisms have developed a series of defence systems to prevent virus infections, including the innate immune system, the adaptive immune system and intrinsic anti-viral defences. The innate and adaptive immune systems have been well studied for many years. In contrast, the intrinsic anti-viral defence is a relatively recent concept and less is known about its function in the process of defence to virus infection. This thesis concentrates on HSV-1 (Herpes Simplex Virus type 1) and HCMV (Human Cytomegalovirus) infection, investigating the role of cellular nuclear sub-structures known as ND10 or PML nuclear bodies in the mechanism of intrinsic anti-viral defence. General reviews of many relevant aspects of these viruses can be found in (Knipe *et al.*, 2006; Reddehase, 2013; Weller, 2011).

1.1 Herpesviridae family

Herpesviridae are a large DNA virus family that cause diseases in mammals, birds, reptiles, amphibians, marine molluscs and fish. Eight human herpes viruses are identified currently, which are Herpes Simplex Virus type 1 (HSV-1), Herpes Simplex Virus type 2 (HSV-2), Varicella Zoster Virus (VZV), Epstein Barr virus (EBV), Human Cytomegalovirus (HCMV), Human Herpesvirus type 6 (HHV-6), Human Herpesvirus type 7 (HHV-7) and Kaposi's sarcoma herpesvirus (KSHV). *Herpesviridae* family includes three subfamilies, the *Alphaherpesvirinae*, the *Betaherpesvirinae* and the *Gammaherpesvirinae*. HSV-1 belongs to the *Alphaherpesvirinae*, and it is neurotropic and establishes latency in neuronal ganglia. HCMV is included in the *Betaherpesvirinae*, and establishes latency in peripheral blood monocytes. Replication of HCMV is slow in cell culture and is restricted to a limited number of cell lines. EBV is a member of the *Gammaherpesvirinae* that has infected more than 90% of the population over the world. It infects and establishes latency in lymphocytes. HSV-1, HCMV and EBV share many properties such as gene expression strategy and host cell interaction targets (such as ND10) and some of these similarities will be investigated in this thesis.

1.1.1 Alphaherpesvirinae

The herpes viruses in *Alphaherpesvirinae* replicate and reproduce more quickly than members of the other two subfamilies. *Alphaherpesvirinae* family members infect humans and animals such as pigs, bovines, horses, cats, chickens and turkeys. The alphaherpesviruses are further divided into four subfamilies, which are Simplexvirus, Varicellovirus, Mardivirus and Iltovirus. HSV-1, HSV-2 and VZV (also known as HHV-1, HHV-2 and HHV-3) are well studied human herpes viruses from the *Alphaherpesvirinae*. HSV-1 is one of the most comprehensively studied of the herpes viruses in *Herpesviridae*. HSV-1 infection in human is separated into latent and lytic stages. The primary infection of HSV-1 occurs in epithelial cells and keratinocytes at mucocutaneous sites including the mouth, eyes, and genitalia (Szostecki *et al.*, 1990). Viral genome hides in sensory and autonomic ganglia of the nervous system to establish latent infections, which only express several latency related untranslated transcripts without virus production (reviewed in (Bloom & Kwiatkowski, 2011; Efstathiou & Preston, 2005; Nicoll et al., 2012)).As described in more detail later, HSV-1 immediate early protein ICP0 was identified as an important protein in activating viral gene expression during lytic and latent infection (Everett, 1984; Gordon et al., 1990; Natarajan et al., 1991; Sacks & Schaffer, 1987; Stow & Stow, 1986). It has been extensively studied for its effects on cellular intrinsic resistance and virus-host interactions (reviewed in (Everett, 2011) and it was studied in different aspects in this thesis.

1.1.2 Betaherpesvirinae

One factor which distinguishes the members of the *Betaherpesvirinae* from other herpes virus family members is their slow reproduction time, at least in cultured cells. Members in this subfamily are further divided into Cytomegalovirus, Muromegalovirus, Proboscivirus and Roseolovirus. Betaherpesviruses infect humans, and animals including rats, elephants, African green monkeys, Rhesus monkeys, Chimpanzees, Orangutans and Night monkeys. They establish latency infection mostly in monocytes, which is different to *Alphaherpesvirinae* and *Gammaherpesvirinae*. Four members of the *Betaherpesvirinae* infect humans, they are Human cytomegalovirus (HCMV also known as human herpesvirus 5, HHV-5), Human herpesvirus 6A and 6B (HHV-6A and HHV-6B) and Human herpes virus 7 (HHV-7). In this thesis, two important proteins, IE1 and pp71, from HCMV were studied to contribute more detail about their roles in evading intrinsic resistance to HCMV infection.

1.1.3 Gammaherpesvirinae

Gammaherpesvirinae reproduce at a variable rate compared to the other two subfamilies of *Herpesviridae* and viral infections in humans are mainly established in lymphocyte cells. The molecular phylogenetic analyses confirmed the close similarity of those viruses and distinguished this subfamily from Alpha and Beta herpesviruses. The *Gammaherpesvirinae* family is further divided into four genera, which are Lymphocryptovirus, Rhadinovirus, Macavirus and Percavirus. EBV (also known as HHV-4) is a member of Lymphocryptovirus, and KSHV (also known as HHV-8) is a member of Rhadinovirus. They are two viruses from *Gammaherpesvirinae* that can cause severe infections in humans and have attracted primary interest of scientists. Three EBV proteins, which are EBNA-1, BNRF1 and EBNA-LP, were studied in this thesis for their interactions with ND10 and their abilities to substitute for the functions of other viral proteins during HSV-1 and HCMV infection.

1.2 The virus particle structure of the Herpesviridae

A typical *Herpesviridae* infectious virion particle includes the lipid bilayer envelope, tegument, capsid and double-stranded DNA (dsDNA) from the very outside to inside (Figure 1.1). The double stranded (ds) DNA inside the virion encodes the information for virus replication. Intracellular capsids can be found in three forms, A-capsids, which are empty, B-capsids that contain scaffolding proteins but no DNA, and C-capsids, which contain viral dsDNA. The tegument is between the inner surface of the lipid bilayer envelope and the outer surface of the capsid. The lipid in the envelope is host-cell derived and contains viral glycoproteins.

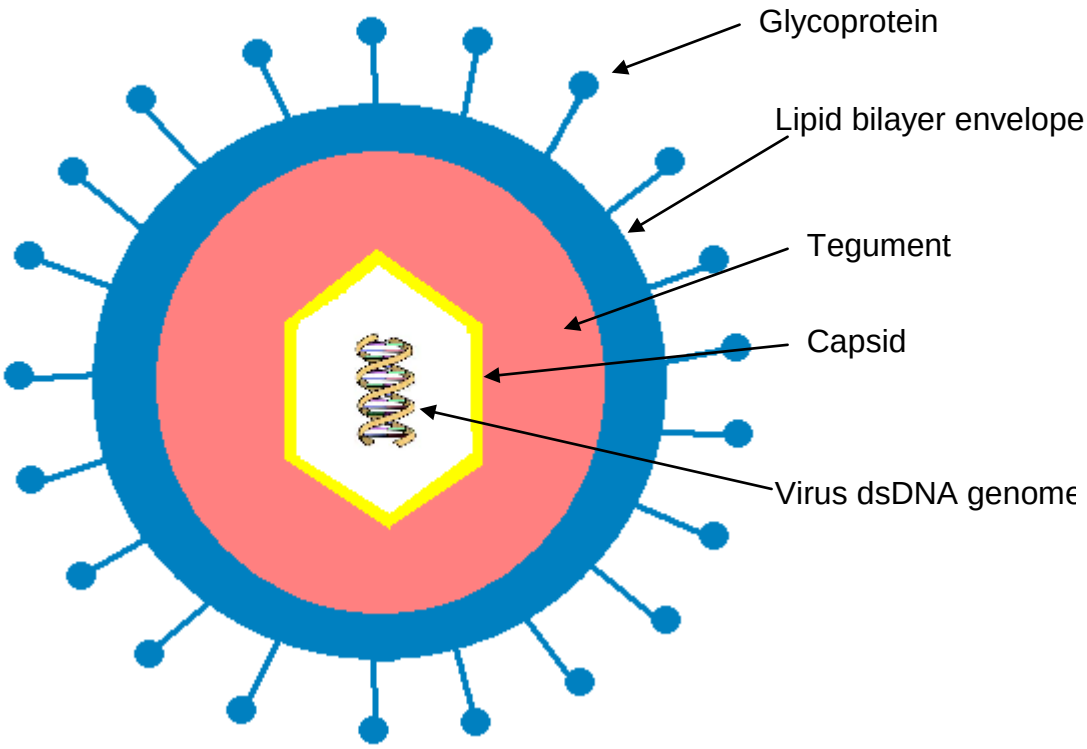

Figure 1.1 General structure of herpesvirus infectious virion particle.

1.2.1 Virus genome structure of the Herpesviridae

Herpesviridae genomes vary in size from the smallest at 124 kbp (Simian Varicella Virus) to the largest at 295 kbp (Koi Herpesvirus). The genomes of HSV-1 and HCMV are 152 kbp and 235 kbp respectively. The genome structures of HSV-1 and HCMV have similar arrangements, consisting of the unique long (U_L) region, the unique short (U_S) region, the terminal repeat long regions (TR_L and IR_L) and the terminal repeat short regions (TR_S and IR_S). At the 3' and 5' termini, and at the junction between the internal repeats (IR_L and IR_S), an additional repeat element the 'a' sequence is found. The 'a' sequence provides signals for cleavage and packaging of the replicated genomes. The arrangement of the different regions in HSV-1 and HCMV genomes is shown in Figure 1.2.

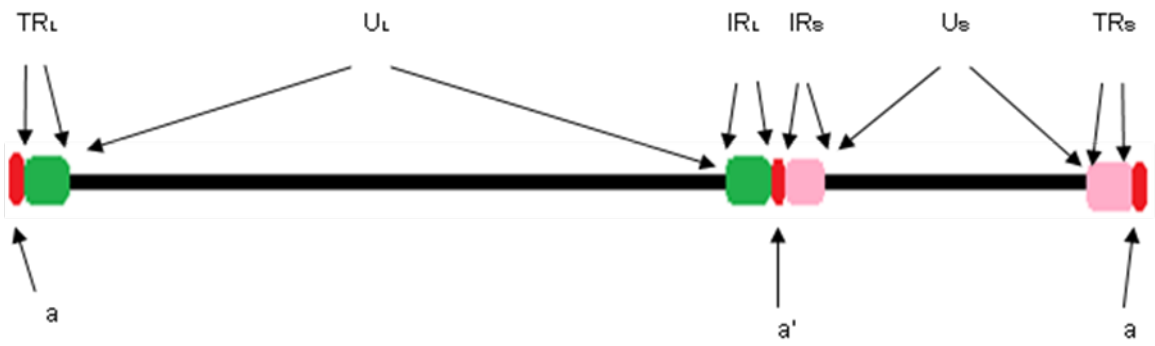

Figure 1.2 The similar Genome organization of HSV-1 and HCMV.

The EBV genome structure is different to that of HSV-1 and HCMV (Straus *et al.*, 1993). It consists of about 172000 base pairs of dsDNA organized in U1 to 5, IR1 to 4, and two TR regions (Figure 1.3).

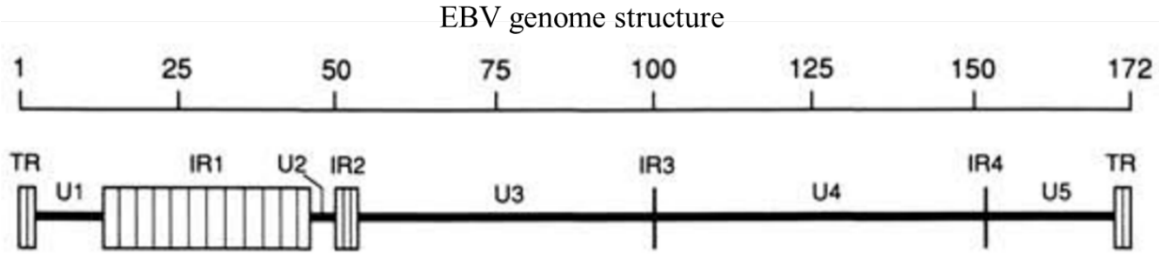

Figure 1.3 The Genome organization of EBV.
Figure is taken from (Straus *et al.*, 1993)

1.2.2 Capsid

Capsid-like structures were first observed in HSV-1 infected cells and further classified into A-, B-, and C-capsids (Gibson & Roizman, 1972). Later on, similar capsid structures were observed in HCMV infected cells (Gibson, 1996; Irmiere & Gibson, 1985). More recently, in Rhesus monkey rhadinovirus infected cells, the comparable chemical composition and structural features of the three types of capsid have been observed, which indicates that a similar manner of capsid assembly process may apply to gammaherpesvirus (O'Connor *et al.*, 2003; Yu *et al.*, 2003b). Of the three different kinds of capsids, A, B and C-capsids, only the C-capsid contains viral DNA (reviewed in (Conway & Homa, 2011)). The procapsid, which is another capsid type, has a distinctive spherical shape compared to A-, B-, and C-capsids under electron microscope observation (Rixon & McNab, 1999; Trus *et al.*, 1996). Procapsids are transiently stable and undergo spontaneous structural rearrangement to form the stable polyhedral structure that is

characteristic of the other types of capsids (Heymann *et al.*, 2003; Yu *et al.*, 2005; Zhou *et al.*, 1998). Capsid assembly starts with the formation of the procapsid in HSV-1. The procapsids spontaneously rearrange into particles resembling the B- capsid, which lacks the DNA inside of the structure. Proteolytic cleavage of the scaffolding protein and VP26 recruitment into the capsid structure are required for B-capsid formation (Chi & Wilson, 2000). Viral genome DNA packaging into the capsid structure is the last step of mature capsid formation. This process is believed to arise spontaneously, but, more investigation is still required (Yu *et al.*, 2005). The proteins that constitute the outer shell of the HSV-1 capsid are the major capsid protein (VP5/UL19), virion protein 26 (VP26/UL35), virion protein 23 (VP23/UL18) and virion protein 19C (VP19C/UL38) and the portal protein UL6. During virion DNA encapsidation, an additional component of HSV-1 premature capsid, VP24, functions as a protease which processes the internal capsid scaffold. HCMV has a similarly capsid structure. Five virion proteins constitute the HCMV capsid, the major capsid protein encoded by UL86, the minor capsid protein, the minor capsid protein binding protein, the portal protein (PORT) encoded by UL104 and the smallest capsid protein (SCP) encoded by UL48A.

1.2.3 Tegument

The inner nucleocapsid and the outer envelope are separated by the tegument. This is composed of multiple proteins, which enter the host cell along with the capsid, and at least some of which regulate early events of the virus infection. Many tegument proteins are phosphorylated, but the significance of this and other post-translational modifications to these proteins remains largely unexplored.

The HSV-1 tegument includes at least 26 tegument proteins. Major components include VP1/2, VP11/12, VP13/14, VP16, VP22 and the virion-induced host shut-off protein (VHS)(Loret *et al.*, 2008; Morrison *et al.*, 1998).ICP0 is also present in the HSV-1 tegument layer (Delboy *et al.*, 2010; Yao & Courtney, 1992). Among these tegument constituents, the most studied are VP16, VP22, VHS and ICP0 (more detail is introduced in section 1.6.1.1). VP16 is encoded by UL48, with 490-amino acids in its sequence and an acidic C-terminal transcriptional activation domain. The association between VP16 and cellular proteins Host Cell Factor (HCF) and Oct-1 activates the Immediate Early (IE) gene transcription, and VP16 is also involved in virion assembly.

The HCMV tegument structure contains at least 76 tegument proteins and less than half of them have been determined and identified (reviewed in (Kalejta, 2008)). Proteins include pp65 (UL83), pp71 (UL82), pp150 (UL32) and largest tegument protein (LTP, UL48 gene product) . Some HCMV tegument proteins are not essential for virion structure, such as pp65 and pp71 (Bresnahan & Shenk, 2000; Reyda *et al.*, 2014), but the deletion of pp71 impairs the viral infection at low MOI infection (Bresnahan & Shenk, 2000).

EBV tegument contains BNRF1, BPLF1, BOLF1, BBLF1, BGLF1, BGLF2 and BVRF1. BNRF1 was investigated to be one of the most abundant tegument proteins in the EBV structure (Johannsen *et al.*, 2004). Although deletion of BNRF1 was initially reported to have no significant effect on viral infection and DNA replication (Feederle *et al.*, 2006), more recent work has shown that it is important for stimulation of viral gene expression in the early stages of lytic infection (Tsai *et al.*, 2011).

1.3 Biology of herpesvirus infections

1.3.1 Viral attachment and penetration into the host cell

The entry process of *Herpesviridae* starts from virus attachment to non-specific cell surface molecules such as heparin sulphate, followed by binding to specific cell surface receptors, then the virus envelope fuses with the cellular membrane and endocytosis occurs (reviewed in (Eisenberg *et al.*, 2011)). Many viral proteins and pathways interact to coordinate cellular signals during virus entry. In addition, the entry process can trigger multiple cellular processes including nuclear processes to facilitate virus entry or induce antiviral responses. HSV-1 entry is mediated by glycoproteins known as gB, gC, gD, gH and gL. There are other glycoproteins such as gE, gG, gI and gM that are components of the HSV-1 envelope but which are not directly involved in entry. Glycoproteins gB, gD, gH and gL are essential for HSV-1 infection in cell culture. Glycoproteins gB and gC bind to host cell surface molecules such as heparan sulphate during initial attachment to the host cell. The interaction between gD with one of three cellular receptors: herpes virus entry mediator (HVEM), nectin-1 or nectin-2, followed by the activity of the gB fusion protein and the gH/gI heterodimer, triggers the fusion of viral envelope with the cell membrane. In HCMV entry, EGFR, PDGFRαm and avb3 integrin have been proposed as specific receptor molecules. However, some study shows EGFR is not expressed on all HCMV-permissive cell lines that are efficiently infected by HCMV (Compton & Feire, 2007;

Wang *et al.*, 2003). The HCMV glycoproteins that are important for virus entry are known as gB, gO, gH, gM and gL (Compton & Feire, 2007).

1.3.2 Capsid transport and DNA entry into the nucleus

Fusion of the viral envelope with the cellular membrane releases the capsid and tegument proteins into the cytoplasm. The capsids are then transported on microtubules to the nuclear envelope, where they dock at nuclear pores and release the viral genome through the pore into the nucleus.

1.3.3 Herpesvirus Gene Expression

The gene expression of herpesviruses is classified into three stages, which are the Immediate-early (IE), Early and Late genes expression. Those viral genes are classified by the expression time during virus infection process. IE genes are the first expressed viral genes after primary infection on host cells, which is followed by Early gene transcription and finally the Late genes expression. IE genes are the only genes expressed when protein synthesis is inhibited, while the expression of other viral genes is activated by the products of the previously expressed genes, such as the initiation of Early and Late gene expression (Figure 1.4).

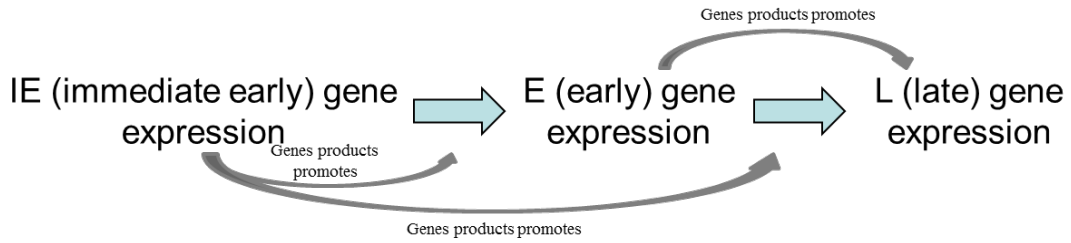

Figure 1.4 Herpesvirus genes expression stimulation.

IE genes are the first ones transcribed in host cell nucleus, and their products can both stimulate viral transcription and gene expression directly, and also inhibit the intrinsic anti-viral defence of the host cell. The mechanism of IE protein inhibition of intrinsic anti-viral defence is introduced in more details in the next paragraphs. IE gene expression is followed by early (E) genes, which encode enzymes that are involved in nucleotide

metabolism and DNA replication. E genes contain two members, E or β1 genes and delayed-early (D-E) or β2 genes, which differ in expression time. The late (L) genes are expressed last, which principally encode the virion structural proteins. Two subclasses constitute the L genes, the early-late (E-L) or γ1 and true L or γ2 genes, which divided by their strict dependence upon viral DNA replication.

IE genes expression in HSV-1 is carried out by the host-cell transcription machinery but requires activation by the viral tegument protein VP16, which is assembled with cellular proteins to form enhancer core complex as illustrated in Figure 1.5 (Preston et al. 1988. Cell 52, 425-434.).

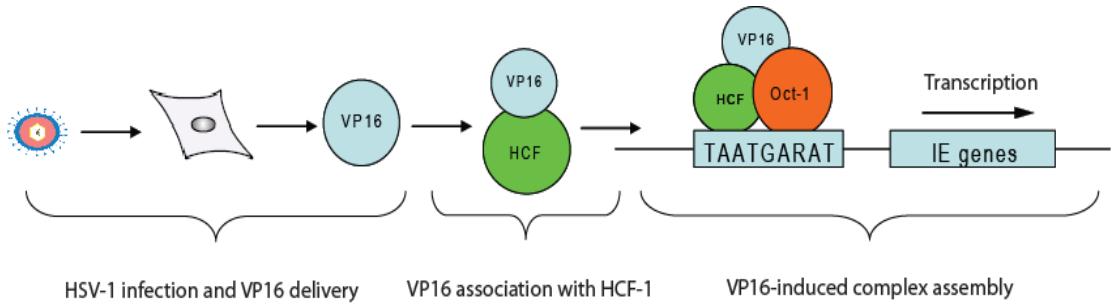

Figure 1.5 The assemble of VP16 with cellular proteins to form enhancer core complex.

VP16 in HSV-1 is responsible for the initiation of IE gene expression. Five IE genes are transcribed at the immediate early stage. They are distinguished from Early and Late genes by specific sequence in the upstream regions of IE promoters termed TAATGARAT sequences, which can be recognized by HSV-1 tegument protein VP16. During the primary HSV-1 infection, VP16 binds as part of a protein complex that contains two cellular factors, the POU-domain transcription factor Oct-1 and the cell-proliferation factor HCF, to transcriptionally activate expression of IE genes (Wysocka and Herr, 2003).

The expression products of HSV-1 IE genes stimulate viral transcription directly (ICP4; (DeLuca, 2011)), promote gene expression at the post-transcriptional level (ICP27; (Sandri-Goldin, 2011)) and antagonize the intrinsic resistance and transfer the infection into the lytic stage (ICP0; (Everett, 2011)).

HCMV infection is divided into latent and lytic stages as HSV-1. The Lytic infection of HCMV is also divided into three phases which are immediate early, early and late

(reviewed in (Fortunato & Spector, 1999)). Once the HCMV capsid enters host cells, the viral genome will transfer into the nucleus, where viral gene expression is established. Initial viral genome expression can be repressed in the nucleus by ND10 components and this may contribute to establishment of a latent infection, or HCMV IE genes are expressed and the cell enters into lytic infection. The activation of HCMV IE gene expression does not require *de novo* viral protein synthesis, but it depends on tegument protein pp71, which is delivered into host cells immediately after infection. Protein pp71 localizes to ND10 and interacts with hDaxx (Hofmann *et al.*, 2002), which is a cellular repressor that silences IE gene transcription (Woodhall *et al.*, 2006). HCMV IE genes express two important proteins, IE1 (IE72) and IE2 (IE86), which are stimulated by the MIEP (major immediate early promoter) (Boshart *et al.*, 1985). hDaxx recruits ATRX in the nucleus to form the hDaxx-ATRX complex which mediates MIEP repression in the absence of pp71. ATRX is dispersed by pp71 prior to hDaxx dispersion (Lukashchuk *et al.*, 2008) and the level of hDaxx is down regulated by pp71 (Saffert & Kalejta, 2006). The de-repressed MIEP stimulates IE gene transcription, and then IE proteins IE1 and IE2 stimulate the HCMV infection into the lytic stage (Figure 1.6). The deletion of pp71 or IE1 can severely impair the HCMV infection at low MOI, but this growth defect can be rescued by high MOI infection (Bresnahan & Shenk, 2000; Gawn & Greaves, 2002). IE2 deletion abolishes the mutant virus replication and infection, and the re-introducing IE2 gene into viral genome can rescue this growth defect (Sanders *et al.*, 2008). HCMV early gene expression requires previously synthesized IE proteins and cellular proteins. In this stage of infection, early gene products are involved in viral replication, preparing the cells for viral DNA replication and repression of host immune responses. Late genes of HCMV are stimulated by viral genome replication. They encode proteins that assemble and constitute the complex virion. HCMV late genes are further divided into two broad classes which are leaky-late class genes and ‘true’ late genes. The leaky-late genes are expressed during the early stage of infection at a low level and are upregulated at a later stage after viral DNA replication has commenced. The ‘true’ late genes are expressed after the early time of infection and are highly dependent on viral DNA replication.

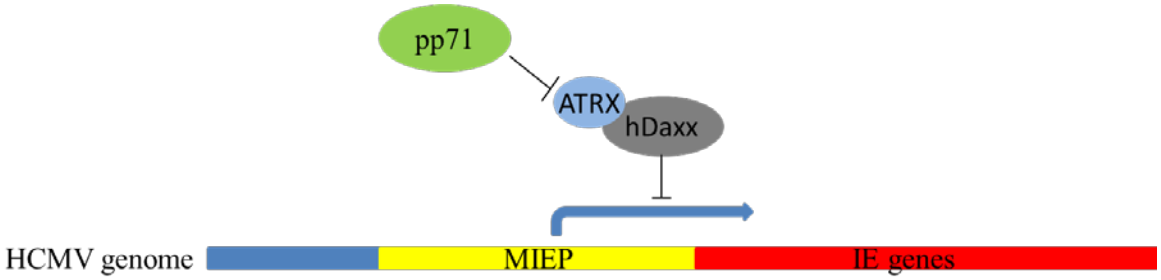

Figure 1.6 pp71 interacts with hDaxx-ATRX complex to de-repress MIEP.

As for HSV-1 and HCMV, EBV infection is separated into latent and lytic stages. Furthermore, EBV infections on different cell lines exhibit different replication strategies. EBV infected epithelia cells always proceed to lytic infection after virus entry, whereas EBV infected B cells enter into a latent stage directly without lytic infection. In the latent stage, the EBV genome circularizes in the host cell nucleus and is copied by host cell DNA polymerase through a mechanism that requires the viral protein known as EBNA1 (Amon & Farrell, 2005). Two EBV latent related proteins interact with ND10 members, EBNA1 and EBNA-LP, which will be investigated in this study.

1.4 Herpesviruses and human disease

The Herpesviruses family infects many kinds of species which include mammals, birds, reptiles, amphibians, marine molluscs and fish. Viruses from Herpesviruses three sub-families can infect human cells. These are HSV-1, HSV-2 and VZV from the α-herpesvirus family, HCMV, HHV-6A, HHV-6B and HHV-7 from the β-herpesvirus and EBV and KSHV from the γ-herpesvirus family (reviewed in (Knipe *et al.*, 2006). Because all these herpes viruses establish latent infection in humans, therefore individuals cannot eradicate the infection. This ensures the herpes viruses are maintained within infected individuals, and can transmit the virus to the individuals around them. In most cases the infections of herpes viruses are non-serious and asymptomatic, but they can still cause serious diseases, particularly the infection in new born and immunocompromised individuals.

1.4.1 Alphaherpesviruses and human disease

HSV-1, HSV-2 and VZV are three important members of the Alphaherpesviruses which have been well studied for causing lifelong infections in humans. HSV-1 and HSV-2 can

infect almost any part of the skin or mucosa on the human body. HSV-1 produces mostly facial cold sores and fever blisters. The virus hides in the cell bodies of neurons to evade the immune system and becomes latent for a long period. HSV-2 produces mostly genital infections and evades the immune system in the same way as HSV-1. HSV-1 tends to hide in the trigeminal ganglia, while HSV-2 tends to hide in the sacral ganglia. Some infected people experience sporadic episodes of viral reactivation or outbreaks after the primary infection. In the virus outbreak, the virus in a nerve cell becomes active and is transported via the axon to the skin causing new sores. Figure 1.7 shows the latent and lytic infection cycles of HSV-1 and HSV-2. HSV infects skin, eye, mucous membrane (SEM) and can cause disseminated infection and encephalitis in neonates. A considered diagnosis and timely treatment to HSV infected patients could relieve the SEM infection efficiently. HSV infections can cause life threatening diseases in central nervous system (CNS). HSV-1 is a major cause of severe viral encephalititis. If no proper treatment is applied to the patients with HSV-1 encephalitits, 70% of patients will die and the infection causes severe sequelae in almost all survivors. HSV infections in neonates and immune compromised hosts are the most severe and even life threatening. HSV infection in immunocompromised patients is slowly progressed and accompanied by extensive tissue damage and necrosis, but fatal infections are not common.

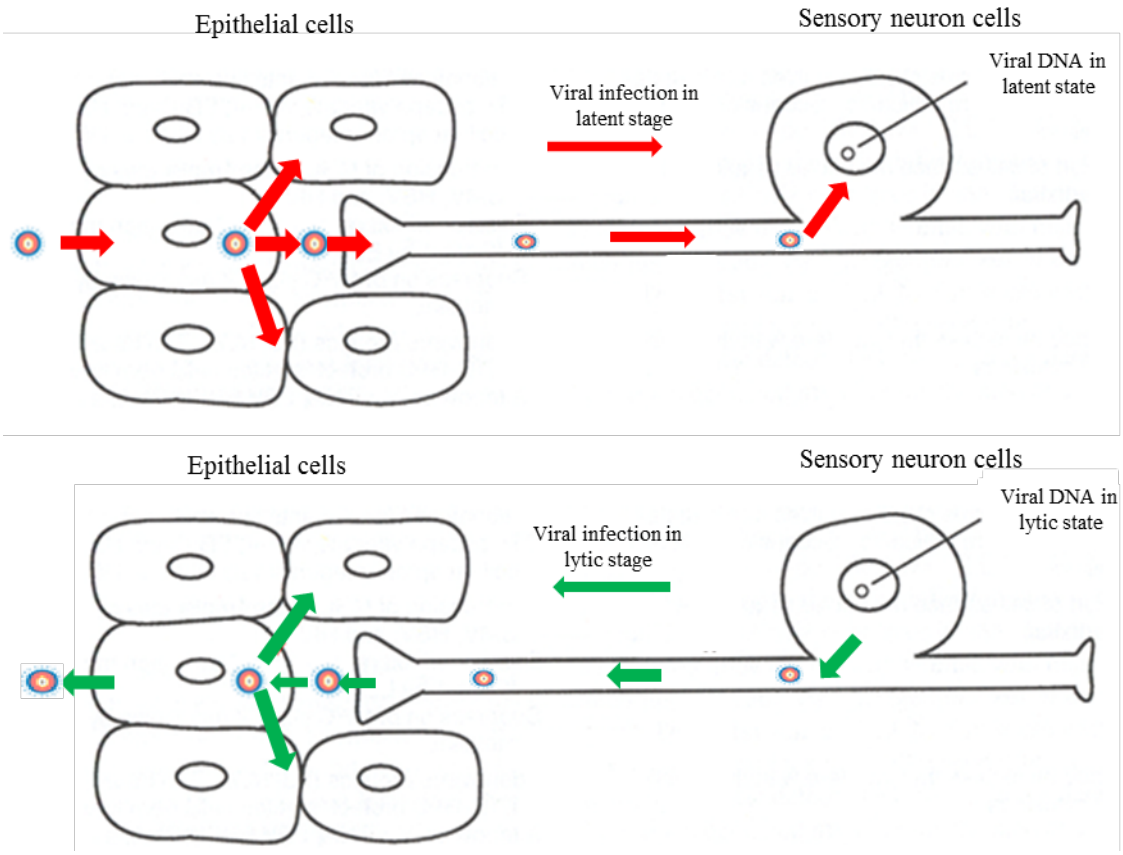

Figure 1.7 Latent and Lytic infection by HSV-1 and HSV-2.
Figure modified from (Knipe & Cliffe, 2008).

VZV causes varicella (chickenpox) on the human body in the primary infection and herpes zoster following reactivation. It evades the immune system in a similar manner as HSV by establishing latency in sensory ganglia. Most adults are immune to VZV infection because of childhood exposure, but immune compromised patients, pregnant women and newborns appear to be predisposed to severe infection. VZV infections in immunocompromised children are life threatening without proper treatment or if treatment is delayed. Acyclovir and its prodrug Valacyclovir are analogues of guanosine, which can selectively inhibit VZV and HSV replication. As an effective treatment to VZV infection, after administration acyclovir can spread throughout the human body, including the CNS, and can be well-tolerated and rarely causes side-effects. A vaccine for VZV has been approved by the FDA in 1995 and is available in many countries over the world (Holmes, 1996).

1.4.2 Betaherpesviruses and human disease

HCMV, HHV-6A, HHV-6B and HHV-7 are members of the Betaherpesviruses which have humans as their primary host. HHV-6A can be found in the patients with neuroinflammatory diseases. Primary infection of HHV-6B causes exanthem subitum in childhood. Furthermore, the reactivation of HHV-6B can cause encephalitis, bone marrow suppression and pneumonitis in transplant recipients and this makes the diagnosis of HHV-6B vital for the patients. HHV-7 can also cause exanthema subitum, but it is not as important as HHV-6B.

HCMV is the best known member in Betaherpesviruses family for its severe infection consequences. HCMV infection is recognized in a high proportion of the population over the world. It is much more common in developing countries for over 90% positive in the population, whereas this number is around 50% in developed countries (Fulop *et al.*, 2013). Most patients get the HCMV infection during childhood through exposure to the virus. HCMV maintains latency in CD34+ haematopoietic stem cells after the primary infection. HCMV can cause sensory impairment, retinitis, encephalitis, hepatitis, gastroenteritis and pneumonitis in immunocompromised hosts such as neonates, organ transplantation recipients and HIV positive patients. For bone marrow transplantation, as the severity of immunosuppression increases, so does the risk of HCMV infection. It is even fatal for bone marrow allograft recipients with a severe HCMV infection. The treatment for HCMV infection includes the competitive inhibitors of HCMV encoded DNA polymerase, immunoglobulin application, and adoptive transfer of immunity. Ganciclovir and Valganciclovir are competitive inhibitors of HCMV DNA polymerase but are not well tolerated by pregnant patients (Sullivan *et al.*, 1992). Therefore immunoglobulin is an effective way for the treatment of pregnant patients.

1.4.3 Gammaherpesviruses and human disease

Gammaherpesviruses are distinguished by their tropism for lymphocytes and are divided into *Lymphocryptoviridae* and *Rhadinoviridae.* EBV, which is one of the best studied gammaherpesviruses belongs to the *Lymphocryptoviridae.* EBV infects T cells, B cells and epithelial cells in the human body, and it has been linked to Burkitt's lymphoma, CNS lymphoma, post-transplant lymphoproliferative syndrome and HIV-associated hairy leukoplakia (Maeda *et al.*, 2009). There is evidence that EBV is also associated with immune mediated diseases such as auto-immune diseases. An asymptomatic EBV

infection usually occurs in the early childhood and is spread by saliva. EBV establishes latency in lymphoid tissues to evade the immune system and is harboured in the host for the remainder of their life.

KSHV (HHV-8) is another important member in gammaherpesvirus that belongs to the *Rhadinoviridae.* Primary target cells of KSHV are lymphocytes. It has been reported that B cells, T cells, monocytes and endothelial cells have been found positive for KSHV DNA. KSHV infection causes Kaposi's sarcoma, primary effusion lymphoma and some types of multicentric Castleman's disease (Boshoff & Weiss, 2002b; Cesarman *et al.*, 1995).

1.5 Host immunity and cellular defence to viral infection

During evolution, the human body has adapted several complicated defence systems to prevent virus infection, which include the innate immune system, the adaptive immune system and intrinsic immunity. The innate and adaptive immune systems have been extensively studied from many different aspects, whereas intrinsic immunity is a relatively recent concept (Bieniasz, 2004; Kerscher *et al.*, 2006; Michaelson & Leder, 2003; Pertel *et al.*, 2011; Yan & Chen, 2012).

1.5.1 Innate immune system

The innate immune system, also known as the first line of defence, plays the earliest role in anti-viral defence in the whole conventional immune system. It includes many cell types, cytokines and chemokines for defending the host from viral infection. On a cellular level, NK cells were identified to be important in controlling herpes virus infection with an efficient response to viral infection (reviewed in (Biron *et al.*, 1999)). NK cells stimulate IFN-γ expression, which mediates many cellular pathways against viral infection. This response happens within the first several hours to several days, and this is more rapid than the adaptive immune response mediated by B and T lymphocytes that take over a week to develop. Helper T cells also respond to IFN-α/β that is produced by infected cells, and the activated helper T cells mediate cytotoxicity to infected host cells and stimulate the adaptive immune response to virus infection.

Some aspects of intrinsic resistance also respond to innate immunity signalling in viral infection. Several components of ND10 are induced by IFN I/II to increase antiviral infection by repressing virus gene expression, notably by PML, hDaxx, ATRX and Sp100 (Everett & Chelbi-Alix, 2007; Tavalai & Stamminger, 2008). For example, HSV-1

infection triggers the innate immunity immediately to control the infection and lysis of the infected cells. This process also facilitates the adaptive immune response to HSV-1 infection. In brief, pathogen-associated molecular patterns (PAMPs, examples including lipopolysaccharide, peptidoglycan and double-stranded RNA) interact with the invading HSV-1, and then are recognized by toll-like receptors (TLRs). Activated TLRs trigger the inflammatory signals that including TLR-mediated Type I IFN-α/β production. In response to the IFN-α/β production, the cellular Janus/Just another kinase (JAK) - signal transducers and activators of transcription (STAT) signalling pathway is activated that induce phosphorylation and formation of the STAT1/STAT2 complex which is then imported into the nucleus. The STAT1/STAT2 complex binds to IFN-stimulated response elements (ISRE) located on interferon-stimulated genes (ISGs) to stimulate ISGs transcription. One of the many ISG transcription products that represses HSV-1 replication is PKR (protein kinase RNA-activated). PML expression in this process is increased in response to IFN-α/β (Chelbi-Alix *et al.*, 1995; Lavau *et al.*, 1995; Regad & Chelbi-Alix, 2001) and it further represses viral infection and replication (more detail will be introduced in section 1.5.3).

1.5.2 Intrinsic resistance to viral infection

1.5.2.1 Intrinsic resistance to herpes virus infection

Intrinsic resistance to virus infection is located at the front line of the intracellular host-cell defence system. It is conferred by constitutively expressed cellular proteins that restrict viral infection. In herpes virus infection, such as HSV-1, HCMV and EBV, components of ND10 have been identified by many groups to restrict viral infection. Meanwhile, the relative viral proteins that repress the host cell intrinsic resistance were also identified (some examples are listed in Table 1.1) (Ahn *et al.*, 1998; Ahn & Hayward, 1997; 2000; Amon *et al.*, 2006; Bell *et al.*, 2000; Everett *et al.*, 1998; Everett & Murray, 2005; Glass & Everett, 2013; Maul *et al.*, 2000; Tavalai *et al.*, 2011; Tavalai *et al.*, 2006; Tavalai & Stamminger, 2009; Tsai *et al.*, 2014).

Table 1.1 ND10 components and the viral proteins that interact with them.

Herpes virus	Viral protein	ND10 interaction components
HSV-1	ICP0 (Everett, 2000; Everett *et al.*, 1998)	PML, Sp100
HCMV	IE1 (Ahn *et al.*, 1998; Ahn & Hayward, 1997)	PML, Sp100
	pp71(Baldick *et al.*, 1997; Ishov *et al.*, 2002; Lukashchuk *et al.*, 2008; Tavalai *et al.*, 2008a)	hDaxx, ATRX
EBV	EBNA1(Sivachandran *et al.*, 2010; Sivachandran *et al.*, 2008; Stenberg *et al.*, 1985)	PML
	EBNA-LP(Echendu & Ling, 2008; Ling *et al.*, 2005)	Sp100
	BNRF1(Feederle *et al.*, 2006; Tsai *et al.*, 2014; Tsai *et al.*, 2011)	hDaxx, ATRX

1.5.2.2 Intrinsic resistance to retroviral infection

The concept of intrinsic resistance as a term to describe the antiviral effects of constitutively expressed cellular proteins was first developed in relation to the restriction of retrovirus infection (Bieniasz, 2004). Cellular proteins, such as APOBEC3G/F and TRIM5α, have been demonstrated to restrict HIV replication (reviewed in (Ishov *et al.*, 2004; Nisole *et al.*, 2005; Sokolskaja *et al.*, 2006)). APOBEC3G (apolipoprotein B mRNA-editing enzyme catalytic polypeptide 3G or A3G, initially known as CEM-15) is a member of cytidine deaminase family that can catalyse the mutation of viral DNA. It was identified as a cellular protein that represses the replication of Vif (viral infectivity factor) gene mutants of HIV-1 (Sheehy *et al.*, 2002). A3G catalyses the hydrolysis of cytidines (C) in the negative sense single-stranded DNA that reverse transcribed into uridine residues (U) (Harris *et al.*, 2003; Yu *et al.*, 2003a). As a consequence, it leads to guanine (G) to adenine (A) changes in the positive sense strand of proviral DNA. These mutations lead to potential damage to viral genome expression and regulatory genetic elements (Figure 1.8). Vif protein of HIV counteracts A3G by targeting A3G to ubiquitylate it, and leads to the degradation of A3G by proteasomes. In the absence of Vif during viral genome expression, A3G is packaged into progeny virions and leads to mutation during progeny virion gene reverse transcription, therefore impairing HIV viral replication (Sheehy *et al.*, 2003; Yu *et al.*, 2003a).

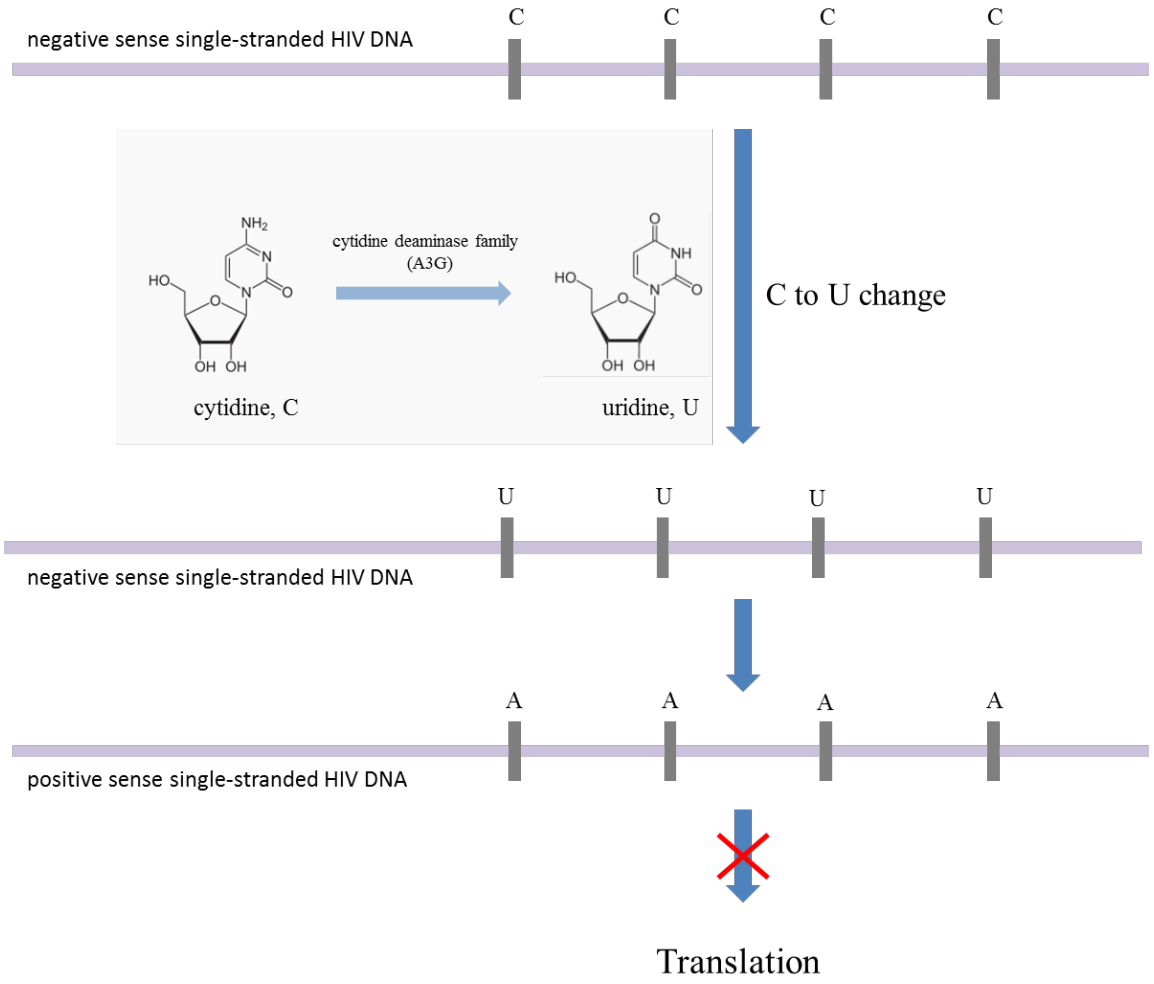

Figure 1.8 Hydrolysis of cytidine catalysed by A3G. A3G changes C to U during reverse transcription.

Thus, the HIV genes structure and its expression are damaged.

TRIM5α is one member of tripartite motif-containing (TRIM) superfamily, whose structural characteristics include a RING domain near the N-terminal region, one or two B-box domains and a coiled-coil domain in the C-terminal region of the motif . TRIM5α was first identified as an inhibitor of HIV-1 replication in rhesus monkey cells (Hatziioannou *et al.*, 2004; Keckesova *et al.*, 2004; Perron *et al.*, 2004; Stremlau *et al.*, 2004; Yap *et al.*, 2004). It has a C-terminal PRY/SPRY domain that includes viral recruitment motifs (Nisole *et al.*, 2005; Yap *et al.*, 2005). The PRY/SPRY domain recognizes the shape of sensitive retroviral capsids, then recruits the TRIM5 enzyme to the incoming virions to repress the viral infection (Stremlau *et al.*, 2004). TRIM5α deficient cells were demonstrated to be more susceptible to infection, further confirming its repression function on HIV infection (Stremlau *et al.*, 2004). The detailed mechanisms of A3G and TRIM5α

repression on HIV infection are still not clear and other repressors still wait to be identified, therefore, further research work is still ongoing. However these two examples illustrate the some of the core principles of intrinsic resistance proteins, in that they are constitutively expressed and in some cases are targeted by viral proteins that counteract their activities.

1.5.3 ND10 and its components

ND10, also known as PML Nuclear Bodies (PML-NBs) were first described in connection with Herpesvirus infection over 20 years ago(Maul *et al.*, 1993), although these electron dense punctuate structures in the nucleus of human cells had first been noted much earlier. ND10 are tightly bound to the nucleus matrix (Stuurman *et al.*, 1992) and electron microscopy studies have shown a ring-like protein structure that apparently in normal circumstances contains no nucleic acids in the centre (Boisvert *et al.*, 2000; Dellaire & Bazett-Jones, 2004). ND10 have many functions in cell biology that have been well studied, such as transcriptional regulation, DNA damage response, regulation of cellular senescence, regulation of neoangiogenesis and apoptosis (reviewed in (Bernardi & Pandolfi, 2003; 2007; Borden, 2002; Eskiw & Bazett-Jones, 2002; Negorev & Maul, 2001; Zhong *et al.*, 2000b)). In recent years, ND10 have been linked to the restriction of replication of both DNA and RNA virus infection (Boutell & Everett, 2013; Michaelson & Leder, 2003; Rivera-Molina *et al.*, 2013; Tavalai & Stamminger, 2008). For instance, accumulating data have shown that ND10 components re-localize to invading viral genomes during HSV-1 infection (Everett & Murray, 2005; Everett *et al.*, 2008; Lukashchuk & Everett, 2010). Knock down of ND10 components has been shown to increase HCMV infection (Lukashchuk *et al.*, 2008; Tavalai *et al.*, 2011; Tavalai *et al.*, 2006; Tavalai *et al.*, 2008b), and the absence of ATRX in ND10 increased EBV gene expression (Tsai *et al.*, 2014).

ND10 undergo significant changes in size, number and location in the nucleus indicating their dynamic nature (Dellaire & Bazett-Jones, 2004; Muratani *et al.*, 2002). One of the main components is the promyelocytic leukaemia (PML) tumour suppressor protein, which is essential for the formation of ND10 (Gareau & Lima, 2010; Ishov *et al.*, 1999). The deletion of PML has been demonstrated to disturb the localization of Sp100 and hDaxx to ND10 (Everett *et al.*, 2006). Other important ND10 members in intrinsic immunity include Sp100, hDaxx and ATRX. Sp100 was demonstrated to localize within ND10 by the interaction with PML through SUMO (Small Ubiquitin-like Modifier) modification (Negorev *et al.*, 2001). It also contributes to the repression of herpes virus infections such

as HCMV and HSV-1 (Everett *et al.*, 2008; Glass & Everett, 2013; Negorev *et al.*, 2006; Tavalai *et al.*, 2011). hDaxx is another important member of ND10, which recruited to ND10 through its SUMO interaction motif (SIM) (Ishov *et al.*, 1999). It also contributes to viral infection repression, especially in immediate early stage of viral infection (Cantrell & Bresnahan, 2006; Lukashchuk & Everett, 2010; Reeves *et al.*, 2010; Tavalai *et al.*, 2008b). ATRX is recruited by hDaxx and predominantly found in ND10 and heterochromatin (Baumann *et al.*, 2008; Berube *et al.*, 2008; Everett *et al.*, 2007; Kerscher *et al.*, 2006; Ritchie *et al.*, 2008; Tang *et al.*, 2004; Xue *et al.*, 2003). ATRX has many features that suggest a role in chromatin structure and control of gene expression (Tang *et al.*, 2004). Recent studies on ATRX have demonstrated its repression function on HCMV and EBV infection and replication, and this repression could be counteracted by viral tegument proteins (Lukashchuk *et al.*, 2008; Tsai *et al.*, 2014; Tsai *et al.*, 2011).

The formation and structure of ND10 is illustrated in Figure 1.9 (adapted from (Bernardi & Pandolfi, 2007)). In brief, PML interacts with itself or other PML isoforms to form the major part of ND10, and PML/PML interaction includes direct interactions involving the coiled-coil element of the TRIM and indirect interactions through SUMO and the SIM (reviewed in (Bernardi & Pandolfi, 2007)). The recruitment of hDaxx to ND10 is through the SIM site on hDaxx, which was proved by mutations in the hDaxx SIM motif that impaired hDaxx localization to ND10 (Ishov *et al.*, 1999; Lin *et al.*, 2006). ATRX interacts with hDaxx through the N-terminal PAH domain of hDaxx and is recruited to ND10 by hDaxx (Tang *et al.*, 2004). Sumoylated Sp100 locates to ND10 by the interaction with sumoylated PML through its SIM (Cuchet-Lourenco *et al.*, 2011). Many other gene regulation proteins can be recruited to ND10, such as ISG20, LYSP100, NDP55, SUMO family members and so on, whose functions and roles in intrinsic immunity (if any) have not been studied (Dent *et al.*, 1996; Gongora *et al.*, 1997; Maul *et al.*, 1995). Thus, in this thesis, the investigation will concentrate on PML, Sp100, hDaxx and ATRX.

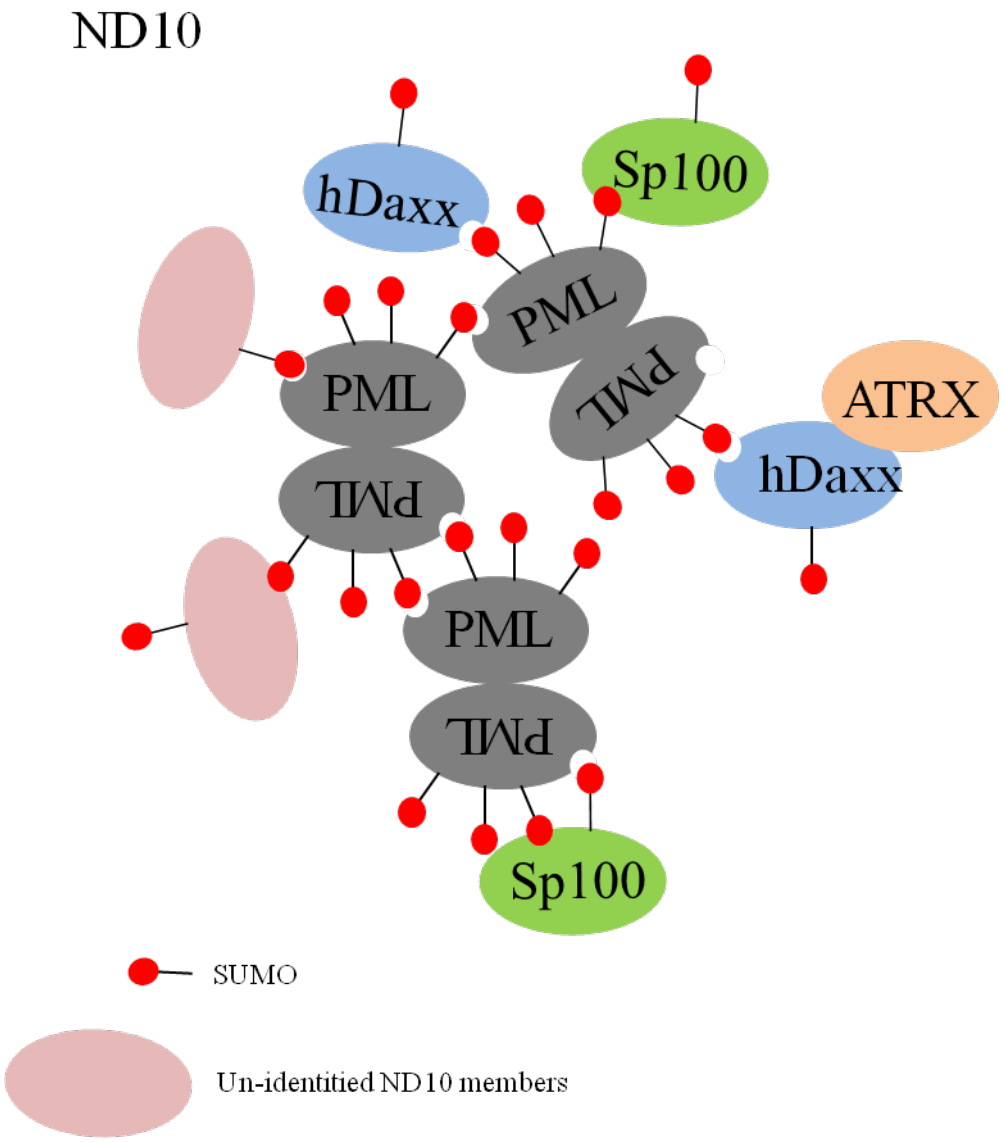

Figure 1.9 A model for the assembly of promyelocytic leukaemia nuclear bodies (ND10). Figure modified from (Bernardi & Pandolfi, 2007)

1.5.3.1 PML

PML is a tumour suppressor protein that is encoded by the PML gene and it is steadily expressed in most human cell lines. The PML gene is a member of tripartite motif (TRIM) family located on chromosome 15q22 that spans ~53,000 bases and nine exons (as indicated in Figure 1.11). PML gene C-terminal exons splicing leads to the expression of seven major isoforms of PML, I-VII (Bernardi & Pandolfi, 2007). Most isoforms (I-VI) predominantly localize within the nucleus due to the nuclear localization signal (NLS) located in exon 6. As Figure 1.11 shows, all PML isoforms contain exons 1-3, which

encode the TRIM/RBCC motif. The TRIM motif contains a zinc-finger structure (RING motif, R), two additional zinc-finger motifs (B-boxes, B) and a coiled-coil domain (CC). The RING domain was shown to be important for PML post-translational modification by SUMO (Meroni & Diez-Roux, 2005; Shen *et al.*, 2006), which is an ubiquitin-like protein (UBL). B-box domains in other TRIM proteins (TRIM5α and TRIM15) were demonstrated to contribute to intrinsic resistance to HIV infection (Brass *et al.*, 2008; Li *et al.*, 2007). The CC domain following the B-box domains is responsible for homomeric and heteromeric interactions among TRIM family members (Cuchet-Lourenco *et al.*, 2011; Lewis *et al.*, 2010; Mische *et al.*, 2005). The whole TRIM motif is required for PML I mediated restriction of HSV-1 infection (Cuchet *et al.*, 2011).

PML proteins were reported to repress VSV, HSV-1, HCMV and influenza A virus infection and replication (Chelbi-Alix *et al.*, 1998; Everett *et al.*, 2006; Ishov & Maul, 1996; Kang *et al.*, 2006; Kyratsous & Silverstein, 2009; Maul *et al.*, 1996; Reichelt *et al.*, 2011; Tavalai *et al.*, 2008b; Wang *et al.*, 2011). Many herpes viral proteins, such as ICP0 from HSV-1, IE1 from HCMV and EBNA1 from EBV, were reported to interact with PML for de-repression of the viral genes expression (Everett *et al.*, 2006; Kang *et al.*, 2006; Lee *et al.*, 2004; Muller & Dejean, 1999; Stenberg *et al.*, 1985). In ND10 structure, PML is the major component protein and indispensable for maintaining ND10 structure (Gareau & Lima, 2010; Ishov *et al.*, 1999). Knock down of PML by siRNA severely damaged the co-localization of Sp100 and hDaxx, and as a consequence, leads to increased viral infection (Everett *et al.*, 2008; Glass & Everett, 2013).

The difference between the PML isoforms is mainly due to alternative C-terminal exons (as indicated in Figure 1.10). PML VII lacks the NLS, thus leading to its spread in the cytoplasm but not mainly in nucleus (Jensen *et al.*, 2001). This PML isoform has been shown to regulate the transforming growth factor-β signal pathway (Newhart *et al.*, 2013). Other PML isoforms have different binding interfaces and functional specificity in nucleus and during herpes virus infection. PML isoform I binds to transcription factor AML1 to stimulate AML1-induced transcription (Abb, 1985). PML III interacts with Aurora A and regulates its kinase activity, which implicates a role of PML III in centrosome duplication and genome stability (Bostikova *et al.*, 2014). PML VI binds to p53 to induce premature senescence (Bischof *et al.*, 2002; Newhart *et al.*, 2012). PML IV is the preferentially interaction target of EBV protein EBNA1, which down regulates PML and stimulate lytic infection (Stenberg *et al.*, 1985). Construction of cell lines that lack wild type PML isoforms and reintroduction of different PML isoforms provided convenient tools to study

each single PML isoforms' function in HSV-1 infection (Cuchet *et al.*, 2011). The PML I or PML II expression in endogenous PML depletion cells can partially reverse ICP0 null HSV-1 infection increase (Cuchet *et al.*, 2011). The same study also showed that each individual PML isoform is capable of recruiting Sp100 into ND10 and to be sumoylated (Cuchet *et al.*, 2011).

Similar to many proteins expressed in a cell, PML is post-translational modified., There are two major types of modification of PML that have been identified, phosphorylation and sumoylation. PML is phosphorylated after translation at Tyr and Ser residues (Chang *et al.*, 1995). This process has been demonstrated to be important for lung cancer development (Scaglioni *et al.*, 2006). The most important post-translational modification of PML that has been studied is sumoylation. Mutation of PML sumoylation sites abolished the recruitment of Sp100 and hDaxx to ND10 (Ishov *et al.*, 1999; Zhong *et al.*, 2000a). Three sumoylation sites of PML have been identified, which are K65, K160 and K490 (Boddy *et al.*, 1996; Duprez *et al.*, 1999; Kamitani *et al.*, 1998). Nevertheless, the expression of PML I isoform in the cells that had been depleted of wt PML identified K616 but not K65 as a sumoylation site in PML I (Cuchet-Lourenco *et al.*, 2011), which might indicate the sumoylation of PML is partially isoform dependent.

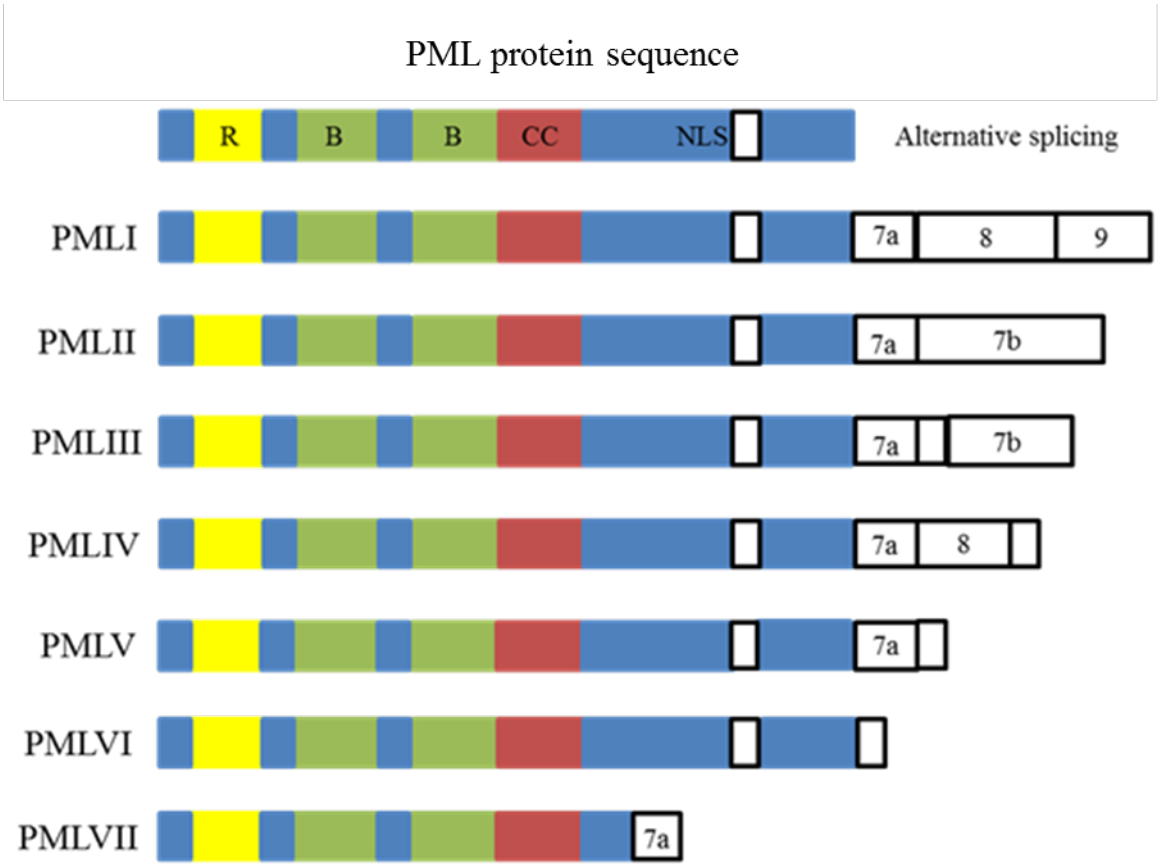

Figure 1.10 PML protein isoforms.
The figure is modified from (Bernardi & Pandolfi, 2007). Key domains of PML isoforms showing the RBCC location in the protein sequence and the NLS sequence location. The SIM is located in exon 7a.

Different herpes viruses interact with PML by different mechanisms to release PML's repression of viral replication. HSV-1 IE protein ICP0 degrades PML to stimulate HSV-1 lytic infection (Boutell *et al.*, 2011; Cuchet-Lourenco *et al.*, 2012; Everett, 2011; Everett *et al.*, 1998; Muller & Dejean, 1999; Perusina Lanfranca *et al.*, 2013). IE1 from HCMV de-sumoylates sumoylated PML and disperses the PML in nucleus to counteract the intrinsic immunity (Kang *et al.*, 2006; Kim *et al.*, 2011b; Lee *et al.*, 2004; Muller & Dejean, 1999; Tavalai *et al.*, 2011). EBV protein EBNA1 was demonstrated to down regulate PML in host cells through interacting with casein kinase 2 (CK2) and ubiquitin specific protein 7 (USP7) (Sivachandran *et al.*, 2010; Sivachandran *et al.*, 2008). Details about the above interactions between PML and viral proteins will be discussed in section 1.6.

PML depleted cells have been widely studied to analyse the effects of PML on herpes virus infection by different labs to support the notion of PML mediated intrinsic immunity. PML knock down cells have been demonstrated to increase ICP0 null HSV-1 infection (Everett *et al.*, 2006). PML depletion was also shown to increase IE gene expression and the plaque

formation efficiency of wt HCMV. In the same experiment, IE gene expression of several mutant HCMVs, in which the IE1 gene, the pp71 gene were deleted or the MIEP (major immediate-early promoter) sequence was altered, was also increased in PML depleted fibroblast cells (Tavalai *et al.*, 2008b). Therefore, the above reports demonstrated the repression function of PML in α and β herpes virus infection. It is important to note however that depletion of PML did not restore replication of these mutant viruses to wt levels. For example, depletion of PML increases ICP0 null mutant HSV-1 plaque formation by about 10-fold, whereas the defect of the mutant virus in the parental cell line is 500- to 1000-fold. Therefore although PML is involved in regulating HSV-1 infection, other factors must also be important.

1.5.3.2 Sp100

Sp100 is another important ND10 component involved in viral gene expression regulation (Negorev *et al.*, 2006; Negorev *et al.*, 2009). It was originally identified by the presence of anti-Sp100 auto-antibodies in the sera of primary biliary cirrhosis patients (Szostecki *et al.*, 1990) and was the first protein identified in the ND10 structure (Negorev *et al.*, 2001; Negorev & Maul, 2001). The human Sp100 gene was originally reported to locate on chromosome 2 and encode a protein of calculated molecular mass of 53 kDa. The sequence of Sp100 reported has an acidic region that leads to a highly aberrant electrophoretic mobility in SDS-PAGE which resolves at the molecular weight near 100 kDa (Szostecki *et al.*, 1990; Szostecki *et al.*, 1987). Sp100 is a single-copy gene that encodes four spliced isoforms, Sp100A, Sp100B, Sp100C and Sp100 HMG (high mobility group, HMG) (Amon & Farrell, 2005). The genome structure of Sp100 isoforms is shown in Figure 1.11. The shortest and most abundantly expressed isoform, Sp100A, which shares 477 amino acids with the other three isoforms, was reported to promote transcription (Negorev *et al.*, 2006; Negorev *et al.*, 2009; Sullivan *et al.*, 1992). Sp100B, Sp100C and Sp100 HMG isoforms contain a SAND domain (named after Sp100, AIRE-1, NucP41/45 and DEAF-1) that binds DNA composed of un-methylated CpG (-C-phosphate-G-) sites (Fulop *et al.*, 2013; Holmes, 1996). The mutation at W655Q in the Sp100B SAND domain was reported to abolish the interaction with DNA, and then promote transcription (Holmes, 1996; Negorev *et al.*, 2006; Negorev *et al.*, 2009). This might indicate the SAND domain possesses transcription repression activity. Sp100C contains a PHD (plant homeo-domain) and Bromo-domain that in some cases are involved in binding to methylated lysines in histones and acetylation of lysines respectively (Baker *et al.*, 2008; Boshoff & Weiss,

2002a). Sp100HMG has a HMG-1/2 family homologous domain that may possess DNA-binding potential (Seeler *et al.*, 1998).

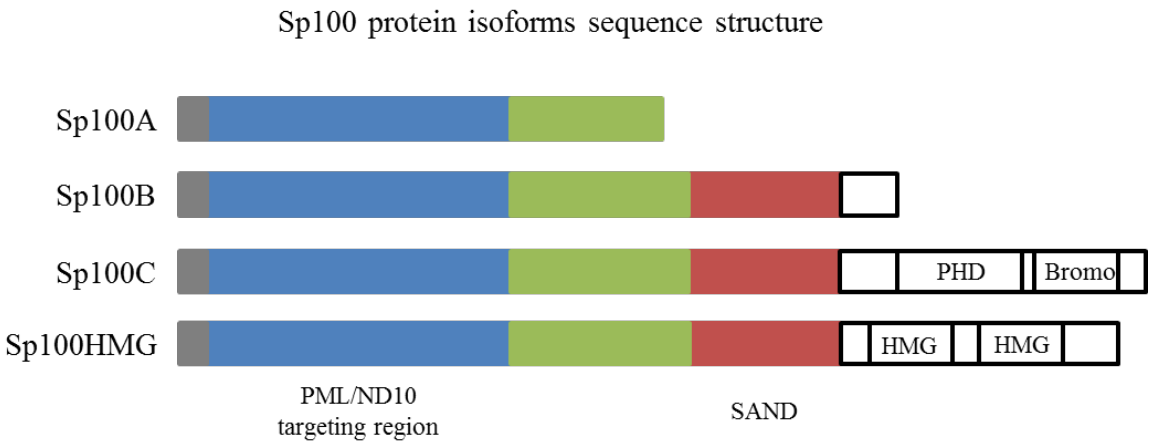

Figure 1.11 Sp100 protein isoforms.
This figure is modified from (Guldner *et al.*, 1999). Key structural features are shown, including the PML/ND10 targeting region near the N- terminal end, the SAND domain location in Sp100B, Sp100C and Sp100HMG, the PHD and Bromo domains in Sp100C, and the HMG domains in Sp100HMG.

In herpes virus infection studies, Sp100 has been identified to regulate HSV-1, HCMV and EBV infection and replication (Bell *et al.*, 2000; Echendu & Ling, 2008; Everett *et al.*, 2008; Ling *et al.*, 2005; Tavalai *et al.*, 2011). Many herpes viral proteins target Sp100 to stimulate virus infection and gene expression, such as ICP0 from HSV-1, IE1 from HCMV and EBNA-LP from EBV (further details will be discussed in section 1.6) (Chelbi-Alix & de The, 1999; Echendu & Ling, 2008; Everett *et al.*, 2008; Ling *et al.*, 2005; Muller & Dejean, 1999). Sp100 is also sumoylated as PML, but this post translational modification is not essential for its localization to ND10 (Sternsdorf *et al.*, 1997). PML has been shown to be important for Sp100 sumoylation (Everett *et al.*, 2008). Further investigation demonstrated Sp100 recruitment to ND10 dependent on its SIM motif. In the same study, the SIM motif, but not sumoylation, has been shown to be important for Sp100A recruitment to invading ICP0 null HSV-1 genomes (Cuchet-Lourenco *et al.*, 2011).

1.5.3.3 hDaxx

hDaxx (human Daxx) is an important ND10 component involved in intrinsic resistance to virus infection. It was first identified as a modulator of apoptotic signalling (Rowe *et al.*, 1956). hDaxx is mainly located to chromatin and ND10, where it is involved in chromatin

assembly and remodelling, transcription, apoptosis regulation and viral gene repression (reviewed in (Maeda *et al.*, 2009)). hDaxx is expressed in most human tissues (Rowe *et al.*, 1956). Its structure contains 740 amino acids and several major domains were identified in the primary work, they include two N-terminal paired amphipathic helices (PAHs), a coiled-coil domain, an acidic region and a C-terminal serine/proline/threonine (S/P/T) rich region (Rowe *et al.*, 1956). hDaxx was reported to interact with numerous proteins, and many of them are related to intrinsic resistance to viral infection and apoptosis (reviewed in (Maeda *et al.*, 2009)). The interaction between hDaxx and FAS, which is a widely expressed cell death receptor that is important to the regulation of the immune system and tissue homeostasis, was originally reported to activate apoptosis (Rowe *et al.*, 1956). Then, it was reported to interact with PML in yeast two-hybrid screening and co-localize with ND10 in immunofluorescence assays (Ishov *et al.*, 1999; Zhong *et al.*, 2000c). The interactions of hDaxx with chromatin components and modifiers, such as H2A, H2B, H3, H4 and HDAC II were also reported (Hollenbach *et al.*, 2002). After that, hDaxx was identified to interact with ATRX and form a complex in ND10 in 2003 and 2004 (Tang *et al.*, 2004; Xue *et al.*, 2003). Furthermore, the hDaxx-ATRX complex was reported to form mainly in the S phase of cell cycle, and this complex is separated during G2 phase. In cells that lacked hDaxx, S phase is accelerated which leads to the formation of binucleated cells (Kerscher *et al.*, 2006). HCMV infection interferes with the formation of the hDaxx-ATRX complex, and also leads to the formation of binucleated cells (Cantrell & Bresnahan, 2006; Foster & Jack, 1971; Ishov *et al.*, 2002; Lukashchuk *et al.*, 2008).

Due to the large number proteins that interact with hDaxx, it is involved in many signaling pathways and cell functions. Some of the reports about hDaxx were not consistent with its function in apoptosis, which indicates its complicated mechanisms of interaction with other proteins. hDaxx was firstly reported to promote apoptosis through the interaction with Jun-N-terminal kinase (JNK), which leads to downstream events and finally apoptosis (Rowe *et al.*, 1956). hDaxx also interacts and activates the JNK upstream kinase Apoptosis signal-regulating kinase 1 (ASK1) that activates JNK after activation (Pluta *et al.*, 1998). Furthermore, TGF-β treatment stimulates the phosphorylation of hDaxx by nuclear kinase HIPK2, which is required for TGF-β induced apoptosis and JNK signalling. This indicates the HIPK2 and hDaxx are involved in the nuclear pathways that activate JNK and apoptosis upon TGF-β (Pertel *et al.*, 2011). Thus, hDaxx was initially identified as a factor that promotes apoptosis. However, researchers also observed anti-apoptotic roles of hDaxx. A Daxx knock out mouse embryo model ($Daxx^{-/-}$) increased apoptosis (Mehle *et al.*, 2004).

The similar apoptosis increase also observed in Daxx knock out embryonic stem cells (Mehle *et al.*, 2004). The apoptosis increase in hDaxx knockdown by RNAi in cells was also observed by other group (Michaelson & Leder, 2003). Furthermore, hDaxx knockdown cells are more sensitive to FAS, UV or tumour necrosis factor α (TNF-α) induced apoptosis (Michaelson & Leder, 2003). Thus, the above studies indicated the complexity of hDaxx in apoptosis, and whether this is related to its interactions with ND10 is as yet un-clear.

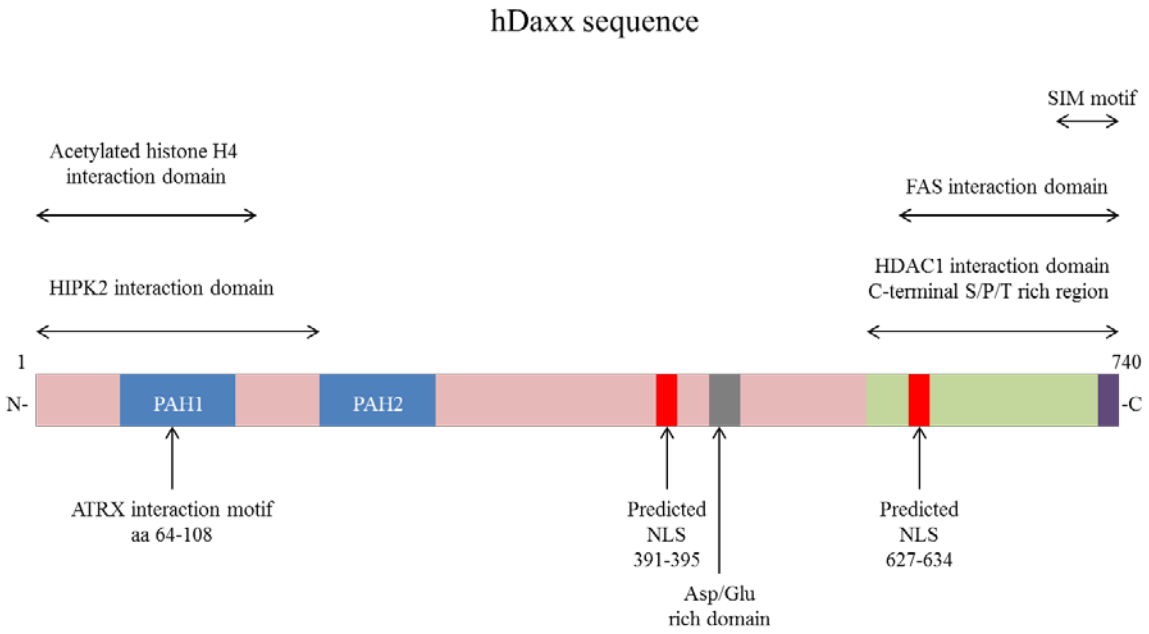

Figure 1.12 The hDaxx protein map.
Figure adapted from (Boshart *et al.*, 1985). The main protein interaction regions are shown as indicated.

hDaxx was reported to be sumoylated by SUMO-1 and to interact with Ubc9 (Everett & Murray, 2005; Ryu *et al.*, 2000). Mutations at K630 and K631 abolished the sumoylation of Daxx. Furthermore, the same study also indicated that the sumoylation of Daxx is not essential for its co-localization with PML (Everett & Murray, 2005). A SIM domain was also reported in the hDaxx sequence. By generating different hDaxx mutation, the SIM site was identified between 733-740 amino acids. Furthermore, the hDaxx-SUMO interaction was reported important for its SUMO conjugation (Lin *et al.*, 2006). The extent of sumoylation of hDaxx under normal circumstances is unclear as, unlike PML and Sp100, modified forms of hDaxx consistent with sumoylation are not readily detectable in whole cell lysates.

In virology, hDaxx performs anti-viral infection functions in many instances. In RNA viruses, integrase from Avian Sarcoma virus (ASV) and HIV-1, DENV C from dengue virus (DENV) and PUUV-N from Puumala virus (PUUV) were reported to modulate hDaxx, and for DNA viruses, BNRF1 from EBV, pp71 from HCMV, protein VI from Adenovirus type 5 and L2 from HPV were reported to interact with hDaxx during viral infection (reviewed in (Schreiner & Wodrich, 2013)). Furthermore, ICP0 from HSV-1 was reported to antagonize hDaxx-ATRX complex repression of viral gene expression although there was no evidence of a direct interaction (Lukashchuk & Everett, 2010). In this study, the interactions between hDaxx and pp71 and BNRF1 will be introduced in more detail in section 1.6.

1.5.3.4 ATRX

ATRX forms a strong complex with hDaxx that accumulates in ND10 (Tang *et al.*, 2004; Xue *et al.*, 2003). Its name came from the mutation in X-linked α-thalassemia/mental retardation syndrome (Gibbons *et al.*, 1995). The ATRX gene contains about 11,000 nucleotides, of which the major ATRX isoform cDNA is approximately 7,500 nucleotides (Brasch & Ochs, 1992; Gibbons *et al.*, 1995). The structure of ATRX includes a SWI/SNF2-type ATPase/helicase motif, a plant homeodomain-like (PHD) zinc finger, a HP1 binding region and hDaxx interaction domain and PxVxL sequence (Amon *et al.*, 2006; Argentaro *et al.*, 2007; Chelbi-Alix *et al.*, 1995; Lechner *et al.*, 2005; Tang *et al.*, 2004). Mutations in ATPase/Helicase domains and PHD zinc finger motif causing a severe mental retardation syndrome, which is associated with urogenital abnormalities, facial dysmorphisms, and frequently α-thalassaemia (the ATR-X syndrome as described above) (Brasch & Ochs, 1992; Gibbons *et al.*, 1995). The structure of ATRX is shown in Figure 1.13.

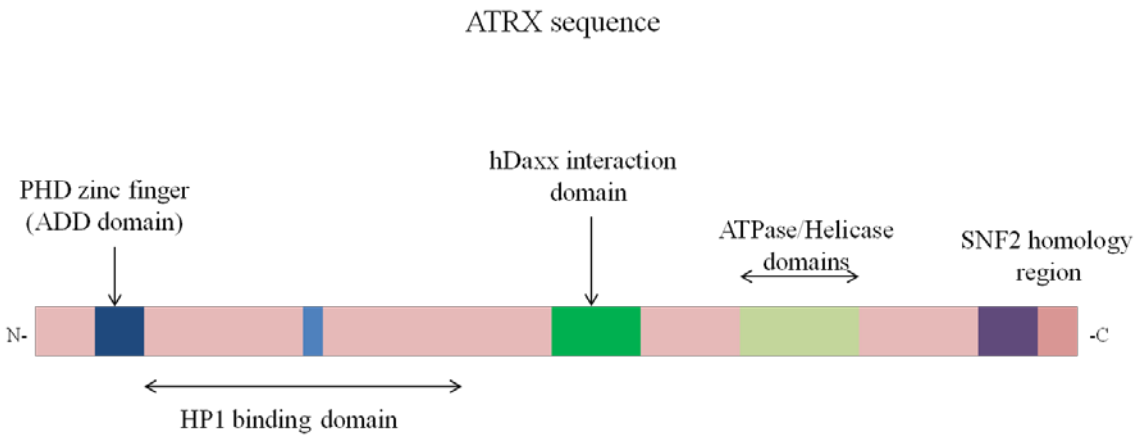

Figure 1.13 The ATRX protein map.
Key structural features showing: PHD zinc finger, HP1 binding domain, hDaxx interaction domain, helicase domains and SNF2 homology region.

ATRX was identified to possess a PHD zinc finger that indicates its potential function in chromatin remodelling. The ATRX PHD zinc finger domain is of the C4HC3 type (four cysteines-one histidine-three cysteines) that coordinates two zinc ions to stabilize the protein fold. Sequence data base searches revealed that DNA methyltransferase DNMT3A, DNMT3B and DNMT3L share the same PHD zinc finger domain structure with ATRX (Meroni & Diez-Roux, 2005). Therefore, this unique domain in ATRX was named the ADD domain (Aapola *et al.*, 2000). The studies on DNMTs indicate the potential of interaction between DNMTs with histones (Dent *et al.*, 1996), and DNMT3L was reported to recognize the H3K4 (lysine 4 on histone H3) methylation status through its ADD domain (Gongora *et al.*, 1997). Accordingly, the above studies suggest the potential interaction between ATRX with histones, and furthermore, it is involved in transcription regulation.

Accumulating evidence demonstrated that ATRX interacts with hDaxx to predominantly locate at ND10 and heterochromatin (Baumann *et al.*, 2008; Berube *et al.*, 2008; Everett *et al.*, 2007; Kerscher *et al.*, 2006; Ritchie *et al.*, 2008; Tang *et al.*, 2004; Xue *et al.*, 2003). In recent report, hDaxx and ATRX were identified in H3.3 immunoprecipitations (Brass *et al.*, 2008). Further investigation indicated the hDaxx is a specific histone chaperone for H3.3, and the interaction between ATRX and hDaxx is essential for H3.3 incorporation at telomeres (Lewis *et al.*, 2010). Thus, it is likely that ATRX cooperates with hDaxx to interact with H3.3 for transcription regulation. More recently, the hDaxx-ATRX-H3.3 complex was reported to be a BNRF1 interaction target for stimulating lytic stage infection

(Tsai *et al.*, 2014). It indicates the hDaxx-ATRX complex interaction with histones involves an anti-viral infection process in host cells.

ATRX interacts with HP1 to perform gene expression regulation (Rivera-Molina *et al.*, 2013), and is recruited to ND10 by hDaxx (Tang *et al.*, 2004; Xue *et al.*, 2003). ND10 have been reported to perform intrinsic immunity functions during viral infection (Ahn *et al.*, 1998; Ahn & Hayward, 1997; 2000; Amon *et al.*, 2006; Bell *et al.*, 2000; Everett *et al.*, 1998; Everett & Murray, 2005; Glass & Everett, 2013; Maul *et al.*, 2000; Tavalai *et al.*, 2011; Tavalai *et al.*, 2006; Tavalai & Stamminger, 2009; Tsai *et al.*, 2014). Therefore, it was reasonable to predict that ATRX is involved in viral gene regulation. Recent reports have indicated the repression function of ATRX in herpes virus infection, which includes examples of herpes viruses from the α, β and γ herpes virus subfamilies (Lukashchuk & Everett, 2010; Lukashchuk *et al.*, 2008; Tsai *et al.*, 2014). Meanwhile, viral proteins that counteract the hDaxx-ATRX repression during viral infection were identified in parallel, and more detail will be introduced in section 1.6.

1.5.3.5 SUMO family

Small ubiquitin-like modifier (SUMO) proteins are a family of small proteins that become covalently bound to other proteins at lysine residues to provide post translational modification. Sumoylation (SUMO modification) alters the interaction patterns between proteins, changes the proteins localization in the cell and changes the activities of the sumoylated proteins (Boddy *et al.*, 1996; Gareau & Lima, 2010; Hay, 2005; Kamitani *et al.*, 1997; Mahajan *et al.*, 1997; Matunis *et al.*, 1996; Shen *et al.*, 1996). This post translational modification is involved in many cellular processes like the stress response, nuclear-cytosolic transport, apoptosis, transcriptional regulation, protein stability and progression through the cell cycle (Bergink & Jentsch, 2009; Gareau & Lima, 2010; Hay, 2005). In ND10, SUMO modifies PML, Sp100 and hDaxx and it is important for maintaining ND10 structure (as indicated in Figure 1.9) (Bernardi & Pandolfi, 2007; Cuchet-Lourenco *et al.*, 2011; Shen *et al.*, 2006). The SUMO protein 3D structure is similar to ubiquitin (as its name indicates), and the covalently attachment on substrates of SUMO and ubiquitin also occur through similar enzymatic cascades that involves an E1 activating enzyme, an E2 conjugating enzyme and an E3 protein ligase (Capili & Lima, 2007; Kerscher *et al.*, 2006). The SUMO modification pathway is shown in Figure 1.14.

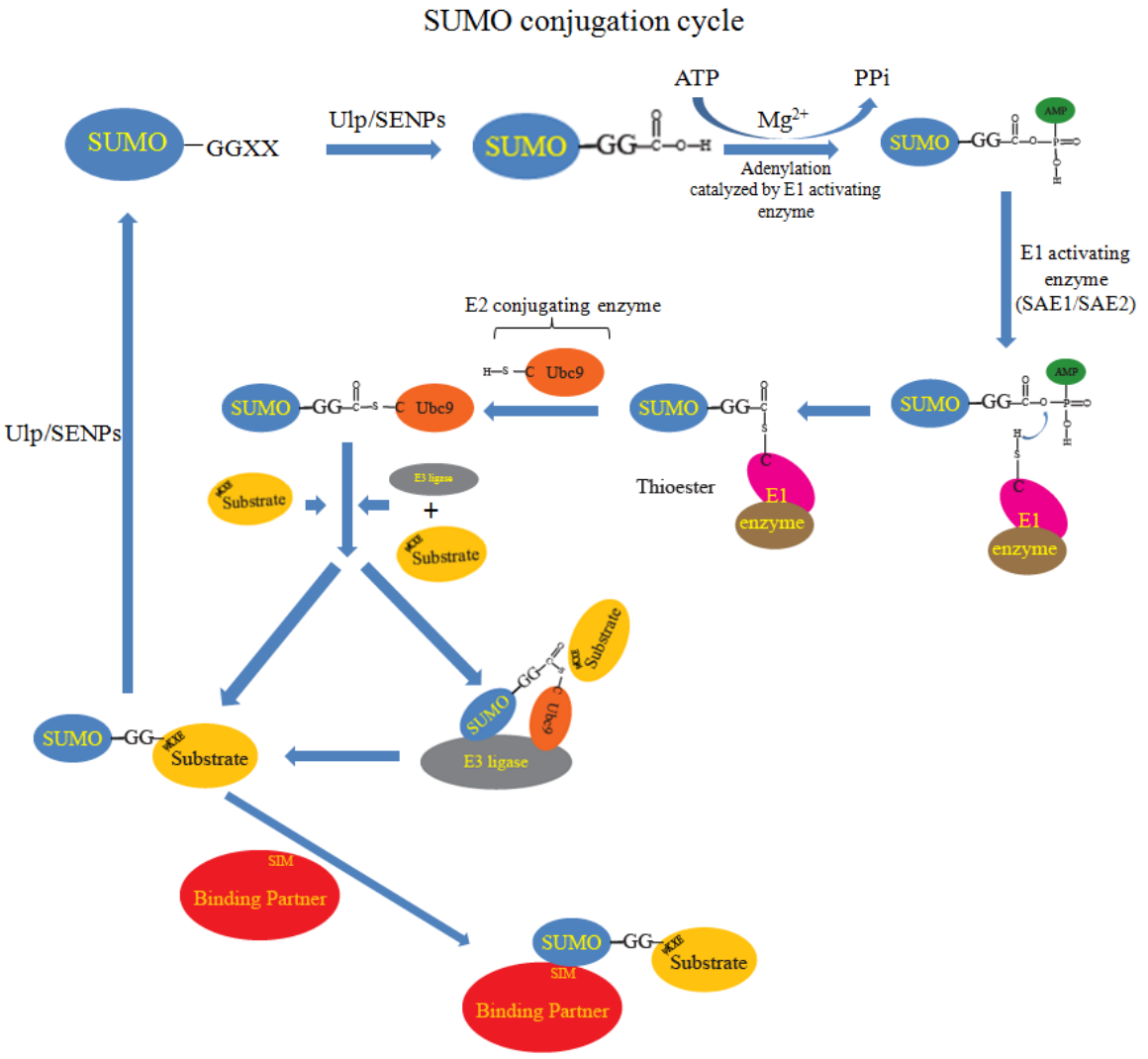

Figure 1.14 The SUMO conjugation cycle.
This figure is adopted from (Everett *et al.*, 2013b; Gareau & Lima, 2010).

SUMO proteins are translated as immature precursors first, then the immature SUMO proteins are modified by Ulps (ubiquitin-like protein-specific protease, Ulp, in yeast) or SENPs (sentrin-specific protease, SENP, in human) to generate the mature form of SUMO, which has a C- terminal di-glycine motif for efficient adenylation (Biron *et al.*, 1999). Adenylated SUMO proteins are attacked by HS- group from the active site Cys on the E1 activating enzyme complex and the -GG of SUMO is covalently conjugated to the Cys on the E1 activating enzyme, which contains SUMO activating enzyme subunit1 (SAE1) and SUMO activating enzyme subunit2 (SAE2) (in yeast the E1 complex is formed by Aos1 and Uba2) (Drane *et al.*, 2010; Nevels *et al.*, 2011), to form the E1~SUMO thioester (chemical groups that have a C-S-CO-C structure). The E2 conjugating enzyme also has a conserved active site Cys residue, and UBC9 (ubiquitin-like conjugating enzyme 9) is the

predominant E2 enzyme that has been identified (Adler *et al.*, 2011; Everett, 2006a; Kerscher *et al.*, 2006; Preston & Nicholl, 2006). Therefore, the E1~SUMO complex transfers SUMO to UBC9 to form the UBC9~SUMO thioester. Following the above conjugation, UBC9~SUMO can directly interact with some SUMO substrates to form covalent bond between SUMO-GG and a Lys residue on the substrates, or alternatively, E3 protein ligases facilitate the conjugation between SUMO with its substrates. In many cases, SUMO substrates have a SUMO conjugation consensus motif that has been characterized as ψKXE. The ψKXE site contains a large hydrophobic amino acid (isoleucine, leucine or valine) which is represented by ψ, a lysine (K) residue for modification, an X residue represents any amino acid and a glutamic acid (E) (Dimitropoulou *et al.*, 2010). Sumoylated proteins can be de-conjugation by Ulps/SENPs to release the SUMO back into the SUMO conjugation cycle (reviewed in (Everett *et al.*, 2013b; Gareau & Lima, 2010)). Sumoylated proteins interact with SIM sites on its binding partners. SIM sites are characterized by a short group of hydrophobic amino acids, such as (V/I)X(V/I)(V/I), that is flanked by acidic residues (Gareau & Lima, 2010).

The SUMO family has 4 members, which are SUMO1, SUMO2, SUMO3 and SUMO4, encoded by different genes. The molecular weight of SUMO1-3 is about 12 kDa. SUMO1 shares about 50% sequence with SUMO2/3, it uses the same E1 complex and Ubc9 (Kerscher *et al.*, 2006). SUMO2 and SUMO3 share 97% sequence identity in their structure, which leads to use of the term SUMO2/3 to represent both of them. Different to other SUMOs, the function of SUMO4 remains unclear in protein modification (Baumann *et al.*, 2008; Berube *et al.*, 2008). SUMO1 and SUMO2/3 may have different conjugation substrates and also differ in SUMO chain formation. For instance, SUMO2/3 has the potential to form SUMO chains in sumoylation of PML and other substrates but this property is not shared by SUMO1 (Kyratsous & Silverstein, 2009; Ritchie *et al.*, 2008).

Sumoylation is also involved in the regulation of viral infections, and more detail about this will be introduced in section 1.6.

1.6 Herpes virus ND10 interaction proteins

As introduced above, ND10 restrict several different virus infections (Boutell & Everett, 2013; Tavalai & Stamminger, 2008). During evolution, viruses have developed complicated mechanisms to counteract host cell defences that are imparted by ND10. Several major viral ND10 interaction proteins from different herpes viruses are listed in

Table 1.1. This chapter will introduce more detail about the interactions between viral proteins and ND10 components, and furthermore the mechanisms of stimulating viral infection through the above interactions.

1.6.1 HSV-1 protein ICP0 interacts with ND10

HSV-1 infects the majority of the population and establishes a life-long latent infection in sensory neurones. The reactivation of HSV-1 infection can cause life threatening diseases in immune compromised patients and neonates (introduced in section 1.4.1). ND10 components were reported to restrict HSV-1 infection, and in parallel, viral proteins that counteract ND10 repression were also identified (Everett *et al.*, 2008; Everett *et al.*, 2009; Everett *et al.*, 1991; Everett *et al.*, 2006; Everett & Zafiropoulos, 2004; Glass & Everett, 2013; Harris *et al.*, 1989; Lukashchuk & Everett, 2010; Maul & Everett, 1994; Natarajan *et al.*, 1991; Wilcox *et al.*, 1997).

1.6.1.1 HSV-1 ICP0 protein

The viral protein identified to interact with ND10 for stimulating HSV-1 infection is ICP0 (Cuchet-Lourenco *et al.*, 2012; Everett, 1987; 1988b; Everett & Maul, 1994; Everett *et al.*, 2006; Glass & Everett, 2013; Harris *et al.*, 1989). ICP0 is expressed by HSV-1 in the IE stage of infection, during which 5 viral proteins are expressed, they are ICP4 (Kim *et al.*, 2011a), ICP27 (Kutluay & Triezenberg, 2009), ICP22 (Lilley *et al.*, 2011; Rice *et al.*, 1995), ICP47 (Lukashchuk *et al.*, 2010) and ICP0. Once ICP0 is expressed, it localizes to ND10 and causes their disruption (Maul & Everett, 1994; Maul *et al.*, 1993). The association of ICP0 with ND10 degrades PML , abrogates sumoylation of Sp100 and disperses Sp100, hDaxx and ATRX from ND10 (Boutell *et al.*, 2011; Boutell *et al.*, 2002; Everett *et al.*, 1998; Everett *et al.*, 2009; Lukashchuk & Everett, 2010; Muller & Dejean, 1999; Parkinson & Everett, 2000).

ICP0 is encoded by the IE-1 gene, which has two copies, within the TR_L and IR_L regions of the genome (herpes virus genome structure is shown in Figure 1.2). ICP0 contains 775 amino acids with a predicted molecular weight about 80 kDa (Perry *et al.*, 1986). The ICP0 molecular weight indicated on polyacrylamide gels is approximately 110 kDa, therefore, ICP0 was referred to as Vmw110 in earlier reports. In the ICP0 structure, several functional groups have been identified (indicated in Figure 1.15). They are the RING finger domain, 3 major phosphorylation sites, a nuclear localization sequence (NLS), the USP7 (ubiquitin-specific processing protease 7) interaction motif (Daubeuf *et al.*, 2009;

Everett *et al.*, 1997; Saffert & Kalejta, 2007) and a region required for ND10 localization (reviewed in (Everett, 2006b)). Studies on ICP0 mutants indicated that the N-terminal half of ICP0 is important for its function on transcription activation for viral promoters (Cai & Schaffer, 1989; Everett, 1987; 1988a; Perry *et al.*, 1986). The RING finger domain is important for ICP0 to perform its E3 ligase activity (Barlow *et al.*, 1994; Boutell *et al.*, 2002). The USP7 interaction motif, as indicated, is responsible for the interaction between USP7 and ICP0, which is important for stabilization of ICP0 and innate response modulation (Daubeuf *et al.*, 2009; Saffert & Kalejta, 2007).

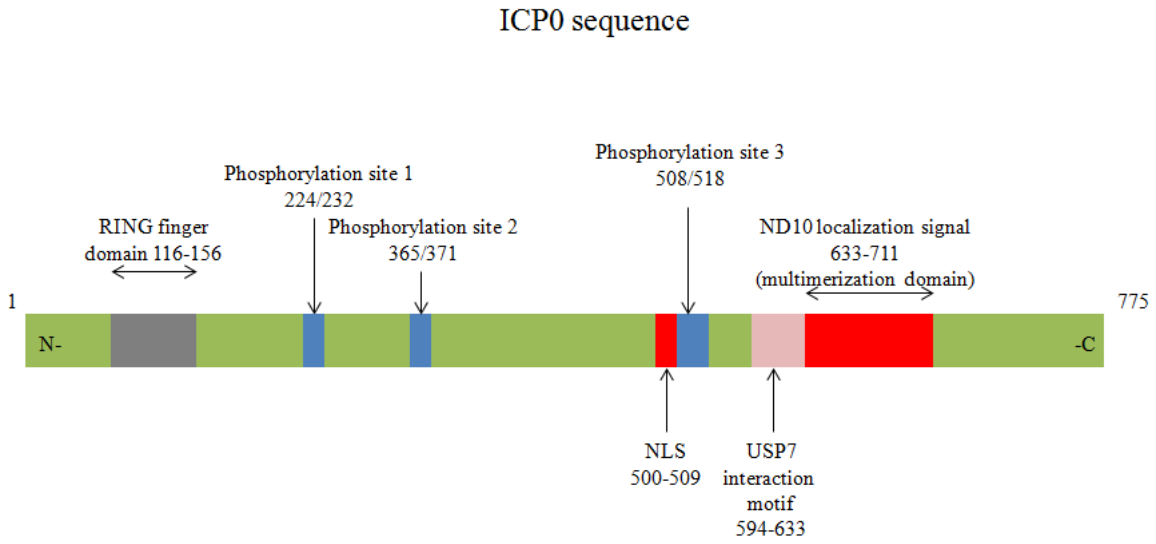

Figure 1.15 A map of the ICP0 protein sequence.
Figure adapted from (Everett, 2006b). Key structures are indicated as a RING finger domain, 3 phosphorylation sites, a nuclear localization sequence (NLS), USP7 interaction motif and ND10 localization signal region.

The RING finger domain in ICP0 was firstly identified as "C_3HC_4" sequence motif located in the N-terminal third of the protein that binds to two Zn^{2+} atoms (Barlow *et al.*, 1994). Many RING finger domain containing proteins perform E3 ubiquitin ligase activities in diverse cellular functions and processes, for instance, the cell cycle, signalling, transcription, DNA repair and apoptosis (Joazeiro & Weissman, 2000). ICP0 also performs E3 ubiquitin ligase activity through RING finger domain (Boutell *et al.*, 2002), which is essential for ICP0 induced PML degradation (Boutell *et al.*, 2003; Chelbi-Alix & de The, 1999; Everett *et al.*, 1998; Everett *et al.*, 2009; Parkinson & Everett, 2000). Mutations within the RING finger domain of ICP0 inactivate its ubiquitin conjugation activity and completely impair its ability to stimulate lytic infection and the reactivation of quiescent viral genomes (Boutell *et al.*, 2002; Everett *et al.*, 1995; Everett, 1987; Everett *et al.*, 2009; Lium & Silverstein, 1997; O'Rourke *et al.*, 1998). Studies on ICP0 mutants demonstrated

that the RING finger domain is not required for ICP0 localization to ND10 but is important for efficient viral infection (Everett *et al.*, 2009).

The ubiquitin conjugation pathway is similar to the SUMO conjugation pathway (Figure 1.15) which requires an E1 ubiquitin activation enzyme, an E2 conjugation enzyme and an E3 ubiquitin ligase. In brief, monomeric ubiquitin is activated by an ATP dependent reaction and covalently conjugated to the E1 activation enzyme by a thioester bond. Then, the activated ubiquitin is transferred to E2 ubiquitin conjugation enzyme, and finally, the ubiquitin in the E2-ubiquitin thioester is mediated by E3 ligase to transfer to its substrates by covalently attachment to the lysine residues on its substrates. Unlike the SUMO conjugation pathway in which there is only one known E2 (Ubc9), there are 20-30 different E2 enzymes and hundreds of E3s (Deshaies & Joazeiro, 2009; Pickart & Eddins, 2004). The ubiquitin chains which have more than 4 ubiquitin monomers are recognized by 26S proteasome. Therefore, the ubiquitin attached substrate is degraded by the proteasome and the monomeric ubiquitin is released back to the ubiquitinization cycle by ubiquitin-specific protease (USP) enzymes (Everett, 2013).

ICP0 interacts with USP7 (or HAUSP, herpesvirus-associated ubiquitin-specific protease) to perform several important functions (Daubeuf *et al.*, 2009; Everett *et al.*, 1997; Saffert & Kalejta, 2007; Shih *et al.*, 2007). This interaction protects ICP0 from auto-ubiquitination in vitro, and prevents RING finger-dependent and proteasome-dependent ICP0 degradation during HSV-1 infection in U2OS osteosarcoma cells (Shih *et al.*, 2007). In converse, ICP0 mediates the ubiquitination of USP7 in a RING finger-dependent manner and induces the proteasome-dependent degradation of USP7 during low MOI HSV-1 infection (Saffert & Kalejta, 2007). In the same study, it was also reported that the binding of ICP0 to USP7 is not important for PML degradation that is induced by ICP0. Furthermore, reducing the expression level of USP7 had a negative effect on HSV-1 gene expression at low MOI, probably because this reduced the stability of ICP0 and therefore its rate of accumulation (Saffert & Kalejta, 2007). The ICP0 and USP7 interaction is also involved in innate immune response repression. USP7 was identified to repress the TLR-mediated NF-κB response, and this property is usurped by ICP0 through the interaction with USP7 during HSV-1 infection (Daubeuf *et al.*, 2009).

ICP0 was reported to repress the interferon response to increase HSV-1 infection (Jamieson *et al.*, 1995b; Smith *et al.*, 2011). Melroe *et al* .(2004) demonstrated that HSV-1 infection reduces IFN-β production by monitoring mRNA accumulation and IFN-β

secretion levels. Then ICP0 was identified to prevent IFN regulatory factor-3 (IRF-3) nuclear accumulation, and thereafter reduce the IFN-β production (Jamieson *et al.*, 1995b). ICP0 deletion mutant HSV-1 was reported to induce interferon-stimulated genes (Everett *et al.*, 2010; Preston & Nicholl, 2005). Eidson *et al*. observed that cells infected with HSV-1 mutant d109, which expresses ICP0 but not the other four IE proteins during infection, reduced the interferon-stimulated gene expression and a similar result was also repeated by expressing ICP0 in adenovirus (Smith *et al.*, 2011). In addition, the studies on E3 ligase function of ICP0 and cellular proteasomal activity indicated the above activities are important for inhibiting toll-like receptor 2 (TLR-2) dependent inflammatory responses and NF-κB signalling (van Lint *et al.*, 2010).

ICP0 interacts with PML isoform I via sequences encoded in the isoform I specific exon and it also targets sumoylated PML and Sp100 through its SIM sites. The SIMs of ICP0 are also important for stimulating HSV-1 lytic infection and reactivation from quiescence (Boutell *et al.*, 2011). Furthermore, a recent study on sequences related to SIMs of ICP0 indicated these motifs cooperatively stimulate viral infection (Roizman *et al.*, 2006).

In addition to degrading PML, ICP0 has been found to degrade a number of other cellular proteins, including RNF8, RNF168, CENP-A, CENP-B, CENP-C, CENP-I, CENP-H, CENP-N, USP7, USP7β, IκBα, IFI16 and E2FBP1 (reviewed in (Boutell & Everett, 2013)). This accumulating evidence indicates the multifunctional roles of ICP0 in HSV-1 infection and replication, which require further investigation on this important viral protein.

1.6.2 HCMV proteins that interact with ND10

HCMV is an important member of the β-herpesvirus subfamily. It infects the majority of the human population especially in developing countries. Similar to HSV-1, the infection of HCMV is separated into latent and lytic stages. The lytic infection is further divided into IE, E and L phases (Hancock *et al.*, 2010; Smith *et al.*, 2013). The two viral proteins that have been identified to interact with ND10 members for stimulating viral infection are tegument protein pp71 and IE protein IE1 (Ahn *et al.*, 1998; Ahn & Hayward, 1997; 2000; Baldick *et al.*, 1997; Cantrell & Bresnahan, 2006; Everett *et al.*, 2013a; Gawn & Greaves, 2002; Greaves & Mocarski, 1998; Hofmann *et al.*, 2002; Homer *et al.*, 1999; Hwang & Kalejta, 2007; Ishov *et al.*, 2002; Kang *et al.*, 2006; Kim *et al.*, 2011b; Korioth *et al.*, 1996; Lee *et al.*, 2007; Lee *et al.*, 2004; Lukashchuk & Everett, 2010; Lukashchuk *et al.*, 2008; Tavalai *et al.*, 2011).

1.6.2.1 HCMV IE1 protein

IE1 is a 491 amino acid phosphoprotein that is expressed within the first 2 h of HCMV infection in the host cell nucleus. The predict molecular weight of IE1 is about 64 kDa (Wang & Dasso, 2009), whereas IE1 migrates to 72 kDa in SDS-PAGE (Foster & Jack, 1971; Gareau & Lima, 2010; Torok & Etkin, 2001; Yap *et al.*, 2005), therefore, IE1 was also known as IE72. IE1 is encoded by the UL123 open reading frame which is located at the abundantly transcribed major IE (MIE) region. The MIE also encodes another important IE protein, IE2 (encoded by UL122) (reviewed in (Scherer & Stamminger, 2014)). IE1 and IE2 share the first 85 amino acids that are encoded by exon 2 and exon 3 (Sobol & Mossman, 2011; Stenberg *et al.*, 1985). MIE expression is stimulated by the MIE enhancer promoter (MIEP), which is one of the most efficient transcriptional enhancers known to date (Sheehy *et al.*, 2002; Sheehy *et al.*, 2003; Sokolskaja *et al.*, 2006). The MIEP is repressed by the hDaxx-ATRX complex in ND10, and during the very early stages of infrection tegument protein pp71 interacts with hDaxx-ATRX to release the MIEP from hDaxx-ATRX complex repression (Cantrell & Bresnahan, 2006; Hofmann *et al.*, 2002; Lukashchuk *et al.*, 2008). The functions of pp71 will be introduced in more detail in the next section. IE1 was identified to de-sumoylate PML and Sp100 and interact with hDaxx (Ahn *et al.*, 1998; Ahn & Hayward, 1997; Korioth *et al.*, 1996; Lee *et al.*, 2004; Muller & Dejean, 1999; Reeves *et al.*, 2010; Tavalai *et al.*, 2011). Mutant HCMVs that are deleted for IE1 cannot perform efficient infection of cultured cells at low MOI, but this defect can be rescued in high MOI infections (Gawn & Greaves, 2002; Greaves & Mocarski, 1998).

The IE1 protein structure contains four important regions (Figure 1.16), they are the nuclear localization signal (NLS, aa 1-24) (Lee *et al.*, 2007; Wilkinson *et al.*, 1998), a globular core domain (aa 25-382), a highly acidic region (373-475) (Huh *et al.*, 2008; Paulus *et al.*, 2006) and chromatin tethering domain (CTD) (Shin *et al.*, 2012). In Figure 1.16, two special amino acids are indicated, K450 and L174. K450 was identified to be a sumoylation site of IE1 (Xu *et al.*, 2001) and L174 is essential for the interaction with PML and targeting ND10 (Lee *et al.*, 2004; Muller & Dejean, 1999). The IE1 NLS motif was identified by expressing fusion proteins that combine IE1 residues 1-24 to the N-terminal end of β-galactosidase (Wilkinson *et al.*, 1998) or EGFP (Lee *et al.*, 2007) in human fibroblast cells. The globular core domain is involved in many protein interactions, and this will be introduced in more detail later. The acidic region of IE1 is important for the interaction with STAT2, which involves in the IFN pathway (Huh *et al.*, 2008; Paulus

et al., 2006). The CTD domain was reported to be involved in the interaction between IE1 and core histones, which leads to the association of IE1 with chromosomes during cell mitosis (Lafemina *et al.*, 1989; Reinhardt *et al.*, 2005; Scherer *et al.*, 2014).

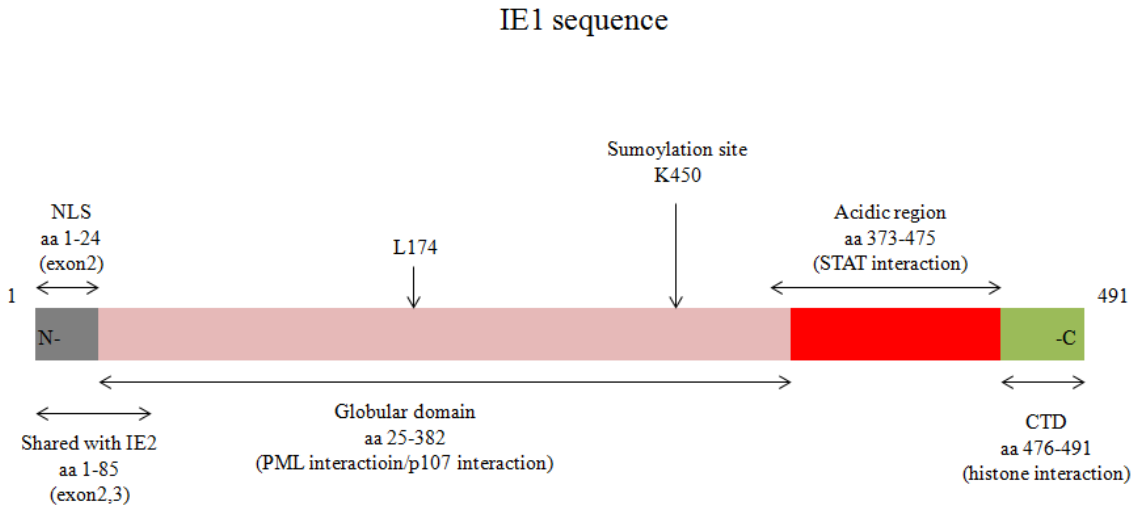

Figure 1.16 The IE1 protein sequence.
Key motifs are indicated as NLS (aa 1-24), globular domain (aa 25-382), acidic region (aa 373-475) and CTD (aa 476-491). Figure is adapted from (Scherer & Stamminger, 2014).

The IE1 globular domain is important for many of the protein's interactions and activities. Sequence deletions within this region were demonstrated to abrogate the transactivation activity of IE1 (Hayhurst *et al.*, 1995; Lee *et al.*, 2004; Malone *et al.*, 1990). The deletion of exon 3 or exon 4 sequences in IE1 was reported to damage the IE1 and IE2 synergistic stimulation of HCMV early promoter activity (Malone *et al.*, 1990). Exon 3 of IE1 was also identified to be important for TATA less DNA polymerase α promoter activation. In the same study, the deletion of aa 105-139 and aa 267-286 were also observed to similarly damage activation of this promoter. In addition, deletion of aa 6-85, which cover exon 2 and exon 3, was observed to abolished nucleus localization of IE1 (Hayhurst *et al.*, 1995). Several mutations within the IE1 globular domain abolished the activities of IE1 on PML de-sumoylation and ND10 disruption. Deletion of aa 132-274, aa 290-320 and aa 232-491 in IE1 were observed to be unable to de-sumoylate PML, whereas a sequence deletion in acidic domain didn't have the same effect (Lee *et al.*, 2004). In the same study, an HCMV-BAC clone containing the aa 290-320 deletion, which is the smallest deletion in the study, was unable to perform infectious activity (Lee *et al.*, 2004). Researchers also tried to identify the sequence region in globular domain that interacts with PML in yeast two-hybrid assays. The results showed that the deletion in globular region, such as deletion of aa 132-274, or in converse, expression the deleted region, such as aa 132-274, all abolished

the interaction with PML (Ahn *et al.*, 1998). The above studies indicated that the globular domain is important for IE1 transactivation activity and interaction with ND10, it was also noticed that this region is very sensitive to mutation (Hayhurst *et al.*, 1995; Lafemina *et al.*, 1989). Therefore, point mutation is a better way than sequence deletion to study the properties of this region.

More recently, Scherer *et al.* reported the 3D structure of the core region of IE1 from rhesus CMV (Scherer *et al.*, 2014), which is highly related to the human CMV protein. The IE1 region responsible for the interaction with PML was identified as a coiled-coil region that is represented by helixes H1, H2 and H3 in Figure 1.17. Furthermore, this globular domain of IE1 was also identified to interact with TRIM5α, which implies the potential mechanism of IE1 interacting with TRIM family proteins through structural mimicking (Scherer *et al.*, 2014).

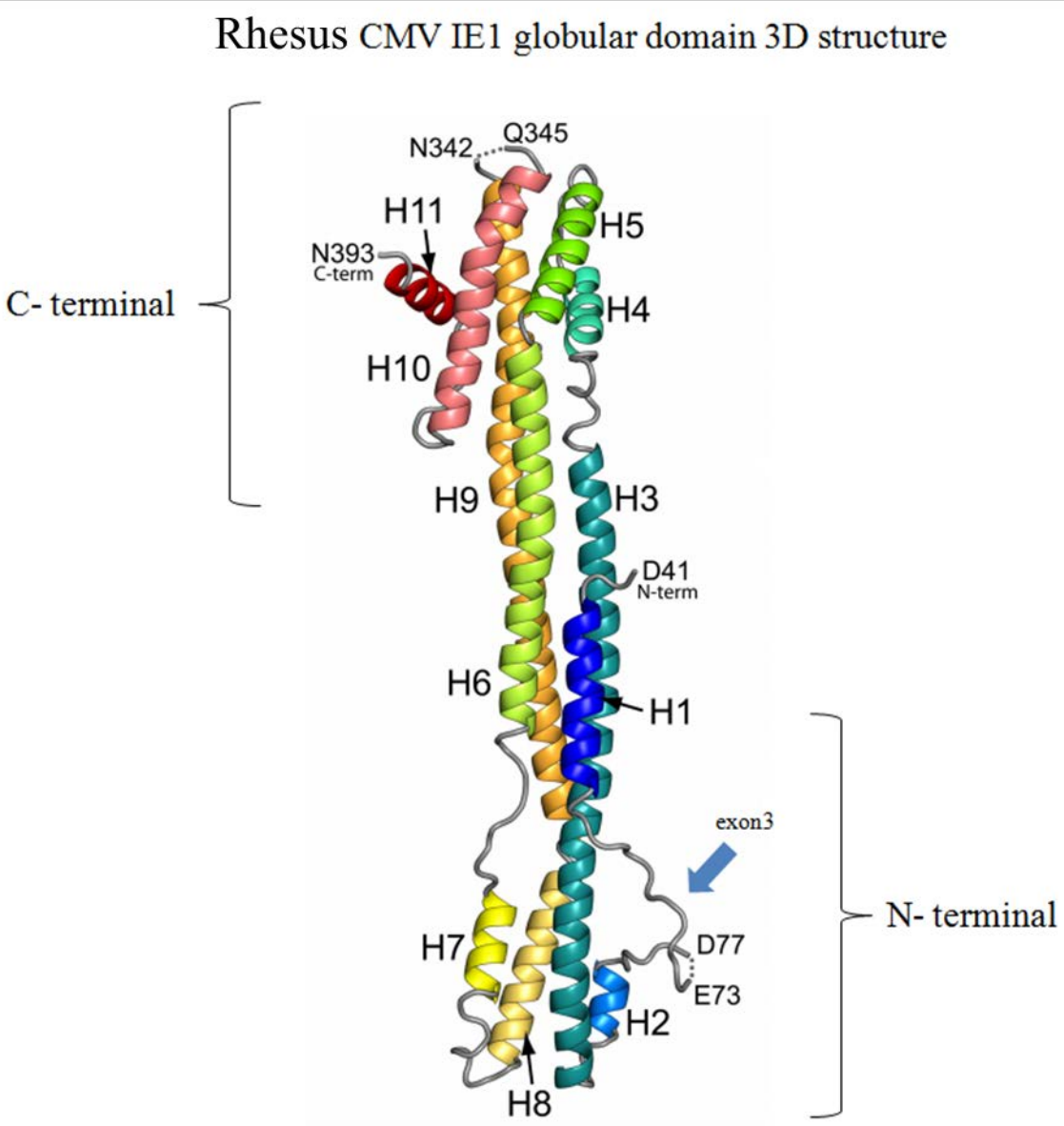

Figure 1.17 3D structure of the rhesus CMV IE1 globular domain.
It represents aa 42-392 of rhesus CMV IE1 which corresponding to aa 27-379 of HCMV IE1. This figure is adapted from (Scherer *et al.*, 2014).

IE1 was reported to repress the IFN response through its acidic domain (Huh *et al.*, 2008; Krauss *et al.*, 2009; Paulus *et al.*, 2006; Reinhardt *et al.*, 2005). Primary HCMV infection stimulates the accumulation of many IFN-stimulated mRNAs, and eventually disarms this antiviral response (Kamitani *et al.*, 1997; Kerscher *et al.*, 2006; Mahajan *et al.*, 1997; Matunis *et al.*, 1996; Scherer & Stamminger, 2014; Shen *et al.*, 1996). By comparing the IFN-responsive transcripts that accumulate to substantially increased levels in IE1 null HCMV and wt HCMV, IE1 was identified to be responsible for this IFN-response repression. The observation was also confirmed using IFN treated IE1 expressing fibroblast cells (Paulus *et al.*, 2006). Meanwhile, the same study also confirmed the colocalization and physical interaction of IE1 with STAT1/STAT2 (Paulus *et al.*, 2006).

There after the acidic domain of IE1 was identified to be responsible for the interaction between IE1 and STAT2, and furthermore, the STAT2 interaction domain of IE1 is separated from the sequences required for ND10 disruption (Huh *et al.*, 2008; Krauss *et al.*, 2009). Even though the sumoylation of IE1 is not essential for IE1 disrupting the ND10 structure and de-sumoylation of PML, it is important for IE1 to interact with STAT2, which further implies the potential role of IE1 in regulating the IFN response (Huh *et al.*, 2008). In addition, IE1 was reported to disrupt inerleukin-6 (IL-6) signalling by sequestering STAT3, which indicated the complexity of IE1 interacting with cellular pathways to regulate HCMV gene expression (Grant *et al.*, 2012).

IE1 disrupts ND10 to stimulate HCMV infection (Ahn *et al.*, 1998; Korioth *et al.*, 1996; Lee *et al.*, 2004; Tavalai *et al.*, 2011; Xu *et al.*, 2001). This process is proteasome independent, which means that IE1 interacts with sumoylated PML and de-sumoylates it instead of degrading PML like ICP0 (Lee *et al.*, 2004; Xu *et al.*, 2001). In the study of Xu *et al.*, the K450 was identified to be essential for IE1 sumoylation, but this point mutation didn't abolish or damage IE1 mediated ND10 disruption (Xu *et al.*, 2001). Other studies on K450 confirmed the dispensable role of this amino acid for IE1 and PML interaction, but the same study observed a reduced HCMV growth kinetics by generating site mutation at this site. These results indicated that the sumoylation of IE1 contributes to efficient HCMV replication (Nevels *et al.*, 2004a). IE1 was also reported to de-sumoylate Sp100 in a similar manner to that found for PML (Tavalai *et al.*, 2011). Four Sp100 isoforms were de-sumoylated and dispersed in the presence of IE1, and furthermore the down regulation of Sp100 by siRNA was shown to stimulate wt HCMV infection, which supported the notion that the interaction between IE1 and Sp100 contributes to the HCMV infection (Tavalai *et al.*, 2011). IE1 directly interacts with hDaxx to activate a putative latency-associated transcript (LUNA) promoter, which indicated the multifunctional role of IE1 during HCMV infection (Reeves *et al.*, 2010).

1.6.2.2 HCMV tegument protein pp71

The tegument protein pp71 from HCMV was originally termed as VP8, which is due to its identification as the eighth largest viral protein (Compton & Feire, 2007). It is encoded by the UL82 gene, and as its name indicates, it is a 71 kDa phosphoprotein (Chee *et al.*, 1990; Wang *et al.*, 2003). The UL82 gene is expressed at the early-late stage of HCMV infection, and the newly synthesised protein also localizes to nucleus (Pickart & Eddins, 2004). Early work identified pp71 as being required to stimulate the MIEP (Liu & Stinski, 1992). More

recently, pp71 was reported to be involved in many viral and cellular process, such as inducing the degradation of hDaxx, degradation of members of the Rb family, stimulating IE gene expression, stimulating cell cycle progression, and MHC expression inhibition (Bresnahan & Shenk, 2000; Homer *et al.*, 1999; Kalejta *et al.*, 2003; Kalejta & Shenk, 2003b; Saffert & Kalejta, 2006; Yongxu Lu, 2014). This thesis will concentrate on the study of interaction between pp71 and hDaxx-ATRX complex in ND10 (Figure 1.6) (Cantrell & Bresnahan, 2006; Lukashchuk *et al.*, 2008).

pp71 was reported to increase HCMV DNA infectivity and expression (Baldick *et al.*, 1997). The co-transfection of HCMV DNA with pp71 expressing plasmids was observed to cause a 30-80 fold increase in plaque forming efficiency (Baldick *et al.*, 1997). pp71 was also observed to increase late gene expression, virus spread and promote plaque development in the same study (Baldick *et al.*, 1997). In addition, Baldick *et al.* also reported that the expression of IE1 and IE2 slightly increased HCMV DNA plaque formation, and IE1 and IE2 together can amplify the pp71 stimulation on HCMV DNA transfection (Baldick *et al.*, 1997). The same study and others reported that pp71 activates the MIEP (Baldick *et al.*, 1997; Liu & Stinski, 1992). The ND10 protein hDaxx, as previous introduced, performs transcriptional repression at ND10, where other viral infection repressors also accumulate. It recruits ATRX to form heterodimeric complex to repress HCMV infection (Hofmann *et al.*, 2002; Ishov *et al.*, 2002; Lukashchuk *et al.*, 2008; McFarlane & Preston, 2011; Saffert & Kalejta, 2006; 2007). Accumulating evidence indicates that the MIEP of the HCMV genome is involved in the assembly of higher order chromatin structure, which represents the cellular regulation of viral genomes (Lecossier *et al.*, 2003; Yu *et al.*, 2003a). hDaxx interacts with histones and histone deacetylase enzymes (HDACs), which are involved in the regulation of chromatin structure (introduced in section 1.5.4.4). Therefore, the study of hDaxx demonstrated its repression of the HCMV MIEP (Woodhall *et al.*, 2006), and pp71 was identified to interact with hDaxx-ATRX complex to rescue the repression of the MIEP (Everett *et al.*, 2013a; Hofmann *et al.*, 2002; Ishov *et al.*, 2002; Lukashchuk *et al.*, 2008; Saffert & Kalejta, 2006). Figure 1.18 shows the pp71 localization and function in HCMV latent and lytic infection. During latent infection, pp71 is located in the cytoplasm, therefore, it is incapable to interact with hDaxx and release the viral genome from repression (Saffert & Kalejta, 2007). In lytic infection, pp71 transfers into the nucleus and displaces ATRX from hDaxx-ATRX complex, and then induces the degradation of hDaxx to release the viral genome from repression (Lukashchuk *et al.*, 2008; Saffert & Kalejta, 2006; 2007).

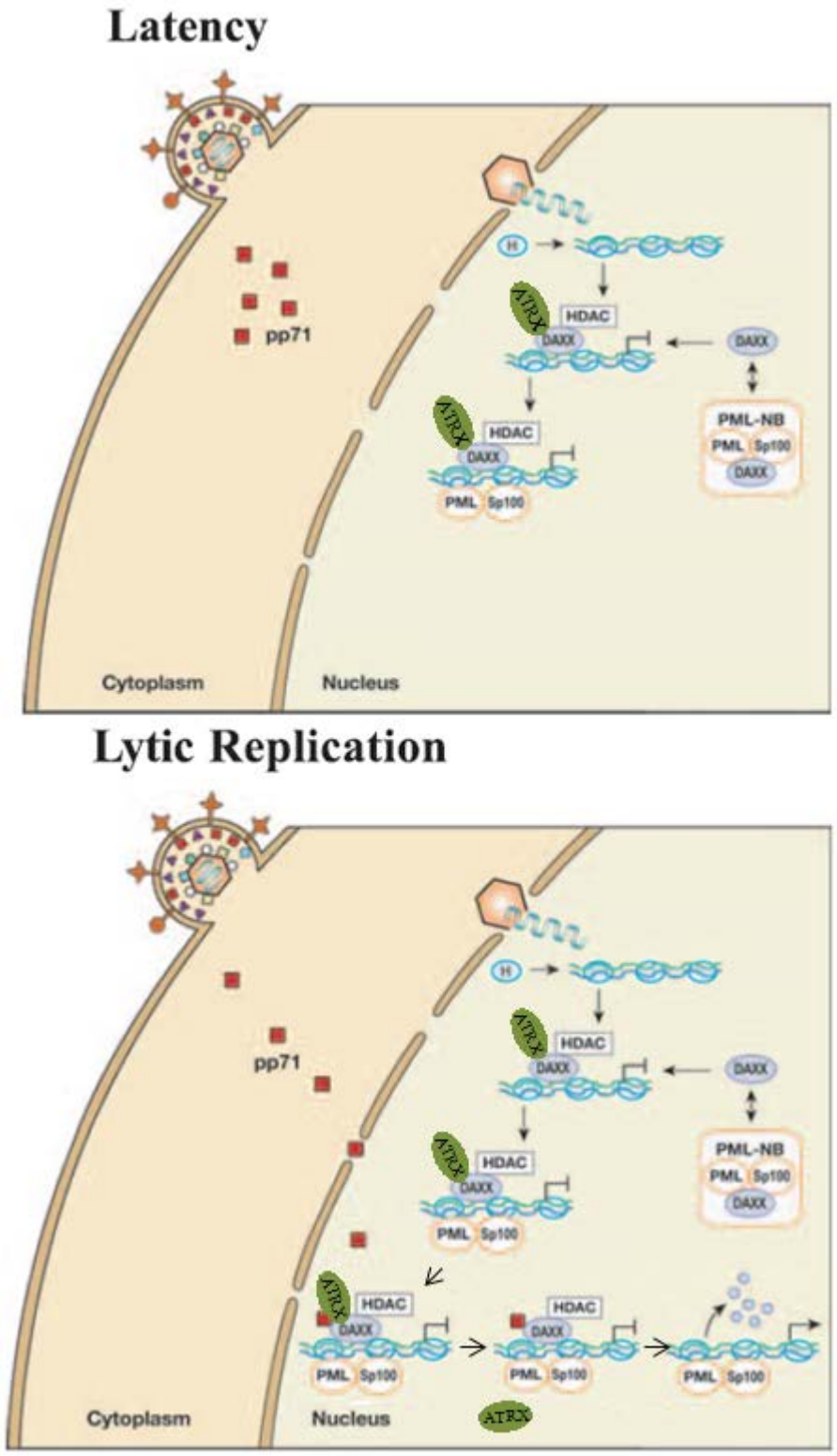

Figure 1.18 pp71 localization and function in HCMV latent and lytic infection.
Figure adapted and modified from (Hayhurst *et al.*, 1995)

Isolation of a pp71 null mutant of HCMV was reported in 2000 (Bresnahan *et al.*, 2000). Meanwhile, Bresnahan and Shenk observed that knock down of UL82 leads to severe impairment of HCMV infection and replication at low MOI, such as 0.01. This damage to HCMV infection efficiency could be at least partially rescued at high MOI infection, such

as 3 pfu per cell (Bresnahan & Shenk, 2000). This observation shares similarities with IE1 null HCMV and ICP0 null HSV-1, which perform impaired infection at low MOI but replicate to similar levels as wt virus in high MOI infections (Greaves & Mocarski, 1998; Sacks & Schaffer, 1987; Stow & Stow, 1986). This might indicate cellular intrinsic resistance to HCMV and HSV-1 infection can be overcome by high doses of virus.

pp71 also involves in the evasion of HCMV from innate immunity. It was reported to limit cell surface MHC class I complex accumulation in glioblastoma cells (Yongxu Lu, 2014). In addition, pp71 induces proteasome-dependent degradation of retinoblastoma family proteins (Rb), which is a tumor suppressor protein that inhibits several major cancers (Kalejta *et al.*, 2003). In this respect, pp71 shares properties with other DNA virus proteins, such as adenovirus E1A, simian virus 40T and papillomavirus E7, on the interaction with Rb, which indicates the similarities of different DNA virus interactions with the host cell.

1.6.3 EBV proteins that interact with ND10

EBV is a member of the γ-herpesvirus subfamily. It has a different genome structure and replication kinetics compared with HSV-1 and HCMV (introduced in section 1.3). ND10 were reported to be dispersed during EBV lytic infection (Bell *et al.*, 2000). Therefore, viral proteins that may be responsible for ND10 interactions attracted researchers' attention. Recently, EBV nuclear antigen 1 (EBNA1), EBNA-leader protein (EBNA-LP) and BNRF1 were reported to interact with ND10 components (Echendu & Ling, 2008; Ling *et al.*, 2005; Sivachandran *et al.*, 2010; Tsai *et al.*, 2014; Tsai *et al.*, 2011). In this section, details about these proteins will be introduced.

1.6.3.1 EBV EBNA1 protein

EBNA1 is one of the six EBV nuclear antigens that may be expressed in latent infections (the other five are EBNA 2 ,3A, 3B, 3C and -LP). It is expressed in most EBV infected cells and EBV associated tumours (Cesarman *et al.*, 1995). EBNA1 is also responsible for the maintenance and replication of the episomal EBV genome (reviewed in (Young & Rickinson, 2004)). The EBNA1 primary structure is separated by a Gly-Ala repeat region in the middle of the sequence. This repeat region was originally suggested to be involved in immune evasion (Guldner *et al.*, 1999), but further studies indicated that it is important for mature protein stabilization (Szostecki *et al.*, 1990; Szostecki *et al.*, 1987).

EBNA1 was reported to disrupt ND10 (Sivachandran *et al.*, 2010; Sivachandran *et al.*, 2008). It was also reported that EBNA1 degrades at least one isoform of PML to stimulate lytic infection (Stenberg *et al.*, 1985). The disruption of ND10 by EBNA1 in latent infection is due to the degradation of PML. This process was indicated to involve USP7 and casein kinase 2 (CK2) (Holowaty *et al.*, 2003; Sivachandran *et al.*, 2010; Sivachandran *et al.*, 2008). USP7 is involved in the regulation of ubiquitination (introduced in section 1.6.1.1) and interacts with another PML interacting protein, ICP0. CK2 regulates several cellular processes by phosphorylation of cellular proteins, including PML (Hatziioannou *et al.*, 2004; Scaglioni *et al.*, 2006). EBNA1 interacts with CK2 to increase phosphorylation of PML, then stimulates the multiubiquitylation and finally degradation of PML (Hatziioannou *et al.*, 2004; Scaglioni *et al.*, 2006; Sivachandran *et al.*, 2010). Further studies demonstrated that each single PML isoform is capable to suppress EBV lytic reactivation. In the same study, PML IV was identified to be the primary degradation target of EBNA1 (Stenberg *et al.*, 1985).

1.6.3.2 EBV EBNA-LP protein

EBV infection of human B cells leads to B cell immortalization (Loret *et al.*, 2008; Yap *et al.*, 2004). This process requires several EBV proteins, and EBNA-LP is one important member of them (Keckesova *et al.*, 2004; Perron *et al.*, 2004). EBNA-LP acts as a coactivator with EBNA2, another nuclear antigen that can be expressed in the latent stage infection, to stimulate the immortalization of B cells (Kalejta, 2008; Kempkes *et al.*, 1995).

Recently, EBNA-LP was reported to interact with Sp100 in ND10 and disperse Sp100 and heterochromatin protein 1α (HP1α) from ND10 (Ling *et al.*, 2005). The interaction between EBNA-LP and Sp100 was confirmed by immunoprecipitation, and immunofluorescence studies indicated the dispersion of Sp100 and HP1α by EBNA-LP. The study also identified that the ND10 targeting domain of Sp100 is the EBNA-LP interaction motif. Furthermore, an Sp100 mutant deleted of the ND10 targeting domain is able to coactivate EBNA2 (Ling *et al.*, 2005). Later studies from the same group reported the Sp100A dimerization domain is highly overlapping with the EBNA-LP interaction domain, which is located within ND10 localization motif. The result also demonstrated that interferon-β is unable to inhibit EBNA-LP function, which indicates the potential function of EBNA-LP in EBV evasion of antiviral responses (Echendu & Ling, 2008).

1.6.3.3 EBV tegument protein BNRF1

BNRF1 is one of the most abundant proteins in the EBV tegument (Johannsen *et al.*, 2004). It contains 1319 amino acids with a molecular weight about 140 kDa (Boshoff & Weiss, 2002b; Stenberg *et al.*, 1985).

The interaction between BNRF1 and hDaxx was reported by (Tsai *et al.*, 2011). The hDaxx interaction motif in BNRF1 was identified as aa 360-600 in this study, which also indicated that BNRF1 co-localizes with hDaxx in ND10 and disperses ATRX to disrupt the hDaxx-ATRX complex (Tsai *et al.*, 2011). Different to pp71, another hDaxx interaction protein, BNRF1 didn't induce the degradation of hDaxx in the above study. More recently, Tsai *et al.* (2014) reported more details about the relationship between BNRF1 and hDaxx-ATRX. They observed that BNRF1 disperses and replaces ATRX in the hDaxx-ATRX complex to form a ternary complex of BNRF1-hDaxx-H3.3-H4. The complex further enhanced EBV gene expression in the early stages of infection (Tsai *et al.*, 2014). The study also compared the difference between ATRX and hDaxx on regulating EBV gene expression. ATRX and hDaxx knock down cell lines were prepared to study the BNRF1 null EBV gene expression. By measuring the immediate early and lytic early protein expression, both ATRX and hDaxx knockdown increased the mutant EBV gene expression. This study further confirmed the repression function of the hDaxx-ATRX complex on EBV.

BNRF1 null EBV was generated and applied in the study of EBV infection on B cells *in vitro* (Feederle *et al.*, 2006). This study didn't observe significant impairment of viral DNA replication and progeny virus production, but the BNRF1 null EBV that was cultivated and collected showed about a 20-fold decrease of infection ability at MOI 10. Furthermore, the study also indicated the importance of BNRF1 for nuclear entry of the EBV genome (Feederle *et al.*, 2006). The above properties of BNRF1 indicated the similarities with pp71. Both proteins interact with the hDaxx-ATRX complex and disperse ATRX from ND10. Mutant viruses that are deleted for BNRF1 or pp71 are able to infect hDaxx and ATRX depleted cells more efficiently (Lukashchuk *et al.*, 2008; Tavalai *et al.*, 2008b; Tsai *et al.*, 2014). Therefore, in chapter 5 in this thesis, the BNRF1 and pp71 were compared in several assays.

1.7 Aims and objectives of the study

Cellular proteins were identified to restrict viral infections. For herpes viruses, ND10 was demonstrated to be important in viral infection regulation. Viral proteins that interact with ND10 to counteract the viral infection restriction were investigated and identified by extensive studies. These viral proteins were considered possible functional counterparts to each other, but only limited information was provided by existing research reports, and little detail about the direct interchangeability among them has been reported (such as ICP0, pp71, IE1, EBNA1, EBNA-LP and BNRF1). The main aim of this project was to analyse the ability of proteins from the different herpesviruses to substitute for each other functionally. Previous work in the Everett lab had demonstrated that the functional requirement of ICP0 to HSV-1 can be largely replaced by the combination of IE1 with pp71. Furthermore, SIM sequence of ICP0 was demonstrated to be essential for the interaction with PML and Sp100. Therefore, the identification of SIMs in IE1 suggested that they could play a role in stimulating ICP0 null HSV-1 infection.

Another important question that rose from previous work is whether ICP0 can replace IE1 or pp71 in HCMV infection. Furthermore, γ herpes viruses are also restricted by ND10 during viral infection. To extend the study, ND10 interaction proteins from EBV were also examined for their ability to stimulate other herpes virus infection, such as HCMV and HSV-1. In the result section, six herpes viral proteins were analysed in ND10 interaction and complementation of mutant herpes viruses that deleted relevant viral genomes. Therefore, the presentation of the results is introduced in three parts, which were concentrated in: (1) Complementation of ICP0 null HSV-1 infection by IE1 and IE1 mutants. (2) Complementation of IE1 null HCMV and pp71 null HCMV by ICP0. (3) Stimulation of ICP0 null HSV-1 and pp71 null HCMV by EBV proteins which had been identified to interact with ND10. To investigate more detail about IE1, several IE1 mutants were prepared in this study based on IE1 sequences analysis.

The data presented in this study provided evidence of the interchangeable role of ND10 interaction proteins from different herpes virus subfamilies. It was also identified that IE1 has HCMV specific functions that ICP0 cannot replace. Furthermore, a HCMV specific region of IE1 was identified in this study. But the mechanism of how this HCMV specific region in IE1 interact with other viral proteins and its functions in other viral and cellular processes are still required further investigation.

2 Materials and Methods

2.1 Materials

2.1.1 Cells

All cells were grown in a humidified incubator at 37 ^{o}C in the presence of 5% CO_2.

2.1.1.1 HEK 293T cells

Originally from HEK 293 cells (Human Embryonic Kidney 293 cells; (Ahn *et al.*, 1998)), these cells (obtained from BD Biosciences) additionally express the Large T antigen of SV40, which can bind to several proteins that inhibit the cell cycle. HEK 293T cells also have neomycin resistance as a result of introducing the Large T antigen into them (DuBridge *et al.*, 1987).

2.1.1.2 HepaRG (HA) cells

This cell line was derived from differentiated human hepatoma cells (Gripon *et al.*, 2002). It can differentiate into two distinct liver cell types. Half the cells differentiate into hepatocyte-like cells and another half of the cells differentiate into biliary-like cells. For the experiments in this thesis they were used without differentiation because they can be readily manipulated while, unlike many permanent laboratory cell lines, they restrict ICP0-null mutant HSV-1 efficiently (Everett *et al.*, 2008).

2.1.1.3 HA-TetR cells

HepaRG cells transduced with a lentivirus vector expressing the EGFPnlsTetR fusion protein and neomycin (G418) resistance (Everett *et al.*, 2009).

2.1.1.4 HFT Cells

This cell line is an immortalized version of limited passage diploid human fibroblasts, constructed by the method of (Smith *et al.*, 2013) and provided by Dr Chris Boutell.

2.1.2 Cell culture media

2.1.2.1 DMEM

Dulbecco's modified Eagle's medium (DMEM) was purchased from Life Technologies (DMEM, high glucose, pyruvate, Catalogue number: 41966-029, 500ml). It was supplemented with 10% foetal calf serum and 100 U/ml penicillin, 100µg/ml streptomycin, and was used for the growth of HEK 293T and HFT cells.

2.1.2.2 William's Medium E

William's Medium E is a commercial product from Life Technologies (William's E Medium, no glutamine, Catalogue number: 22551-022) and was used for the growth of HepaRG cells. It was supplemented with 5 ml L-Glutamine-200 mM (100X, Life Technologies, Catalogue number: 25030-24), 10% foetal calf serum (Life Technologies, Catalogue number: 10270-106), 100 U/ml penicillin, 100 µg/ml streptomycin (Life Technologies, Catalogue number: 15140-122), 5 µg/ml insulin and 0.5 µM hydrocortisone. The insulin and hydrocortisone maintain the cells in the undifferentiated condition (Gripon *et al.*, 2002).

2.1.2.3 Cell culture solutions

Versene: This medium is for washing cells before trypsin digestion. It is made of 0.6 mM EDTA with 0.002% phenol red in phosphate buffered saline (PBS).

Trypsin: 10X Trypsin solution was purchased from Life Technologies (Sigma, Catalogue number: T4549-100 ml) and was diluted 1 in 10 in Versene before use.

2.1.3 Yeast strains

2.1.3.1 AH109 yeast strain

The yeast 2 hybrid assay used in the work presented in this thesis was based on the Matchmaker 3 system (Clontech). The yeast strain AH109 uses three reporter genes to eliminate false positive results. These are genes *ADE2*, *HIS3* and *MEL1* (or *lacZ*) which are under the control of promoters that incorporate GAL4 upstream activating sequences

(UAS) and TATA boxes, and thus are only expressed in cells expressing GAL4 DNA binding domain and activation domain fusion proteins that interact.

2.1.3.2 Y187 yeast strain

Yeast strain Y187 contains the lacZ reporter gene under control of a promoter the GAL1 UAS. The yeast strains AH109 and Y187 were purchased from Clontech.

2.1.4 Viruses

2.1.4.1 HSV-1 strains

The wild type (wt) HSV-1 strain used in this laboratory is strain 17 syn+, known as 17+ for short (Hollenbach *et al.*, 2002). The ICP0 deletion mutant derivative of 17+ is dl1403 (Stow & Stow, 1986). Mutant dl1403/CMV lacZ (herein termed ΔICP0) includes the lacZ gene under the control of HCMV promoter/enhancer and was kindly provided by Dr Chris Preston. This virus can be titrated conveniently by detection of β-galactosidase activity (blue plaque assay, section 2.2.5.2) (Jamieson *et al.*, 1995a). The ΔICP0 HSV-1 virus stocks were grown in BHK cells and titrated on U2OS cells, and aliquots for use in the work for this thesis were provided by Anne Orr.

2.1.4.2 HCMV strains

HCMV strain Towne wt (TNwt):

TNwt was a gift from Dr. Michael Nevels. TNwt was derived from a bacmid of strain Towne, and it includes a SV40-driven EGFP marker gene inserted into a non-essential region of the Us segment of the viral genome (Marchini *et al.*, 2001). The TNwt used in this thesis was grown and titrated on HFT.IE1 cells (see below).

AD169:

This virus is an alternative and commonly used laboratory HCMV strain (Chee *et al.*, 1990; Rowe *et al.*, 1956). AD169 stocks used in this thesis were cultivated and titrated in HFT.IE1 expression cells. In this way, the virus titre increased and cultivation time could be reduced to 7 days.

HCMV stain TBE40 wt (TBwt):

TBwt, also a laboratory strain but more closely related to clinical HCMV strains, with fewer deletions and other mutations compared to strains Towne and AD169, was also a gift from Dr. Michael Nevels (Bernardi & Pandolfi, 2007).

IE1 deleted mutant HCMV strains:

A derivative of TNwt with a deletion of the IE1 specific coding sequences (TNdlIE1) was a gift from Dr. Michael Nevels and it was derived from the same bacmid as TNwt (Knoblach *et al.*, 2011). The TNdlIE1 used in this study was grown and titrated on HFT.IE1 cells. The TBE40 IE1 deletion mutant TBdlIE1 and its revertant version TBrvIE1were gifts from Dr. Michael Nevels (Zalckvar *et al.*, 2013). Stocks of these viruses were titrated on HFT-IE1 cells.

pp71 deleted mutant HCMV:
AD169subUL82 (herein named Δpp71) was kindly provided by Steven McFarlane (Chris Boutell's laboratory). It was originally made in Thomas Shenk's laboratory by deleting the UL82 gene which encodes the pp71 protein in AD169 genome. This mutant also expresses enhanced green fluorescent protein as a marker (Bresnahan *et al.*, 2000).

2.1.5 Bacteria

2.1.5.1 DH5α Chemically Competent *E. coli*

This is a commercial product from Invitrogen (Catalogue Number: 18265-017). These bacteria were used for routine plasmid transformation, DNA manipulation and for large scale plasmid preparation.

2.1.5.2 Stbl3 Chemically Competent *E. coli*

Commercial product of Invitrogen (Catalogue Number: C7373-03). These bacteria were necessary for the construction of lentivirus vectors expressing IE1 as such plasmids were very unstable in DH5α bacteria.

2.1.6 Plasmids

Table 2.2 lists the lentiviral vector plasmids used in this study. Where a reference is given, the plasmid was provided by others for use in this work (usually from the group of Professor R.D. Everett). Those for which notes on the construction are given in the 'source' column were constructed by the author during the course of this work. Further details on the construction, structure and functions of these plasmids are given in the relevant results chapters.

Table 2.1 List of plasmids used in this study.

Plasmid	Source	Application
pLKOneo.EGFPnlsTetR	(Everett *et al.*, 2013a)	Expresses EGFPnlsTetR in target cell line.
pLDT.IE1	(Everett *et al.*, 2013a)	Expresses IE1 in target cell line in an inducible manner. The transduced cells were selected by puromycin.
pLDT.IE1.YL1-YL7	Replacement of the wt IE1 sequence in pLDT.IE1 by IE1 mutant segments including mutations YL1 to YL7. Constructed by the author (Everett *et al.*, 2013a).	Each expresses an IE1 YL series mutant protein in target cell line in an inducible manner.
pLDT.IE1 K450R	Replacement of the wt IE1 sequence in pLDT.IE1 by IE1 mutant segment K450R. Constructed by the author (Everett *et al.*, 2013a).	Expresses IE1 mutant K450R in target cell line in an inducible manner.
pLDT.myc.pp71	(Everett *et al.*, 2013a)	Expresses myc tagged pp71 in target cell line in an inducible manner. The transduced cells were selected by blasticidin.
pLDT.myc.EBNA1	The EBNA1 sequence was a kind gift from Dr. Joanna Wilson. A myc tag is attached on the 5' end of the EBNA1 DNA sequence	Express myc tagged EBNA1 in target cell line in an inducible manner. The

	(Cerboni *et al.*, 2000). Constructed by the author.	transduced cells were selected by puromycin.
pLDT.FLAG.BNRF1.puro	Provided by the Everett laboratory (unpublished). The FLAG-tagged BNRF1 sequence was provided by Paul Lieberman (Tsai *et al.*, 2011). The BNRF1 coding sequence was inserted into a pLDT lentivirus vector.	Expresses FLAG tagged BNRF1 in target cell line in an inducible manner. The transduced cells were selected by puromycin.
pLDT.FLAG.BNRF1.bla	Replacement of the myc.pp71 sequence in pLDT.myc.pp71 by the FLAG.BNRF1 segment. Constructed by the author.	Expresses FLAG tagged BNRF1 in target cell line in an inducible manner. The transduced cells were selected by blasticidin.
pLDT.FLAG.EBNA-LP.neo	The FLAG tagged EBNA-LP sequence was a kind gift from Dr. Paul D. Ling (Ling *et al.*, 2005). This sequence was inserted into an pLDT vector expressing neomycin (G418) resistance. Constructed by the author.	Expresses FLAG tagged EBNA-LP in target cell line in an inducible manner. The transduced cells were selected by neomycin.
pLDT.EYFP.TetR.IRES.P	This plasmid was gift from Dr. Chris Boutell. The backbone is termed a 'single inducible vector' as it incorporates both the inducible gene of interest and expression of the TetR repressor. Puromycin resistance is expressed from the TetR transcription unit by an internal ribosome entry site (IRES).	Expresses EYFP in target cell line in an inducible manner after a single transduction. The transduced cells were selected by puromycin.
pLDT.ICP0.TetR.IRES.P	The EYFP segment in pLDT.EYFP.TetR.IRES.P was replaced by the cICP0 sequence. Constructed by the author.	Expresses ICP0 in target cell line in a single inducible manner.
pLDT.IE1.TetR.IRES.P	The EYFP segment in pLDT.EYFP.TetR.IRES.P was replaced by wt IE1 sequence. Constructed by the author.	Expresses IE1 in target cell line in a single inducible manner.
pLDT.IE1.YL1.TetR.IRES.P and related plasmids incorporating the YL2, YL3, YL4, YL7 and K450R mutant	EYFP segment in pLDT.EYFP.TetR.IRES.P was replaced by IE1 YL and K450R mutant segments.	Express IE1 mutant proteins in target cell line in a single inducible

forms of IE1.	Constructed by the author.	manner.
pLDT.myc.EBNA1.TetR.IRES.P	A single inducible vector version for the expression of myc tagged EBN1, derived from the mycEBNA1 vector described above. Constructed by the author.	Expresses myc tagged EBNA1 in target cell line in a single inducible manner. The transduced cells were selected by puromycin.
pLKO.shPML1	(Everett *et al.*, 2008)	Expresses an shRNA that targets all isoforms of PML. The transduced cells were selected by puromycin.
pLNGY.PML.I	(Cuchet *et al.*, 2011)	Expresses EYFP tagged PML isoform I in target cell line. The transduced cells were selected by neomycin.
pLBG.myc.PML.VI	Constructed by the author.	Express myc tagged PML isoform VI in target cell line. The competent cells were selected by blasticidin.
pCMV.DR.8.91	A gift from Prof. Didier Trono	Expresses the lentivirus helper functions.
pVSV-G	BD Biosciences	Expresses G protein of the Vesicular Stomatitis Virus (VSV-G) envelope gene.
pGBK.ICP0	(Cuchet-Lourenco *et al.*, 2012)	Used as a vector backbone for expressing BD fusion proteins in yeast.
pGBK.IE1	The cICP0 sequence in pGBK.ICP0 was replaced by the IE1 sequence. Constructed by the author.	Expresses a BD-IE1 fusion protein in yeast cells.
pGBK.IE1.YL3, YL4 and K450R	The cICP0 sequence in pGBK.ICP0 was replaced by IE1 YL3, YL4 or K450R sequences. Constructed by the author.	Expresses BD-IE1 YL3, YL4 and K450R fusion proteins in yeast cells.

pGBK.PML.I	(Cuchet-Lourenco *et al.*, 2012)	Expresses a BD-PML isoform I fusion protein in yeast cells.
pGBK.SUMO1	(Vanni *et al.*, 2012)	Expresses a BD-SUMO1 fusion protein in yeast cells.
pGAD.PML.I	Constructed by Delphine Cuchet.	Expresses an AD-PML.I fusion protein in yeast cells.
pGAD.PML.VI	Constructed by Delphine Cuchet.	Expresses an AD-PML.VI fusion protein in yeast cells.
pGAD.PML.I ΔBB1, ΔBB2, ΔCC, ΔRING	The PML.I ΔBB1, ΔBB2, ΔCC, and ΔRING mutations in PML.I lentivirus vector plasmids (Cuchet *et al.*, 2011) were inserted into pGAD.PML.I. Constructed by the author.	Express AD-PML.I ΔBB1, ΔBB2, ΔCC, ΔRING fusion proteins in yeast cells.
pGAD.SUMO1	(Vanni *et al.*, 2012)	Expresses an AD-SUMO1 fusion protein in yeast cells.
pGAD.empty	Clontech	Negative control
pGBK.empty	Clontech	Negative control

2.1.7 Primers

All primers were purchased from Sigma-Aldrich. Primers were provided as lyophilised solids and re-suspended in distilled water to a final concentration of 100 µM.

Table 2.2 List of primers.

Primer	Sequence	Application
IE1 YL1 Forward	5'-TCCTCTGCCAAGAGAAAGATGGACCCTGATAATGGTGACGGGGGCCCTTCCTCCAAGGTG-3'	Generating IE1 YL1 mutant vector
IE1 YL1 Reverse	5'-GCGCAGAATTCTTACTGGTCAGCCTTGCTTC-3'	Generating IE1 YL1 mutant vector
IE1 YL2 Forward	5'-CAGCTGAGTCTGGGAGCACCGGCAGCTCCAGAGTTGGCCGAA-3'	Generating IE1 YL2 mutant vector
IE1 YL2 Reverse	5'-TTCGGCCAACTCTGGAGCTGCCGGTGCTCCCAGACTCAGCTG-3'	Generating IE1 YL2 mutant vector
IE1 YL3 Forward	5'-CAGAATGCCGGAGATGGCGGAGATAAGGTTCAT-3'	Generating IE1 YL3 mutant vector
IE1 YL3 Reverse	5'-AACCTTATCTCCGCCATCTCCGGCATTCTGCAA-3'	Generating IE1 YL3 mutant vector
IE1 YL4 Forward	5'-CTGTGCTGCGGTGGCGGAGAGGAGACTAGT-3'	Generating IE1 YL4 mutant cell line
IE1 YL4 Reverse	5'-AGTCTCCTCTCCGCCACCGCAGCACAGCAC-3'	Generating IE1 YL4 mutant vector
IE1 YL5 Forward	5'-TGCTGCTATGTCTTAGCGGCGACTAGTGTGATGCTG -3'	Generating IE1 YL5 mutant vector
IE1 YL5 Reverse	5'-CTCCTCAGCTCCGGCTCCTAGGTCATCCAC-3'	Generating IE1 YL5 mutant vector
IE1 YL6 Forward	5'-CTGTCCTCAGGAGGTGGGGCTGAGAACAGT-3'	Generating IE1 YL6 mutant vector
IE1 YL6 Reverse	5'-GTTCTCAGCCCCACCTCCTGAGGACAGAGG-3'	Generating IE1 YL6 mutant vector
IE1 YL7 Forward	5'-ATATAGTCGACCCCATGGAGTCCTCTGCCAAGAG 3'	Generating IE1 YL7 mutant vector
IE1 YL7 Reverse	5'-GCGCAGAATTCTTAGCTCTTGCCTCCAGAGGCGGTGGGTTCCTC-3'	Generating IE1 YL7 mutant vector
IE1 K450R Forward	5'-GACACTGTGTCTGTCAGATCTGAGCCAGTGTCTG-3'	Generating IE1 K450R mutant cell line
IE1 K450R Reverse	5'-CAGACACTGGCTCAGATCTGACAGACACAGTGTC-3'	Generating IE1 K450R mutant vector

myc-EBNA1 Forward	5'-CGTGGGTCGACCCATGGCATCAATGCAGAAGCTGATCTCAGAGGAGGACCTGCTTATGGCCATGTCTGACGAGGGGCCAGGTACAGGACCTGGAAATGGC-3'	Generating myc tagged EBNA1 vector
myc-EBNA1 Reverse	5'-CGTGAGAATTCTCACTCCTGCCCTTCCTCACCCTCATCTCCATCACC-3'	Generating myc tagged EBNA1 vector

2.1.8 Antibodies

2.1.8.1 Primary Antibodies

Table 2.3 List of primary antibodies

Antibody	Origin	Application	Source
IE1 (1B12)	Mouse	IF/WB	Thomas Shenk lab (Zhu *et al.*, 1995)
IE1+ IE2 (E13)	Mouse	IF/WB	Serotec
IE2 (5A8.2)	Mouse	IF/WB	Millipore
ICP0 (11060)	Mouse	IF/WB	(Everett *et al.*, 1993)
pp71 (UL82)	Mouse	WB	Thomas Shenk lab (Bresnahan & Shenk, 2000)
myc (9E10)	Mouse	IF/WB	Santa Cruz
myc (Ab9106)	Rabbit	IF/WB	Abcam
FLAG (M2)	Mouse	IF/WB	SIGMA
pp52 (UL44, Sc-56971)	Mouse	IF/WB	Santa Cruz
pp28 (5C3)	Mouse	IF/WB	Abcam
EGFP (ab290)	Rabbit	WB	Abcam
PML (A301-167A)	Rabbit	IF/WB	Bethyl Laboratories
PML (5E10)	Mouse	WB	Gift from Roel van Driel (Stuurman *et al.*, 1992).
Tubulin (DM1A)	Mouse	WB	Abcam

2.1.8.2 Secondary antibodies

Table 2.4 List of secondary antibodies

Antibody	Application	Source
Sheep anti-mouse IgG hrp conjugated antibody (A4416)	WB	Sigma
Goat anti-rabbit IgG hrp conjugated antibody (A0545)	WB	Sigma
Donkey anti-mouse Alexa 555 conjugated antibody (A31570)	IF	Invitrogen
Goat anti-rabbit Alexa 633 conjugated antibody (A21071)	IF	Invitrogen
Goat anti-mouse Alexa 633 conjugated antibody (A21050)	IF	Invitrogen
Donkey anti-rabbit Alexa 555 conjugated antibody (A31572)	IF	Invitrogen

2.1.9 Restriction endonucleases

All restriction endonucleases and the respective buffers in this study were ordered from New England Biolabs.

2.1.10 General Solutions

Lauria-Bertani (LB) broth: 10 g NaCl, 10 g Bactopeptone, 5 g yeast extract in 1 L water, pH 7.5

Phosphate buffered saline (PBS): 170 mM NaCl, 3.4 mM KCl, 10 mM Na_2HPO_4, 1.8 mM KH_2PO_4, pH 7.2

SDS-PAGE loading buffer: 50 mM Tris-HCl, pH 6.8, 2.24% SDS (w/v), 11.1% (v/v) glycerol, 666.6 mM β-mercaptoethanol

STET: 8% (w/v) sucrose, 5% (v/v) Triton-X 100, 50 mM EDTA pH 8.0, 50 mM Tris-HCl pH 8.0

40×TAE: 40 mM Tris, 1 mM EDTA, 5 mM sodium acetate, glacial acetic acid to pH 7.6

Tris-EDTA (TE): 10 mM Tris-HCl, pH 8.0, 1 mM EDTA

Versene: 0.6 mM EDTA in PBS, 0.02% phenol red

X-gal solution: 5 mM potassium ferrocyanide, 5 mM potassium ferricyanide, 2 mM magnesium chloride, 0.01% NP 40, in PBS; X-gal in DMSO (40 mg/ml) added to a final concentration of 2.4 mM

2.2 Methods

2.2.1 Polymerase chain reaction (PCR)

Polymerase chain reaction (PCR) was used for making mutations in the IE1 sequence, using Phusion DNA polymerase (Thermo Scientific, catalogue number: F-530S) and buffers supplied by the manufacturer.

2.2.1.1 Standard PCR reaction mixtures

Standard PCR mixtures were prepared as follows:

Table 2.5 Reagents for PCR

Reagent	Quantity
Template DNA	50 ng
Primer 1	1 µl (10 µM stock)
Primer 2	1 µl (10 µM stock)
5x HF Phusion Buffer (Thermo Scientific, catalogue number: F-518)	10µl
dNTPs (New England Biolabs, catalogue number: N0447S)	1 µl
Phusion polymerase	1 µl
dH_2O	to 50 µl

2.2.1.2 Standard PCR cycling conditions

Standard PCR cycling programmes were set up as follows:

Initial denaturation at 98℃ for 30 seconds

Cycle number set up for 25-30 times repeat of the following:

98℃ for 30 seconds

60℃ for 30 seconds (this temperature was adjusted for annealing temperatures of primers used)

72℃ for 30 seconds

Final elongation:

72℃ for 5 min

Holding process:

4℃ hold

2.2.1.3 Purification of PCR products

PCR products were isolated using 1.2% agarose gels, then purified using a commercial PCR fragment purification kit (Dundee Cell Products).

2.2.1.4 PCR fragment digestions

Purified PCR fragments were treated by restriction endonuclease digestion to create suitable 5' - and 3' ends for ligation.

DNA fragment digestion conditions:

Table 2.6 Reagents for DNA fragment digestion

Reagent	Quantity
PCR fragment	5-10 µl (depending on the concentration of fragment)
Restriction endonuclease	1 µl
10X restriction endonuclease buffer (New England Biolabs)	3 µl
dH_2O	to 30 µl

The DNA digestion mixture was incubated at 37℃ for 1-2 h, and then the fragments were separated and isolated by DNA agarose electrophoresis. The fragments were purified again using the commercial PCR fragment purification kit.

2.2.1.5 PCR fragment ligations

The PCR products and vector fragments for ligation were isolated by 1.2% DNA agarose gel electrophoresis and purified using commercial DNA purification columns. Generally, vector fragments were prepared by digesting 10 µg of plasmid DNA. Purified DNA segments were eluted from the columns in 30 µl elution buffer.

The PCR segments were digested by the same enzymes used to cut the plasmid vectors, by virtue of the appropriate recognition sequences within the primers used to generate the PCR fragments.

Ligation mixtures:

Table 2.7 Reagents for DNA ligation

Reagent	Quantity
PCR fragment (enzyme digested)	5 µl
Plasmid vector fragment	5 µl
10x Ligase buffer (New England Biolabs, Catalogue number: B0202S)	3 µl
T4 DNA Ligase (New England Biolabs, Catalogue number: M0202S)	1 µl
dH_2O	to 30 µl

Control ligation mixture:

Table 2.8 Reagents for DNA ligation control

Reagent	Quantity
Plasmid vector	5 µl
10x Ligase buffer (New England Biolabs, Catalogue number: B0202S)	3 µl
T4 DNA Ligase (New England Biolabs, Catalogue number: M0202S)	1 µl
dH_2O	to 30 µl

The ligations were done at RT for 8 h or overnight.

2.2.2 DNA manipulation

2.2.2.1 Small scale DNA purification

Boiling method

This method is a home-made plasmid extraction method for small scale *E. coli* cultures. Plasmid quality obtained by this method is not as clean as that using a commercial kit, but it is quicker and cheaper. This method is suitable for testing ligation products purified from the transformed colonies.

Transformed *E. coli* cultures were plated on selective plates and incubated at 37℃ overnight. The following day, single colonies were inoculated into 5 ml liquid broth containing appropriate selection antibiotics, then incubated at 37℃ overnight. On the next day, 1.3 ml of the culture was transferred into 1.5 ml Eppendorf tubes, and then the bacteria were pelleted by centifugation at 13,000 rpm for 1 min. If growth of the cultures

was poor (often the case with lentiviral vector plasmids) a pipette was used to take out the supernatant and add an extra 1.3 ml of the *E. coli* culture medium, and the centrifugation was repeated. The supernatant was removed, then 200 µl STET (10 mM Tris-HCl pH 8.0, 1 mM EDTA, 100 mM NaCl, and 5% Triton™ X-100 (v/v)) buffer was added. The pellet was vortexed to re-suspend the bacteria, then 5 µl of 10 mg/ml lysozyme (freshly made, dissolved in STET buffer) was added to the re-suspended bacteria, then vortexed to mix. The Eppendorf tubes were immediately transferred into a boiling water bath for 50 sec, then the mixture was centrifuged at 13,000 rpm for 15 – 30 min. 180µl of the supernatant was transferred to a new Eppendorf tube, supplementing the volume with fresh STET if necessary, then 165 µl of isopropanol was added. After vortexing, the mixture was centrifuged at 13,000 rpm for 2 min. At this stage, the precipitate was usually visible in the bottom or on the sides of the Eppendorf tube. The supernatant was removed, and then 200 µl of 80% ethanol was added before another centrifugation for 30 sec. The supernatant was removed and the tube centrifuged for another 30 sec so that the last of the supernatant could be removed. The pellet was air dried then dissolved in 30 µl dH2O or TE buffer. This is an economical method to test DNA ligations to identify the required clone. The DNA purified by this method is not suitable for transformation and needed to be further purified using the commercial PCR fragment isolation kit for further application.

2.2.2.2 Large scale DNA purification

Once suitable clones were identified, large scale plasmid DNA preparations were made by inoculating a single colony from a fresh transformation plate into 300 ml liquid bacterial medium containing selection antibiotics. After incubation at 37℃ with shaking (180 rpm) for 12 h or overnight, a Plasmid Xtra Midiprep Kit (MACHEREY-NAGEL, ref. 740410.100) was used for plasmid extraction. All protocols were according to the manufacturer's instructions.

2.2.2.3 DNA sequencing

DNA sequencing in this study was performed by the Dundee Sequencing Service. Primers used for DNA sequencing were purchased from Sigma-Aldrich. All protocols for plasmid and primer preparation were as advised by Dundee Sequencing Service.

2.2.2.4 DNA agarose gel electrophoresis

DNA segments were separated using electrophoresis on 1% or 1.2% (w/v) agarose gels in 1 X TBE buffer) at 100 V. DNA gels were stained by incubation in ethidium bromide (EB, 0.5 µg/ml) for 30 min, then gels were photographed using a GelDoc (BioRad) imager under UV light. For DNA fragment isolation, the gels were examined using a long wave UV transilluminor, then the DNA segments were cut from the gel and purified using commercial kits (Dundee Cell Products).

2.2.2.5 Bacterial transformation

Commercial chemically competent DH5α and Stbl3 *E.coli* strains were aliquoted and stored in a -70℃ freezer to maintain viability. Before transformation, the competent cells were thawed on ice for 15 mins and then 3-5 µl of ligation mixture (or 0.5 µg of plasmid DNA) was added to 30 µl competent cells. The plasmid was incubated with the cells on ice for 30 min, then the mixture was heat shocked for 45 sec in a 42℃ water bath before returning to ice for 1 min. Then 300 µl of liquid bacteria medium was added to the heat-shocked cells which were then incubated at 37℃ with shaking (200 rpm). After 1 h of incubation, the whole culture was plated on bacterial agar plates with selection antibiotics, which were then incubated at 37℃ overnight.

2.2.3 Generating lentivirus transduced cell lines

2.2.3.1 Transfection of HEK-293T cells

$1.5x10^6$ HEK-293T cells were seeded into 60 mm plates with 4 ml DMEM medium (DMEM with 10% FCS, 0.1% P/S). On the next day, the HEK-293T cells were 50-70% confluent and ready for transfection.

The production of lentivirus requires co-transfection of three plasmids as follows: a pLKO-based lentivirus vector plasmid, pVSV-G to provide the envelope protein, and pCMV-DR8.91 to provide lentiviral helper functions. 3µg of each plasmid was used for each transfection.

In the first step of transfection, a mixture of 8 µl Lipofectamine PLUS reagent, 250 µl serum-free DMEM medium and 3µg of each plasmid was made then incubated at RT for 15 min. In the second step, 12 µl lipofectamine reagents was added to 250 ul of serum-free DMEM, mixed, and then added to the plasmid-containing mixture that was made in the first step. This was then incubated at RT for 15 min. During the incubation time in the

second step, the HEK-293T cells that had been seeded one day before were washed with serum-free DMEM medium twice. In the third step of the transfection, 850 µl serum-free DMEM medium was added to each DNA/PLUS/lipofectamine mixture. Then this final mixture was added to the pre-washed HEK-293T cells. After incubation of the cells for 3 h at 37℃, 3 ml DMEM complete medium with 30% FCS was added to each plate and incubated at 37℃ overnight or 12 h.

After this primary incubation, the plasmids should have gained entry into the HEK-293T cells. The mixture was removed and replaced with 4 ml of fresh DMEM medium containing 30% FCS.

24h later, the supernatant was collected and another 4 ml of fresh DMEM medium containing 30% FCS was added to the cells. On the next day, the supernatant was collected again and added to the previously collected medium. This lentivirus containing medium was centrifuged at 1500 rpm (Sorvall bench top centrifuge) and then filtered through a 45 micron sterile filter to remove debris and dead cells. The lentivirus supernatant was then ready for use, or alternatively it could be stored at 4℃ for 24 h before use.

2.2.3.2 Lentivirus infection

HepaRG or HFT cells were set up the day before lentivirus infection at $6x10^5$ cells in each 60 mm dish. When infecting the cells, 1.5 ml lentivirus containing medium was added to each plate with 1.5 µL polybrene at 5 µg/ml. The plate was then agitated every 10 min at 37℃ (for giving a better lentivirus attachment) and after 1h the supernatant was removed and add another 1.5 mL of lentivirus medium with polybrene was added. The plate was then incubated at 37℃ for 1 h without shaking. Infection with lentivirus-containing medium was then repeated for a third time before finally the remaining lentivirus medium with the same concentration of polybrene was added for overnight infection. On the next day, the medium was changed and the appropriate antibiotic was added to select for the transduced cells.

The selection antibiotics used in this study were G418 (used at 500µg/ml), puromycin (used at 1 µg/ml) and blasticidin (used at 1 µg/ml).

2.2.3.3 Inducing protein expression

In this study, Tet-ON control system was used for making inducible cell lines. The induction of cell lines to express proteins from the genes inserted into the lentiviral vectors

was achieved by adding doxycycline (100 ng/ml for final concentration) to the cell culture, usually 24 h before further experimentation. Details of the expression system and other aspects of the lentiviral vectors used in this study are explained in sections 3.3 and 4.2.1.

2.2.4 Western blot analysis

Western blotting buffers

Western blotting was conducted on standard Tris-glycine gels using the following buffers and reagents:

Table 2.9 List of western blot butters and components

Buffers and solutions	Components
Resolving buffer (RGB)	181.5 g/L Tris-HCl pH 8.8, 4 g/l SDS
Stacking buffer (SGB)	59 g/L Tris-HCl pH 6.8, 4 g/l SDS
Running buffer	6.32 g/L Tris base, 4 g/l glycine, 1 g/l SDS
Transfer buffer (TOWBIN)	20% methanol, 25 mM Tris, 192 mM glycine, pH 8.3
Blocking solution	5% (w/v) skimmed milk in PBST
Stripping buffer	2% SDS, 62.5 mM Tris-HCl, 100 mM β-mercaptoethanol, pH 6.7
Washing buffer (PBST)	PBS with 0.1%Tween 20

PBS solution was made by diluting 10X PBS, which was provided by Sigma-Aldrch, with dH_2O.

Table 2.10 List of western blotting reagents

Reagents	Source
Acrylamide :(N,N′-methylene-bis acrylamide) (30:1 w/w), 30% solution	BioRad
Ammonium Persulphate (AP), made up to 10% w/v with dH_2O	BioRad
TEMED (N,N,N',N'-tetramethylethylenediamine)	Sigma-Aldrich
Rainbow markers	Invitrogen
Photographic film	Kodak Ltd
Hybond (H^+) nylon membrane	GE Healthcare (cat. #10600015)
ECL Western Blotting Detection Reagents	Perkin-Elmer (cat. # NEL 101001EA)
ECL Plus Western Blotting Detection Reagents	Perkin-Elmer (cat. # NEL 103001EA)
ECL Prime Western Blotting Detection Reagent	GE Healthcare (cat. # RPN2236)

2.2.4.1 Protein sample preparation

The composition of the 3X sample loading buffer was as follows: 1 ml SGB, 1 ml 20% SDS, 1 ml glycerol, 0.5 ml 14 M β-mercaptoethanol, bromophenol blue dye. Stored at –20℃. Diluted to 1X loading buffer by addition of water.

For cells in 24-well plates, 70µl of 1X loading buffer was added to each well to prepare whole cell protein samples, which were boiled the samples for 5 min and then centrifuged for 1 min before 10-30 µl aliquots were loaded on a gel.

2.2.4.2 Preparation of the resolving gel

For the preparation of 7.5% acrylamide gels, 5 ml dH_2O, 2.5 ml RGB, 2.5 ml acrylamide solution (30:1) were mixed, then 80µl 10% APS and 8µl TEMED were added to catalyse polymerisation. For 10% polyacrylamide gels the mixture contained 4.2 ml dH_2O, 2.5 ml RGB, 3.3 ml acrylamide, 80µl 10%APS, and 8µl TEMED. The resolving gel solution was poured immediately into glass gel plate sandwiches, and then dH_2O was carefully overlaid on top of the resolving gel solution. The stacking gel solution was prepared while the gel set.

2.2.4.3 Preparation of the stacking gel

For all gels, the stacking gel solution contained 1.4 ml dH_2O, 0.6 ml SGB, 0.4 ml acrylamide (30:1), 20µl 10%APS, and 6µl TEMED.

The water on the top of the resolving gel was poured off after the gel had set, then the stacking gel solution was added on top before fixing the gel the gel comb in place. The gel was then left to set firm before the comb was gently removed and the wells washed with dH_2O before the completed gel sandwich was placed in the electrophoresis apparatus.

2.2.4.4 Gel running and transfer

A BioRad MiniProtean II kit was used for gel electrophoresis and western blot transfer. The protein samples were loaded on the gel and electrophoresis performed at a constant 100 V for 2 h (10% resolving gels) or 1 h (7.5% resolving gels), or until the bromophenol blue dye reached the bottom of the gel. After electrophoresis had been completed, the gel was removed from the gel plates and placed in a sandwich between filter papers with a nitrocellulose filter in contact, while immersed in transfer buffer. This sandwich was then inserted into a transfer holder with nylon pads, and the proteins were transferred to the nitrocellulose membranes by electrophoresis for 2-3 hours at a constant 250m Amps in transfer buffer (TOWBIN).

2.2.4.5 Membrane blocking and antibody blotting

After the Western Blot transfer, the nitrocellulose membrane was washed in PBST, placed into 20 ml PBST with 5% dried milk and blocked by incubating the membrane at 4℃ overnight or for 2 h at RT with shaking. Subsequently, the primary antibody dilution was added to the membrane and incubated at RT for 2 h with shaking. Alternatively, the primary antibody incubation could be done at 4℃ with overnight shaking. Then the membrane was washed at least three times with PBST within 20 min before the secondary antibody dilution was added to the membrane. Incubation was continued at RT for 1-2 h before the membrane was again washed at least three times with PBST in 20 min prior to the ECL reaction. Membranes soaked in ECL detection reagent were exposed to X-ray film for a range of times before the films were developed in a Konica X-Omat machine.

2.2.5 Herpes Virus infection and Cultivation

2.2.5.1 HSV-1 infection

HSV-1 was used to infect HepaRG and HFT cell lines in this study. Where necessary, the relevant cell lines were induced to express inserted genes by addition of doxycycline (100 ng/ml final concentration) for 24 h before infection. Virus dilutions were prepared in culture medium in order to infect the cells at the required multiplicity of infection (moi). Leaving 100 µl of cell culture medium in the wells of 24-well plates to ensure the cells did not dry out during virus adsorption, 100 µl of HSV-1 dilution was added to each well and the plate was shaken every few min to mix the virus dilution with the cell culture in the first hour. After 3h incubation, the mixture was removed from cells and 0.5 ml of fresh cell culture medium was added.

For plaque assays, this overlay included 1% human serum and also doxycycline to maintain induction of protein expression when required. Doxycycline was omitted for uninduced cells. The human serum prevents virus released into the medium from one cell infecting other cells, which means the virus can only transmit by cell-cell contact. HSV-1 virus used in this study could form plaques that were clearly detected by staining for the β-galactosidase marker gene within 24 h. The next day, the cell culture medium was removed from cells, then the cells were washed, fixed with glutaraldehyde and stained for β-galactosidase activity (see 'blue plaque' assay method, Section 2.2.5.2).

2.2.5.2 Titration of HSV-1 – 'blue plaque' assay

The titre of stocks of ICP0 null HSV-1 mutant dl1403CMVlacZ (ΔICP0) was determined on U2OS cells, and aliquots of these stocks for use in the work of this thesis were kindly provided by Anne Orr. For titration in other cell lines of interest, the mutant HSV-1 has a lacZ marker gene whose activity can be detected by blue plaque assay, as follows:

In the first step, cell medium was removed from the infected cells (infection processes were introduced in section 2.2.5.1) and they were washed with PBS for one time.

Then, 1% glutaraldehyde in PBS was prepared. The stock glutaraldehyde was warmed to 37℃ before dispensing. The steps involving glutaraldehyde were done in the fume hood with the fan on, and all glutaraldehyde solutions were disposed down the drain in

the fume hood. Pipette tips were rinsed under the tap in the fume hood before discarding.

In the next step, 0.5ml PBS/1% glutaraldehyde was added to each well on 24-well plates. The plates were then incubated in the fume hood with the lid on at room temp for 20-40 min.

Then, the PBS/1% glutaraldehyde fix solution was removed from the cells, and the fixed cells were washed with PBS for two times. The following steps were done on normal bench.

Blue plaque assay reagent solution (0.5ml for each well on 24-well plate) was prepared as follows:

Table 2.11 HSV-1 blue plaque assay reagents

Reagent Solution	Composition
5 mM potassium ferrocyanide	1 ml stock 100 mM solution (in fridge)
5 mM potassium ferricyanide	1 ml stock 100 mM solution (in fridge)
2 mM MgCl2	0.4 ml 100 mM solution
0.01% NP40	2 ml 0.1% solution
PBS to required volume	15.6 ml for prepare 20 ml reagent solution.

Reagent solution was pre-warmed in 37℃ water bath.

Then, 40 mg/ml X-gal (Melford) in DMSO (Sigma-Aldrich) (20 mg in 500 ul for 20 ml reagent solution) was prepared. Also warm X-gal solution to 37℃. This solution was prepared freshly for each experiment.

In the next step, the X-gal solution was added drop-wise while vortexing and swirling to mix. This step reduces the formation of X-gal crystals.

Then, the final reagent mix was filtered through a 45 micron filter. This step was done immediately before dispensing the reagent mix. In the following step, the PBS wash solution was removed from the cells, and 0.5ml of the final reagent mix was added immediately.

Then, fixed cells were incubated with the final reagent mix at 37℃ for 30-120 min.

When a good blue colour had developed, the plates were washed with water and left on the bench to dry.

In the final step, the blue plaque numbers were counted and the virus titre was worked out.

X-gal is digested by lacZ gene product, which is β-galactosidase, and the digestion product dimerizes and oxidizes into an indigo coloured molecule. The reaction is illustrated as follows (Figure 2.1).

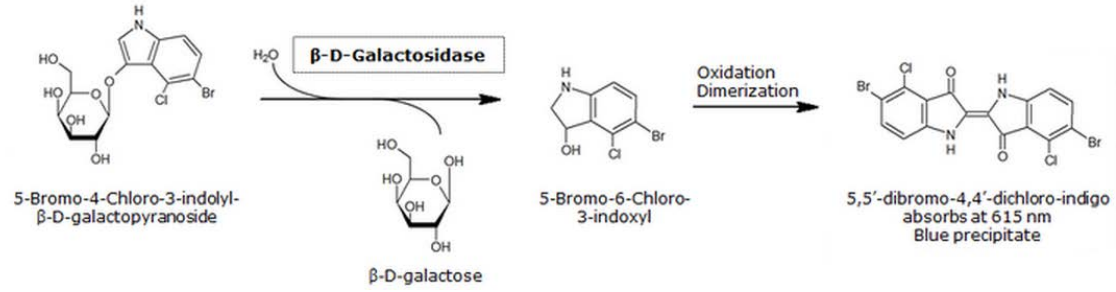

Figure 2.1 Digestion of X-gal by lacZ gene expression protein (β-galactosidase).

2.2.5.3 HCMV infection

Three HCMV wt strains and various mutants were used in this thesis (see section 2.1.5). Histological staining using an antibody against the UL44 Early HCMV protein was used to detect the plaques formed on immortalized human fibroblast cell lines and modified to express different inserted genes. The infection by HCMV was similar to HSV-1 infection after induction of protein expression using doxycycline. In the infection process, the virus dilution was prepared first and then the cell culture medium was removed from the cells, leaving 100 µl of medium in each well of a 24-well plate. Then the virus dilution was added to each well and the plate shaken to mix it. As the HCMV replication cycle is longer than HSV-1, the virus inoculum could be left on the cells for 24 h but no longer than 48 h. After the primary infection, the virus was removed from the cells and fresh cell culture medium with 1% human serum and doxycycline (where required) was added. The HCMV plaques were allowed to develop during 7 to 10 days of incubation. During the incubation time, it was necessary to add fresh medium or change the medium once or twice.

2.2.5.4 Cultivating HCMV

Stocks of HCMV strains and mutants TNwt, TNdlIE1, AD169 and AD169sub82 (Δpp71) HCMV were grown on modified HFT cells as follows. TNwt, TNdlIE1 and AD169 were grown on HFT.IE1 cells while Δpp71HCMV was grown on HFT.ICP0 cells. As described in the results section, ICP0 and IE1 can increase the infection of HCMV on HFT cells, but these cells cannot tolerate ICP0 expression for extended time periods. HFT cells can however tolerate IE1expression, which makes the HFT.IE1 cell line a better host for

cultivating both wt HCMV and the IE1 mutant TNdlIE1. As pp71 is required for HCMV to express immediate early genes, the Δpp71 HCMV mutant is severely impaired for HCMV infection and gene expression. Expression of ICP0 in host cells can complement the mutant virus infection (see the relevant Results sections), therefore stocks of Δpp71 HCMV were grown on HFT.ICP0 cells. In all cases, cell monolayers were infected at moi=1 then the cells were cultivated for 15 days before the virus-containing supernatant was collected.

2.2.5.5 HCMV plaque assay

Immunostaining of HCMV plaques

The titres of stocks of HCMV TNdlIE1, TNwt and AD169 were determined on HFT.IE1 cells while that Δpp71 HCMV was tested on HFT.pp71 cells and HFT.ICP0 cells. Infections in subsequent experiments were performed at multiplicities based on these titres, for reasons that will be explained in the Results sections. Plaques were detected by histological staining for UL44 expression, as follows:

Cells were seeded in 24-well plates at $1x10^5$ /well, then the next day, doxycycline (100 ng/ml) was added for induction when necessary. After a further 24 h, the cells were infected with HCMV, as described above. After 7 to 10 days of incubation, the cell monolayers were washed twice with 0.5 ml PBS and simultaneously fixed and permeabilized (F/P) with F/P solution (F/P solution contains 16 ml PBS, 1 ml 10% NP40 and 3 ml methanol buffered formaldehyde (37% solution) for 10 to 20 min. The cells were then washed twice with 0.5 ml PBST before incubation with 0.5 ml 5% skimmed milk in PBST for 30 min at RT on a table shaker. The block solution was removed then the primary antibody dilution (anti-UL44, 1:250) was added to the cells at 0.3 ml/well. Following incubation at RT for 2 h with horizontal shaking, the primary antibody solution was removed and stored for re-use. The cells were washed with 1 ml PBST three times, and then the secondary antibody solution (horseraddish peroxidase conjugated antibody in 5% milk in PBST) was added to the cells at 0.5 ml/well and incubated at RT for 1 h. The secondary antibody solution was removed and the cells were washed with 0.5 ml PBST three times. In the final step, 200 μl TRUE BLUE peroxidise stain (KPL, Lot No. 140590, Product Code: 50-78-02) was added to each well. The plates were then incubated at RT for 5-10 min for development of the blue colour. When the blue plaques had formed clearly, the TRUE BLUE solution was removed and the cells were washed with water. The plaques

were counted soon after staining as the colour fades quite rapidly, and when necessary the plates were also scanned to record the data.

2.2.6 Yeast 2 hybrid assay

2.2.6.1 Yeast Growth supplements, media and cultures

All Y2H strains detail is specified in section 2.1.3. The commercial Y2H analysis reagents, application and sources are described in Table 2.12.

Table 2.12 List of yeast growth supplements and media.

Reagent	Preparation	Purpose
YPD broth/medium (Sigma-Aldrich)	Add 50 g of YPD broth to 1 L of deionized H_2O, then Mix to dissolve. Autoclave at 121 °C for 15 min. Store autoclaved medium at room temperature.	Liquid yeast incubation culture including essential amino acids.
Adenine supplement (Clontech)	Added to normal YPD medium or agar as required to make YPDA culture medium or selection plates. Added at 55 ℃ after autoclaving the YPD agar.	Prevents yeast strains harbouring ADE1 and ADE2 mutations and enhances growth of Y187 with ade2-101 mutation
YPD agar (Sigma-Aldrich)	Resuspend 65 g YPD agar in 1 L medium. Then autoclave and keep at 55 ℃ water bath for adding medium supplements. YPD agar containing 15 g/L agar.	Agar medium base including essential amino acids.
Drop-out Medium Supplements (DOBA) (Sigma-Aldrich)	1.92 g will supplement 1 L of medium.	Drop-out agar medium base lacking essential amino acids
DO growth supplement -Leu (-L) (Clontech)	0.69 g will supplement 1 L of medium.	Yeast selection supplement for *LEU2* expression (pGAD plasmid transformed strains)
DO growth supplement -Trp (-W) (Clontech)	0.74 g will supplement 1 L of medium.	Yeast selection supplement for *TRP1* expression (pGBK plasmid transformed strains)
DO growth supplement -Leu-Trp (-L-W) (Sigma-Aldrich)	1.54 g will supplement 1 L of medium.	Yeast selection supplement for both *TRP1* and *LEU2* expression (pGAD and pGBK plasmids contained strains)
DO growth supplement -Leu-Trp-His (-L-W-H) (Clontech)	0.62 g will supplement 1 L of medium.	Yeast selection supplement for both *TRP1*, *LEU2* and *HIS3* interaction reporter gene expression (mated yeast strains selection)

Polyethylene glycol 3350 (PEG)	Store at room temperature.	Increase the binding of plasmid DNA to the surface of intact yeast cells during transformation.
5-bromo-4-chloro-3-indolyl-β-D-galactopyranoside (X-gal) (Melford)	Store at room temperature.	Analysis reagent for lacZ gene expression.
1 M 3AT	Added to -L-W-H agar as required. Autoclave the 3AT separately with the agar. 1mM and 5mM 3AT used as final concentration in the -L-W-H agar plate.	Eliminate background expression of *HIS3* gene

2.2.6.2 Reviving glycerol stocks

Yeast strains were stored in glycerol solution at -70 ℃. It was important to avoid frequent thaw of the yeast strain stocks as the transformation efficiency goes down dramatically after each time the stock were thawed. A sterile yellow tip was used to pick up an aliquot of the frozen stock and this was streaked onto a pre-warmed YPDA plate. The thawed yeast strain could be grown on the plate for a maximum of 3 days before re-streaking onto a fresh YPDA plate.

2.2.6.3 Preparation of Yeast Strain Stocks

A single colony on a YPDA plate was picked and inoculated into 1 ml YPDA media in an Eppendorf tube , then this was cultivated the inoculated media at 30 ℃ overnight. On the next day, 100 µl 80% glycerol was added into 400 µl of the yeast culture, then the mixture was vortexed and frozen down immediately on dry ice. The yeast strain stocks were stored at -70 ℃ and could be maintained for 1 year.

2.2.6.4 Preparation of the parental yeast strains for transformation

To maintain high transformation efficiency, it was important to re-streak the parental yeast strains on YPDA plates at least twice after reviving from the glycerol stocks. Several parental yeast strain colonies with 1-2 mm size were selected from a freshly streaked plate and inoculated into a 3 ml YPDA yeast media before being cultivated overnight at 30 ℃ with shaking. Strain AH109 was used for pGAD plasmid transformations (cultivated in medium lacking leucine (-L)) and strain Y187 was used for pGBK plasmid transformations (cultivated in medium lacking tryptophan (-W)).

2.2.6.5 Transformation of parental yeast strains

Transformation buffers

50X TE: 25 ml 1 M Tris-HCl pH 8.0, 10 ml 0.25 M EDTA pH 8.0, made up to 50 ml with dH_2O (final concentrations 500 mM Tris-HCl pH 8.0, 50 mM EDTA).

10X TE: 100 mM Tris-HCl pH 8.0, 10 mM EDTA, autoclaved.

10X LiAc: 1.02 g/ml Lithium acetate, autoclaved.

50% PEG: 40 g polyethylene glycol (PEG 3350) dissolved in 40 ml dH_2O, autoclaved.

TE/LiAc solution: 1ml 10X TE, 1ml 10X LiAc, 8 ml dH_2O.

TE/ LiAc /PEG solution: 0.5 ml 10X TE, 0.5 ml 10X LiAc, 4 ml 50% PEG.

Transformation of parental yeast stains was performed by following the manufacturer's instructions. In brief, the protocols are as follows:

In the first day, 3-5 single colonies from AH109 and Y187 yeast strains were picked up to inoculate 750 µl yeast culture. Then the yeast was incubated overnight. In the following day, 750 µl parental yeast culture was added to 15 ml fresh YPDA medium and incubated for 4 h at 30 ℃ with constant shaking at 200 rpm (final OD_{600} is about 0.7). In the third day, yeast cells were harvested by centrifugation at 3.5 k/min for 5 min. Then, yeast cells were washed twice by 2 ml dH_2O and two times by 2 ml 1x TE/LiAc solution. In the next step, the yeast cells were re-suspended in 75 µl 1x TE/LiAc solution. 50 µl yeast suspension, 25 µg denatured herring tested carrier DNA and 1-2 µg plasmid DNA are used for each transformation. The transformation mix was incubated in room temperature for 15 min. And 150 µl TE/LiAc/PEG solution was added to the transformation mix (mix gently). In the next step, the transformation mix was incubated for 1 h at 30 ℃ with shaking at 200 rpm. After the incubation, the transformation mix was heat-shocked at 42 ℃ for 20 min. In the following step, 700 µl dH_2O was added to the transformation mix and mixed gently. The mixture in the last step was centrifuged at 6 K rpm for 1 min. The supernatant was discarded and the yeast cell pellet was re-suspended in 400 µl pre-warmed medium. AH109 yeast strain was re-suspended in -L medium and Y187 was re-suspend in -W medium. In the next step, 200 µl re-suspend yeast cells was plated out onto the appropriate pre-warmed -L or -W drop-out agar plates. Then, the transformed yeast strains were incubated at 30 ℃. After 4 days incubation, 2 mm diameter yeast colonies were selected and re-streaked onto fresh –L or –W drop-out agar plates.

2.2.6.6 Mating single transformed yeast strains

The haploid yeast strains used in this Y2H system could be mated with each other to form diploids. The mating between transformed AH109 and Y187 strains formed a diploid strain which expressed both AD fusion and BK fusion proteins and which were able to grow in the absence of both leucine and tryptophan.

Several colonies of 2-3 mm diameter of the relevant single transformed yeast strains were picked from fresh yeast plates, noting that the size and the number of the colonies from two single strains should be keep consistent for getting a maximum mating rate. The colonies were inoculated into 0.5 ml YPDA medium and incubated overnight at 30℃ with shaking (200 rpm). On the next day, 200 µl of the mating culture was plated onto pre-warmed -L-W plates. The mated yeast diploids were grown to form colonies during incubation at 30℃ over the next 3days. The plates could then be stored at 4℃ for 2 months, but it was better to proceed directly to the 3AT growth phenotype assay in order to obtain the most reliable data.

2.2.6.7 3AT based growth phenotype interaction assay

Diploids in which the BD and AD fusion proteins interact are able to activate expression of two reporter genes, one which enables growth in the absence of histidine and the other that imparts β-galactosidase activity (lacZ gene product). The presence of 3AT decreases the growth of false positive yeast clones. Therefore diploids initially selected on -L-W plates could be screened for interactions by patching onto -L-W-H plates in the presence of 3AT, then the strength of the interaction could be assessed by staining for β-galactosidase activity. The protocols for this assay are as follows.

In the first day, 10 diploid colonies of 2 mm diameter were picked up from -L-W agar plates into 0.5 ml -L-W medium. Then the colonies were mixed by vortexing. Mixed yeast was incubated over night at 30 ℃ with constant shaking at 200 rpm for 16 h. In the following day, OD_{600} of the yeast culture was measured and the yeast culture was diluted to OD_{600}=0.2 by fresh -L-W medium. In the next step, 7 µl dilutions was applied onto -L-W and -L-W-H agar plates containing 0, 1, and 5 mM 3-AT. Agar plates in the last step were incubated at 30℃ for positive yeast cells growth. (The reporter genes expression enable the yeast cells to grow on -L-W-H plates with 3-AT)

2.2.6.8 X-gal staining assay

X-gal staining solutions

K_2HPO_4 solution: 68.5 g $K_2HPO_4(3H_2O)$ dissolved in 300 ml dH_20, pH 10 (with HCl) (final concentration 1 M), filter sterilised with vacuum pump.

KH_2PO_4 solution: 40.8 g KH_2PO_4 dissolved in 300 ml dH_2O, pH 5.5-6.0 (final concentration 1 M), and filter sterilised with vacuum pump.

1M Phosphate buffer solution: 61.5 ml K_2HPO_4 solution, 38.5 ml KH_2PO_4 solution, heated to 50℃ before use.

1% agarose: 1% (w/v) agarose dissolved by autoclaving and then kept at 50℃ in a water bath before use.

20% SDS (w/v): dissolve SDS in dH_2O.

40% X-gal solution: 0.16 g X-gal power dissolved in 400 µl DMF.

The protocol for this assay is as follows:

Yeast colonies grow on -L-W-H agar plates indicating the successfully mated diploid yeast strains. Whereas the -L-W-H agar plates with 3-AT repress back ground growth of diploid yeast strains. Another reporter gene in Y2H assay system is the lacZ gene, which is tested by X-gal staining. The protocols for X-gal staining are as follows.

In the first step of this protocol, all buffers were pre-warmed in 50℃ water bath. Then, 5 ml KPO_4 with 600 µl DMF, 50 µl 20% SDS and 40% X-gal solution in DMF were mixed for preparing the reactivation solution. In the next step, 5 ml 1% agarose (in dH_2O) was added to the mixture. Then, the mixture was pipetted above to the yeast agar plates immediately and gently. Agar plates were incubated over night at 37℃. In the next day, the agar plates were imaged.

2.2.6.9 Y2H analysis of protein-protein interaction based on His3/lacZ reporter gene expression

Mated yeast strains were selected on -L-W medium, and then -L-W-H medium. To eliminate background growth on -H medium, 1 or 5 mM 3-AT was added into the selection medium. The principle of Y2H assay used in this assay is illustrated in Figure 2.2.

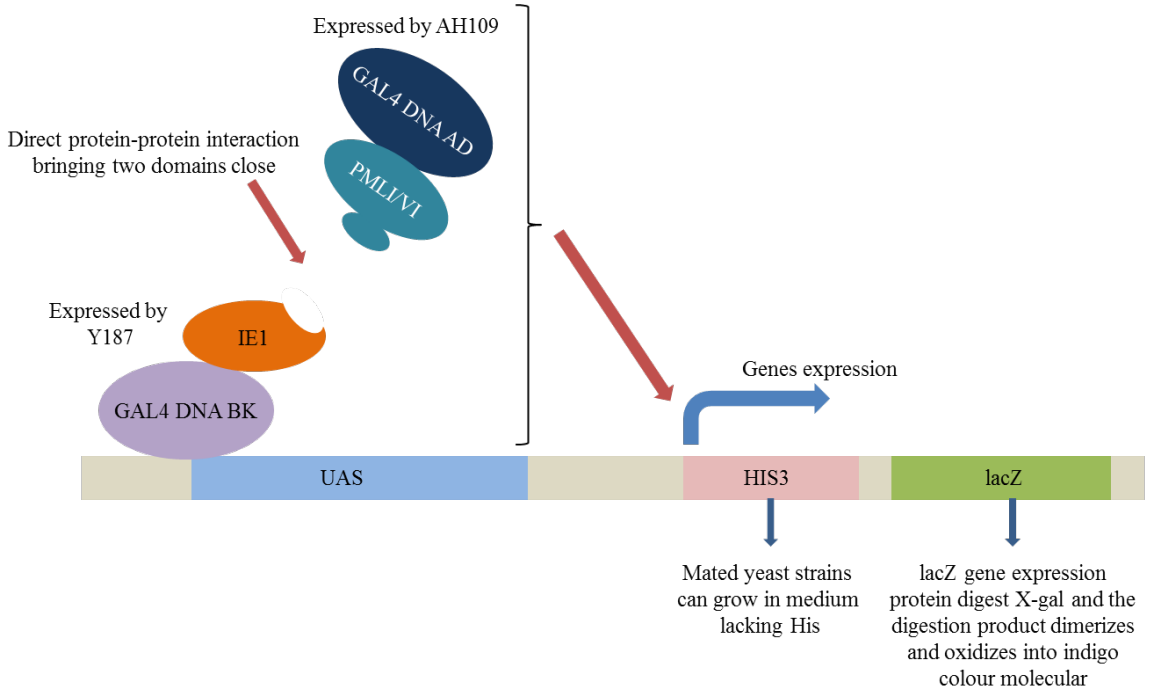

Figure 2.2 Principles of Y2H analysis for protein/protein interaction.

The X-gal digestionby lacZ protein (β-galactosidase) was introduced in section 2.2.5.1.

The GAL4 transcription factor is divided into two domains, which are the DNA binding domain (BK) in plasmid pGBK (plasmid information in section 2.1.6) and the activating domain (AD) in plasmid pGAD (detailed in section 2.1.6). Target proteins are expressed as fusion proteins with the above two transcription factor domains in yeast strains. The pGBK plasmids are transformed into Y187 yeast strain and the pGAD plasmids are transformed into AH109 yeast strain. Mated yeast strains are selected by -L-W, and then incubated in -L-W-H medium to select the interaction between BK fusion protein (BK+Bait) and AD fusion protein (AD-Prey). 3AT eliminates the back ground growth of mated yeast strains on -L-W-H agar. Furthermore, protein/protein interactions between BK+Bait and AD-Prey is visualized by X-gal staining.

2.2.7 Immunofluorescence and confocal microscopy

2.2.7.1 Preparation of coverslips

Commercial 13 mm round coverslips were autoclaved in a beaker before using.

2.2.7.2 Seed cells on the coverslips

For observing protein expression in cells, and for virus infection, HepaRG and HFT cells were seeded at $1x10^5$ cells per well, resulting in cells at about 50% confluence on the next day.

2.2.7.3 HCMV infection on coverslips

When infecting cells on the coverslips, most of the medium was removed to leave 100 µl medium on the coverslips. Then 100 µl of virus dilution was added and the cells incubated for 3 h, after which all medium was removed from the coverslips and replaced with cell culture medium with 1% human serum.

2.2.7.4 Fixing

20 ml of fixing solution contains 19 ml PBS, 1 ml 37% formaldehyde and 0.4 g sucrose. The cell culture medium was removed and the coverslips washed twice with PBS before 0.5 ml fixing solution was added in a fume hood. After 5 min of treatment with the fix at RT, the coverslips were washed twice with PBS. At this stage, the coverslips could be used directly in the next stage or stored at 4℃ with 0.5 ml PBS/1% calf serum.

2.2.7.5 Permeabilisation

20 ml permeabilisation solution contains 19 ml PBS, 1 ml 10% NP40 and 2 g sucrose. This permeabilisation solution (0.5 ml per well) was added to each coverslip and incubated for 5 min at RT. Then the coverslips were washed twice with PBS/1% calf serum.

2.2.7.6 Primary antibody staining

Primary antibodies were used at different dilutions for staining, as indicated in Table 2.13 The appropriate dilutions of primary antibodies were made up in PBS/1% calf serum. Cells could be stained with as many as three primary antibodies simultaneously. In this stage, too much antibody could increase background.

Table 2.13 List of primary antibodies for IF.

Antibody	Dilution
mouse anti ICP0 (11060)	1/2000
mouse anti IE1 (E13)	1/1000
mouse anti IE1 (1B12)	1/1000
mouse anti IE2 (5A8.2)	1/1000
mouse anti pp52 (UL44)	1/1000
mouse anti myc (9E10)	1/500
mouse anti FLAG (M2)	1/2000
rabbit anti PML (A301-167A)	1/1000
rabbit anti myc (Ab9106)	1/1000

Most antibodies could be diluted to an intermediate concentration using PBS/1% calf serum in the presence of 1% sodium azide, then stored at 4℃ for several months without loss of functionality.

For each coverslip, 15-20 µl antibody dilution was enough for staining. The coverslip was placed upside down on an antibody dilution drop on the lid of a 24-well culture dish and incubated at room temperature for 1-2 h. Then the coverslips were washed at least three times with PBS/1% calf serum over 20 min.

2.2.7.7 Secondary antibody staining

This was similar to the primary antibody staining. Dilutions of secondary antibodies could be prepared at an intermediate concentration using the same storage solution as above and stored in 4℃.

Table 2.14 List of secondary antibodies for IF

Antibody	Dilution
anti-mouse Alexa555 antibody	1/2000
anti-rabbit Alexa 633 antibody	1/1000
anti-mouse Alexa 633 antibody	1/2000
anti-rabbit Alexa 555 antibody	1/1000

Secondary antibodies were incubated with the coverslips in the same manner as described above, and then washed several times with PBS/1% calf serum as before. As a final step, an extra wash with de-ionized water was required to remove salts from the surface of the sample to give cleaner images. Finally, the coverslips were dried and mounted on galas

slides with a drop a Citifluor AF1 glycerol-based mounting medium, which includes and anti-fade reagent.

2.2.7.8 DAPI staining

DAPI (4', 6-diamidino-2-phenylindole) is a fluorescent stain that binds to DNA. It was diluted to 0.5 μg/ml for staining the nucleus of cells. DAPI was added with secondary antibodies for staining.

2.2.7.9 Confocal Microscopy

Confocal microscopy analysis was carried out using a Zeiss LSM 510 or a Zeiss LSM 710 confocal microscope with 488 nm, 543 nm (561 nm for the LSM 710) and 633 nm laser lines, capturing images for each channel sequentially. Samples were observed with a ×63 (NA 1.4), or ×40 NA oil immersion objective lenses. The images were exported as files in tif format using the Zeiss software then edited and assembled for presentation using Adobe Photoshop and Adobe Illustrator.

3 Complementation of ICP0 null HSV-1 infection by IE1 and its mutants

3.1 Introduction to the similarity between IE1 and ICP0

As described in detail in Chapter 1, IE1 and ICP0 are immediate early proteins expressed by HCMV and HSV-1, and they are required for viral infection at low MOI for efficient entry into the lytic stage (Everett, 2006b). Although they share no similarities within their amino sequences, they still initially co-localise with the same host proteins located in ND10. ICP0 degrades PML and SUMO-modified Sp100 in infected cells, whereas IE1 induces desumoylation of PML and Sp100 instead of degrading them, and disperses them into the general nucleoplasm. ICP0 also disperses hDaxx and ATRX from ND10, whereas in HCMV the tegument protein pp71 inhibits the repressive activity by interfering with their complex formation (Lukashchuk *et al.*, 2008). Previous data have shown the expression of IE1 also disperses hDaxx and ATRX from ND10, but this is an indirect consequence of PML dispersal(Everett *et al.*, 2013a). An interaction between IE1 and hDaxx has been reported, and this was found to rescue the LUNA promoter in latent and lytic infection from repression mediated by ATRX (Reeves *et al.*, 2010). The above information gave rise to the possibility that the functional similarities between IE1 and ICP0 might allow their functional interchange between HSV-1 and HCMV.

In the work conducted by others prior to initiating the work of this thesis, expression of wt IE1 in an inducible cell line system was found to substantially increase plaque formation by ICP0 null mutant HSV-1 (Everett *et al.*, 2013a). The work described in this chapter investigated characteristics of IE1 that were required for this activity.

3.2 Generation of IE1 mutant sequences

Previous studies in the laboratory showed that the replication defect of ICP0-null mutant HSV-1 could be partially overcome by HCMV protein IE1 (Everett *et al.*, 2013a). Here, this study was extended to several IE1 mutants. By analysing IE1 protein sequences from different primate CMVs (as indicated in Figure 3.1 A; original alignments provided by Dr Andrew Davison), a number of conserved regions and potential SUMO interaction motifs (SIMs) were identified. The potential SIMs (characterised by a quartet of residues rich in leucine, isoleucine and valine residues (Song *et al.*, 2004) were of interest because one potential mechanism of IE1 inducing desumoylation of PML might involve SUMO-SIM

interactions. Conserved amino acid residues within these regions were changed to glycine or alanine by site directed mutagenesis. The IE1 mutants prepared in this stage were later assayed for complementation of ICP0-null HSV-1 infection to analyse the properties of the mutants.

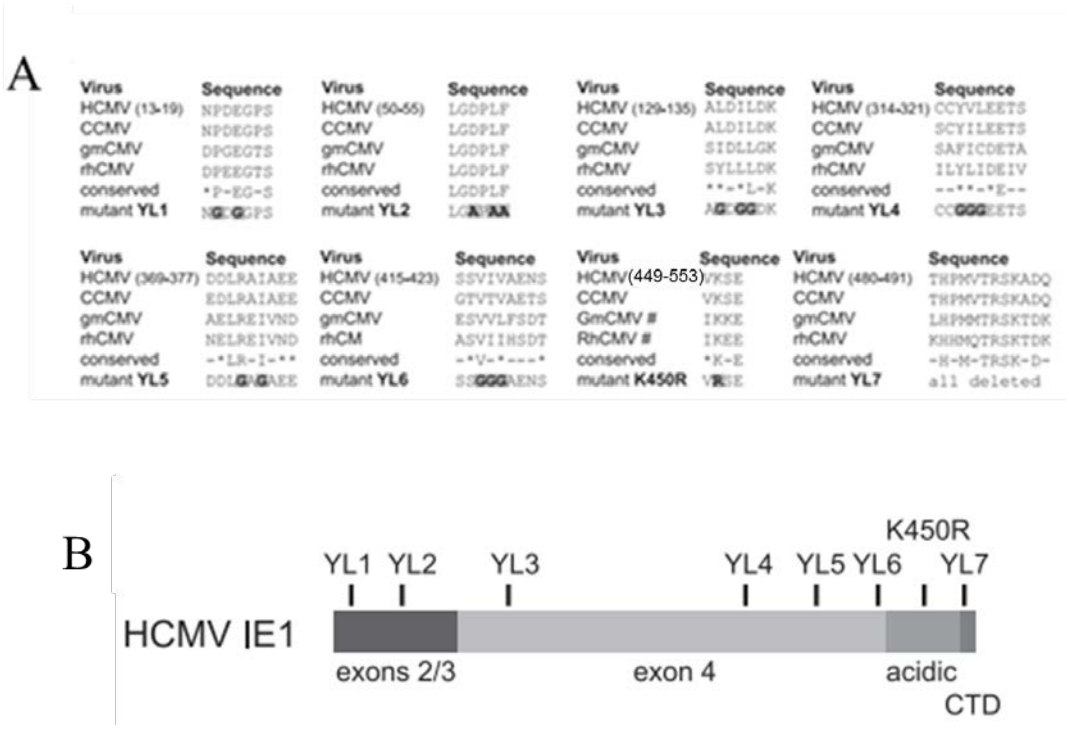

Figure 3.1 A map of the locations of the IE1 mutants analysed in this study.

(A) IE1 sequences of the regions chosen for mutagenesis, showing the aligned sequences of human, chimpanzee, green monkey, and rhesus macaque CMVs (HCMV, CCMV, gmCMV, and rhCMV). The conserved residues are indicated, with an asterisk indicating similar residues rather than precise conservation in all sequences. The lowermost row shows the sequences of the mutants, with the mutated residues highlighted. (B). A map of the IE1 coding sequence showing the locations of the exon2 and exon3 sequences shared with IE2, the acidic C-terminal region, the chromatin tethering domain (CTD) and the positions of IE1 mutants. Figure taken from (Everett *et al.*, 2013a).

YL1 and YL2 are located in the region that is shared between IE1 and IE2. The mutation sites of YL3 and YL4 are located within the hydrophobic core of IE1 and the mutations also affect the hydrophobic groups within YL3 and YL4. Although these are substitution rather than more drastic deletion mutations, these might lead to instability of the IE1 3D structure and therefore impair its function. YL5 and YL6 were identified as potential SIMs for which the importance required investigation. YL7 deletes 12 amino acids of the C-terminal domain where contains an acidic domain that plays a regulatory role and a chromatin-tethering domain (Reinhardt *et al.*, 2005). Furthermore, the investigation by

different groups demonstrated the dispensable role of this region during HCMV infection (Reinhardt *et al.*, 2005; Shin *et al.*, 2012). IE1 mutant K450R was reported to be deficient in SUMO modification but it had no effect on IE1 bioactivity when analysed in transfection assays (Xu *et al.*, 2001), although it does reduce virus growth in the context of the viral genome (Nevels *et al.*, 2004a).

3.3 HepaRG cells expressing IE1 wt or IE1 mutants

The IE1 mutant sequences were inserted into lentivirus plasmid vectors for transduction into HepaRG-based cells (for convenience, all cells based on HepaRG are named with the prefix HA-). The inducible expression system used is controlled by Tet-On elements that are provided by two lentivirus plasmids. Lentiviruses produced by the pLKOneo.CMV.EGFPnlsTetR vector produce a fusion protein EGFPnlsTetR that localizes in the nucleus, provides EGFP for visualisation and has tetracycline repressor activity (Everett *et al.*, 2009). Cells produced by transduction with this vector are named HA-TetR. The IE1 sequence was inserted into another lentivirus vector plasmid, pLDT.IE1 (Everett *et al.*, 2013a). In this plasmid, the IE1 coding sequence is located downstream of TetO operator sequences with a truncated HCMV promoter/enhancer (DCMV) upstream. HA-TetR cells transduced with this vector are named HA-TetR-IE1 wt.

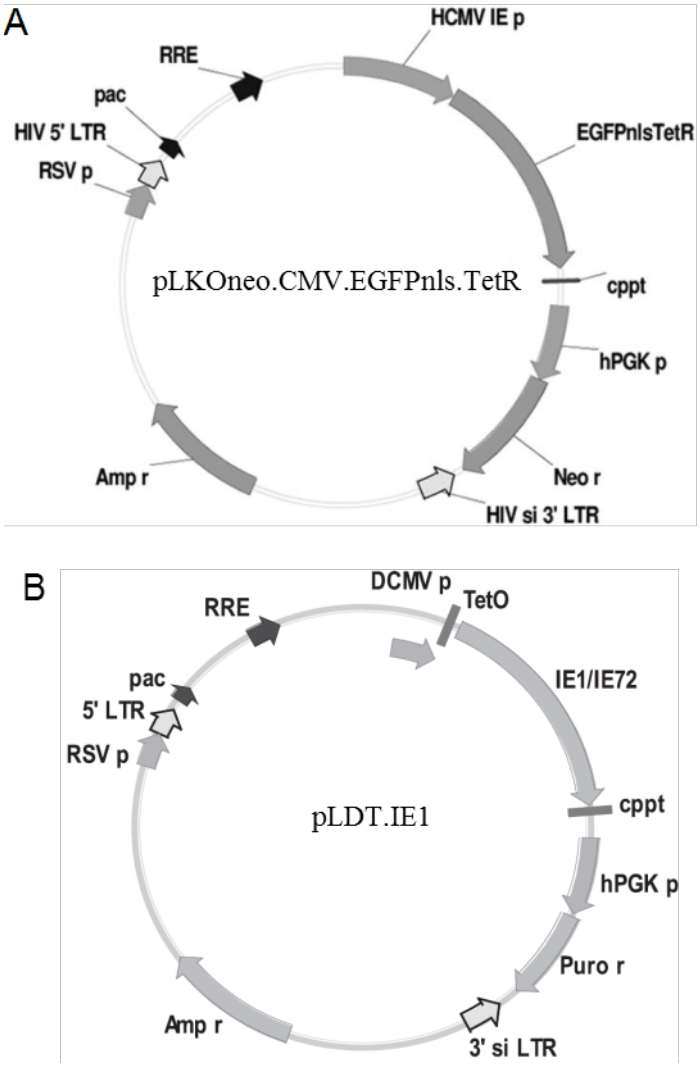

Figure 3.2 Plasmid map of pLKOneo.CMV.EGFPnlsTetR and pLDT.IE1.

(A) Plasmid map of pLKOneo.CMV.EGFPnlsTetR vector. This plasmid encodes the EGFPnlsTetR fusion protein under the control of the HCMV IE promoter. The key features of the lentivirus vector are noted: pac, HIV packaging sequence; RSVp, RSV promoter; RRE, Rev response element; hPGK, human phosphoglycerate kinase promoter; Neo r, G418 resistance coding sequence. (B) Plasmid map of pLDT.IE1. The expression of IE1 is controlled by TetO operator sequences and promoted by a truncated HCMV promoter-enhancer. Puro r indicates puromycin resistance.

This system has been used extensively in our laboratory (Everett *et al.*, 2009) and has been used to express IE1 in MRC-5 cells successfully (Knoblach *et al.*, 2011). Three vectors were used in this system for transduction. They are pVSV-G, pCMV.DR.8.91 and pLKOneo.EGFPnlsTetR or pLDT.IE1. Plasmids functions were described in Table 2.1. HEK-293T cells were transfected with the plasmid mixture in order to cultivate lentivirus for transduction. HA cells were transduced with the EGFPnlsTetR lentivirus in the first

step, then the resulting HA.TetR cells (selected with G418 resistance) were used for secondary transduction to insert the IE1 gene into the cellular genome. In uninduced cells, the tetracycline repressor fusion protein binds to the TetO operator sequences and inhibits transcription of the IE1 coding sequence. Treatment with doxycycline inhibits the binding of the EGFPnlsTetR to TetO sequences and thus allows IE1 gene expression.

To make each mutant, the IE1 sequence was modified by a PCR splicing approach. For each mutant, forward and reverse DNA primers were designed to change the IE1 sequence in the PCR amplification process, and in the initial PCR these were used with primers encoding the N- or C-terminal ends of IE1, as relevant. These latter primers also included restriction sites to enable later insertion into the vector. The information on the primers is shown in Table 2.2. The two PCR products were then mixed and used as a template for a second PCR reaction with the N- and C-terminal primers only, to produce a full length IE1 coding sequence product with the required mutations. The IE1 mutant sequences were digested by restriction enzymes and then ligated with the pLDT vector to replace the IE1 wt sequence. Ligation products were transformed into Stbl3 chemical competent *E.coli* cells and plated on agar plates with selection antibiotics. Single colonies were picked up for miniprep analysis, then purified plasmids were sequenced and analysed to confirm the IE1 mutation sequence.

HA.TetR.IE1 YL1-YL7 and K450R cells were generated by the same methods as used for the HA.TetR.IE1 wt cells. The resulting cell lines were analysed by WB (Figure 3.3) and IF (Figure 3.5) to investigate IE1 expression after induction with doxycycline.

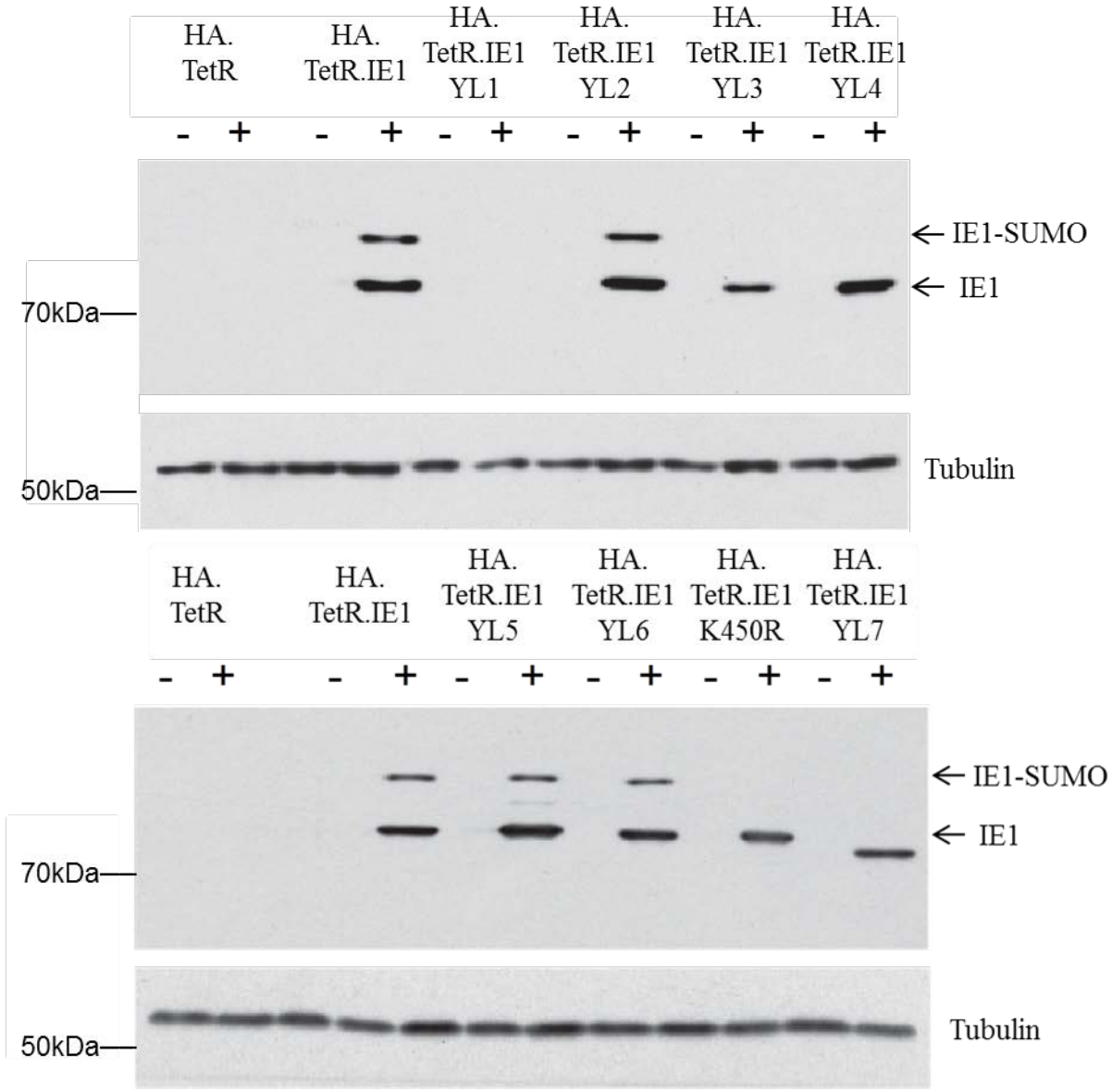

Figure 3.3 WB analyses of HA.TetR.IE1 and IE1 YL1-YL7 and IE1 K450R cell lines.

Cells were induced by treatment with 100 ng/ml doxycycline for 24 h (+) or left untreated (-). The induced and uninduced whole cell lysates were collected and analysed by western blotting using anti-IE1 (mAb E13) and anti-tubulin antibodies as indicated. The positions of molecular weight standards (in thousands) are indicated to the right of each panel.

All IE1 mutant cell lines expressed similar levels of IE1 after 24 h induction by doxycycline. The anti-IE1 mAb used in this experiment (mAb E13) recognizes an epitope in the first 24 amino acid residues of IE1 (Mazeron *et al.*, 1992). It appears that the mutation sites of IE1 YL1 at residues 14 and 16 damage the binding site of this IE1 antibody. Thus, anti-IE1 E13 mAb detected IE1 very inefficiently in Figure 3.3. SUMO modification of IE1 YL2, IE1 YL5 and IE1 YL6 were similar to IE1 wt, whereas IE1 YL3, IE1 YL4, IE1 K450R and IE1 YL7 were not SUMO modified. The absence of sumoylation

of mutant K450R is expected from the published mapping of the sumoylation site of IE1 (Nevels *et al.*, 2004a; Xu *et al.*, 2001), whereas mutations YL3 and YL4 in the hydrophobic core of the protein may destabilise the whole structure, as noted above. Deletion of the conserved C-terminal motif (residues 480-491) in YL7 also disrupts sumoylation, perhaps by affecting the conformation of the protein in the vicinity of the nearby K450 residue, or interactions with the sumoylation machinery. Reduction of sumoylation of IE1 lacking the CTD is consistent with other recent work (Shin *et al.*, 2012).

3.3.1 Characterisation of the effects of the IE1 mutants on sumoylation of PML

IE1 interacts with ND10 and de-sumoylates PML, activities that are important functions for HCMV to counter the intrinsic immune resistance of host cells. Desumoylation of PML was analysed in IE1 mutant expressing cell lines. (Figure 3.4)

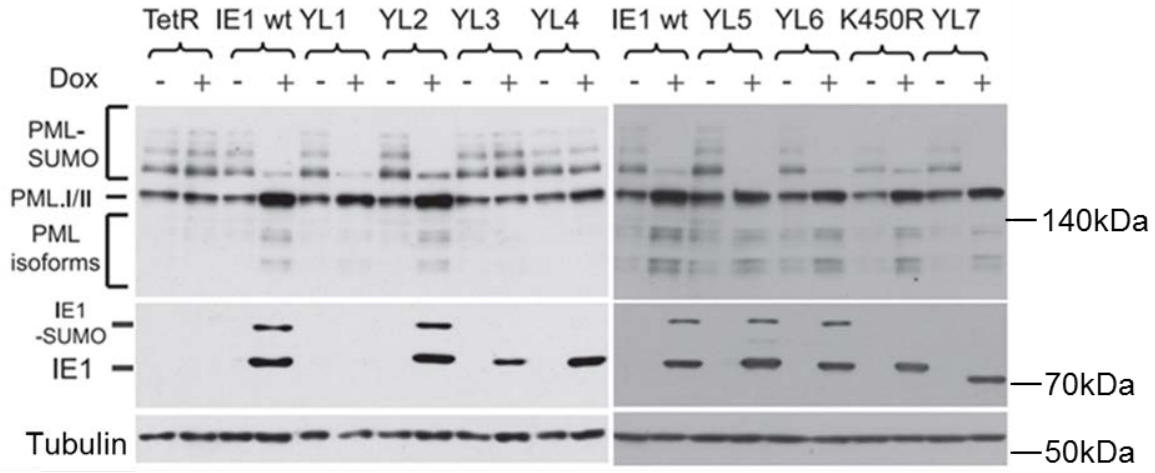

Figure 3.4 WB analysis of HA.TetR.IE1 wt and IE1 YL1-YL7 and IE1 K450R cell lines.
Cells were treated with 100 ng/ml doxycycline for 24 h. The induced and uninduced cell lysates were collected and analysed by western blotting, then probed by anti-IE1 mAb, anti-PML rAb and anti-Tubulin mAb as indicated. (IE1 expression images are also shown in Figure 3.3). The positions of molecular weight standards (in thousands) are indicated to the right of each panel.

Figure 3.4 shows that PML was de-sumoylated by IE1 YL1 in the same manner as IE1 wt, confirming the expression and activity of IE1 YL1 despite it not being detected by mAb E13. Mutants IE1YL3 and IE1 YL4 cannot de-sumoylate PML in HA cells. These two mutant sequences are located in the hydrophobic core of IE1, therefore, changing the

amino acids from Y or L to G deletes the hydrophobic groups which may influence the hydrophobic interaction between amino acids and destabilize the whole protein 3D structure. Mutants IE1 YL2, YL5, YL6, K450R and YL7 all de-sumoylated PML in a similar manner as IE1 wt, indicating that the mutated amino acids are dispensable for IE1's effects on PML.

3.3.2 IF analysis of the IE1 mutants

IE1 initially co-localises with PML in ND10, then desumoylates PML and disperses PML and the other ND10 proteins. These functions are important for HCMV to progress into lytic infection. HA.TetR.IE1, IE1 YL1-YL7 and IE1 K450R cells were induced to express the inserted viral genes to investigate IE1 and the IE1 mutants' interaction with PML and ND10. The confocal microscopy images are shown in Figure 3.5.

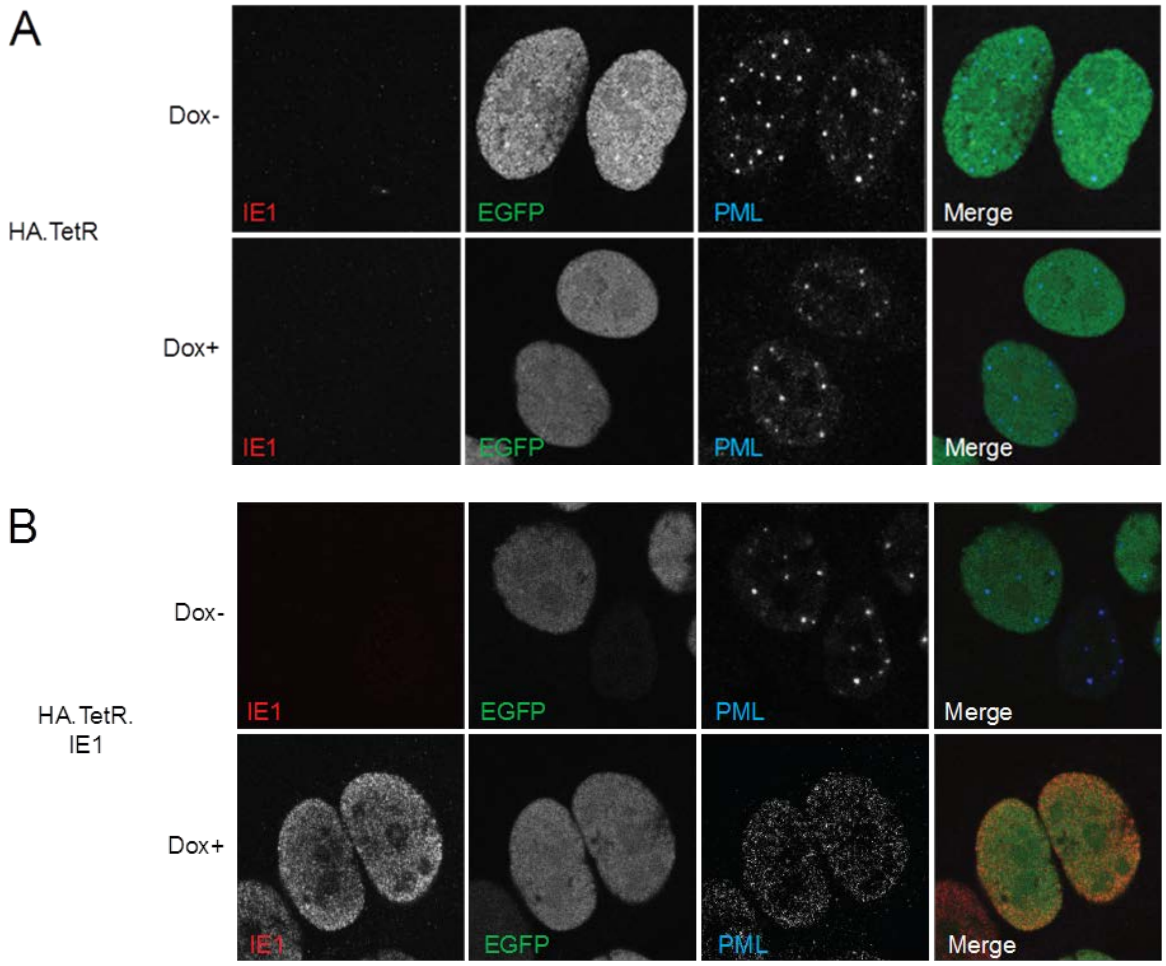

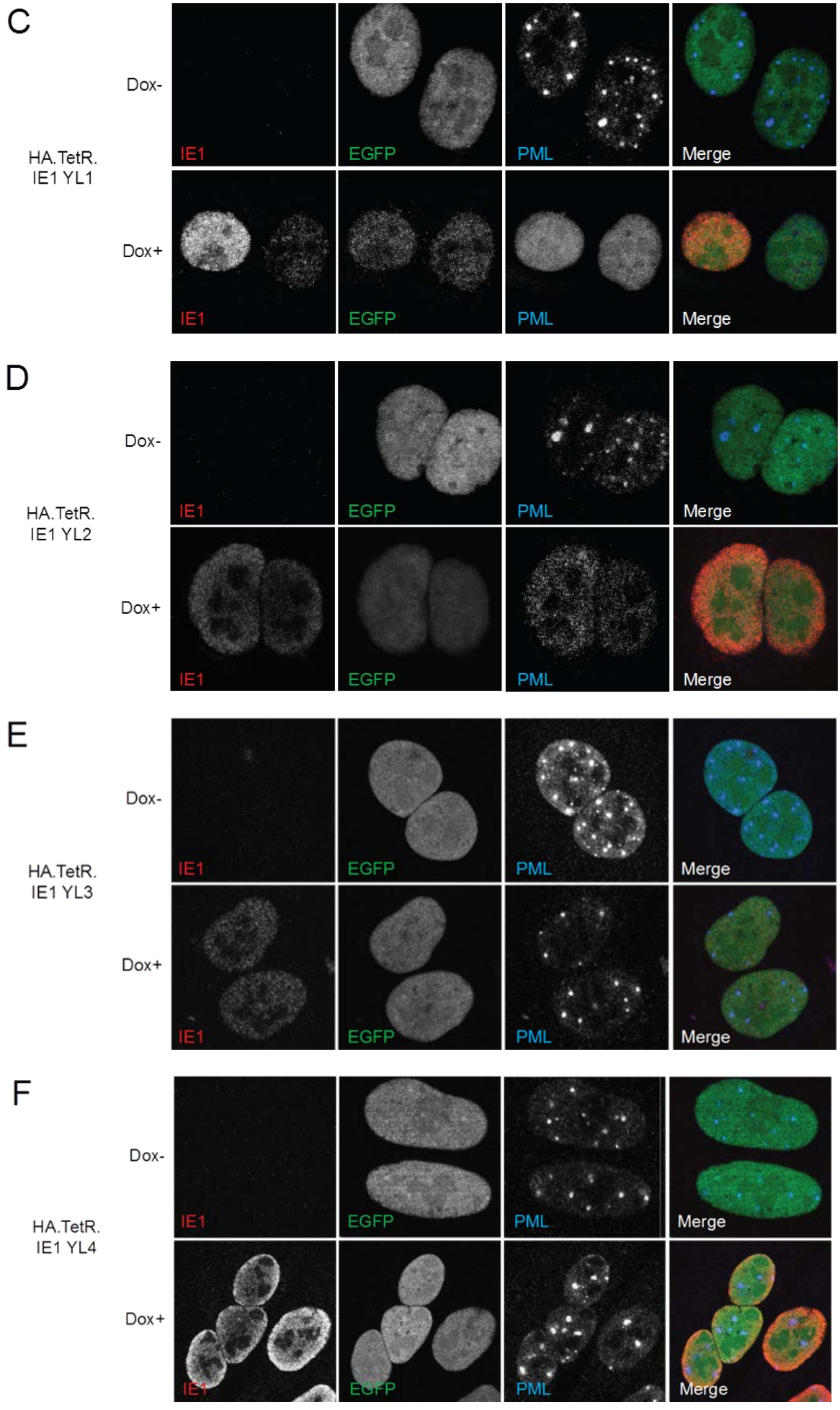
C
Dox-
HA.TetR.
IE1 YL1
IE1
EGFP
PML
Merge
Dox+
IE1
EGFP
PML
Merge
D
Dox-
HA.TetR.
IE1 YL2
IE1
EGFP
PML
Merge
Dox+
IE1
EGFP
PML
Merge
E
Dox-
HA.TetR.
IE1 YL3
IE1
EGFP
PML
Merge
Dox+
IE1
EGFP
PML
Merge
F
Dox-
HA.TetR.
IE1 YL4
IE1
EGFP
PML
Merge
Dox+
IE1
EGFP
PML
Merge

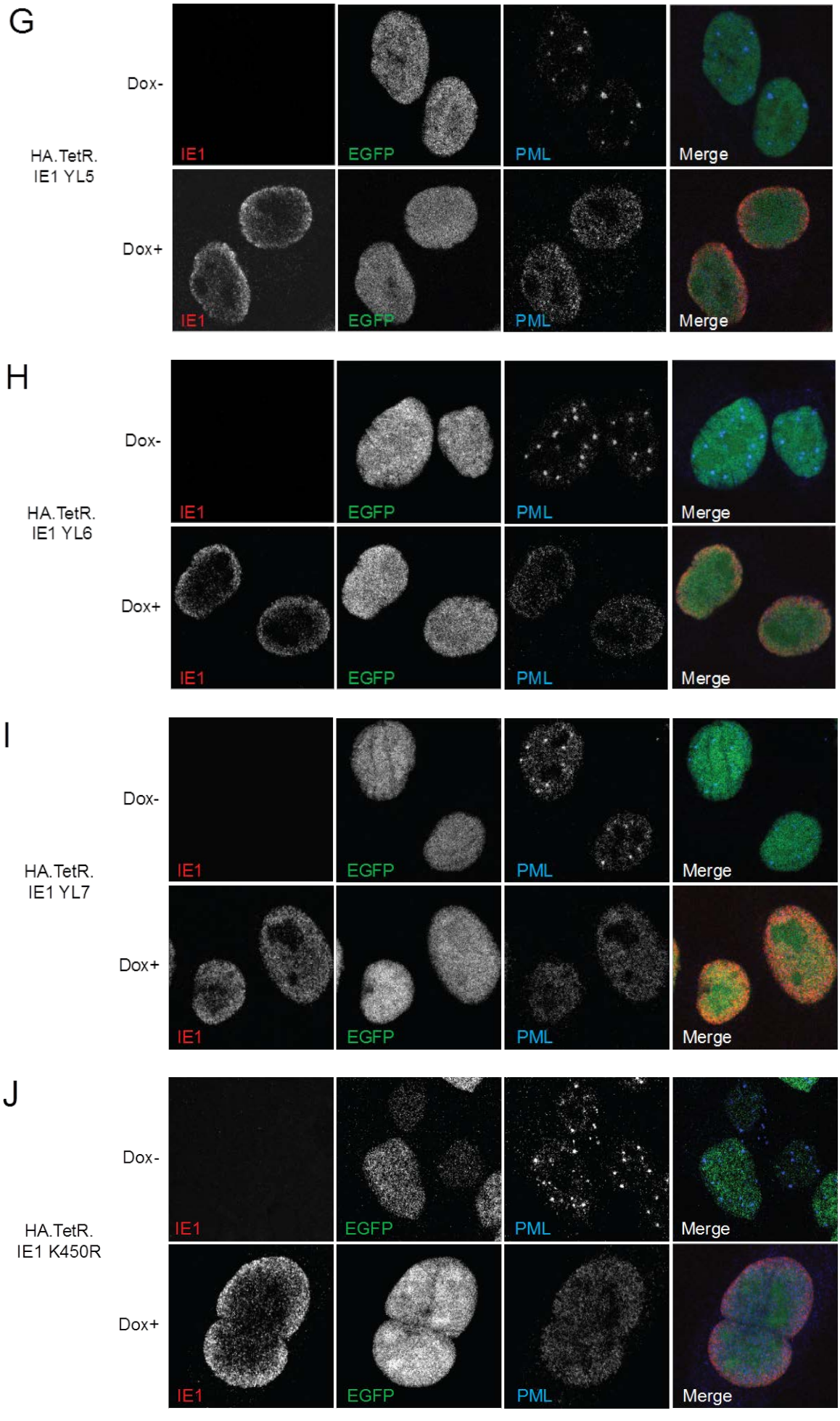
G
Dox-
HA.TetR.
IE1 YL5
Dox+
IE1
EGFP
PML
Merge
H
Dox-
HA.TetR.
IE1 YL6
Dox+
IE1
EGFP
PML
Merge
I
Dox-
HA.TetR.
IE1 YL7
Dox+
IE1
EGFP
PML
Merge
J
Dox-
HA.TetR.
IE1 K450R
Dox+
IE1
EGFP
PML
Merge

Figure 3.5 IF assay of the interaction between IE1 and PML.

Panels A, B, C, D, E, F, G, H, I, J are the IF images of HA.TetR cells expressing IE1, IE1 YL1, IE1 YL2, IE1 YL3, IE1 YL4, IE1 YL5, IE1 6YL, IE1 YL7, IE1 K450R respectively. EGFP images indicate EGFPnlsTetR expression in the HA cell lines. Induced cells were incubated with medium containing 100 ng/ml doxycycline for 24 h. Induced and uninduced cells were fixed and permeabilized, then stained with anti-IE1 mAb and anti-PML rAb primary antibodies, followed by anti-mouse Alexa 555 and anti-rabbit Alexa 633 conjugated secondary antibodies.

Figure 3.5 (A) shows EGFPnlsTetR expression in HA.TetR cells and doxycycline treatment of these cells had no effect on PML localization. In Figure 3.5 (B), HA.TetR.IE1 cells expressed IE1 after induction. IE1 dispersed PML in the nucleus and de-SUMO modified PML, which was shown in Figure 3.4. Figure 3.5 panels (C), (D), (G) and (H) show expression of IE1 YL1, IE1 YL2, IE1 YL5 and IE1 YL6 mutants in HA-TetR cells. These IE1 mutants have different mutation sites in the IE1 sequence that are conserved among different primate CMVs and they have some similarity to SIMs. WB analysis showed that these mutations had no effect on the ability of IE1 to desumoylate PML (Figure 3.4). In the IF analysis, these IE1 mutants dispersed PML in nucleus in the same manner as IE1 wt. In Figure 3.5 (J), IE1 K450R (which cannot be SUMO modified but can de-sumoylate PML (Figure 3.4)) was also able to disperse PML, which is consistent with reported data (Spengler *et al.*, 2002; Xu *et al.*, 2001). Figure 3.5 (I) shows IE1 YL7 expression in HA-TetR cells. IE1 YL7 has a deletion of residues 480-491, and these 12 amino acids at the C- terminal end of IE1 were shown to be important for SUMO modification, but dispensable for PML desumoylation (Figure 3.4) and dispersal of PML in the nucleus. Mutants IE1 YL3 and IE1 YL4, which had no effect on PML in the WB assay (Figure 3.4), were unable to disperse PML from ND10 (Figure 3.5 parts E and F).

The viral protein expression system that has been used in this study allows a minor amount of expression prior to induction (less than 1% cells observed are IE1 positive). This leakiness provides a chance to observe the activity of IE1 and its mutants when expressed in amounts insufficient to disperse PML.

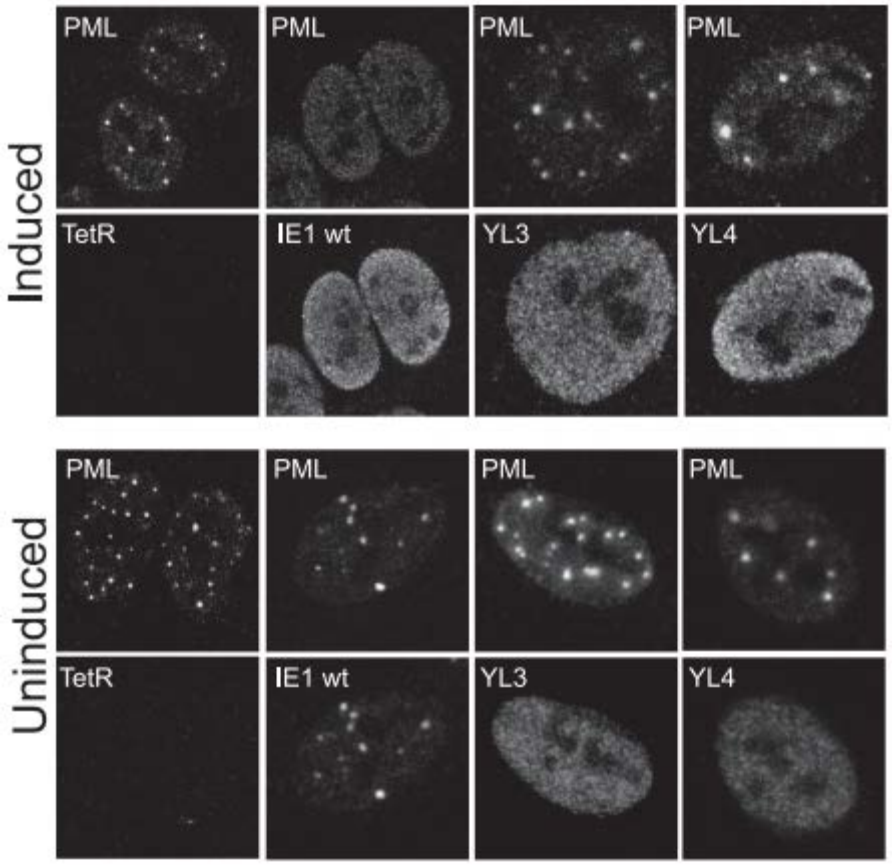

Figure 3.6 Localisation of IE1 wt and the YL mutants when expressed at low levels.
IF images of induced and uninduced HA.TetR.IE1 and IE1 YL3, YL4 cells. Cells were treated with medium containing 100 ng/ml doxycycline for 24 h, or left uninduced. Induced and uninduced cells were fixed and permeabilized, then stained for IE1 (lower row of each pair of rows) and PML as described for Figure 3.5.

Figure 3.6 shows that IE1 wt co-localizes with PML expressed at low levels within leaky uninduced cells and disperses PML when the cells were induced to express high levels of IE1. On the other hand, mutants IE1 YL3 and IE1 YL4 didn't co-localize with PML when expressed at low levels or disperse it after induction. These results indicate the importance of the YL3 and YL4 sequences for the ability of IE1 to co-localise with PML.

3.4 Complementation of ICP0 null HSV-1 by IE1 and its mutants

Previous work in the laboratory conducted by MRes student Adam Bell had shown that wt IE1 can partially complement ICP0-null mutant HSV-1 infection. Therefore the HA.TetR.IE1 mutant cell lines constructed in this study were investigated for their ability to complement ICP0 null HSV-1. Induced cells were infected by ICP0-null mutant HSV-1 (dl1403CMVlacZ; indicated as ΔICP0 in this thesis) and plaque assays were performed by

staining for the β-galactosidase marker gene after 24 h to evaluate the plaque formation efficiency. HA.TetR and HA.TetR.IE1 cells were used as negative and positive controls in this study. The same experiment was performed three times to work out an average figure and standard deviation. Figure 3.7 shows the results of the above experiment.

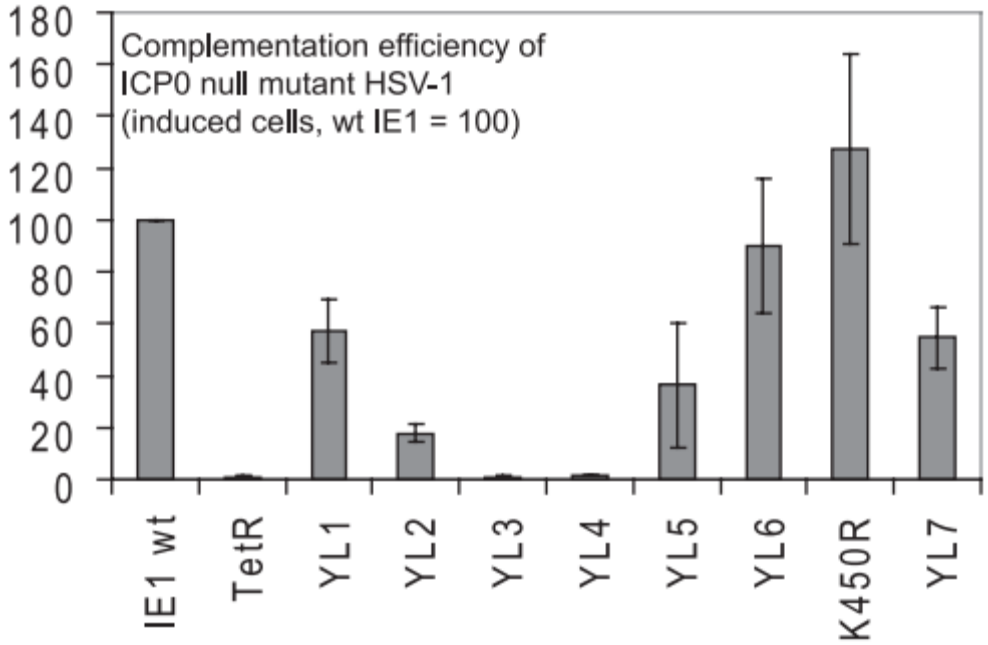

Figure 3.7 Complementation assay of ΔICP0 HSV-1 infection on HA.TetR.IE1 wt and IE1 mutant expression cell lines.

Cells were induced by doxycycline treatment for 24 h before infection. Induced cells were infected by ΔICP0 HSV-1 at a series of MOIs from 0.004 to 1. At 4 h post infection, the cell medium was changed and medium containing 100 ng/ml doxycycline and 1% human serum was added. After 24 h of infection, infected cells were fixed and blue plaque assays were performed to determine the plaque formation efficiency data. The results are expressed as a percentage in absolute titre (PFU per ml) in each cell type over that in HA.TetR.IE1 cells.

Fold increases in plaque formation in the IE1 wt expression cells were calculated and then expressed as a percentage of that of the wt in the data analysis in Figure 3.7. In these experiments, IE1 wt stimulated plaque formation by ΔICP0 HSV-1 by an average of 120-fold, and therefore mutants with as little as 20% of the activity of the wt protein still enable a considerable increase in plaque formation. IE1 mutant K450R produced similar complementation efficiency as IE1 wt, which was consistent with previous data reported (Xu *et al.*, 2001). IE1 mutants YL1, YL5, YL6 and YL7 have retained 40-80% of the activity of the wt protein in complementing ΔICP0 HSV-1 infection. YL7 can't be SUMO modified, but this didn't impair its complementation efficiency. This is consistent with a

previous report from another research group who examined a similar deletion in other assays (Shin *et al.*, 2012). IE1 YL2 complemented the ΔICP0 HSV-1 infection at about 20% efficiency, while mutants YL3 and YL4 were completely negative in this assay. The WB analysis in Figure 3.4 showed that IE1 YL2 can be SUMO modified, and it also dispersed PML in a similar manner as IE1 wt in (Figure 3.5D). It is possible that the mutation site in YL2 damages the 3D structure of IE1 more than other mutants except YL3 and YL4, but it still retains significant activity. Mutants YL3 and YL4 have completely lost the ability to complement ΔICP0 HSV-1 infection, also to desumoylate and disperse PML in WB and IF assays (Figures 3.4 and 3.5). Therefore, along with a previously characterised point mutant in the central hydrophobic region (Muller & Dejean, 1999), changing the hydrophobic residues of the YL3 and YL4 regions into neutral residues such as glycine may severely damage the IE1 3D structure and lead to the loss of IE1 activity in several assays.

3.5 Yeast-2-Hybrid analysis of IE1 and PML interaction

PML is a major component of ND10. It is sumoylated and co-localizes with ND10 in the nucleus. IE1 is responsible for de-sumoylation of PML and dispersal of ND10 during HCMV infection. IE1 and PML were confirmed to interact directly by Y2H in previous reports (Ahn *et al.*, 1998).

Several important amino acids were identified to be essential for IE1 function in section 3.1.4. Therefore, the interactions between these IE1 mutants and PML were investigated by Y2H analysis in this section. The study was also extended to include two PML isoforms (PML.I and PML.VI) and several PML.I mutants which have lesions in different structural elements of PML. The aim of this experiment was to extend previous work (Ahn *et al.*, 1998; Kang *et al.*, 2006; Lee *et al.*, 2007; Tavalai *et al.*, 2008b) on the characteristics of PML that are required for the IE1 interaction. The PMLI mutants used in these Y2H assays were previously studied for their restrictive effects on ICP0-null mutant HSV-1 plaque formation (Cuchet *et al.*, 2011) and the detail of these PML.I mutants is shown in Figure 3.8.

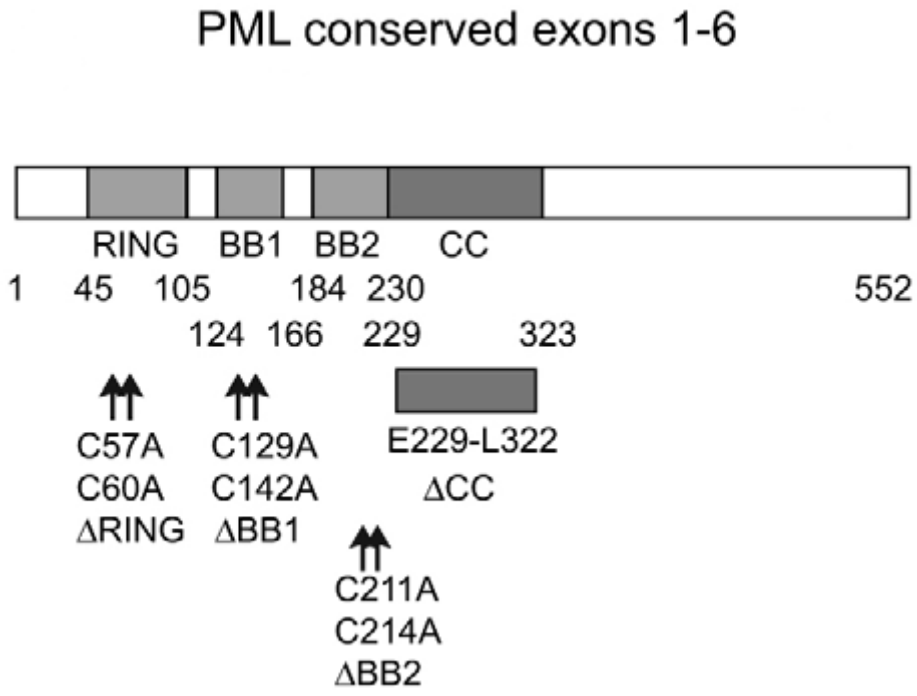

Figure 3.8 Sites of the mutations in PML used in this study.
The figure shows a map of the conserved exons 1 to 6 of PML that are present in all isoforms (detail about PML isoforms is shown in Figure 1.10), and the RING, B-box 1 (BB1), B-box-2 (BB2) and coiled-coli (CC) elements of the tri-partite motif. The actual residues mutated in each mutant (designated ΔRING, ΔBB1, ΔBB2 and ΔCC) are shown. These mutants were provided by Dr Delphine Cuchet-Lourenco and the figure is taken from (Cuchet *et al.*, 2011).

Figure 3.8 shows the detail of PML.I mutants used to study the IE1 - PML.I interaction. ΔRING, ΔBB1 and ΔBB2 are located in conserved cysteine residues in the three zinc binding elements within the tri-partite motif (TRIM) region. The entire TRIM region of PML is required for antiviral defence against HSV-1 infection (Cuchet *et al.*, 2011). The mutation changes the cysteine to alanine residues that delete the –SH groups that are involved in zinc coordination. The ΔCC mutation deletes the coiled-coil region, which is responsible for homomeric and heteromeric interactions among TRIM family members (Ozato *et al.*, 2008).

Three IE1 mutants were used in this study of IE1-PML interactions, namely IE1 YL3, IE1 YL4 and IE1 K450R. It was shown above that IE1 YL3 and IE1 YL4 neither co-localize with PML nor disperse PML in nucleus. IE1 K450R dispersed PML in the nucleus but is not SUMO modified. SUMO1 was used in this Y2H experiment as a positive control for

interaction with PML.I, whereas the empty vector was used as a negative control. The results of the Y2H analysis are shown in Figure 3.9.

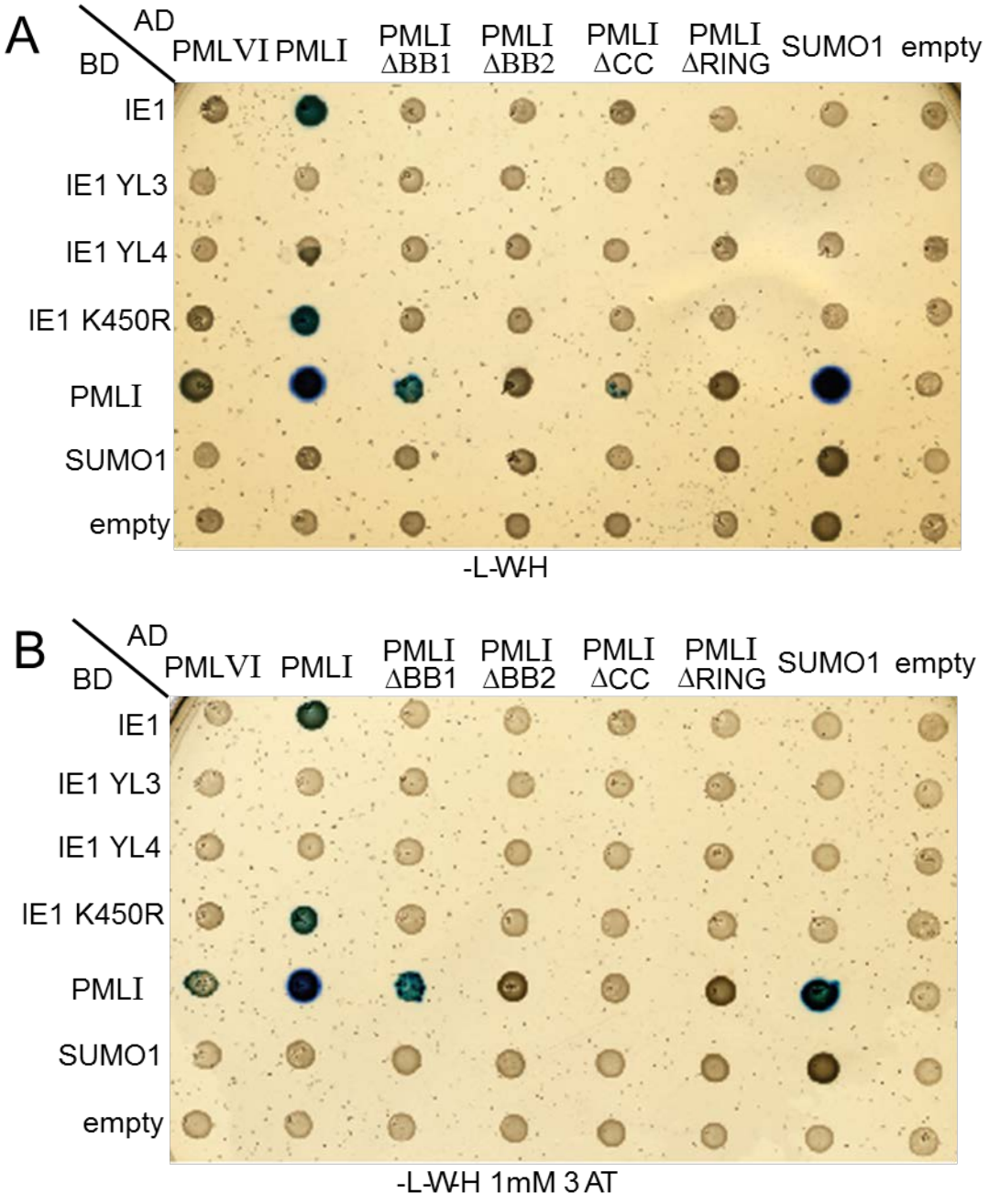

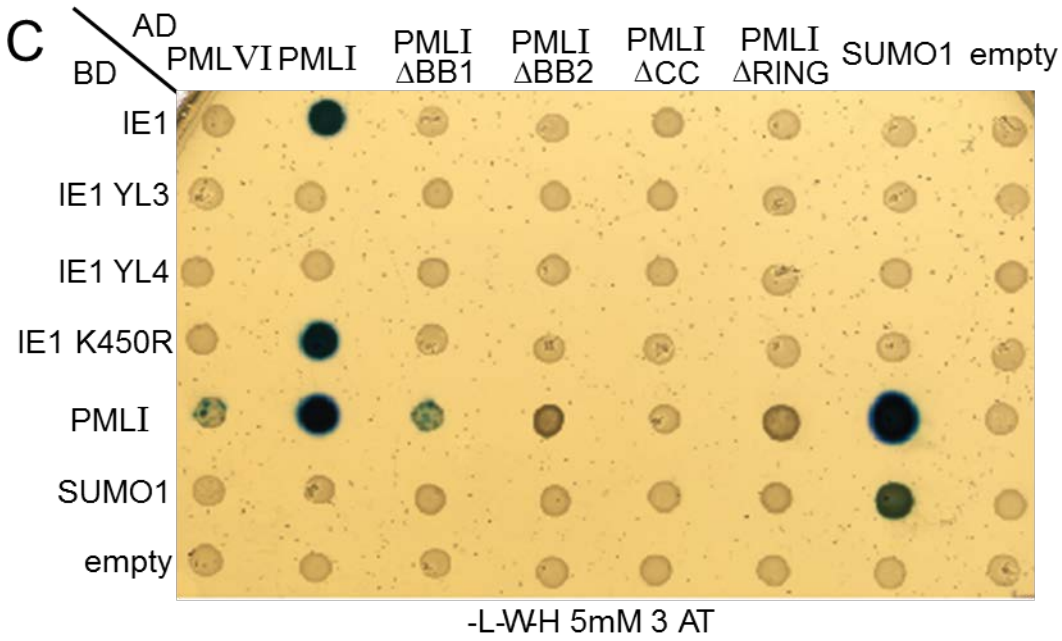

Figure 3.9 Y2H assay of the PML - IE1 interaction.

Mated yeast strains were grown on –L-W-H agar plates (A), –L-W-H plates with 1 mM 3AT (B) and –L-W-H plates with 5 mM 3AT (C). The PML.I and PML.VI matings were done partially in both orientations, with the proteins fused to either the GAL4 activation domain (AD) or DNA binding domain (BD).

In Figure 3.9 (A), AD fusion protein and BD fusion protein interact with each other and express reporter genes which can be detected by X-gal staining. But the background HIS3 gene expression could infect the sensitivity of the assay. In B and C, by adding 3AT in increasing concentration, which is a competitive inhibitor of the HIS3 gene product (Joung *et al.*, 2000) , the background expression of HIS3 can be reduced, thereby reducing the possibility of false positive results.

Despite several repeated experiments and much exploratory work not shown here, these results illustrate some unexpected difficulties with the Y2H system. For example, previous work found that IE1 interacted with PML.VI, and this worked best when IE1 was used on the AD side of the hybrid interaction (Ahn *et al.*, 1998). In the current study, an interaction between IE1 and PML.VI was not observed in either orientation (Figure 3.9 and data not shown). Indeed, the expected interaction between PML.VI and PML.I was weak in this study. Another issue is that the positive control interaction between PML.I and SUMO1 was detected only when SUMO1 was on the AD side (Figure 3.9). These considerations

weaken the interpretation of the data, but nonetheless the strong interactions between PML.I and PML.I, and PML.I and IE1 in the appropriate orientations allow some conclusions to be made.

IE1 and IE1 K450R interacted strongly with PML.I under all conditions in Figure 3.9 parts A, B and C. The IE1 and SUMO1 interaction in Y2H was negative, which is consistent with another publication reported (Xu *et al.*, 2001). IE1YL3 and IE1 YL4 showed no interaction with PML.I or any PML.I mutants, while neither wt PML.I nor IE1 interacted with any of the PML.I mutants. These data indicate that the integrity of all elements of the TRIM motif is required for the PML.I-PML.I interaction, not only coiled-coil motif, and this is also true for the IE1-PML.I interaction. Therefore mutations YL3 and YL4 affect the structural interface between PML.I and IE1, and on the PML side this interface includes the entire TRIM region.

3.5.1 Does IE1 affect the PML - PML interaction?

ND10 structures are a complex of many proteins, of which PML is a major component. PML has 6 major isoforms in the nucleus, of which PML.I is the most abundant, that all co-localize with ND10 (Condemine *et al.*, 2006; Jensen *et al.*, 2001). The infection of HCMV disperses the PML from ND10 and IE1 is responsible for this effect. The results of Figure 3.8 confirm the interaction between IE1 and PML.I in the Y2H assay. IE1 also induces the desumoylation of PML, but the mechanism of this effect is so far not understood. For example, there is no evidence that IE1 itself possesses a SUMO protease-like activity, or interacts with SENPs (Kang *et al.*, 2006). Sumoylation of PML requires all elements of the TRIM but can occur in heterodimers between wt and certain TRIM element mutants (Cuchet *et al.*, 2011). Since the IE1 interaction with PML requires the same structural elements as the PML-PML interaction (Figure 3.8), it is possible that the IE1-PML interaction disrupts PML-PML interactions that are required for PML sumoylation. Thus, the following experiments were designed to investigate whether the PML-PML interaction could be interrupted by IE1 expression.

The initial approach taken was to express different isoforms of PML in the absence of endogenous PML (which would complicate the results), then to use the inducible IE1 expression system to provide IE1. This would allow analysis of the interaction between IE1 and PML, and the PML-PML interaction, by immunoprecipitation from cell extracts.

This required the construction of lentiviruses that could express both an anti-PML shRNA and EYFP-tagged PML.I, another expressing myc tagged PML.VI, and a third expressing IE1 inducibly from a single vector that includes both IE1 and TetR elements. Although cells expressing both PML.I and PML.VI with depleted endogenous PML were established, and co-immunoprecipitation of the two PML isoforms was demonstrated, it was found that the amount of IE1 expressed was not sufficient to disrupt the ND10 structures formed by the over-expressed PML.I and PML.VI (data not shown). Therefore a simpler approach was adopted which involved expression of IE1 during HCMV infection.

Therefore in this part, PML was knocked down firstly with lentivirus made from pLKO.shPML1 (Everett *et al.*, 2008), then these cells were transduced sequentially with lentiviruses made from pLNGY.PML.I (Cuchet *et al.*, 2011) and pLBG.myc.PML.VI in the same cell line. HCMV only infects and replicates efficiently in human fibroblast cells. Thus, the above procedures were applied on immortalized human fibroblast cells (HFT). The resulting cell line was infected by HCMV to study the effect of HCMV infection and IE1 expression on the PML-PML interaction. Those techniques have been used extensively to knock down ND10 components and express different isoforms of PML (Cuchet et al., 2011; Glass & Everett, 2013), and should in principle allow investigation of the effects of IE1 on the physical interaction between different PML isoforms.

The cell lines generated for this assay were analysed by WB and IF. Figure 3.10 shows the WB analysis results, and the IF analysis is shown in Figure 3.11

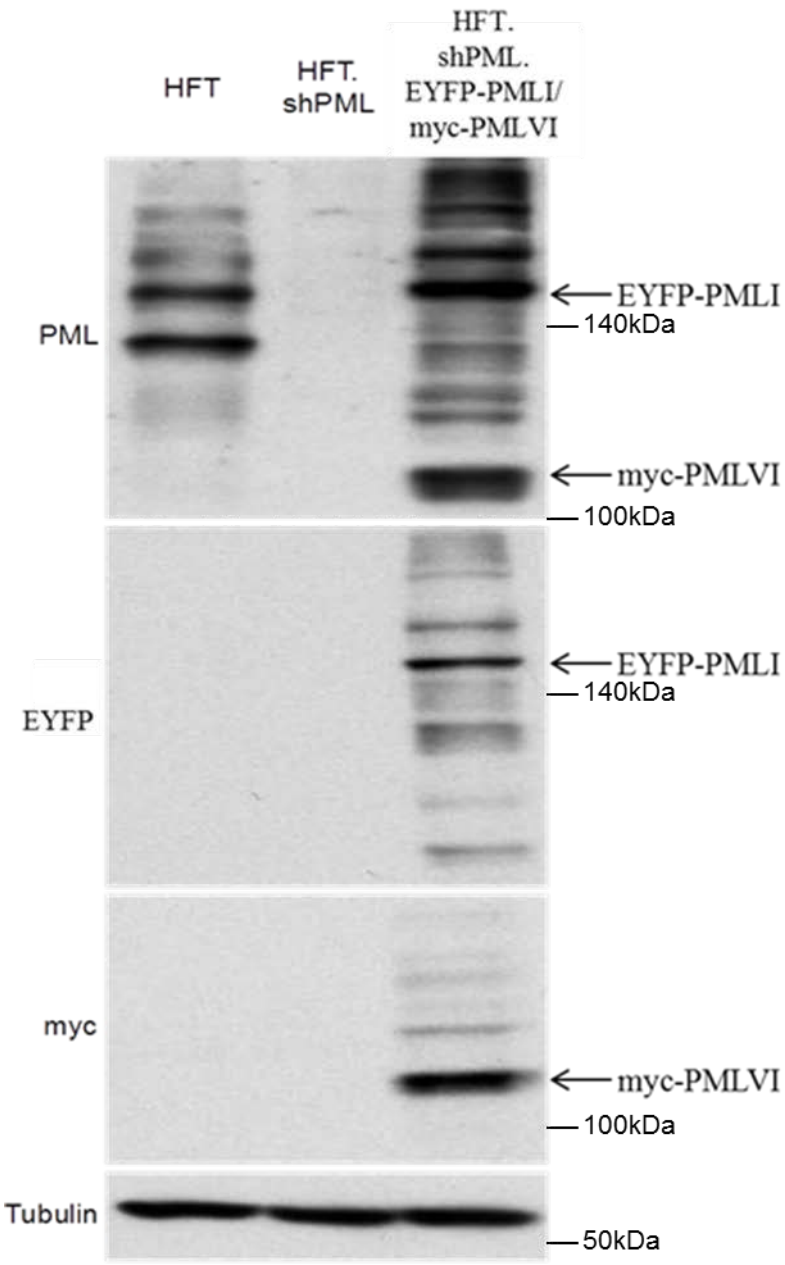

Figure 3.10 WB analysis of PML expression in HFT, HFT.shPML and HFT.shPML.EYFP-PMLI/myc-PMLVI cells.

PML was probed by anti-PML rAb, EYFP-PMLI was probed by mouse anti-EGFP mAb and myc-PML VI was probed by mouse anti-myc mAb. Tubulin was used as loading control**.** The positions of molecular weight standards (in thousands) are indicated to the right of each panel.

In Figure 3.10 an HFT cell extract was used in the WB analysis for an endogenous PML expression control. PML expression in HFT.shPML cells has been efficiently repressed. PML.I and PML.VI have a 322 amino acid residue difference in size, which allows easy identification by WB. HFT.shPML.EYFP-PMLI/myc-PMLVI cells only express these two isoforms of PML which form two strong bands at the tagged PML.I and PML.VI positions,

as indicated. Probing of the blots for EYFP and the myc tag further confirmed the expression of EYFP-PML.I and myc-PML.VI in HFT.shPML.EYFP-PML.I/myc-PML.VI cells. The results also confirmed the SUMO modification of EYFP-PML.I and myc-PML.VI by WB blot analysis.

To investigate the properties of expressed EYFP-PML.I and myc-PML.VI, HFT.shPML.EYFP-PML.I.myc-PML.VI cells were analysed by IF (Figure 3.11)

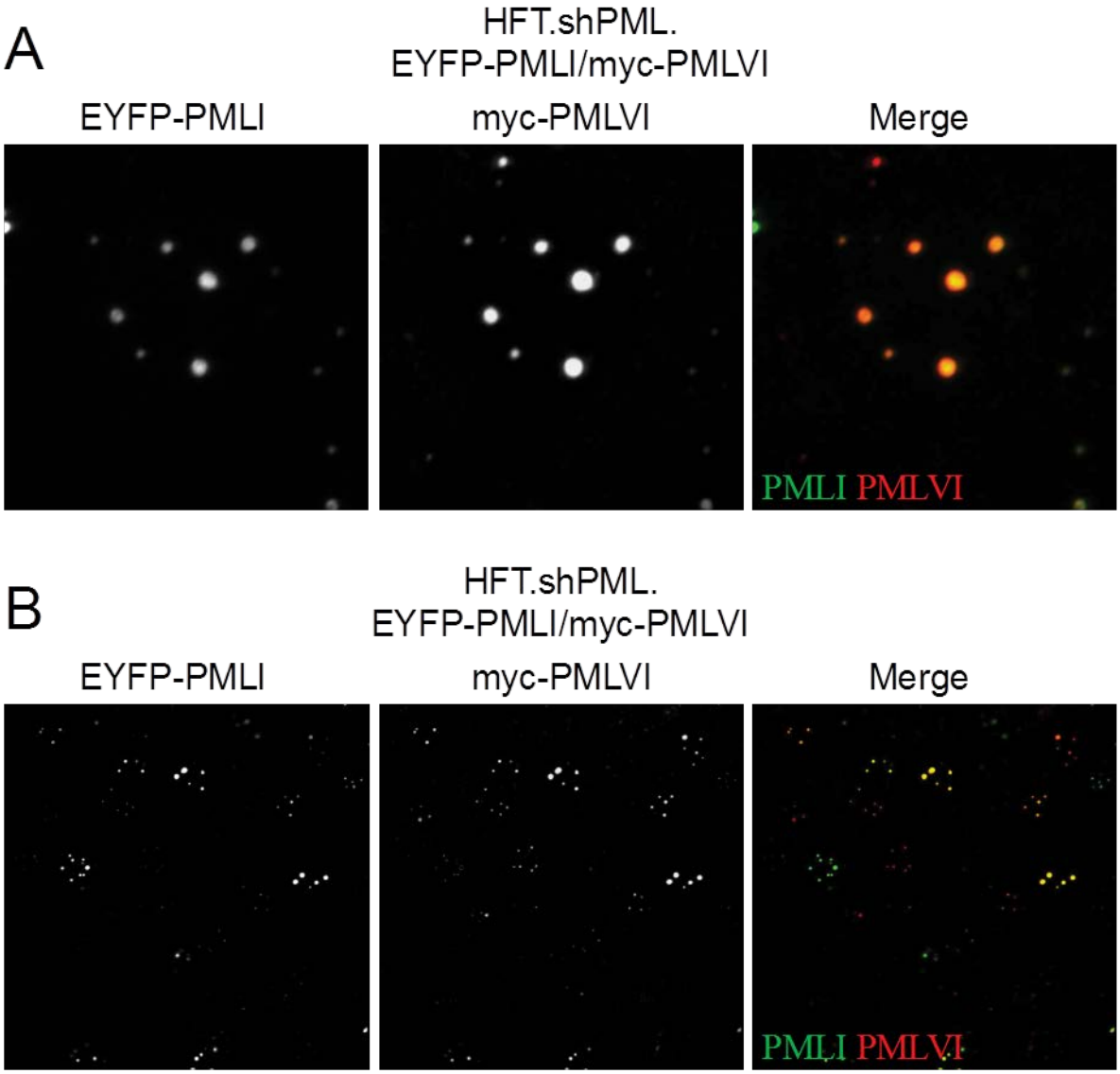

Figure 3.11 IF analysis of HFT.shPML.EYFP-PML.I/myc-PML.VI cells.
(A) The co-localization of EYFP-PML.I and myc-PML.VI in a single cell. (B) IF images of a wide field view. Cells were fixed and permeabilized then stained for the myc tag using anti-myc rAb staining after 24 h incubation on coverslips. EYFP-PML.I was detected by auto fluorescence.

More than 90% of the cells expressed both EYFP-PML.I and myc-PML.VI. As with endogenous PML in normal cells, the EYFP-PML.I and myc-PML.VI expressed in HFT.shPML both co-localized in ND10-like structures and were observed as dots in the nucleus. The knock down of PML in HFT cells didn't appear to cause damage to HFT cells and neither did the expression of EYFP-PML.I and myc-PML.VI, as the cells could be propagated normally. That EYFP-PML.I co-localized with myc-PML.VI is consistent with a previous report that different PML isoforms can co-localize with ND10 (Cuchet *et al.*, 2011).

3.5.2 HCMV infection disperses co-localized PML.I and PML.VI

Several HCMV proteins interact with ND10. Tegument protein pp71 interacts with hDaxx (Hofmann *et al.*, 2002) and disrupts the ATRX-hDaxx complex (Everett *et al.*, 2013a), while IE1 desumoylates and disperses PML and Sp100 in nucleus (Ahn & Hayward, 1997; Korioth *et al.*, 1996). IE2 also co-localizes with ND10 but it neither desumoylates nor disperses any ND10 components (Ahn & Hayward, 1997). The development of HFT.shPML.EYFP-PML.I/myc-PML.VI cell line has built up a model to study the interaction between viral proteins and PML isoforms I and VI in the absence of other PML isoforms.

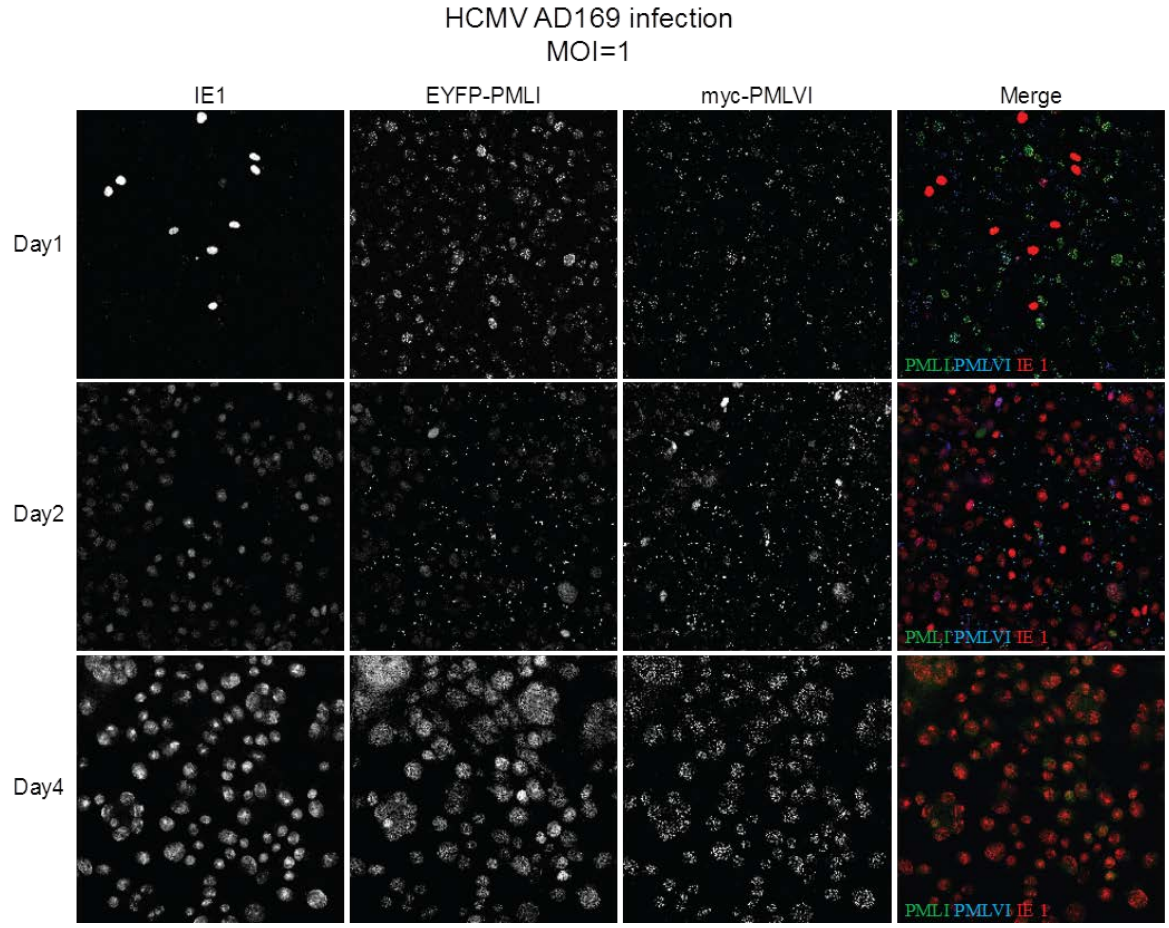

Figure 3.12 IF analysis of HCMV infection of HFT.shPML.EYFP-PML.I/myc-PML.VI cells.

$1x10^5$ cells were seeded on coverslips in a 24-well plate 24 h before infection. On the next day, the cells were infected by HCMV AD169 at MOI 1 (titred on HFT cells). IF images were taken at different time point as indicated. Infected cells were fixed and permeabilized, then stained with anti-myc rAb and anti-IE1 mAb antibodies. EYFP-PML.I was detected by auto fluorescence.

At 24 h post infection, the IE1 expression in some cells reached a high level, but most of the infected cells were expressing the IE1 at a low level which was not sufficient to disperse EYFP-PML.I and myc-PML.VI. After 2 days infection, the infected cells expressed high levels of IE1 as indicated in Figure 3.12. But at this stage, the IE1 expressed in some cells was still not enough to disperse the PML proteins. In the EYFP-PML.I and myc-PML.VI images, both proteins were still co-localizing with each other within about 50% of the infected cells. At 4 days post infection, high level IE1 expression was observed in every single cell, and meanwhile there were no PML dots observed. By observation of single infected cells at the different time points, the interaction process between IE1 and PML was recorded. Figure 3.13 shows IF images of single infected HFT.shPML.EYFP-PML.I.myc-PML.VI cells.

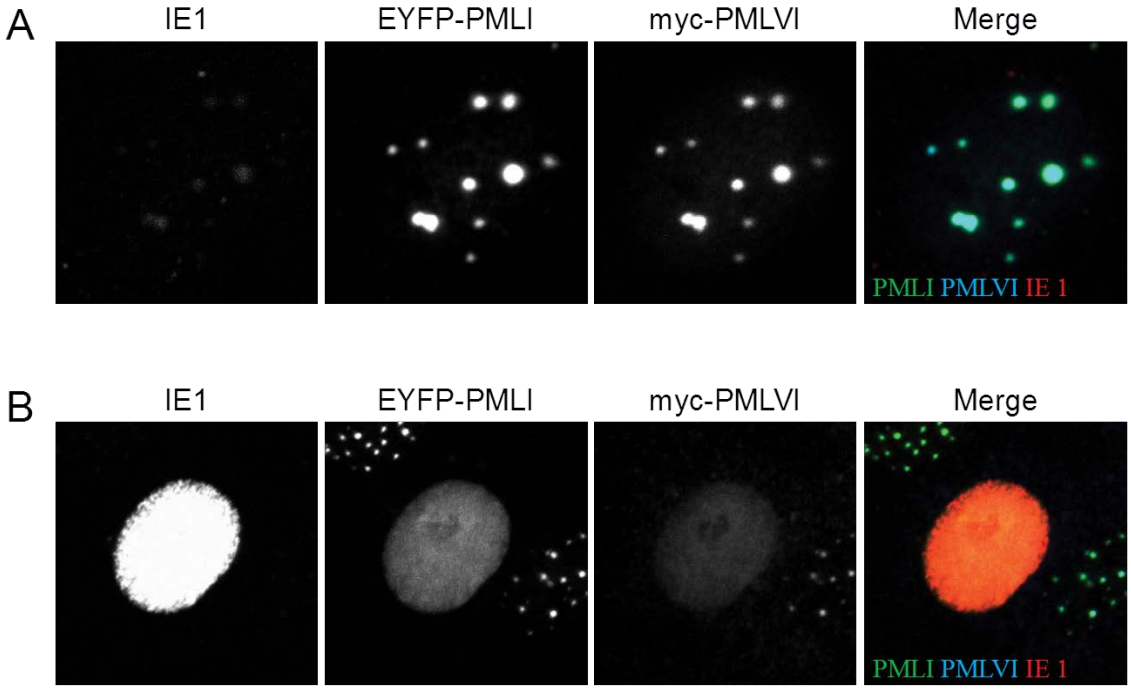

Figure 3.13 IF images of single HCMV infected cell.
(A) An infected cell expressing IE1 at an insufficient amount for PML dispersion (1 day post infection). (B) An infected cells expressing IE1 at an amount sufficient for PML dispersion (1 day post infection). Infected cells were fixed and permeabilized then stained for anti-myc rAb and anti-IE1 mAb, with EYFP-PML.I detected by auto fluorescence.

Previous data showed that IE1 expression in HA cells can desumoylate and disperse PML in the nucleus. When expressed at low levels the IE1 co-localized with PML. In this assay, it was confirmed that the IE1 co-localized with PML.I and PML.VI in the early stages of HCMV infection. Once the IE1 expressed by HCMV reached a high level, it dispersed the PML.I and PML.VI simultaneously, which implies that IE1 co-localized with ND10 and then interferes with the co-localization of specific PML isoforms in the absence of endogenous PML.

This experimental system therefore should in principle allow the study of the physical interaction between PML.I and PML.VI and the effects of IE1 on this interaction using co-immunoprecipitation analysis of infected cell extracts. Unfortunately there was insufficient time during the work for this thesis to conduct these interesting experiments.

3.6 Conclusions and discussion

ND10 contribute to intrinsic immunity to resist herpes virus infection. The research work among different herpes virus labs discovered many viral proteins that target ND10 members to overcome the repression of viral genes expression (for example (Everett *et al.*, 2013b; Tavalai & Stamminger, 2008; 2009); see Chapter 1 for more complete references). IE1 is indispensable for lytic HCMV infection at low MOI (Greaves & Mocarski, 1998), and it has been shown to be an important factor for HCMV infection and gene expression in many scientific reports (Davis *et al.*, 1987; Hermiston *et al.*, 1987; Scherer & Stamminger, 2014). IE1 de-SUMO modifies PML and Sp100 during HCMV infection and disperse them in the nucleus (Kang *et al.*, 2006; Kim *et al.*, 2011b; Lee *et al.*, 2004; Muller & Dejean, 1999; Tavalai *et al.*, 2011). Another research paper also indicated that IE1 interacts with hDaxx to stimulate HCMV gene expression (Reeves *et al.*, 2010). For the reasons stated above, understanding IE1 function and properties is essential for the control of HCMV infection. In the experiments described in this Chapter, the functional and physical interactions between IE1 and PML have been studied from different aspects. To extend the study, PML - PML interactions were also studied in different aspects.

The expression of IE1 was isolated from HCMV infection in this study. In this scenario, the interaction between IE1 and PML was studied independently of infection. Furthermore, the properties of IE1 were also explored by constructing several IE1 mutants that mutated potential SIM sites or sequences that are conserved among different primate CMVs. Some of the IE1 mutants prepared in this chapter have similarities to mutants that were reported before, but the aim here was to study their effects on IE1 complementation of ICP0 null mutant HSV-1 infection. The IE1 mutant YL1 which is located in the exon 2, a common region shared by IE1 and IE2, is mutated at the 14^{th} and 16^{th} amino acids to glycine. This is a less invasive mutation than the deletion of sequences within this region studied previously. A previous paper reported that the first 24 amino acids in the IE1 N-terminal region were responsible for nuclear localization (Lee *et al.*, 2007). This was not observed in IE1 YL1 expression cells. IE1 YL1 can be SUMO modified and can de-SUMO modify PML in the same manner as IE1 wt, which indicates that these conserved amino acids located in the IE1 N-terminal region are dispensable for IE1 localization and function. The IE1 YL2 mutation is located in exon 3 which is also a common region shared by IE1 and IE2. It changes the 52^{nd}, 54^{th} and 55^{th} amino acids to alanine within a highly conserved sequence motif. This region was previously investigated by mutations that deleted the first 69 amino acids of the N-terminal region and it was reported that the Δ69 IE1 cannot

disperse PML in the nucleus (Lee *et al.*, 2007). A similar HCMV mutant virus was also prepared in another HCMV laboratory. Deletion of IE region exon 3 sequence residues 33-77 severely impaired the virus infection even at high MOI, but this mutation affects both IE1 and IE2 in the context of the viral genome (White & Spector, 2005). In this studies described above, IE1 YL2 de-SUMO modified PML and dispersed it in the nucleus. The major difference between IE1 YL2 with IE1 wt was lower complementation activity on ICP0 null HSV-1 infection, where IE1 YL2 retained 25% of the activity of IE1 wt. Therefore, the mutants within exon 2/3 showed that the conserved motifs were not essential for IE1 activity in the above assays. Further studies of those mutants' properties will be introduced in next chapter. IE1 YL3 mutated the 130th, 132nd and 133rd amino acids to glycine. This mutation impaired the functional interactions between IE1 and PML in WB, IF and Y2H assays. It also abolished the ability of IE1 to complement ICP0 null HSV-1. These results indicate the importance of this region for IE1 bio-activity. Previous work reported that deletion of IE1 amino acid residues 132-274 (Δ132–270 IE1) impaired the interaction between IE1 and PML in Y2H assays. The WB analysis also showed that this mutant cannot de-SUMO modify PML (Lee *et al.*, 2004). IE1 YL3 has two mutation sites located in the deleted region of the above IE1 mutant. Therefore, these results indicate that two amino acids, the 132nd and 133rd, might be essential for IE1 bio-activity. IE1 YL4 has the same properties as IE1 YL3 in the above investigation. It also lost the ability to interact with PML and complement ICP0 null HSV-1 infection. Lee *et al.* also produced a deletion mutant that encompasses the IE1 YL4 in a previous publication. (Lee *et al.*, 2004) They deleted 30 amino acids from residues 290 to 320 (Δ290–320 IE1) in the IE1 sequence, whereas IE1 YL4 mutated the 316th, 317th and 318th amino acids to glycine. Deletion mutant Δ290–320 IE1 performed in a similar manner to Δ132–270 IE1 in PML interaction and PML de-sumoylation. Thus, YL4 defines three amino acids within this IE1 sequence that are essential for IE1 function. One interesting difference between Δ290–320 IE1 and IE1 YL4 is in IE1 SUMO modification. Lee *et al.* reported that Δ290–320 IE1 can be SUMO modified whereas IE1 YL4 performed the opposite way. This difference may reflect the different cell types, expression methods and expression levels in the two studies. Mutation on IE1 L174 was reported incapable on co-localization with PML and SUMO-1, and further more PML and Sp100 de-sumoylation (Muller & Dejean, 1999; Xu *et al.*, 2001). YL3 is close to L174 in IE1 sequence, and this mutation also abolished the IE1 function on PML co-localization and de-sumoylation. The above information indicated the importance of this hydrophobic region on IE1 function.

IE1 YL5 and YL6 performed in the same manner as IE1 wt in all the assays above. These studies confirmed that these two mutation sites are neither important for sumoylation nor indispensible for PML interaction. IE1 K450R has been studied in many aspects by different research groups (Lee *et al.*, 2004; Spengler *et al.*, 2002; Xu *et al.*, 2001). This mutant showed no difference from IE1 wt on PML interaction but IE1 sumoylation was abolished, as expected from previous results, confirming the conclusion that the SUMO modification of IE1 is dispensable for IE1 bio-activity. Furthermore, IE1 K450R was able to complement the ICP0 null HSV-1 infection to the same extent as IE1 wt. Despite having no apparent effects in the assays performed in this chapter, IE1 K450R was reported to be important for HCMV replication (Nevels *et al.*, 2004a). Thus, further investigation of IE1 K450R in HCMV infection will be performed in next chapter. IE1 YL7 deleted the last 12 amino acids at the C–terminal end of the protein, another highly conserved region that has been defined as the chromatin tethering domain (Reinhardt *et al.*, 2005; Wilkinson *et al.*, 1998). This deletion region was found to be essential for sumoylation in the current study (Figure 3.3), which is consistent with a previous study that found that sumoylation of IE1 was impaired by deleting the 16 amino acids at the C-terminal end (Kim *et al.*, 2011b). The un modified IE1 YL7 performed in the same way as IE1 wt in the ΔICP0 HSV-1 complementation assay, indicating the deletion of the C-terminal end did not have a negative effect on IE1 bio-activity. Table 3.1 summarizes the properties of the IE1 mutants in the above investigation.

Table 3.1 Summary of IE1 mutants properties

IE1 mutants	IE1 SUMO modification	PML de-SUMO modification	IE1 PML co-localization	ICP0 null HSV-1 complementation
YL1	+	+	+	+
YL2	+	+	+	20%
YL3	-	-	-	-
YL4	-	-	-	-
YL5	+	+	+	+
YL6	+	+	+	+
YL7	-	+	+	+
K450R	-	+	+	+

To minimize the damage that the mutation cause to the IE1 structure, site mutation was applied in this study instead of sequence deletion. By using specific designed primers (detail in section 2.1.7), single amino acids in IE1 sequence were mutated to A or G

through PCR amplification. This provided direct testing of the role of conserved motifs and less chance of drastic structural defects and hence complete protein destabilisation.

Y2H assay was applied to study the interaction between IE1 and PML and the interaction between PML and PML. Table 3.2 presents the summary of the Y2H analysis.

Table 3.2 Summary of Yeast 2 Hybrid assay.

AD / BD	PML VI	PML I	PML I ΔBB1	PML I ΔBB2	PML I ΔCC	PML I ΔRING	SUMO 1	empty
IE1 wt	-	+	-	-	-	-	-	-
IE1 YL3	-	-	-	-	-	-	-	-
IE1 YL4	-	-	-	-	-	-	-	-
IE1 K450R	-	+	-	-	-	-	-	-
PML I	-/+	+	-/+	-	-	-	+	-
SUMO 1	-	-	-	-	-	-	+	-
empty	-	-	-	-	-	-	-	-

The data confirmed a direct interaction between IE1 and PML. Meanwhile, the amino acid sequences located at the IE1 YL3 and IE1 YL4 mutations was shown to be essential for the IE1 and PML interaction. Surprisingly, PML.I and PML.VI showed no interaction in this Y2H assay, but given the established abilities of different PML isoforms to interact through the coiled-coil domain this result is likely to illustrate a weakness in this particular assay method rather than a true lack of interaction. Meanwhile, PML.I interacted with itself in a strong manner. PML.I ΔCC shown no interaction with PML.I in the Y2H assay, which confirm that the coiled-coil motif is essential for self-association of TRIM proteins (Ozato *et al.*, 2008). PML.I ΔBB1, PML.I ΔBB2 and PML.I ΔRING also showed no interaction with PML.I, indicating that the entire N-terminal RBCC motif is essential for PML.I/PML.I interaction. IE1 wt didn't interact with SUMO1 in the Y2H assay. This is consistent with previous report that IE1 neither interacted with SUMO1 nor Ubc9 in the Y2H assay (Xu *et al.*, 2001).

While many of the results of the Y2H analysis replicate or are consistent with previously published data, the results do extend the known information on the motifs of PML that are

required for its interaction with IE1. The data show that these motifs are also required for PML-PML interactions, suggesting the same interface is required for both. This led to the hypothesis that IE1 might interfere with PML sumoylation through disruption of PML-PML interactions. This is consistent with several published observations. Tools were generated to test this hypothesis more directly, but insufficient time was available to complete this part of the study.

4 Analysis of complementation of IE1 null HCMV and pp71 null HCMV infection by ICP0

4.1 Introduction

Previous studies demonstrated that ICP0 is largely interchangeable with the combination of IE1 and pp71 in complementation assays of ICP0 null HSV-1 (Everett *et al.*, 2013a). These results confirmed the activity of IE1 and pp71 on complementing ICP0 but gave no information about whether ICP0 could replace IE1 or pp71. ICP0 not only de-sumoylates PML and disperses it like IE1, but it also degrades PML in nucleus. It also disperses hDaxx and ATRX in nucleus, an activity shared with pp71, but unlike pp71 it does not disrupt the hDaxx-ATRX complex. Therefore ICP0 combines many ND10 interactions and activities of IE1 and pp71, and this makes it a potential candidate to complement IE1-null HCMV and pp71-null HCMV. In this chapter, ICP0 was investigated for its ability to complement HCMV mutants that lack IE1 or pp71.

Three HCMV strains were used in this study, namely TBE40 (TB), Towne (TN) and AD169. AD169 and TN have been extensively used in HCMV labs over decades and are highly laboratory adapted. Previous reports have shown that these two intensely passaged strains lack many genes that are found in low passaged clinical strains (Cha *et al.*, 1996), although they do encode pp71 and IE1. To further support this study, therefore, strain TBE40 was included as it has been described as a relatively low passage strain with greater similarity to clinical isolates (Zalckvar *et al.*, 2013).

HCMV infects and replicates in human fibroblasts in vitro, but not in HepaRG based cell lines. Thus, an immortalized human fibroblast (HFT) cell line was applied in this study. Details about HFT cells were introduced in section 2.1.1.

4.2 Development of IE1, pp71 and ICP0 expression HFT cell lines

4.2.1 ICP0 expression cell line

A single lentivirus vector expression system was used for this study. The TetR repressor protein coding sequence was inserted into pLDT vectors after hPGK promoter, followed by an internal ribosome entry site (IRES) and the puromycin resistance coding sequence. This new system combined the two plasmids used in the HepaRG cell based system for

expressing viral proteins in an inducible manner and simplified the cell line generating process to a single transfection (with no need for TetR expression vector transfection). The basic vector for this system was constructed in the laboratory of Dr Chris Boutell, and was derived from the pLDT vectors described in Chapter 3. A minor negative effect of this new expression system was a weakened expression of puromycin resistance and in some cases a reduced expression of the inducible gene.

Plasmid pLDT.EYFP.TetR.IRES.P was constructed as a single inducible vector to express EYFP (Chris Boutell, personal communication). To prepare a derivative that could express ICP0 (pLDT.ICP0.TetR.IRES.P) (Figure 4.1), the EYFP coding sequence in pLDT.EYFP.TetR.IRES.P was replaced by the ICP0 cDNA sequence which is present in the pLDT.ICP0 vector. Plasmids pLDT.EYFP.TetR.IRES.P and pLDT.ICP0 were digested by the same restriction enzymes which have sites located at the 3' and 5' ends of the EYFP and ICP0 coding sequences. The fragments were separated by DNA gel electrophoresis and purified using a commercial DNA extraction kit. The purified DNA segments were ligated overnight and transformed into Stbl3 chemical competent *E.coli* strain the next day. Transformed bacteria were plated on to agar plates with 100 µg/ml ampicillin for selection. Single colonies were picked to inoculate small scale liquid cultures, then miniprep plasmids were extracted using the boiling method (section 2.2.2.1) and analysed by restriction enzyme digestion. Plasmids with the correct digestion segments were purified using a commercial DNA purification kit and sent for DNA sequencing to further confirm the vector structure and viral gene sequence. A large scale plasmid stock was prepared by transformation of the purified miniprep DNA into DH5α *E.coli* strain.

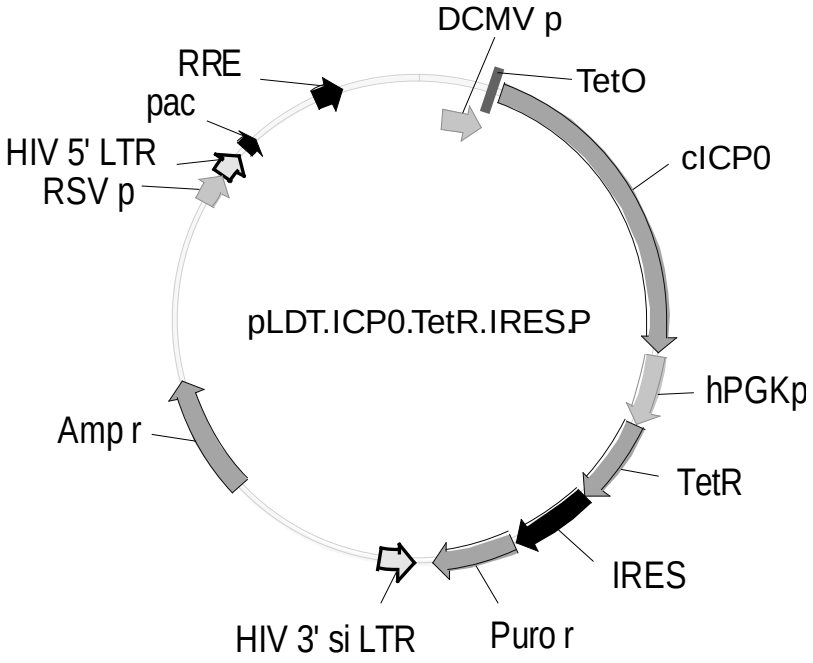

Figure 4.1 Plasmid map of pLDT.ICP0.TetR.IRES.P.

This vector encodes TetR protein under the promotion from the hPGK promoter. The key features of the lentivirus vector are noted: pac, HIV packaging sequence; RSVp, RSV promoter; RRE, Rev response element; hPGK, human phosphoglycerate kinase promoter; IRES, internal ribosome binding site; Puro r, puromycin resistance coding sequence.

Plasmid pLDT.ICP0.TetR.IRES.P was used to transfect HEK-293T cells together with plasmids pCMV.DR.8.91 and pVSV-G to produce lentivirus vector particles. HFT cells were transduced with the resulting lentivirus and selected with puromycin for 2 weeks. The resulting HFT.ICP0 cell line was analysed by IF (Figure 4.2 A) and WB (Figure 4.2 B).

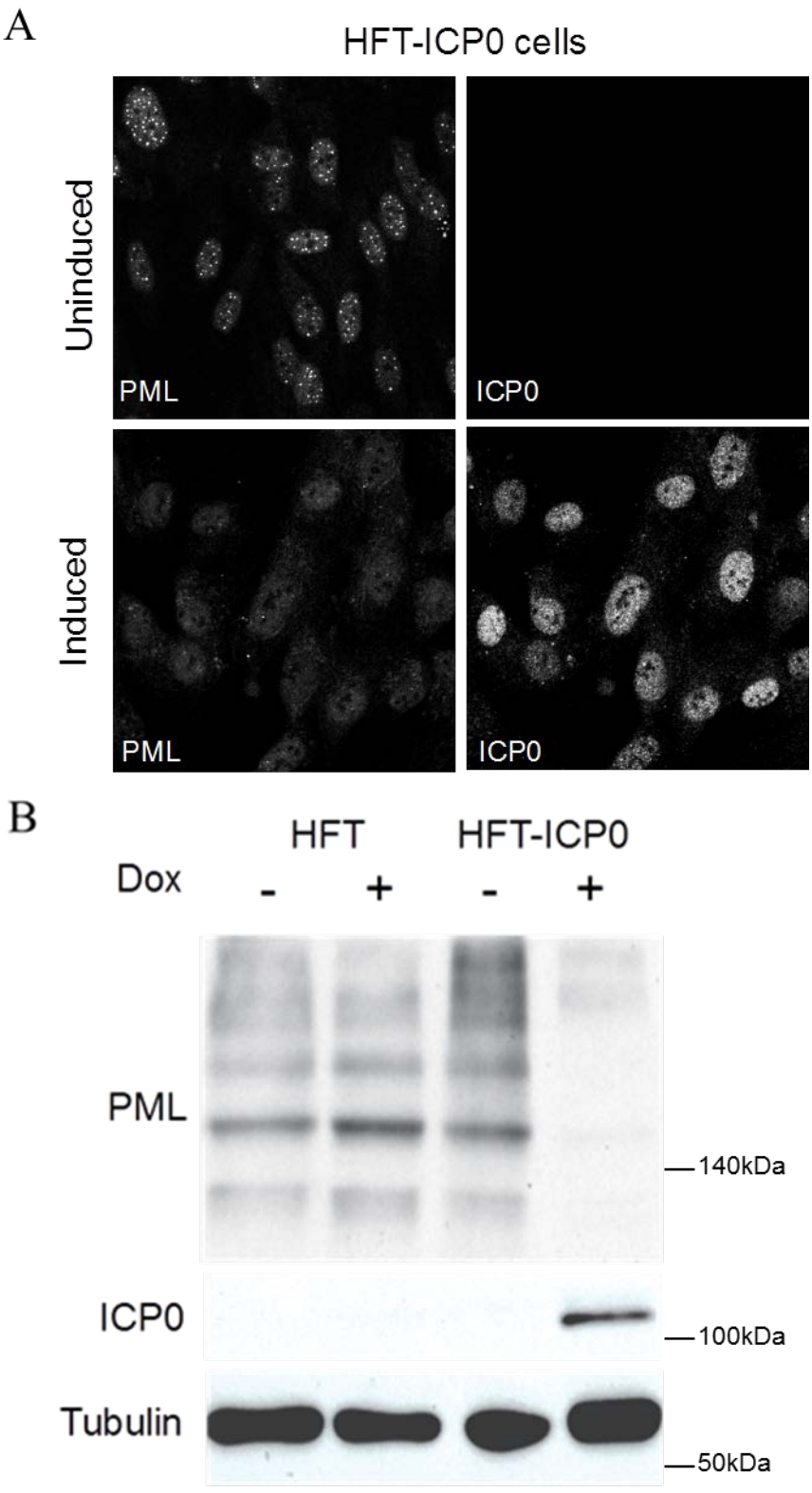

Figure 4.2 IF and WB analysis of HFT.ICP0 cells.

(A) HFT.ICP0 IF images of ICP0 expression. HFT and HFT.ICP0 cells were treated with 100 ng/ml doxycycline or left untreated, then stained by anti-ICP0 mAb and anti-PML rAb 24 h later. (B) WB analysis of ICP0 expression and degradation of PML. Cells were treated as in A then whole cell extracts were prepared for WB analysis. PML was probed for using rabbit anti-PML antibody and ICP0 was probed using mouse anti-ICP0 antibody. Tubulin was used as the loading control. The positions of molecular weight standards (in thousands) are indicated to the right of each panel.

The treatment with doxycycline had no effect on PML or ICP0 expression in the parental HFT cells. The induced and uninduced HFT.ICP0 cells have significant differences in the PML and ICP0 signals in both assays. PML localized at ND10 to form bright dots in uninduced HFT.ICP0 cells, but after ICP0 expression the PML signal was weak and dispersed in more than 90% of HFT.ICP0 cells at 24 h after induction (Figure 4.2 A). ICP0 also degraded the PML signal in the WB analysis (Figure 4.2 B).

The function of ICP0 in HFT-ICP0 cells was also analysed by a ΔICP0 HSV-1 complementation assay. HFT.EYFP cells (constructed using the single inducible EYFP expression vector described above) were used in parallel as a control to analyse the effect of inducible system control elements on ΔICP0 HSV-1 infection. Another negative control for the complementation assay was the parental HFT cells. Cells were seeded in 24-well plates at $1x10^5$cells/well. Seeded cells were induced in the next day for 24 h by treatment with 100 ng/ml doxycycline, then the induced cells were infected with ΔICP0 HSV-1 at different MOIs from 0.004 to 1. At 4 h post infection, the cell culture medium was changed routinely to medium with 100 ng/ml doxycycline and 1% human serum. After 24 h of infection, the cells were fixed and blue plaque assays were performed for collecting plaque formation efficiency data (Figure 4.3).

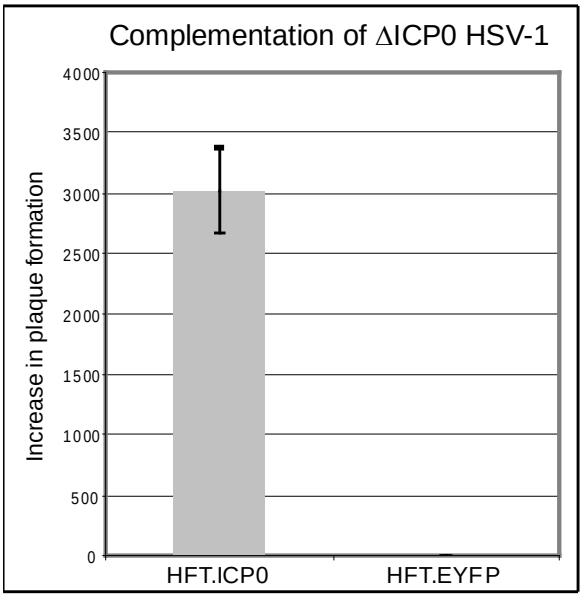

Figure 4.3 Complementation assay of ΔICP0 HSV-1 on HFT.ICP0 cells.

Induced cells were treated with DMEM containing 100 ng/ml doxycycline for 24 h prior to infection. At 4 h post infection, cell medium was changed to DMEM with 100 ng/ml doxycycline and 1% human serum. Blue plaque assays were performed at 24 h after infection. The results are expressed as fold-increase in absolute titre (PFU per ml) in each cell type over that in HFT cells. This experiment was performed three times independently to work out an average figure and standard deviation.

ICP0 expression in HFT-ICP0 cells complemented the ΔICP0 HSV-1 infection about 3000-fold compared to parental HFT cells (Figure 4.3). This was similar to previous work reported (Everett *et al.*, 2013a), except that the effect in these HFT derived cells is even greater than in the HepaRG cell based system. HFT.EYFP cells could not complement ΔICP0 HSV-1 infection, which is consistent with expectation.

In this part of the study, the single inducible system has been proved to be a reliable system. The preparation of the HFT.ICP0 cell line has been simplified to one transduction and the ICP0 expressed in HFT cells has the same functions as that expressed in HA-TetR-cICP0 cells.

4.2.2 IE1 expression cell line

HFT.IE1 cells were constructed using the same lentivirus system as HFT.ICP0 cells. The ICP0 coding sequence in plasmid pLDT.ICP0.TetR.IRES.P was replaced by the IE1 coding sequence to make plasmid vector pLDT.IE1.TetR.IRES.P (Figure 4.4).

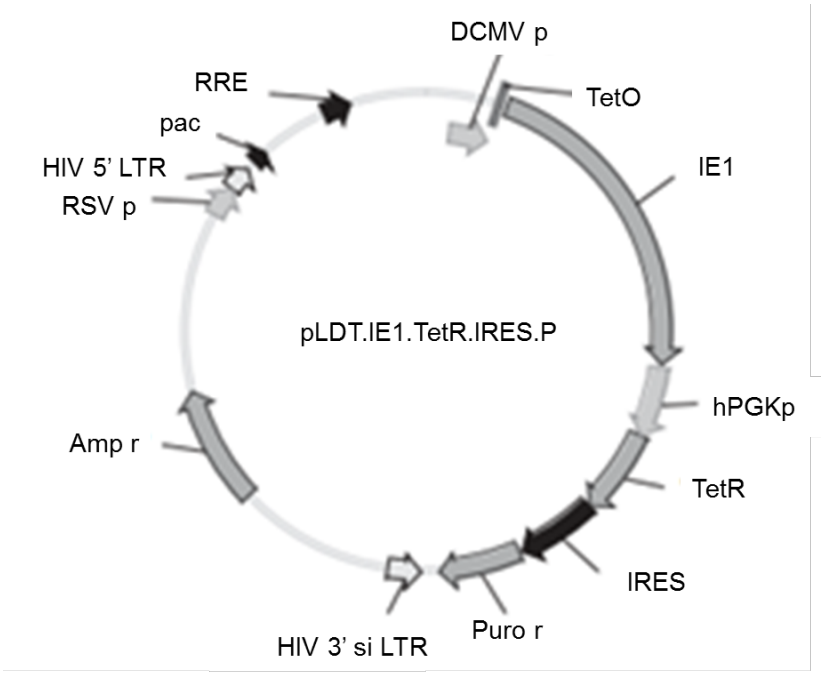

Figure 4.4 Plasmid map of pLDT.IE1.TetR.IRES.P vector.
The features of the plasmid are as described in the legend to Figure 4.1.

Plasmid pLDT.IE1.TetR.IRES.P was constructed in the same way as plasmid pLDT.ICP0.TetR.IRES.P. In brief, the ligation product was transformed into Stbl3 chemical competent *E.coli*. The resulting transformation mixture was plated on selective agar plates for overnight incubation. Single colonies were selected in the next day for miniprep plasmid extraction. Purified plasmids were sent for sequencing to confirm the viral gene sequence and plasmid structure. A maxiprep stock was prepared after DNA sequencing and this was then transfected into HEK-293T cells (with the helper plasmids) for lentivirus cultivation. HFT cells were tranduced by the resulting lentivirus for 24 h, then the transduced HFT cells were selected using puromycin for 2 weeks. The resulting HFT.IE1 cells were analysed by IF and WB (Figure 4.5).

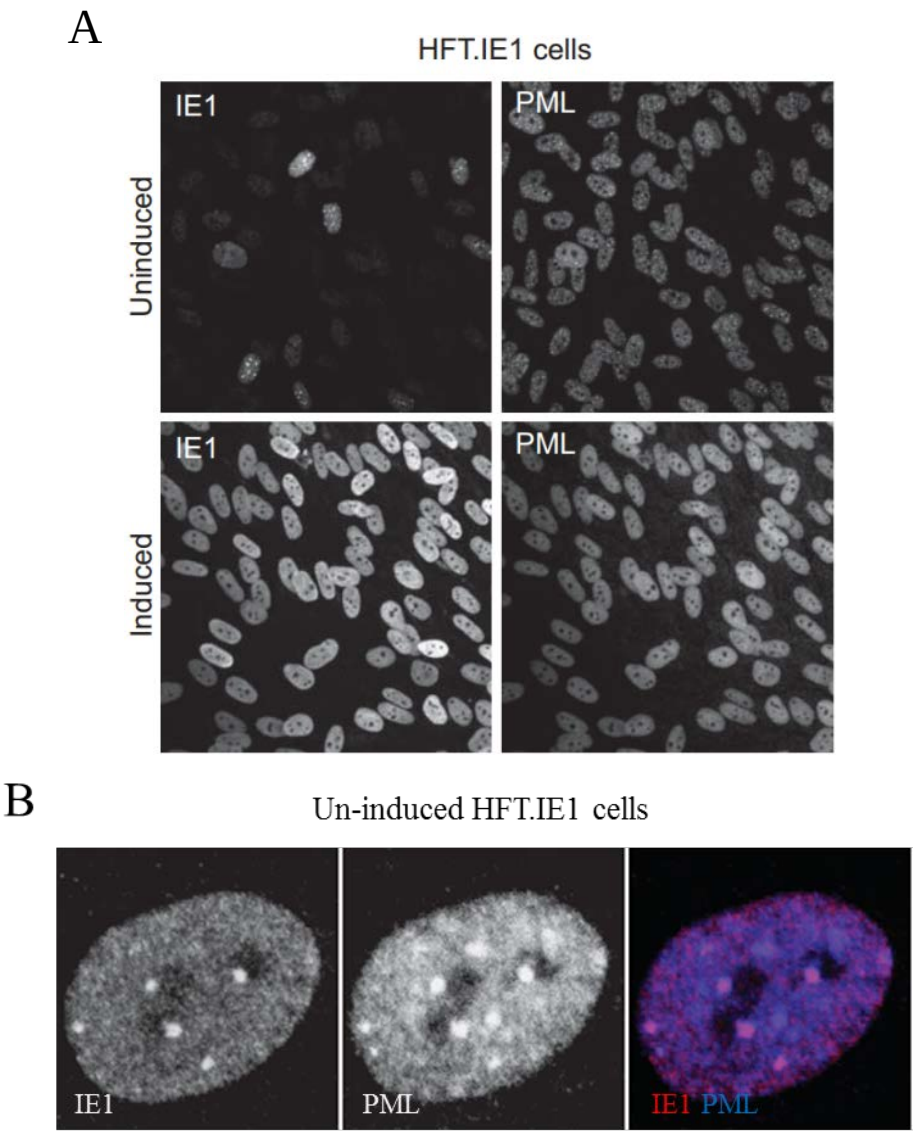

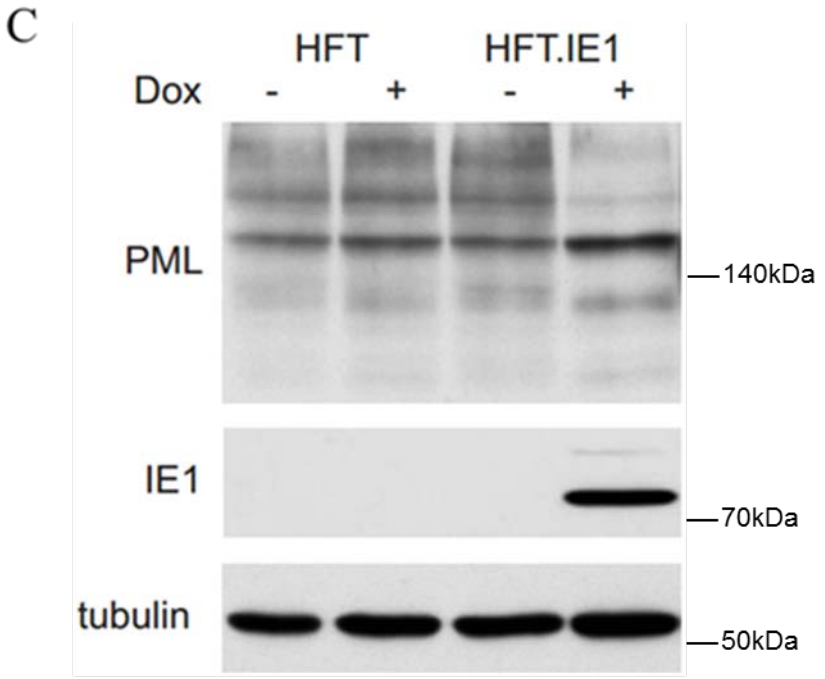

Figure 4.5 IF and WB analysis of HFT.IE1 cells.

(A) IF images of IE1 expression in HFT.IE1 cells. Induced cells were treated with DMEM containing 100 ng/ml doxycycline for 24 h. Uninduced and induced cells were fixed and permeabilized then stained with anti-IE1 mAb and anti-PML rAb as indicated. Secondary antibodies were AlexaFluor-conjugated anti-rabbit 633 and anti-mouse 555. (B) IF images of the IE1 signal in a proportion of uninduced HFT.IE1 cells. (C) WB analysis of IE1 expression. Induced and uninduced cells were treated with the same medium as for the IF assay. Cell lysates were collected and analysed by western blotting, probing with anti-IE1 mAb and anti-PML rAb as indicated. The positions of molecular weight standards (in thousands) are indicated to the right of each panel.

A proportion of uninduced HFT.IE1 cells expressed low levels of IE1 that could be detected by IE1 staining in IF (Figure 4.5 A), but this leaky expression of IE1 wasn't sufficient to disperse PML and it was not detected by WB (Figure 4.5 B, C). More than 95% of HFT.IE1 cells expressed IE1 after 24 h of induction, and this induced IE1 was sufficient to de-sumoylate PML (Figure 4.5 C) and disperse the PML in nucleus (Figure 4.5 A). Unlike the IE1 that was expressed at low level prior to induction (which co-localised with PML in ND10; Figure 4.5 B), induced high level expressed IE1 was dispersed throughout the nucleus (Figure 4.5 A). This functional analysis of IE1 expressed in HFT cells was consistent with that in HA.TetR.IE1 cells (Figure 3.3). PML expression in uninduced HFT.IE1 cells was the same as HFT controls, which is consistent with the IF analysis. The above data show that the IE1 expressed by lentivirus made from plasmid vector pLDT.IE1.TetR.IRES.P performed the same bioactivities as that expressed in HA.TetR.IE1 cells.

4.2.3 pp71 expression cell lines

A myc-tagged pp71 coding sequence was also inserted into the same vector used for inducible ICP0 and IE1 expression. However, it was found that the expression of myc-pp71 in the transduced cells was not high enough to give a detectable signal in WB analysis. Thus, the expression of myc-pp71 was achieved using the double vector system as introduced in section 3.1.2. A pp71 mutant (pp71 DID2/3) lentivirus vector (Everett *et al.*, 2013a) was also used as a control for expression of an inactive form of pp71 in this part of the experiments.

HFT cells were transduced by the lentivirus cultivated from HEF-293T cells transfected with plasmid pLKOneo.CMV.EGFPnlsTetR. The resulting cell line was selected using neomycin for 2 weeks. The second transduction used lentivirus cultivated from transfection with pLDT.myc.pp71 or pLDT.myc-pp71 DID2/3, and the transduced HFT.TetR cells were selected using blasticidin for 2 weeks. The study was also extended to express pp71 and IE1 simultaneously. Thus, HFT.TetR.myc-pp71 cells were transduced for the third time by pLDT.IE1.TetR.IRES.P and the resulting cells were selected using puromycin for 2 weeks. HFT.TetR, HFT.TetR.myc-pp71 DID2/3, HFT.TetR.myc-pp71 and HFT.TetR.myc-pp71.IE1 cells were induced and probed using anti-myc and anti-IE1 monoclonal antibodies (Figure 4.6).

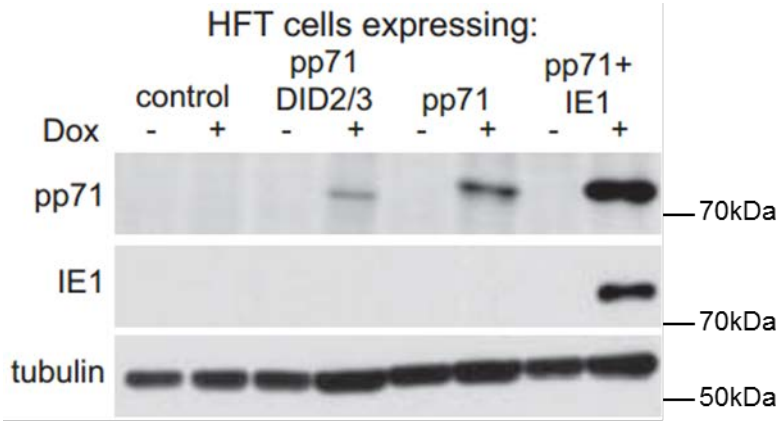

Figure 4.6 WB analysis of HFT.TetR, HFT.TetR.myc-pp71 DID2/3, HFT.TetR.myc-pp71 and HFT.TetR.myc-pp71.IE1 cell lines.

Cells were induced using DMEM with 100 ng/ml doxycycline for 24 h. Uninduced and induced cell lysates were collected and probed using anti-myc mAb, anti-IE1 mAb and anti-tubulin mAb as indicated. The positions of molecular weight standards (in thousands) are indicated to the right of each panel.

The pp71 protein was tagged with myc to simplify the detection by antibodies in this study. This approach has been applied in cellular expression systems in the laboratory and was also found suitable for functional pp71 expression (Everett *et al.*, 2013a). Expression of pp71 and IE1 together has been shown to largely complement the ΔICP0 HSV-1 infection in HepaRG-based cell lines (Everett *et al.*, 2013a). To confirm this activity in the HFT cell system, HFT.TetR.myc-pp71.IE1 cell line was also generated. The mutant pp71 DID2/3 protein was expressed in a lower amount compared with wt myc-tagged pp71, which was consistent with previous studies (Everett *et al.*, 2013a). Expression of pp71 in HFT.TetR.myc-pp71.IE1 cells was much higher than HFT.TetR.myc-pp71 cells (Figure 4.6), which might be due to a higher efficiency of transduction with the double vector system (perhaps because of reduced puromycin resistance expression from the single inducible vector, as noted above). Functional analysis of myc-pp71 and IE1 expressed in the above cell lines is described in the following sections.

4.3 IE1 and pp71 complement ICP0 null HSV-1 infection in HFT cells

That ICP0 can be replaced almost entirely by IE1 and pp71 acting together has been reported in previous work in HepaRG-based cells (Everett *et al.*, 2013a). The viral gene expression cell lines constructed here provide a chance to confirm this in HFT cells.

4.3.1 IE1 improves ICP0 null HSV-1 infection in HFT cells

HFT and HFT.EYFP cells were used as negative controls for HFT.IE1 cells in ΔICP0 HSV-1 complementation assays. The ΔICP0 HSV-1 infection protocols were similar to those used in the complementation assays described in section 4.2.1. Complementation efficiency in HFT.EYFP and HFT.IE1 cells was expressed as fold-increase in plaque formation over that in HFT cells (Figure 4.7).

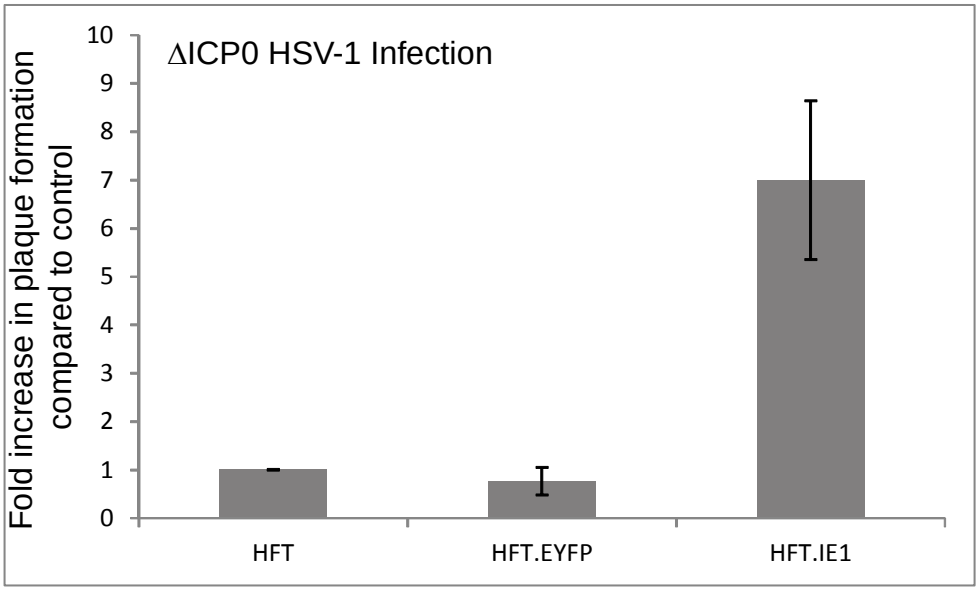

Figure 4.7 ΔICP0 HSV-1 complementation assays on HFT, HFT.EYFP and HFT.IE1 cell lines.

Induced cells were treated with DMEM containing 100 ng/ml doxycycline for 24 h prior to infection. At 4 h post infection, cell medium was replaced with DMEM with 100 ng/ml doxycycline and 1% human serum. Blue plaque assays were performed 24 h after infection. The results are expressed as fold-increases in absolute titre (PFU per ml) in each cell type over that in HFT cells. The same experiment was performed three times to work out an average figure and standard deviation.

Induced HFT.IE1 cells increased ΔICP0 HSV-1 plaque formation about 7-fold compared to HFT cells, which is lower than the same complementation assay performed in HA.TetR.IE1 cells (Everett *et al.*, 2013a). This might be related to differences between HFT and HepaRG-based cells or perhaps the expression level of IE1. To investigate in more detail about the consequences of IE1 expression in HFT cells, the same complementation assay was performed on pp71 and IE1 expression cell lines (see Section 4.3.3 below).

4.3.2 pp71 increases ICP0 null HSV-1 infection in HFT cells

It was found that pp71 can also complement ΔICP0 HSV-1 infection in HepaRG-based cells in a previous study (Everett *et al.*, 2013a) increasing the mutant virus plaque formation about 10-fold compared with control cells. Here, similar experiments were also performed on HFT.TetR.myc-pp71 cells, using. ΔICP0 HSV-1 infection protocols that were the same as the complementation assay described in section 4.2.1. Complementation efficiency of HFT.EYFP and HFT.TetR.myc-pp71 was expressed as fold-increase over that in HFT cells (Figure 4.8).

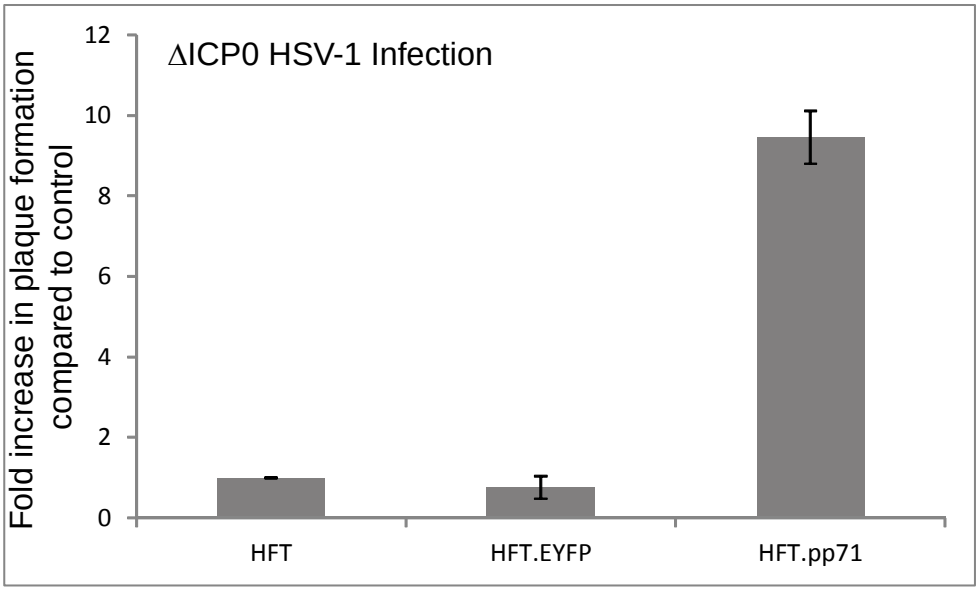

Figure 4.8 ΔICP0 HSV-1 complementation assays on HFT, HFT.EYFP and HFT.TetR.myc-pp71 cells.

Induced cells were treated with DMEM with 100 ng/ml doxycycline for 24 h prior to infection. At 4 h post infection, cell medium was replaced with DMEM with 100 ng/ml doxycycline and 1% human serum. Blue plaque assay were performed 24 h after infection. The results are expressed as fold-increases in absolute titre (PFU per ml) in each cell type over that in HFT cells. The same experiment was performed three times to work out an average figure and standard deviation.

4.3.3 IE1 and pp71 acting together can largely complement ICP0 null HSV-1 infection in HFT cells

It was demonstrated in a previous report that single expression of IE1 or pp71 increased ΔICP0 HSV-1 infection about 100- and 10-fold in HepaRG-derived cells respectively. The expression of IE1 and pp71 together achieved a greater increase, which was 400-fold (about half that of ICP0 in this cell type), on complementing ΔICP0 HSV-1 infection (Everett *et al.*, 2013a). To analyse the HFT.TetR.myc-pp71.IE1 cell line, the same experiment was performed. HFT, HFT.EYFP, HFT.TetR.myc-pp71.IE1 and HFT.ICP0 cells were seeded on 24-well plates and 24 h after treatment with 100 ng/ml doxycycline the cells were infected by ΔICP0 HSV-1 at different MOIs. On the next day, blue plaque assays were performed to collect the plaque formation efficiency data (Figure 4.9).

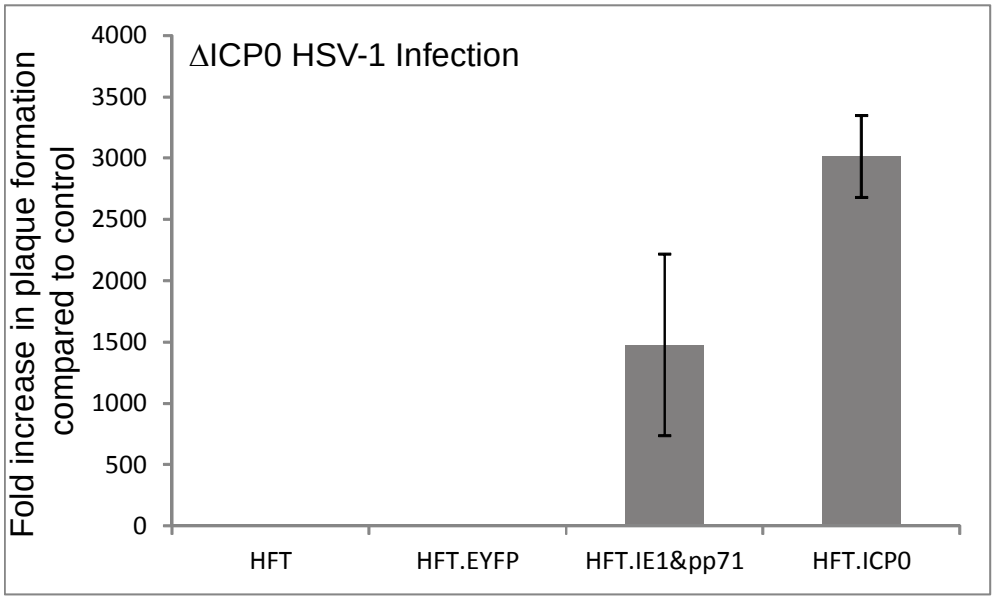

Figure 4.9 ΔICP0 HSV-1 complementation assays on HFT, HFT.EYFP, HFT.TetR.myc-pp71.IE1 and HFT.ICP0 cell lines.

The above cell lines were seeded on 24-well plates at $1x10^5$ cells/well. In the next day, cells were induced with DMEM containing 100 ng/ml doxycycline for 24 h prior to infection. Induced cells were infected by ΔICP0 HSV-1 at different MOIs from 0.004 to 1. At 4 h post infection, the cell medium was replaced with medium containing 100 ng/ml doxycycline and 1% human serum. Blue plaque assays were performed 24 h after infection. The results are expressed as fold-increases in absolute titre (PFU per ml) in each cell type over that in HFT cells. The same experiment was performed three times to work out an average figure and standard deviation.

HFT.ICP0 cell lines achieved a 3000-fold increase in plaque formation of the mutant virus over that in HFT cells, which was a further increase compared with the same experiment performed on HA.TetR.cICP0 cells. Meanwhile, the ΔICP0 HSV-1 infection complementation by HFT.TetR.myc-pp71.IE1 cells was also improved substantially from that achieved in cells expressing either IE1 or pp71 alone (compare Figures 4.7, 4.8 and 4.9). In general, the simultaneous expression of IE1 and pp71 achieved about 50% of the activity of ICP0 in this study, which is consistent with the previous report in HepaRG-based cells. Previous work using single knock down or triple knock down cell lines demonstrated that PML, Sp100 and hDaxx cooperatively repress HSV-1 infection (Glass & Everett, 2013). However, the triple knock down cell lines based on HFs and HepaRG cells increased ΔICP0 HSV-1 plaque formation by about 20- and 50-fold respectively, much less than that achieved by ICP0 itself. Taken with the 3000-fold increase in ICP0-expressing HFT cells in this study, the knock down of PML, Sp100 and hDaxx is not as efficient as either ICP0, or IE1 and pp71 acting together. This implies that ICP0 has additional functions besides the interaction with ND10 components, or possibly that

residual protein expression in the shRNA expressing cells is sufficient to mediate significant repression. Meanwhile, the cooperation of IE1 and pp71 increase the infection of ΔICP0 HSV-1 about 1500-fold which is still much more efficient than knock down in HFT-derived cells of three ND10 components that are affected by ICP0. This illustrates the notion that IE1 and pp71 not only share common targets within ND10 with ICP0, but also perhaps other mechanisms to stimulate HSV-1 gene expression.

4.4 IE1 and ICP0 enhance wt HCMV infection

Plaque formation by wt HCMV was increased about 20-fold in HF cells that had been depleted of PML, Sp100 and hDaxx by shRNA (Glass & Everett, 2013), and wt HCMV infection is also increased in cells singly depleted of PML, hDaxx or Sp100, or a combination of PML and hDaxx (Tavalai *et al.*, 2006; Tavalai *et al.*, 2008b). Because PML was degraded by ICP0 expression in HFT.ICP0 cells (Figure 4.2), and by extension from the known effects of ICP0 on Sp100 and hDaxx, plaque formation and viral gene expression of wt HCMV on HFT.ICP0 and HFT.IE1 cells were investigated.

4.4.1 Cultivation of wt HCMV

HCMV strains Towne (TNwt) and AD169 are widely studied laboratory HCMV strains which have been highly passaged and adapted to infect and replicate in cultured human diploid fibroblasts. An earlier study using cells analogous to HFT.IE1 cells (made using the double transduction method) found increased wt HCMV infection on induced cells, with a reduced cultivation time and higher titres (Knoblach *et al.*, 2011). In this study, stocks of TNwt and AD169 that had been cultivated in human fibroblasts were obtained and then cultivated on induced HFT.IE1 cells. After the initial infection for 2 days, the medium was changed so that the eventual virus stocks were in doxycycline-free medium. Virus stocks were then titrated on HFT.IE1 cells.

4.4.2 Prior expression of IE1 and ICP0 facilitates wt HCMV infection

To investigate whether prior expression of ICP0 and IE1 could enhance wt HCMV infection, three wt HCMV strains were used to infect HFT.IE1 and HFT.ICP0 cells. These were TNwt, AD169 and strain TBE40 (TBwt). TNwt and AD169 were cultivated in HFT.IE1 cells whereas TBwt was a relatively low passage strain that was provided by Dr Michael Nevels and was used without further passage in the laboratory here. Meanwhile,

another HCMV strain, TBrvlIE1, an IE1 repaired version of the TBE40 IE1 deletion mutant TBdlIE1 (see below), was also used in this study.

Doxycycline treated or untreated HFT, HFT.IE1 and HFT.ICP0 cell lines were infected by TNwt at sequential dilutions determined empirically to give countable numbers of plaques on each cell line. At 4 h post infection, cell medium was changed to DMEM with 100 ng/ml doxycycline (for induced cells only) and 1% human serum. Infected cells were incubated at 37℃ for a further 7 days. The infected cells were fixed and permeabilized for histochemical staining of HCMV plaques to collect the plaque formation efficiency data. The same experiment was performed three times to work out an average figure and standard deviation.

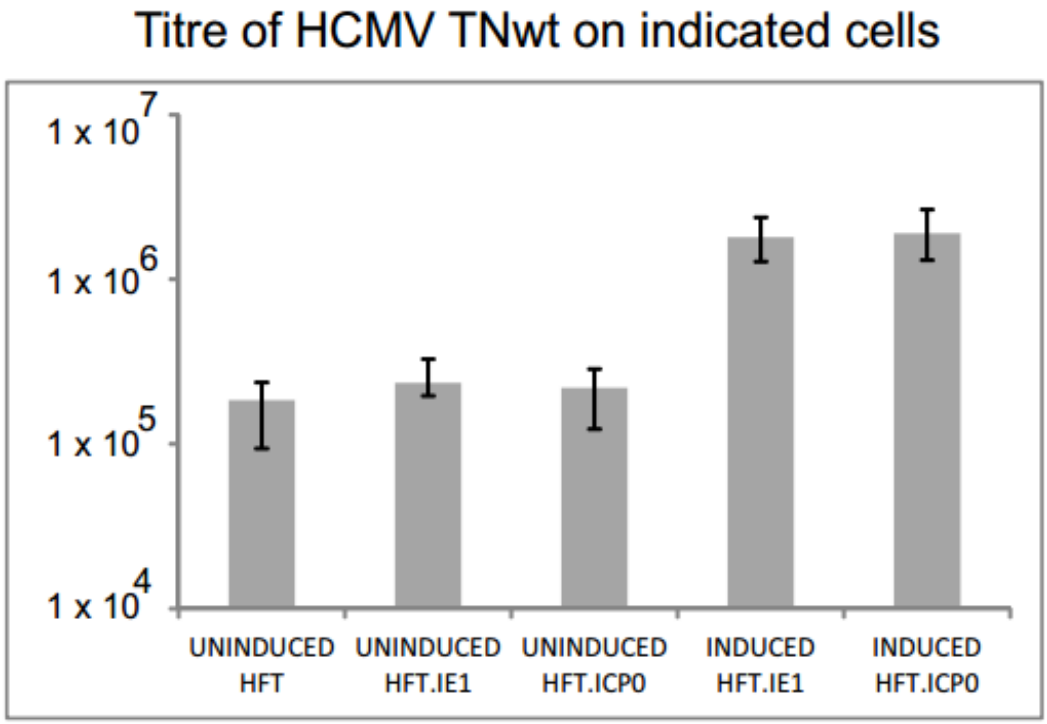

Figure 4.10 TNwt infection on HFT, HFT.IE1 and HFT.ICP0 cell lines.
Induced cells were incubated in DMEM with 100 ng/ml doxycycline for 24 h prior to infection. Uninduced and induced cells were infected by TNwt at different MOIs. At 4 h post infection the cell medium was replaced to routinely maintain cell culture with 100 ng/ml doxycycline (for induced cells) and 1% human serum. HCMV plaque assays were performed by histochemical staining at 7 days after infection. Anti-UL44 mAb was used to detect HCMV plaques. The secondary antibody was sheep horse radish peroxidase conjugated anti-mouse IgG antibody A4416. The results are expressed as PFU per ml in each cell type.

Both IE1 and ICP0 enhanced the TNwt plaque formation by about 20-fold compared with HFT and uninduced cells, which is similar to the increase in wt HCMV plaque formation

in triple knock down cell lines (PML, hDaxx and Sp100) described in previous work (Glass & Everett, 2013). The expression of IE1 by TNwt was sufficient for estimating the efficiency of viral infection observed in HFT cells, whereas prior expression of the extra IE1 expressed in the HFT.IE1 cells created a scenario similar to a higher MOI infection. These data are consistent with the hypothesis that even wt HCMV infection is restricted by cellular factors that reduce the probability of plaque formation, and that prior expression of IE1 or ICP0 increases the probability that a cell receiving a virus particle will become lytically infected. AD169 was also used in the same study and performed in a similar manner as with TNwt, giving essentially similar results. (Figure 4.11)

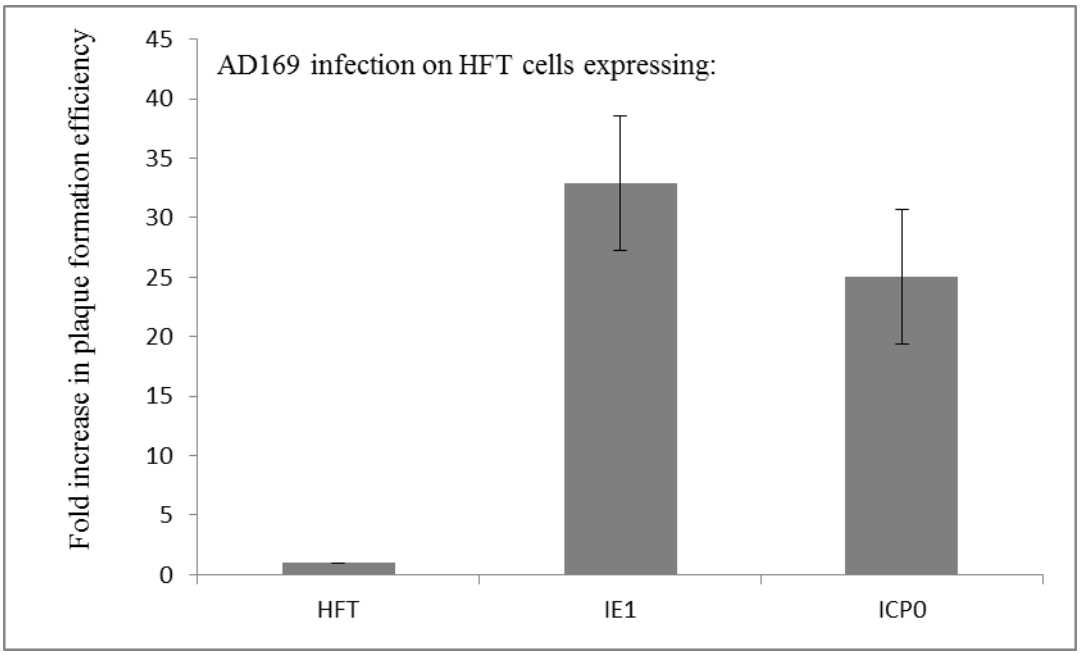

Figure 4.11 AD169 infections on HFT, HFT.IE1 and HFT.ICP0 cell lines.

Cells were induced by treatment with DMEM containing 100 ng/ml doxycycline for 24 h prior to infection. Then, the cells were infected by AD169 at sequential dilutions determined empirically to give countable numbers of plaques on each cell line. At 4 h post infection, the cell medium was replaced with DMEM containing 100 ng/ml doxycycline and 1% human serum. HCMV plaque assays were performed at 7 days after infection. Anti-UL44 mAb was used to detect HCMV plaques. The results are expressed as fold-increase in absolute titre (PFU per ml) in each cell type over that in HFT cells. The same experiment was performed three times to work out an average figure and standard deviation.

TNwt and AD169 are extensively passaged HCMV strains that lack several genes possessed by clinical isolated strains. To investigate whether this phenomenon occurred only with laboratory adapted strains, the same infection experiment was performed using stocks of TBwt titrated on HFT.IE1 cells. Doxycycline induced cells were infected with

TBwt at different MOIs. The results are expressed as plaque formation efficiency relative to that in HFT cells (Figure 4.12).

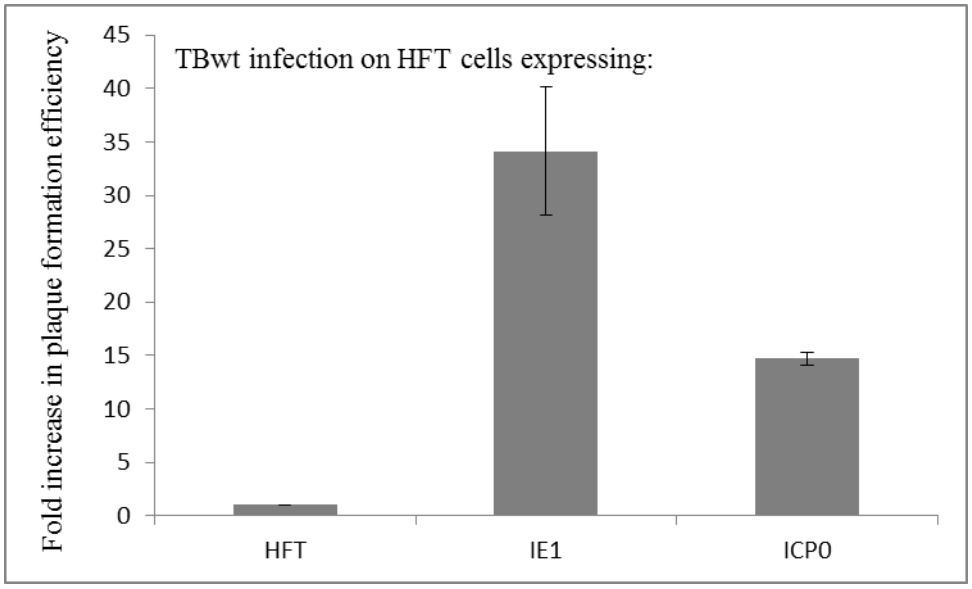

Figure 4.12 TBwt plaque assays on HFT, HFT.IE1 and HFT.ICP0 cell lines.

Cells were seeded on 24-well plates at $1x10^5$/well. In the next step, cells were treated with DMEM with 100 ng/ml of doxycycline for 24 h and infected by TBwt at sequential dilutions determined empirically to give countable numbers of plaques on each cell line. At 4 h post infection, the cell culture was changed to routine culture medium with 100 ng/ml doxycycline and 1% human serum. HCMV plaque assays were performed 7 days after infection by anti-UL44 mAb staining. The results are expressed as fold-increase in absolute titre (PFU per ml) in each cell type over that in HFT cells. The same experiment was performed three times to work out an average figure and standard deviation.

HCMV strain TBwt infection was increased by IE1 and ICP0 in a similar manner as TNwt and AD169, with IE1 being around 2-fold more effective than ICP0. The data above confirmed that even though the IE1 expressed by HCMV is efficient enough to initiate the lytic infection in host cells, the prior expression of these ND10 disrupting proteins increases the probability of lytic viral infection. Considering the similarities between IE1 and ICP0, it is perhaps not surprising that ICP0 could facilitate the infection of HCMV.

TBrvIE1 is a revertant of TBdlIE1 HCMV strain (Zalckvar *et al.*, 2013) that performed in a similar manner as TBwt during titration on HFT.IE1 and HFT.ICP0 cells (Figure 4.13).

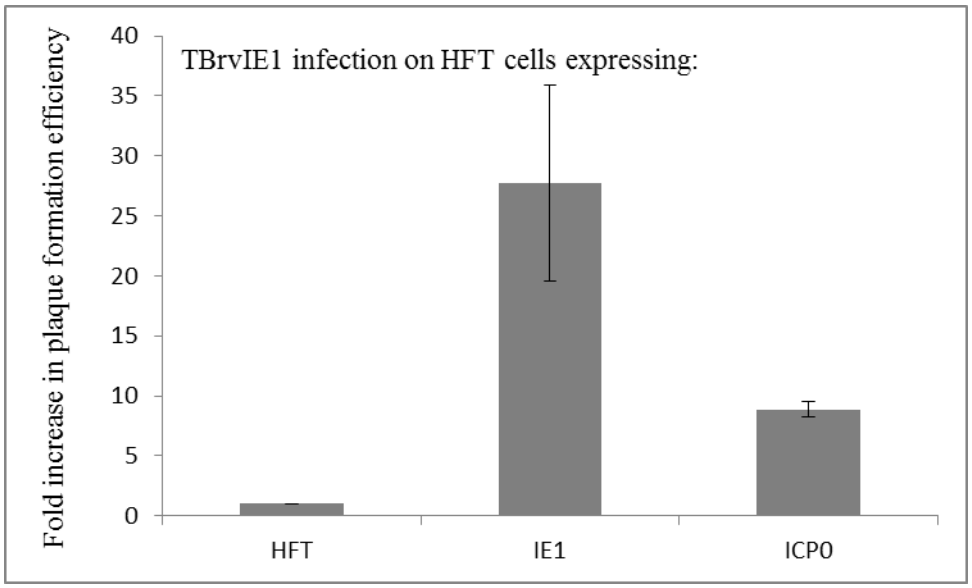

Figure 4.13 TBrvIE1 infections of HFT, HFT.IE1 and HFT.ICP0 cell lines. Experimental details are as described in the legends to figures 4.10 – 4.12.

The plaque assays presented above illustrate that the titre of any stock of even wt HCMV varies with the cell type or line in which it was determined. Conventionally, most studies have used titres determined in normal human diploid fibroblasts as the basis for calculating the amount of virus stock to be used for a given multiplicity of infection. The work presented in this chapter, however, analyses a number of IE1 mutant HCMV strains whose titres must of necessity be determined on IE1 complementing cells. In order to maintain consistency between the amounts of wt and mutant viruses when used in parallel, it was therefore important to use the wt viruses according to their titres on IE1 complementing cells. The results of Figures 4.10 – 4.13 indicate that these MOIs will be 10- to 30-fold lower than if the MOIs were calculated on the basis of titres in ordinary HFT cells. In consequence, in the experiments presented below, all experiments were performed at what would be defined as low MOI on the basis of titres in HFT cells.

4.4.3 IE1 and ICP0 enhance immediate-early and late gene expression of wt HCMV

The data above demonstrated the plaque formation efficiency of wt HCMV can be increased by prior expression of IE1 and ICP0. In this section, WB and IF were applied to observe the enhancement of HCMV infection in HFT.IE1 and HFT.ICP0 cells. Different gene expression products were detected by WB to investigate HCMV replication (Figure 4.14). HFT.ICP0 cells were seeded in a 24-well plate, induced on the next day, then the induced cells were infected by TNwt at MOI 1 after 24 h of induction. At 4 h post

infection, the cell medium was replaced with DMEM containing 100 ng/ml doxycycline and 1% human serum. A control experiment using uninduced cells was performed in parallel. Cell lysates were collected at 24 h, 48 h, 72 h and 96 h post infection and probed by antibodies as indicated. A mock infected cell lysate was collected at 48 h post induction.

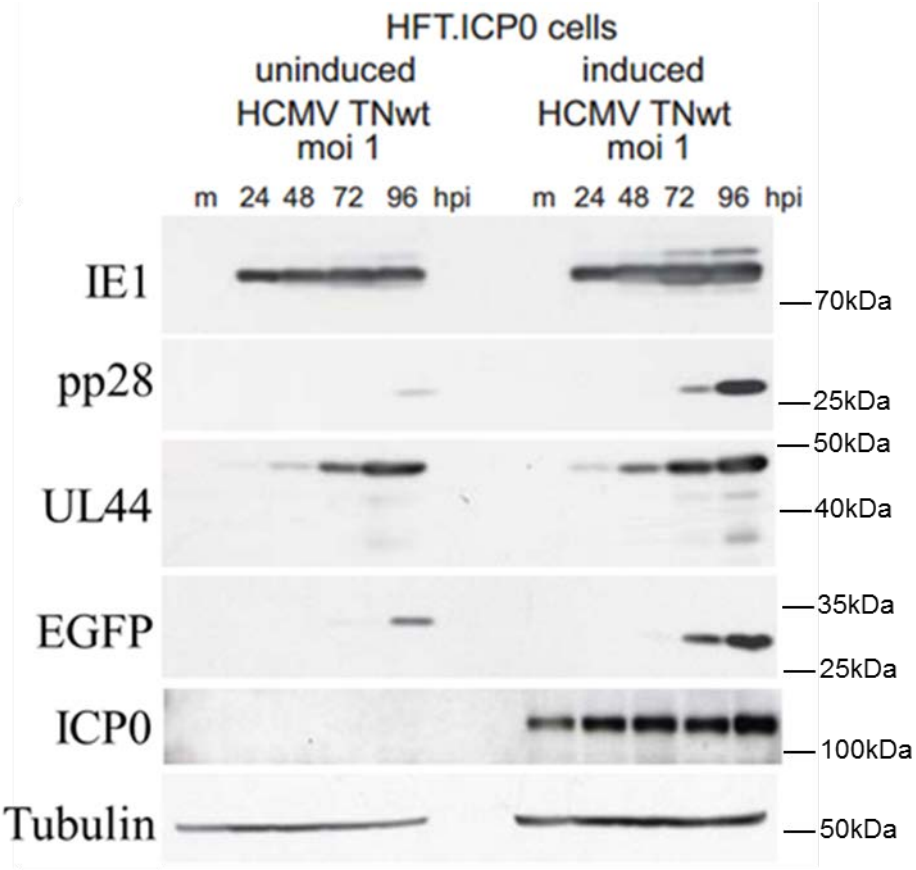

Figure 4.14 WB analysis of gene expression during wt HCMV infection in HFT.ICP0 cells.

HFT.ICP0 induced cells and uninduced cells were infected by TNwt at MOI 1. Samples were collected at 24 h, 48 h, 72 h and 96 h after infection then probed with anti-IE1 mAb E13, anti-pp28 mAb, anti-UL44 mAb, anti-GFP rAb, anti-ICP0 mAb 11060 and anti-tubulin mAb, as indicated. Tubulin was a loading control. The positions of molecular weight standards (in thousands) are indicated to the right of each panel.

HCMV genes expressed at different stages of HCMV infection were probed with relevant antibodies: IE1 is expressed at the immediate early stage of HCMV infection, UL44 is expressed in the early phase prior to DNA replication and pp28 is expressed in the late stage after DNA replication has commenced. EGFP is a SV40-driven EGFP marker gene inserted into a non-essential region of the U_S segment of TNwt viral genome that was shown to express in early or late stage of viral infection (Marchini *et al.*, 2001). ICP0 was

steadily expressed in HFT cells with a slight increase within 96 h of HCMV infection. Prior and continuing ICP0 expression stimulated HCMV immediate-early, early and late gene expression as indicated in WB analysis, with the effect on IE1 being relatively slight, but expression of both UL44 and pp28 started earlier and accumulated to higher levels in the induced HFT.ICP0 cells. These data are consistent with the plaque formation data presented above.

IF analysis provides detail of gene expression in single HCMV infected cells and also plaque forming efficiency. HFT cells were seeded on coverslips at $1x10^5$ cells/well in 24-well plates. After 24 h induction by doxycycline, cells were infected by TNwt at different MOIs as indicated in Figure 4.15. After 4 days of infection, the infected cells were fixed and permeabilized for IF analysis using anti-IE2 mAb staining and EGFP autofluorescence detection as a surrogate for Late gene expression.

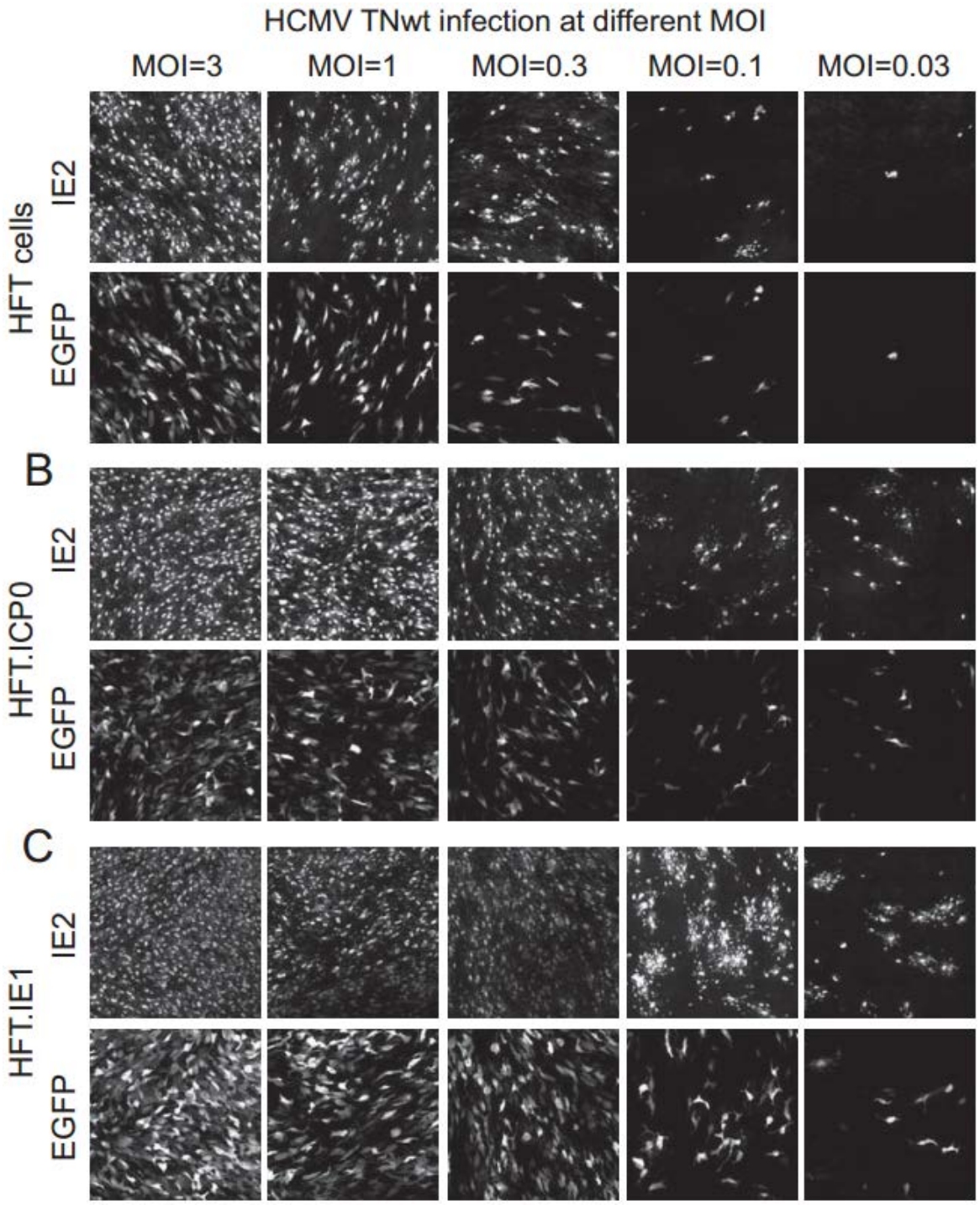

Figure 4.15 IF analysis of TNwt infection on HFT, HFT.IE1 and HFT.ICP0 cell lines.

Cells were treated with DMEM containing 100 ng/ml doxycycline for 24 h prior to infection. HFT, HFT.IE1 and HFT.ICP0 induced cells were infected by TNwt at different MOI as indicated. Cell medium was replaced to DMEM with 100 ng/ml doxycycline and 1% human serum at 4 h post infection. Coverslips were collected after 4 days infection. Then the cells were fixed and permeabilized for anti-IE2 mAb staining.

TNwt infection at MOI 3 was similar among three cell lines with slightly stronger EGFP expression in HFT.IE1 cells. In this scenario, more than one virus particle invaded a single cell and hijacked the host cell machinery to express viral genes. This led to a certain

amount of cell death or cytopathic effect during the 4 day incubation. Differences between HFT and the IE1 and ICP0 expressing cell lines begin to appear when the MOI was lowered to 1. For HFT.IE1 cells, every viable HCMV viral particle could infect a single cell under the facilitation provided by the IE1 expressed in the host cell, and there was a similar situation in HFT.ICP0 cells during HCMV infection at MOI 1. The infection in HFT cells was different than in the other two cell lines, as the effective MOI was effectively lower than 1 in this cell line and this was indicated by IE2 staining and particularly EGFP expression. The increase in HCMV infection by IE1 and ICP0 compared to the situation in HFT cells was more significant at MOI 0.3 and MOI 0.01. At MOI 0.03, there was only one positive cell observed on the HFT cell coverslip, whereas around 20 plaques were observed in the fields of view of HFT.ICP0 and HFT.IE1 cells. At this MOI the proportion of initially uninfected cells allows the development of plaques. This increase in plaque number represents the IE1 and ICP0 enhancement of HCMV infection, while the increase in viral gene expression, is indicated by detection of IE2 and EGFP. The IF images of TNwt infection at MOI 0.03 indicate that the expression of IE2 and EGFP were more efficient in HFT.IE1 than HFT.ICP0 cells.

Plaque formation efficiency assays in section 4.4.2 demonstrated that IE1 and ICP0 expression also increased TBwt infection. To investigate more detail about TBwt infection on HFT.IE1 and HFT.ICP0 cells, IF analysis was performed. TBwt virus stock was titrated on HFT.IE1 cells prior to IF analysis. HFT, HFT.IE1 and HFT.ICP0 cells were infected by TNwt at MOI 1, then at 4 days post infection, the cells were fixed and permeabilized for anti-IE2 mAb and anti-UL44 mAb staining (Figure 4.16).

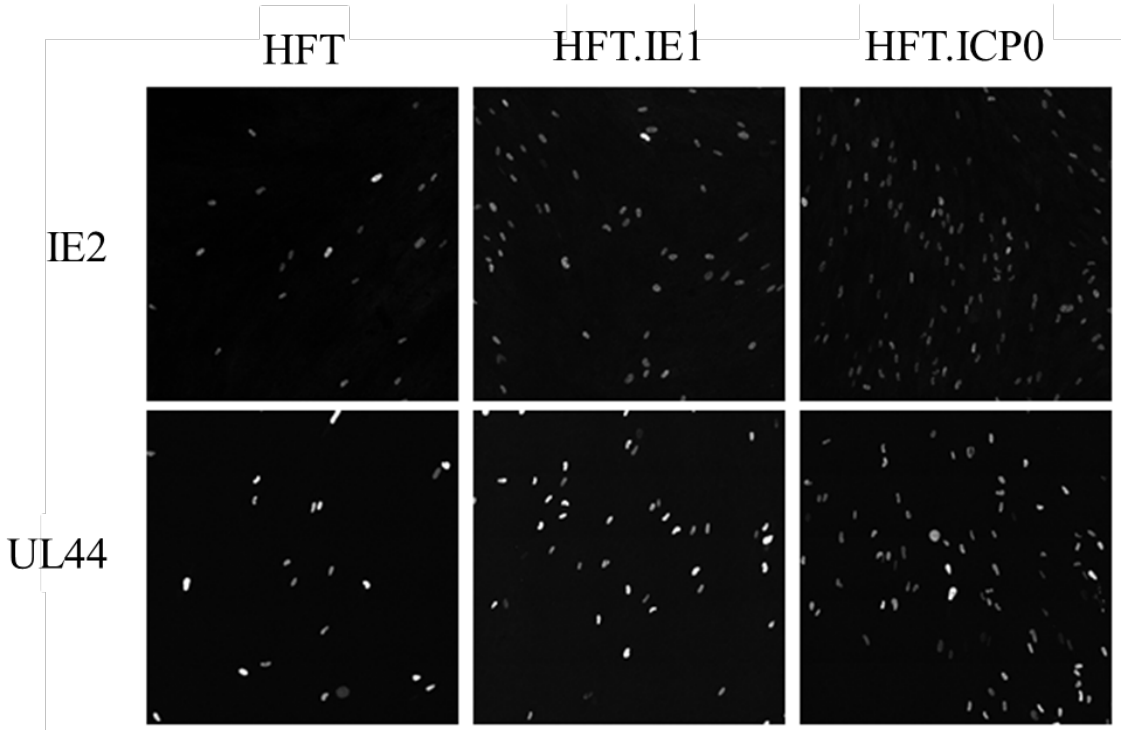

Figure 4.16 Confocal immunofluorescence images of TBwt infection on HFT, HFT.IE1 and HFT.ICP0 cell line.

Cells were induced with DMEM contains 100 ng/ml of doxycycline for 24 h prior to infection. HFT, HFT.IE1 and HFT.ICP0 induced cells were infected by TBwt at MOI 1, then at 4 h post infection, the cell medium was replaced with DMEM with 100 ng/ml doxycycline and 1% human serum. Coverslips were collected after 4 days infection, then the cells were fixed and permeabilized for anti-IE2 mAb and anti-UL44 mAb staining as indicated.

The IE2 and UL44 expression were increased in HFT.IE1 and HFT.ICP0 cells compared with HFT cells, consistent with the TNwt infection. The viral gene expression was different between TNwt and TBwt. The IE2 expression of TBwt was less efficient than TNwt in the same cell line infection. This might be due to the TNwt strain's adaptation to human fibroblast cells, but these experiments were done when time for experimental work was very limited. It would be necessary to confirm any differences between TBwt and TNwt infections using independently grown and titrated stocks before any firm conclusions could be reached.

4.5 IE1 but not ICP0 complements IE1-null mutant HCMV infection

The infection of ΔIE1 HCMV is highly impaired at low MOI but similar to wt HCMV at high MOI (Greaves & Mocarski, 1998). It is likely that the accumulation of IE and E gene

products is necessary for efficient HCMV lytic infection. The previous section demonstrated that ICP0 increases HCMV plaque formation efficiency and viral gene expression. Furthermore, IE1 was demonstrated to complement ΔICP0 HSV-1 infection and achieved 50% of the complementation efficiency of ICP0 when expressed simultaneously with pp71. The similarities between IE1 and ICP0 led to studies on the potential complementation activity of ICP0 on ΔIE1 HCMV strains. In this section, whether ICP0 could replace IE1 was investigated using strain Towne and TBE40 IE deletion mutants, TNdlIE1 and TBdlIE1, in complementation assays. The results are described below.

4.5.1 IE1 complements IE1 null HCMV infection

Many laboratories working on HCMV grow ΔIE1 HCMV mutants using IE1 expression cell lines (Gawn & Greaves, 2002; Greaves & Mocarski, 1998; Mocarski *et al.*, 1996). The IE1 mutant TNdlIE1 (Knoblach *et al.*, 2011) used in this section was also grown and titrated on HFT.IE1 cells. To keep the 'clinical' HCMV strain TBE40 and its IE1 deletion mutant derivative TBdlIE1 (Zalckvar *et al.*, 2013) within a low passage number, TBdlIE1 was not further cultivated on HFT.IE1 cells and was used direct from the stock provided by Dr Michael Nevels. For preparation of stocks of TNdlIE1, induced HFT.IE1 cells were infected at MOI 1 in 90 mm plates, then at 12 h post infection, the cell medium was replaced to DMEM without doxycycline. After 10 days of infection, the infected HFT.IE1 cell medium was collected, centrifuged to clarify, and titrated on induced HFT.IE1 and HFT cells. The collected TNdlIE1 stock was kept at -70 ℃ to maintain infectivity.

To ensure that equivalent amounts of potentially infectious TNwt and TNdlIE1 were used, both viruses were titrated on HFT.IE1 cells. The virus titre was expressed as PFU per ml for each HCMV strain. Both HCMV strains were used to infect $1x10^5$ HFT cells at MOI 1, then the infected cell medium was changed to DMEM with 1% human serum at 4 h post infection. The infected cell lysates were collected at different time points as indicated in Figure 4.17. The WB membrane was probed for HCMV proteins expressed at different infection stages.

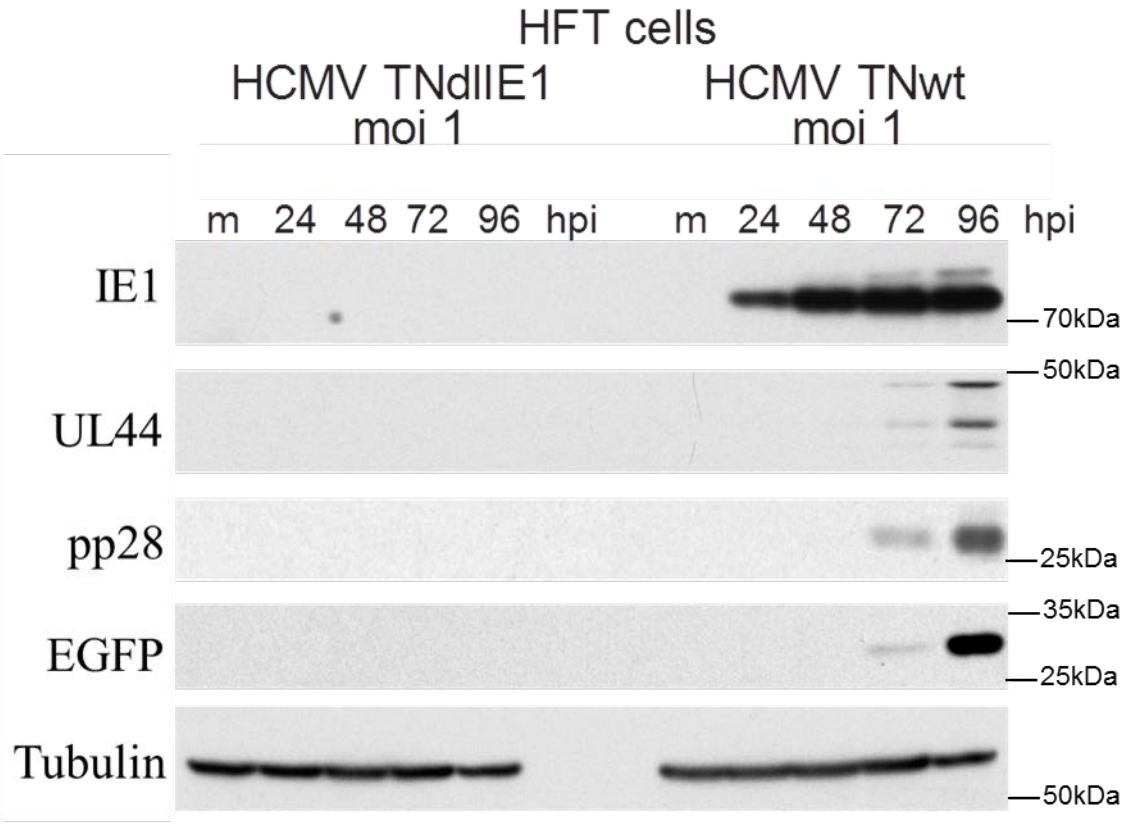

Figure 4.17 WB analysis of TNdlIE1 and TNwt infection of HFT cells.

HFT cells were seeded on 24-well plates at 1 x 10^5 cells/well. On the next day, the cells were infected by TNwt and TNdlIE1 at MOI 1 (titrated on induced HFT.IE1 cells). Cell lysates were collected at 24 h, 48 h, 72 h and 96 h post infection and probed with anti-IE1 mAb, anti-pp28 mAb, anti-UL44 mAb, anti-GFP rAb and anti-Tubulin mAb as indicated. The positions of molecular weight standards (in thousands) are indicated to the right of each panel.

At MOI 1, TNwt infected and replicated efficiently in HFT cells, whereas viral gene expression by TNdlIE1 was highly impaired. This is consistent with the previous report (Greaves & Mocarski, 1998) given that, as explained above, this was effectively a low MOI infection of HFT cells.

Figure 4.18 demonstrates the complementation of TNdlIE1 by IE1 expressed in HFT.IE1 cells. The expression of IE1 in HFT cells efficiently complemented the TNdlIE1 infection. The previously observed IE1 expression in HFT.IE1 cells prior to induction (Figure 4.5) was not sufficient to stimulate TNdlIE1 into lytic infection.

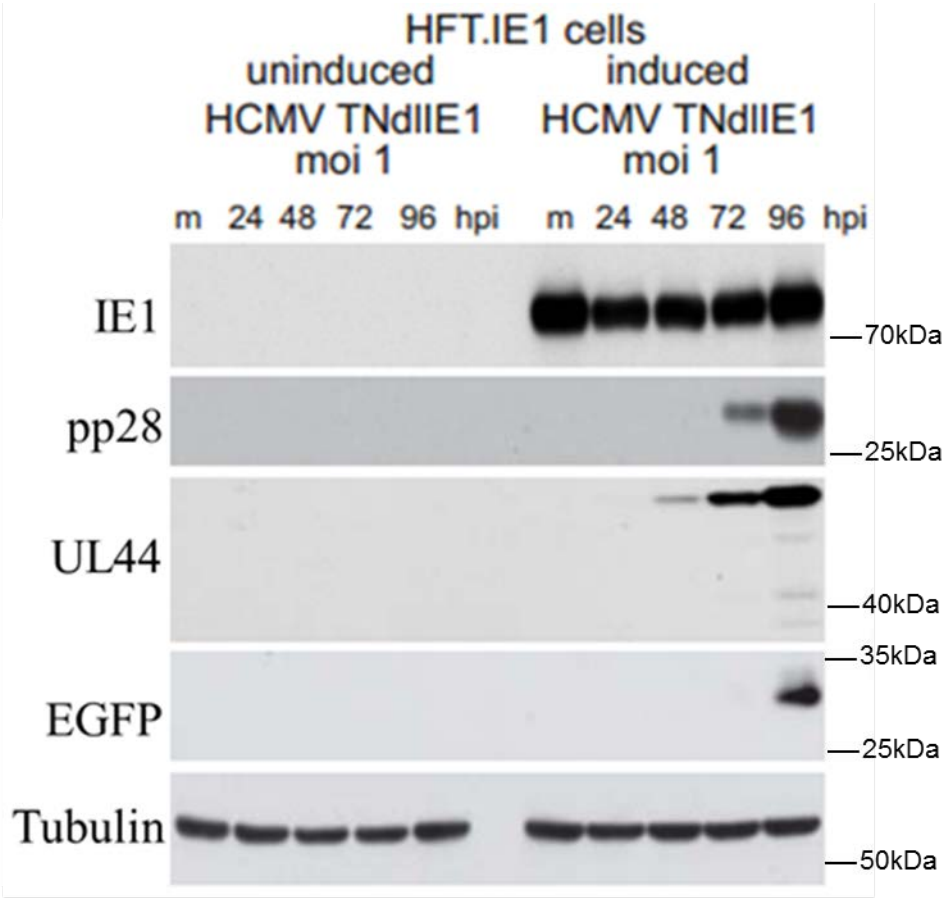

Figure 4.18 WB analysis of TNdlIE1 infection of HFT-IE1 cells.

Induced and uninduced HFT.IE1 cells were infected by TNdlIE1 at MOI 1. Cell lysates were collected at 24 h, 48 h, 72 h and 96 h post infection and probed with anti-IE1 mAb, anti-pp28 mAb, anti-UL44 mAb, anti-GFP rAb and anti-Tubulin mAb as indicated. The positions of molecular weight standards (in thousands) are indicated to the right of each panel.

4.5.2 ICP0 does not complement IE1 null HCMV lytic infection but does enhance IE2 expression

ICP0 expressed in HFT cells was shown to efficiently complement ΔICP0 HSV-1 infection and induce PML degradation in section 4.2.1. Therefore, whether ICP0 complements for the absence of IE1 during HCMV infection could be investigated by TNdlIE1 infection of induced HFT.ICP0 cells. The potential complementation by ICP0 of IE1 null mutant HCMV infection was investigated by WB, IF and plaque assays using both the laboratory strain TNdlIE1 and relatively low passage strain TBdlIE1. The results are shown below.

WB analysis of TNdlIE1 complementation assay on HFT.ICP0 cells was performed in a similar manner to that of TNdlIE1 infection of HFT.IE1 cells. Briefly, HFT.ICP0 cells were seeded in the first day in 24-well plates. After 24 h induction, induced and uninduced

cells were infected by TNdlIE1 at MOI 1 (titrated on induced HFT.IE1 cells), then infected cell lysates were collected at 24 h, 48 h, 72 h and 96 h post infection. Samples were resolved on 7.5% and 10% polyacrylamide gels and viral genes products were detected using different antibodies as indicated (Figure 4.19). The infected cell samples were analysed by WB and probed for HCMV immediate early, early and late protein expression.

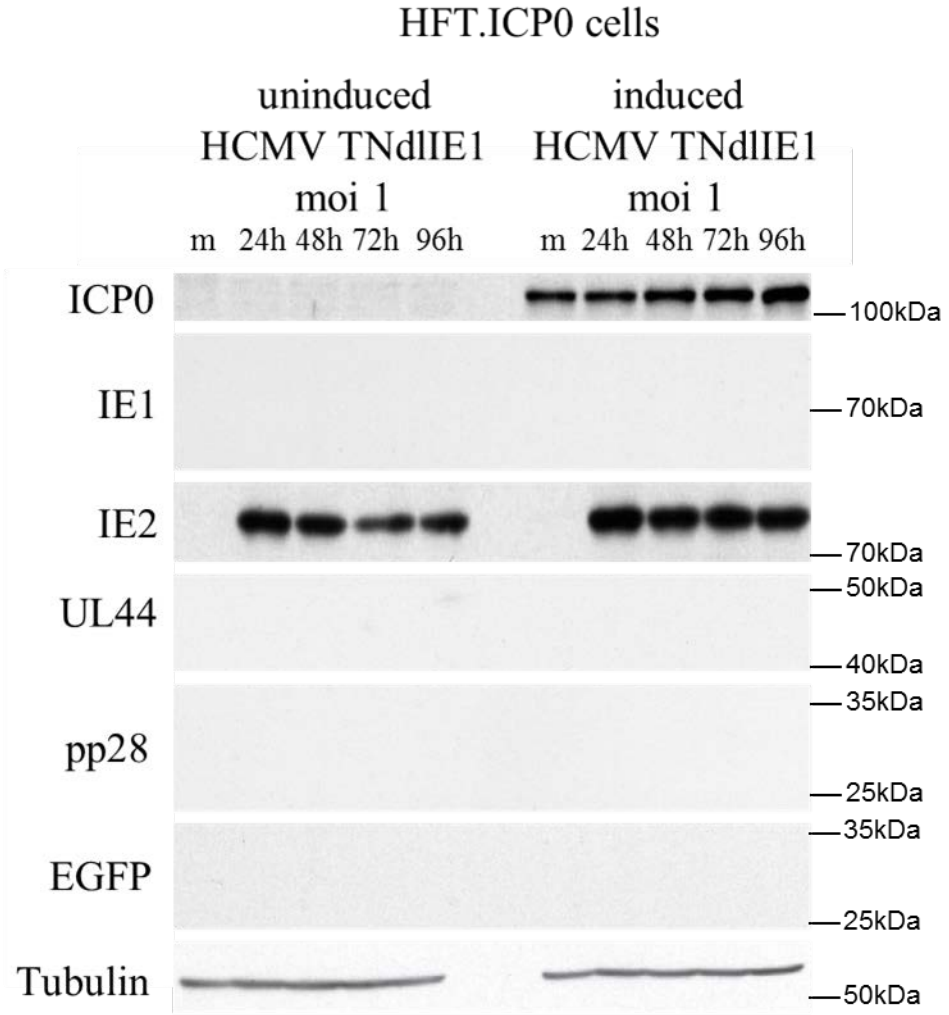

Figure 4.19 WB analysis of TNdlIE1 infection on induced and uninduced HFT.ICP0 cells.

HFT.ICP0 cells were seeded on 24-well plates at $1x10^5$cells/well. Induced cells were treated with doxycycline for 24 h before infection. Uninduced and induced cells were infected by TNdlIE1 at MOI 1, then at 4 h post infection, the medium was replaced to routine medium with 100 ng/ml doxycycline and 1% human serum for induced cells and routine medium with 1% human serum for uninduced cells. Samples were collected at 24 h, 48 h, 72 h and 96 h post infection then probed with anti-ICP0 mAb, anti-IE1 mAb, anti-pp28 mAb, anti-UL44 mAb, anti-GFP rAb and anti-Tubulin mAb as indicated. The positions of molecular weight standards (in thousands) are indicated to the right of each panel.

Even though ICP0 degrades PML and Sp100 more efficiently than IE1, it cannot replace IE1 in stimulating Early and Late IE1 mutant HCMV gene expression, although some increase in IE2 expression was observed. This indicated that besides its effects on PML and Sp100, IE1 has HCMV specific activities that cannot be provided by ICP0 and which are required to initiate efficient lytic infection.

A similar experiment was performed to investigate plaque formation by TNdlIE1 on HFT-ICP0 cells, also with negative results, with no plaques formed by the mutant virus in induced HFT-ICP0 cells at any dilution used. Compared to the number of plaques obtained with the same dilutions in induced HFT-IE1 cells, the plaque forming defect of TNdlIE1 in HFT-ICP0 cells was estimated to be at least 5000 times.

In order to investigate in more detail TNdlIE1 infection of HFT.ICP0 cells, IF analysis was performed. HFT, HFT.IE1 and HFT.ICP0 cells were seeded on coverslips and infected by TNdlIE1 at MOI 1, then at 5 days post infection the cells were fixed and permeabilized for anti-IE2 mAb staining. The secondary antibody for IE2 was AlexaFluor 555-conjugated anti-mouse IgG. EGFP expression from the reporter gene inserted into a non-essential region of the Us segment of TNdlIE1 is indicative of viral replication and Late gene expression (Figure 4.20).

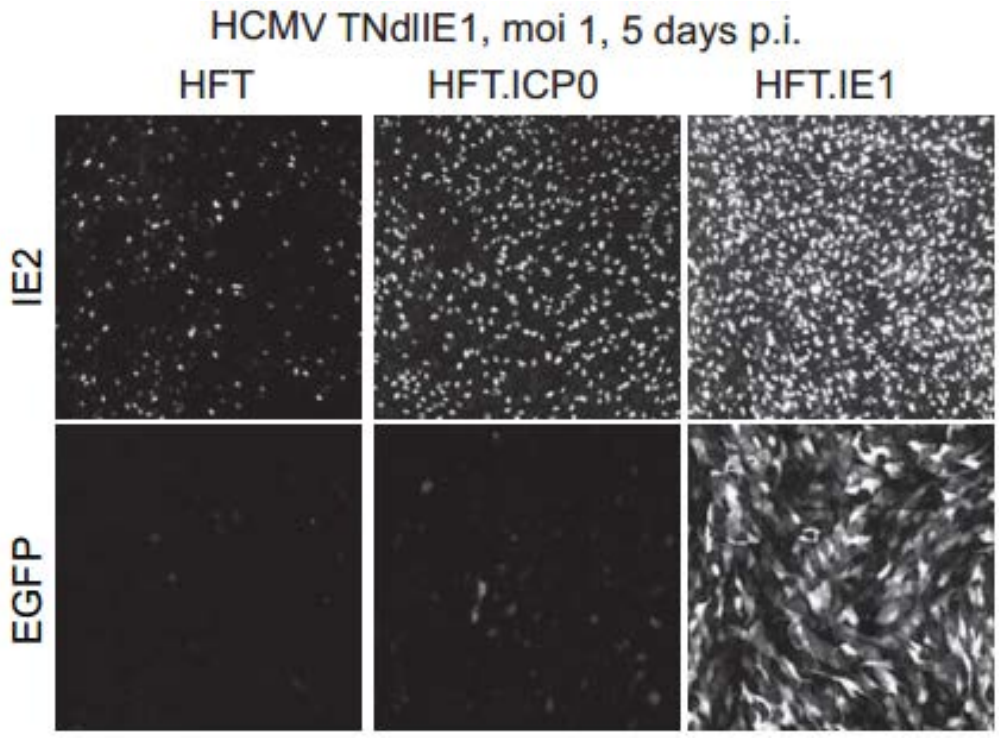

Figure 4.20 IF images of TNdlIE1 infection on HFT, HFT.IE1 and HFT.ICP0 cell lines.
Cells were induced by treatment with DMEM containing 100 ng/ml of doxycycline for 24 h prior to infection. Induced cells were infected by TNdlIE1 at MOI 1, then the

medium was replaced with routine cell culture medium with 100 ng/ml doxycycline and 1% human serum after 4 h of infection. At 5 days post infection, the cells were fixed and permeabilized for anti-IE2 mAb staining. EGFP expression indicates virus Late gene expression.

Consistent with the previous observation in the WB assay, ICP0 did not complement TNdlIE1 infection even though the IE2 expression was increased by ICP0 expression. In this scenario, ICP0 de-represses the MIEP thus stimulating IE2 expression. TNdlIE1 infected HFT cells expressed IE2 in a relatively low proportion of cells compared with infected HFT.IE1 cells. This indicates that even in the absence of IE1 a proportion of infected HFT cells are able to express IE2, but this is insufficient to allow efficient Early gene expression, even when the proportion of IE2 positive cells is increased by ICP0. That the viral gene expression stimulated by ICP0 was restricted to that of IE2 in HFT.ICP0 cells potentially indicates that IE1 is required for IE2 to stimulate downstream viral gene expression efficiently. The presence of IE1 in HFT.IE1 cells allows efficient complementation of TNdlIE1, and therefore at this time point all the cells become highly infected.

HCMV lab strains don’t express a number of genes that are expressed by clinical low passage strains. To investigate whether a relatively low passage HCMV strain performed in a similar manner to TNdlIE1 in HFT.ICP0 cells, TBdlIE1 was studied in the same complementation assay. TBdlIE1 was titrated on HFT.IE1 cells and used to infect induced HFT, HFT.IE1 and HFT.ICP0 cells in a series of MOI from 0.01 to 3. Figure 4.21 shows the plaque assay results at MOI 1.

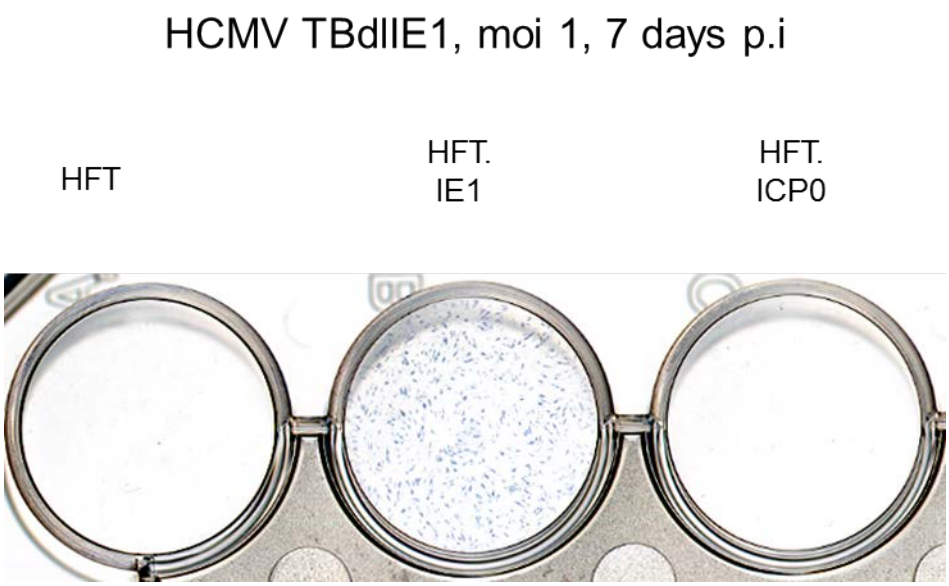

Figure 4.21 HCMV plaque assay of TBdlIE1 infection on HFT, HFT.IE1 and HFT.ICP0 cells.

Cells were treated with DMEM containing 100 ng/ml of doxycycline for 24 h prior to infection. Induced cells were infected with TBdlIE1 at MOI 1, and then at 7 days post infection, the cells were fixed and permeabilized for HCMV plaque assay by staining for UL44.

Due to the attenuated gene expression of TBdlIE1 that was observed in previous report (Zalckvar *et al.*, 2013), a notable smaller plaque size of TBdlIE1 was observed after 7 days infection, but the plaque formation efficiency of TBdlIE1 was similar to that of TNdlIE1 in HFT-IE1 cells. As with TNdlIE1, ICP0 could not complement the infection of TBdlIE1.

4.6 Reactivation of IE1 null HCMV infection in HFT cells

HCMV viral genomes localize adjacent to ND10 in the early stages of infection (Ishov *et al.*, 1997), and IE1 was found to disrupt with ND10 to stimulate viral gene expression and lytic infection (Ahn *et al.*, 1998; Korioth *et al.*, 1996; Wilkinson *et al.*, 1998). Even though IE1 is dispensable in high MOI infections, it is still an important element for HCMV infection in vivo as IE1-null mutant HCMV is impaired for viral infection and gene expression in low MOI infections. This scenario could be modified as model for quiescent infection in cultured cells, analogous to that developed for studying HSV-1 quiescence (Ferenczy *et al.*, 2011; Preston & Nicholl, 1997; Russell *et al.*, 1987; Samaniego *et al.*,

1998), for investigating the process of HCMV transfer into lytic infection from a quiescent state. The processes involved might have some relationship to reactivation of latent infections in vivo. The availability of HFT-IE1 and HFT-ICP0 cells enables studies on the potential roles of IE1 and ICP0 in reactivating quiescent HCMV genomes. In this part of the study, a re-activation assay was designed to mimic quiescent infection in the first 4 days of infection by TNdlIE1 of uninduced HFT-IE1 and HFT-ICP0 cells, followed by induction of IE1 or ICP0 expression to potentially initiate lytic infection on the 4th day.

4.6.1 IE1 reactivates IE1 null mutant HCMV infection

TNdlIE1 was used to infect uninduced HFT.IE1 cells on the first day at MOI 1. After 4 days of infection, the cell culture medium was changed to DMEM with 100 ng/ml doxycycline to trigger high level IE1 expression. After 4 days of induction, the cells were collected for IF analysis of viral gene expression and replication. The uninduced cells were analysed in parallel as controls.

At 4 days post infection in the absence of induction, TNdlIE1 infected HFT.IE1 cells expressed IE2 (data not shown) in the same manner as TNdlIE1 infection on HFT cells (Figure 4.20). On the 2nd day after induction, the induced cells expressed more IE2 under the stimulation of IE1, but at this stage there was no significant reporter gene EGFP expression (Figure 4.22). After the accumulation of IE2 expression and other HCMV gene expression products, infected cells in the 4th day post infection expressed high levels of EGFP, whereas the uninduced cells had no expression of EGFP or any increase in IE2 expression.

In this assay, the lytic infection was controlled by the time of IE1 expression. During the first 4 days post infection, in the absence of induced IE1, the viral genome were held in a repressed state in host cell nucleus without expressing early or late genes. Even though a certain amount IE2 was expressed in the uninduced cells, it was not sufficient to initiate lytic infection. Following induction on the 4th day, doxycycline stimulated IE1 expression and released the genome from repression, therefore this increased IE2 expression and allowed the transfer of the viral infection into the lytic stage.

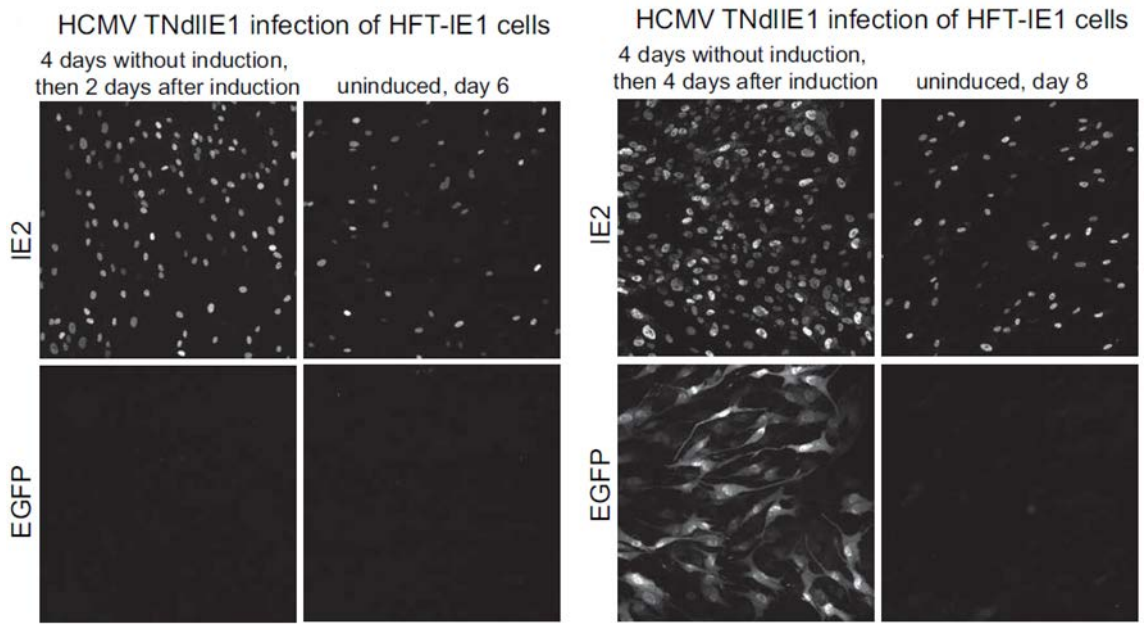

Figure 4.22 Confocal immunofluorescence images of TNdlIE1 re-activation assay on HFT.IE1 cells.

HFT.IE1 cells were infected with TNdlIE1 at MOI 1 on day 1. On the 4th day, doxycycline containing medium was added to the cells for induction of IE1 expression. IF images were taken at 2 and 4 days post induction, after the cells were fixed and permeabilized for anti-IE2 mAb staining. The left side images in Figure 4.22 show the results at 2 days after induction and the right side shows the images at 4 days after induction.

4.6.2 ICP0 cannot reactivate IE1 null HCMV infection but it does increase IE2 expression

HTF.ICP0 cells were investigated in the same re-activation assay in parallel with HFT.IE1 cells (Figure 4.23). As the previous complementation assays had shown, ICP0 was insufficient to stimulate IE1 null HCMV lytic infection, but it could increase IE2 expression, probably by in part by substituting for the activities of pp71 (see Section 4.8 below) but also in an analogous manner by which it re-activates expression from the MIEP when present in quiescent HSV-1 genomes (Baldick *et al.*, 1997; Chau *et al.*, 1999; Homer *et al.*, 1999; Liu & Stinski, 1992; Preston & Nicholl, 2005; Samaniego *et al.*, 1998) However, in this HCMV re-activation assay, ICP0 was still unable to stimulate TNdlIE1 into full lytic infection. To summarise the TNdlIE1 complementation and re-activation assays, IE1 can be replaced by ICP0 on stimulating IE2 expression but is indispensible for efficient expression of other HCMV genes expression in a low MOI infection. This raises the possibility that IE1 is specifically required by IE2 to stimulate lytic infection.

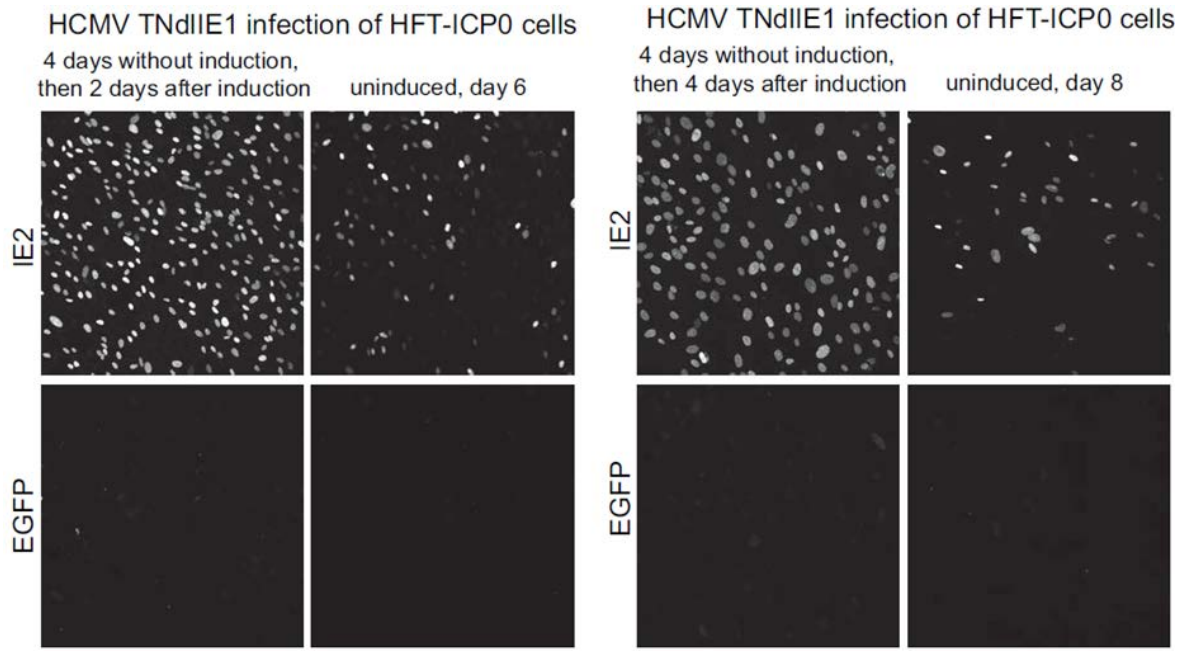

Figure 4.23 Confocal immunofluorescence images of TNdlIE1 re-activation assay in HFT.ICP0 cells.

HFT.ICP0 cells were infected with TNdlIE1 at MOI 1 on day 1, then on the 4th day, doxycycline containing medium was added to the cells to induce ICP0 expression. IF images were taken at 2 and 4 days post induction, the cells were fixed and permeabilized for anti-IE2 mAb staining. The left side images in Figure 4.23 show the results at 2 days after induction and the right side shows the 4 days post induction images.

4.7 Analysis of sequences within IE1 that are important for its stimulation of HCMV infection

4.7.1 Expression of IE1 mutants in HFT cells

Chapter 3 described the construction and study of a series IE1 mutant for their interactions with PML, their effects on PML sumoylation and ND10 integrity, and their complementation of ICP0 null HSV-1. Two of these mutants identified motifs in IE1 that were indispensable for IE1 and PML interaction and the other functions, namely YL3 and YL4. Of the other mutants, YL1 and YL2 are located in the sequence shared by IE1 and IE2, YL7 and K450R were shown unable to be SUMO modified but could still de-sumoylate PML and disperse it into nucleus. Furthermore, a previous report indicated the K450 site of IE1 is important for HCMV replication (Nevels *et al.*, 2004a). Thus, the above IE1 mutants were inserted into the single inducible lentivirus vector and transduced HFT cells were produced for investigating their properties on complementing IE1 null HCMV infection. Figure 4.24 shows the mutation sites of IE1 YL1, YL2, YL3, YL4, K450R and YL7.

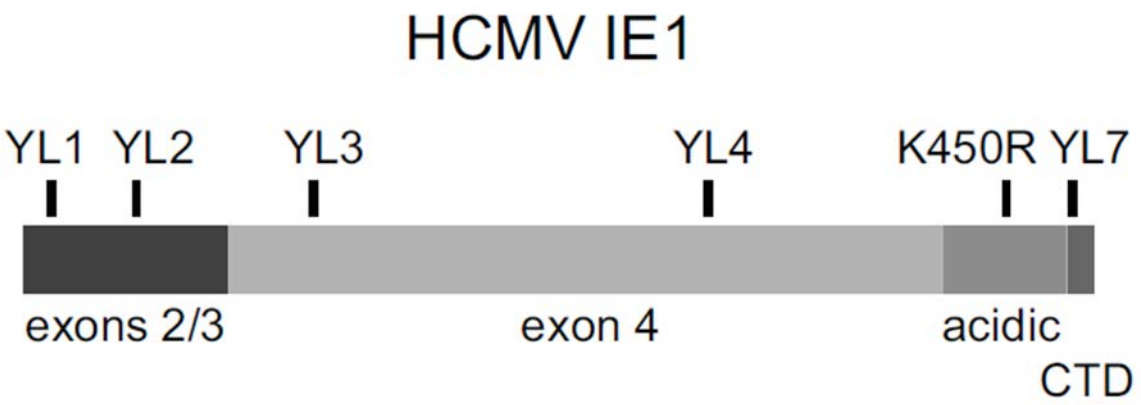

Figure 4.24 A schematic representation of the IE1 protein with its mutation locations.
YL1 and YL2 located in exons2/3 which is the common sequence with IE2. YL3 and YL4, located in exon 4, are located in the hydrophobic region of HCMV IE1 sequence. K450R is located in the acidic domain that is indispensable for IE1 SUMO modification. YL7 deletes the last 11 amino acids of IE1 sequence. Figure taken from (Everett *et al.*, 2013a).

IE1 YL1-YL4, YL7 and K450R sequences were extracted from pLDT.IE1 YL1-YL4, YL7 and K450R vectors using unique restriction enzyme digestion sites in the 3' and 5' ends and the fragments were used to replace the wt IE1 sequence in pLDT.IE1.TetR.IRES.P. HFT.IE1 YL1-YL4, IE1 K450R and IE1 YL7 cells were prepared with the same lentivirus transduction methods as introduced in section 4.2.1. The resulting cell lines were seeded in 24-well plates at $1x10^5$cells/ well and induced by doxycycline on the next day, then the induced cells were infected with TNdlIE1 at MOI 1. DMEM with doxycycline and 1% human serum replaced the infection medium after 4 h. At 10 days post infection, cell lysates were collected and resolved by 7.5% and 10% polyacrylamide gels and viral gene products were probed using antibodies to detect HCMV immediate early, early and late proteins (Figure 4.25).

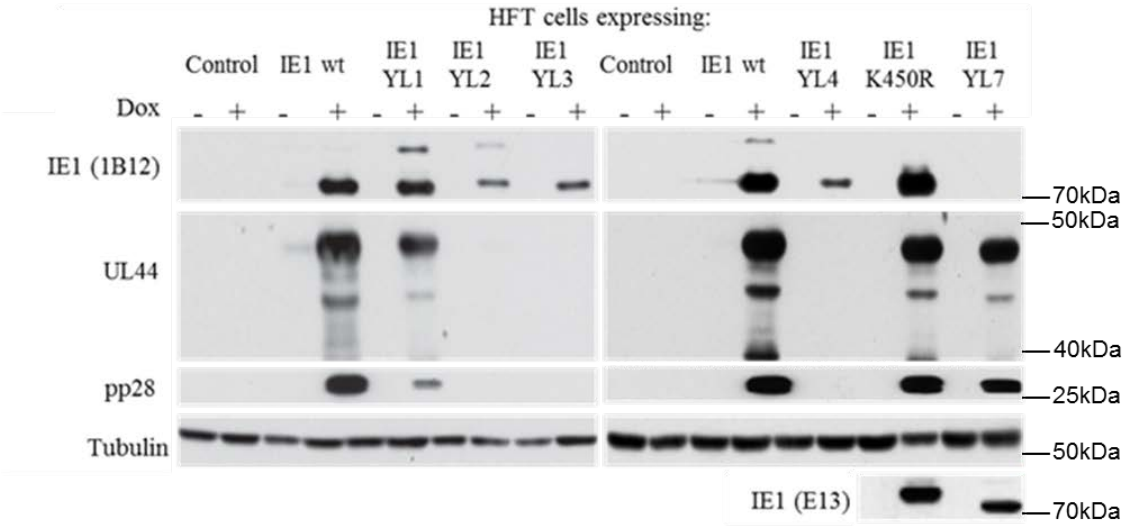

Figure 4.25 WB analysis of TNdlIE1 infection on HFT.IE1 and HFT.IE1 mutant YL1, YL2, YL3, YL4, K450R and YL7 cell lines.

Cells were induced by doxycycline 24 h before infection. The induced cells were infected by TNdlIE1 at MOI 1. After 10 days' incubation, samples were collected and probed by anti-IE1 1B12, anti-IE1 E13, anti-UL44 mAb, anti-pp28 mAb and anti-Tubulin mAb as indicated. The positions of molecular weight standards (in thousands) are indicated to the right of each panel.

Consistent with previous results, anti-IE1 (mAb E13) wasn't able to detect IE1 YL1 expression in HFT by WB (data not shown). To confirm IE1 YL1 expression, anti-IE1 (mAb 1B12) (Zhu *et al.*, 1995) was applied to detect IE1 mutant protein expression in WB. However, anti-IE1 (1B12) mAb could not detect IE1 YL7 in WB because the antibody was raised using a fragment of IE1 that is deleted in YL7. Thus, anti-IE1 (mAb E13) probing image is presented in Figure 4.25 as additional information for IE1 YL7 expression.

As in the complementation assays of ICP0 null mutant HSV-1, IE1 mutants YL3 and YL4 were unable to complement TNdlIE1 infection. They had been shown to be unable to de-sumoylate PML in WB and disperse PML in IF in section 3.3. The functional analysis in TNdlIE1 complementation assay further confirmed that the sequences located in the YL3 and YL4 regions are essential for IE1function and may be required for the stability of the whole protein. IE1 K450R and IE1 YL7 cannot be sumoylated (as shown in the anti-IE1 antibody probed image), but they are still able to complement TNdlIE1 infection as indicated by anti-UL44 and anti-pp28 probing. Consistent with previous data, IE1 mutants YL1 and YL2 expressed in HFT cells were sumoylated. IE1 YL1 complemented TNdlIE1 less efficiently than IE1 wt, indicated by lower UL44 and pp28 expression. The complementation assay of ICP0 null HSV-1 also indicated an attenuated activity of IE1

YL1 (Section 3.4). The expression of IE1 YL2 was less efficient than IE1 wt, but the sumoylated form of IE1 YL2 could also be detected. Surprisingly, the mutation in IE1 YL2 completely abolished the ability to complement TNdlIE1 infection.

To rule out the possibility that this abolishment was due to lower expression of IE1 YL2, the IE1 wt and IE1 YL2 proteins were expressed in HFT cells by the same double transduction lentivirus vector system described in Chapter 3.3 and the data are shown in the following section.

4.7.2 Complementation of IE1 null mutant HCMV plaque formation by IE1 mutants

To quantify the complementation activity of the IE1 mutants, the plaque formation efficiency of TNdlIE1 was performed on HFT.IE1 and the IE1 mutant cell lines.

IE1 expression HFT cell lines were seeded in 24-well plates at $1x10^5$cells/well. On the next day, the cells were induced by treatment with 100 ng/ml doxycycline for 24 h. Induced HFT.IE1 and HFT.IE1 mutant cell lines were infected with TNdlIE1 at sequential dilutions determined empirically to give countable numbers of plaques on each cell line. At 4 h post infection, infection medium was replaced by DMEM containing doxycycline and 1% human serum. At 7 days after infection, the infected cells were fixed and permeabilized for anti-UL44 mAb staining. The same experiment was performed three times to work out average data and standard deviation. Figure 4.26 shows the complementation assay of TNdlIE1 on HFT.IE1 and mutant cell lines.

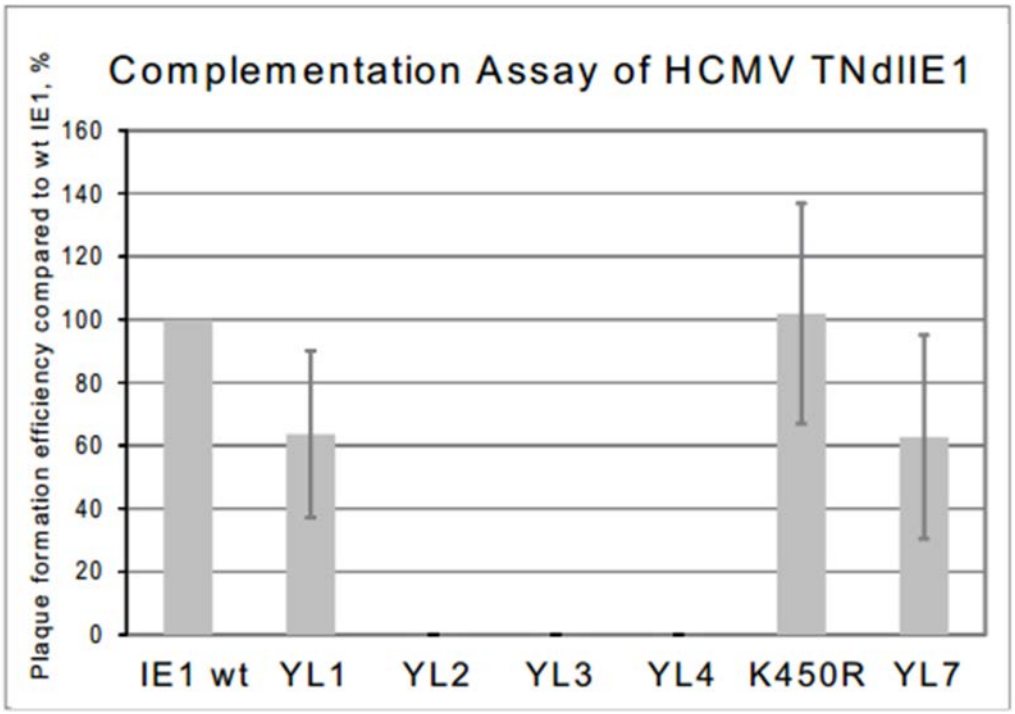

Figure 4.26 Complementation assay of TNdlIE1 on HFT.IE1 and HFT.IE1 mutant cell lines.

HFT.IE1, HFT.IE1 YL1, HFT.IE1 YL2, HFT.IE1 YL3, HFT.IE1 YL4, HFT.IE1 K450R and HFT.IE1 YL7 cells were infected with TNdlIE1 at sequential dilutions determined empirically to give countable numbers of plaques on each cell line. At 7 days post infection, the cells were fixed and permeabilized for anti-UL44 mAb staining. The results are expressed as percentage in each cell type of the titre obtained in HFT.IE1 cells.

The plaque assay shows that YL1 and YL7 complemented the TNdlIE1 at about 60% of the efficiency of IE1 wt. This was highly consistent with the ICP0 null HSV-1 complementation assay on HepeRG-derived cells, indicating that the mutations in YL1 and YL7 cause only partial damage to IE1 activity. YL3 and YL4 were unable to complement TNdlIE1 even at high MOI, which was also consistent with the ICP0 null HSV-1 complementation assay and the analysis by WB in section 4.7.1. IE1 K450R complemented TNdlIE1 infection as efficiently as IE1wt, which is consistent with the previous analysis of (Xu *et al.*, 2001) but apparently different from the situation when the mutation is present within the viral genome (Nevels *et al.*, 2004a). As seen in the WB assay, IE1 YL2 completely lost the ability to stimulate TNdlIE1 infection in this assay despite maintaining 20% activity in complementing ICP0 null HSV-1 infection in HA-IE1 YL2 cells (Section 3.4).

IE1 YL2 expression in HFT.IE1 YL2 cells was lower than IE1 wt in Figure 4.25, which could contribute to its reduced activity. In order to improve expression of IE1 YL2 in HFT

cells, HFT.TetR.IE1 and HFT.TetR.IE1 YL2 cell lines were generated by the double transduction method that was described in Section 2.2.3. Briefly, HFT cells were transduced with lentivirus stock derived from pLKOneo.CMV.EGFPnlsTetR. The resulting cell line was maintained in 0.5 mg/ml neomycin for selection. HFT.TetR cells selected from the above were transduced again by pLDT.IE1 and pLDT.IE1 YL2 derived lentiviruses respectively. The transduced cell lines were selected with 0.5 µg/ml puromycin. Selected cell lines were grown in DMEM containing 0.5 mg/ml neomycin and 0.5 µg/ml puromycin. Western blot analysis of the resulting cell lines using antibodies against PML and IE1 indicated that the IE1 YL2 was expressed in HFT.TetR cells at levels much closer to those of the IE1 wt than from the single inducible vector, and it de-sumoylated PML almost as efficiently as IE1 wt (Figure 4.27). There is a slight mobility difference between wt and YL2 forms of IE1, which is most likely due to the YL2 mutations themselves as the complete IE1 open reading frame in pLDT.IE1 YL2 was confirmed by DNA sequence analysis.

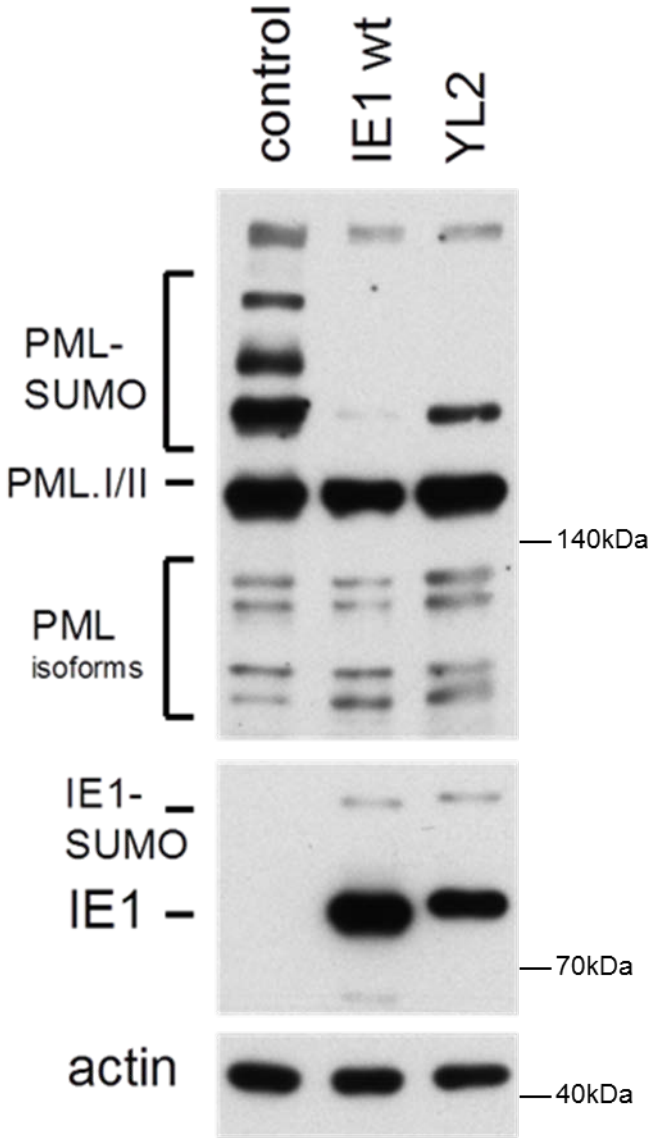

Figure 4.27 WB analyses of HFT.TetR, HFT.TetR.IE1 and HFT.TetR.IE1 YL2 cell lines. Cells were induced with doxycycline for 24 h. The induced cell lysates were collected and probed by anti-IE1 1B12, anti-PML rAb and anti-actin mAb as indicated. The positions of molecular weight standards (in thousands) are indicated to the right of each panel.

The above IE1 wt and IE1 YL2 expression cell lines were infected by TNdlIE1 in complementation assays. The infection protocols were the same as described in section 4.7.2. Induced cells were infected by TNdlIE1 at different MOIs from 0.01 to 3 (TNdlIE1 was titrated on HFT.IE1 cells), then HCMV plaque assays were performed as described in Chapter 2. An anti-UL44 mAb was used to detect the HCMV plaques. High MOI infection on HFT.TetR.IE1 cells formed large plaques and caused high cell death rate but no plaques were formed in HFT.TetR.IE1 YL2 cells (data not shown). To illustrate the

complementation assay clearly, the image of the MOI 0.1 infection is shown in Figure 4.28.

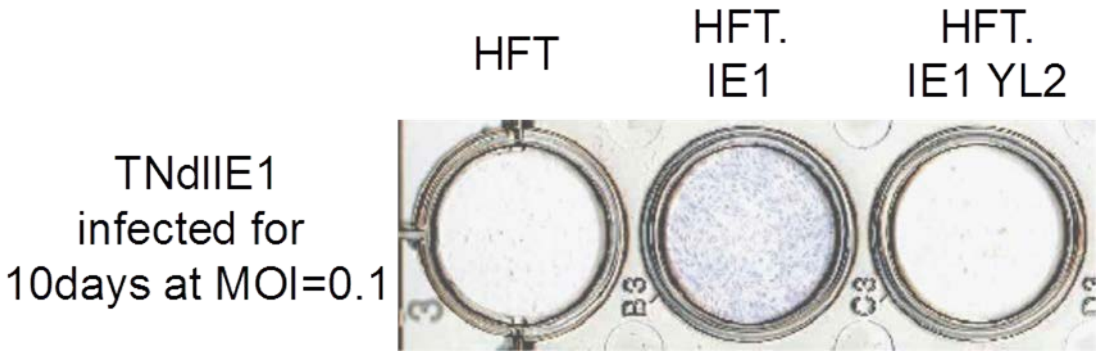

Figure 4.28 HCMV plaque assays of TNdlIE1 infection on HFT, HFT.TetR.IE1 and HFT.TetR.IE1 YL2 cells.

Cells were induced with doxycycline 24 h before infection. The infected cells were incubated at 37℃ for 10 days then fixed and permeabilized for anti-UL44 mAb staining. The secondary antibody was sheep anti-mouse IgG hrp conjugated antibody A4416.

Consistent with the data in Figure 4.26, IE1 YL2 did not complement TNdlIE1 infection even though the activity of the mutant protein on PML was only slightly reduced from that of IE1 wt (Figure 4.27).

To further investigate the early and late stages of TNdlIE1 infection on HFT.TetR.IE1 wt and HFT.TetR.IE1 YL2 cells, both cell lines were infected by TNdlIE1 at MOI 1. At 10 days post infection, the infected cells lysates were collected and resolved by 10% polyacrylamide gel electrophoresis and western blotting. The Early stage of infection was indicated by detection of UL44 expression and late stage was probed by anti-pp28 mAb (Figure 4.29).

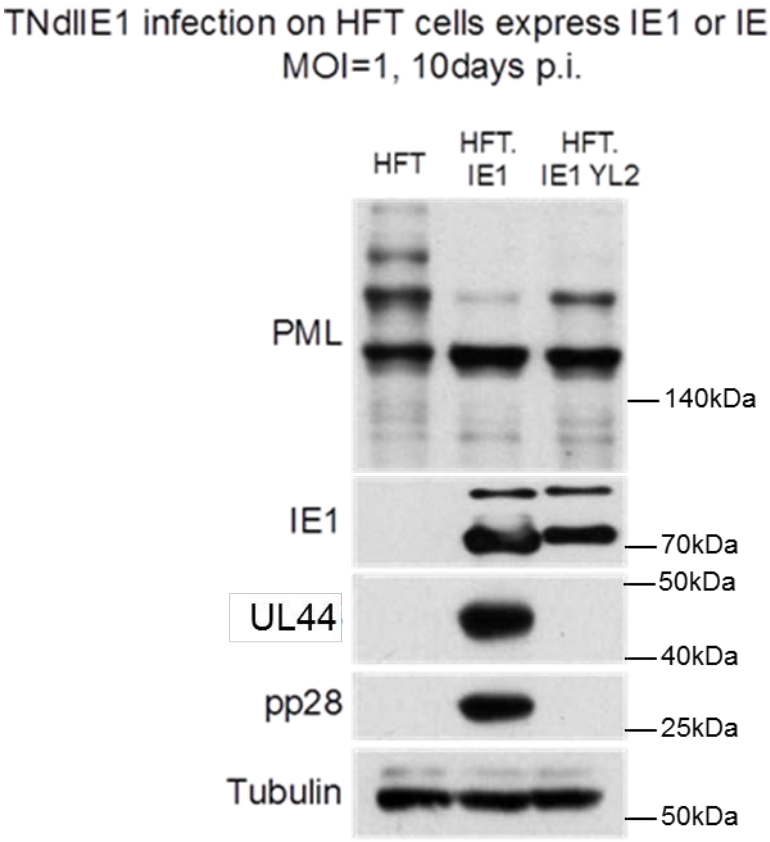

Figure 4.29 Western blot analysis of TNdlIE1 infection on HFT, HFT.TetR.IE1 and HFT.TetR.IE1 YL2 cell lines.

Cells were induced by doxycycline treatment 24 h before infection. The induced cells were infected with TNdlIE1 at MOI 1, then at 4 h post infection, cell medium was replaced with DMEM with 100 ng/ml doxycycline and 1% human serum. After 10 days of infection, samples were collected and probed by anti-PML rAb, anit-IE1 mAb, anti-UL44 mAb, anti-pp28 mAb and anti-Tubulin mAb as indicated. The positions of molecular weight standards (in thousands) are indicated to the right of each panel.

Western blot analysis indicated that at 10 days after infection, IE1 YL2 and IE1 wt were expressed at similar levels and IE1 YL2 de-sumoylated PML, albeit a little less efficiently than the wt protein. IE1 wt but not IE1 YL2 complemented TNdlIE1 as indicated by UL44 and pp28 expression (Figure 4.29). This is consistent with the earlier experiments. This indicates that the amino acids sequence located in IE1 YL2 perform functions that are essential for IE1 activity during HCMV lytic infection.

4.7.3 IE1 YL2 maintains partial activity to enhance ICP0 null HSV-1 infection on HFT cells

The issue of the expression level and activity of IE1 YL2 arose at the very end of the time available for experimental work for this thesis. The experiments for the following two Figures were performed by Anne Orr after the deadline for finishing practical work had passed, but they are included here for completeness and because the issue of the potential activity of IE1 YL2 is important for the overall analysis.

When IE1 and pp71 are expressed together in either HFT or HepaRG cells they complemented 50% of the ICP0 function in HSV-1 infection ((Everett *et al.*, 2013a) and Section 4.3.3). The single expression of IE1 in HA.TetR cells can also rescue about 10% of the activity of ICP0 on complementing ICP0 null HSV-1 (Everett *et al.*, 2013a). In this section, ICP0 null HSV-1 complementation assay was performed on HFT.TetR.IE1 wt/IE1 YL2 cells and on HFT.TetR.myc-pp71.IE1 wt/IE1 YL2 cells to investigate any differences in activity between IE1 wt and IE1 YL2 (Figure 4.30).

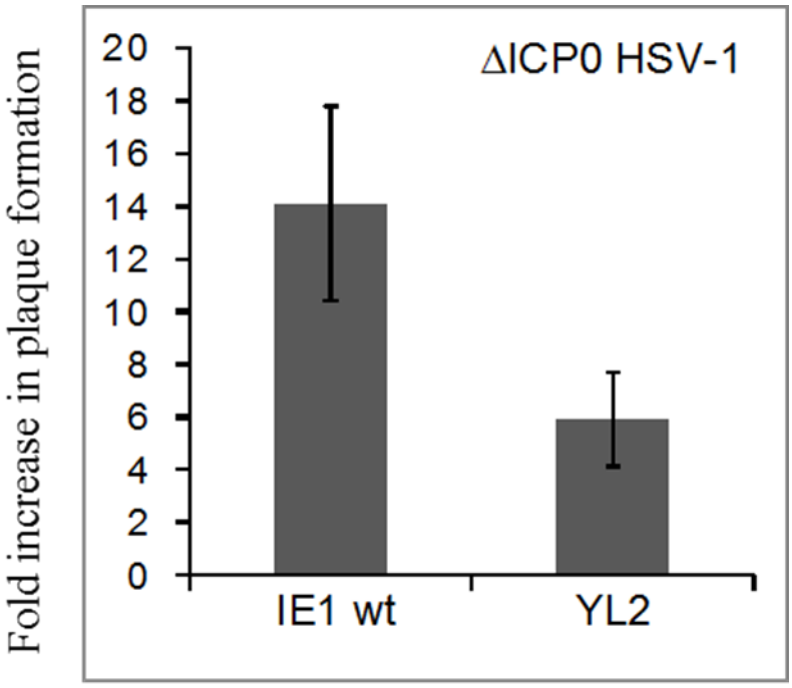

Figure 4.30 Complementation assay of ΔICP0 HSV-1 on HFT.TetR.IE1 and HFT.TetR.IE1 YL2 cells.

HFT.TetR.IE1 and HFT.TetR.IE1 YL2 cells were induced by doxycycline treatment 24 h before infection. The induced cells were infected with ΔICP0 HSV-1 at an appropriate series of dilutions. At 4 h post infection, cell medium was changed to DMEM with 100 ng/ml of doxycycline and 1% human serum. At 24 h post infection, the infected cells were fixed and blue plaque assay were performed to collect the plaque formation efficiency data. The same experiment was performed twice, and the data presented show

the mean and range of the two values obtained. The results are expressed as fold-increase in absolute titre (PFU per ml) in each cell type over that in HFT.TetR cells. This experiment was performed by Anne Orr.

Induced HFT.TetR.IE1 cells complemented ICP0 null HSV-1 infection at a similar level as that in HFT.IE1 cells (see Section 4.3.1). In this assay IE1 YL2 complemented ΔICP0 HSV-1 infection by about 6-fold, which was about 40% of the activity of IE1 wt. This figure was about twice that obtained in the HFT.IE1 YL2 cells produced by the single vector transduction (see Section 3.4), which may reflect the relatively greater expression level of YL2 in the HFT-TetR based cells.

To compare IE1 YL2 with IE1 wt in more detail, both proteins were introduced into HFT cells together with pp71. HFT.TetR.myc-pp71.IE1 wt and HFT.TetR.myc-pp71.IE1 YL2 were prepared by lentivirus transduction. HFT.TetR.IE1 and HFT.TetR.IE1 YL2 cells were infected by lentivirus derived from pLDT.myc-pp71 vector separately. Then the resulting cells were selected with 1 μg/ml blasticidin. The resulting cell lines were maintained in DMEM containing 1 μg/ml blasticidin, 0.5 mg/ml neomycin and 0.5μl/ml puromycin. HFT.TetR.myc-pp71.IE1 wt and HFT.TetR.myc-pp71.IE1 YL2 were analysed by WB to detect protein expression (Figure 4.31 A) and ΔICP0 HSV-1 complementation assays were performed to test their activity (Figure 4.31 B). The three cell lines analysed in the WB expressed similar levels of myc-pp71 as indicated. In the plaque assays, pp71 cooperated with IE1 and complemented ΔICP0 HSV-1 by about 700-fold over that in HFT.TetR.mycpp71 cells. Meanwhile, co-expression of IE1 YL2 with pp71 increased ΔICP0 HSV-1 infection 600-fold over that produced by pp71 alone. This assay indicated that IE1 YL2 was capable of achieving almost the same activity of the wt protein in the presence of pp71. Thus, these experiments demonstrate that the failure of IE1 YL2 to complement HCMV TNdlIE1 cannot be explained by reduced expression levels or complete disruption of the protein structure. Therefore, the amino acids located in the IE1 YL2 region are essential specifically to mediate IE1 function in the context of HCMV infection.

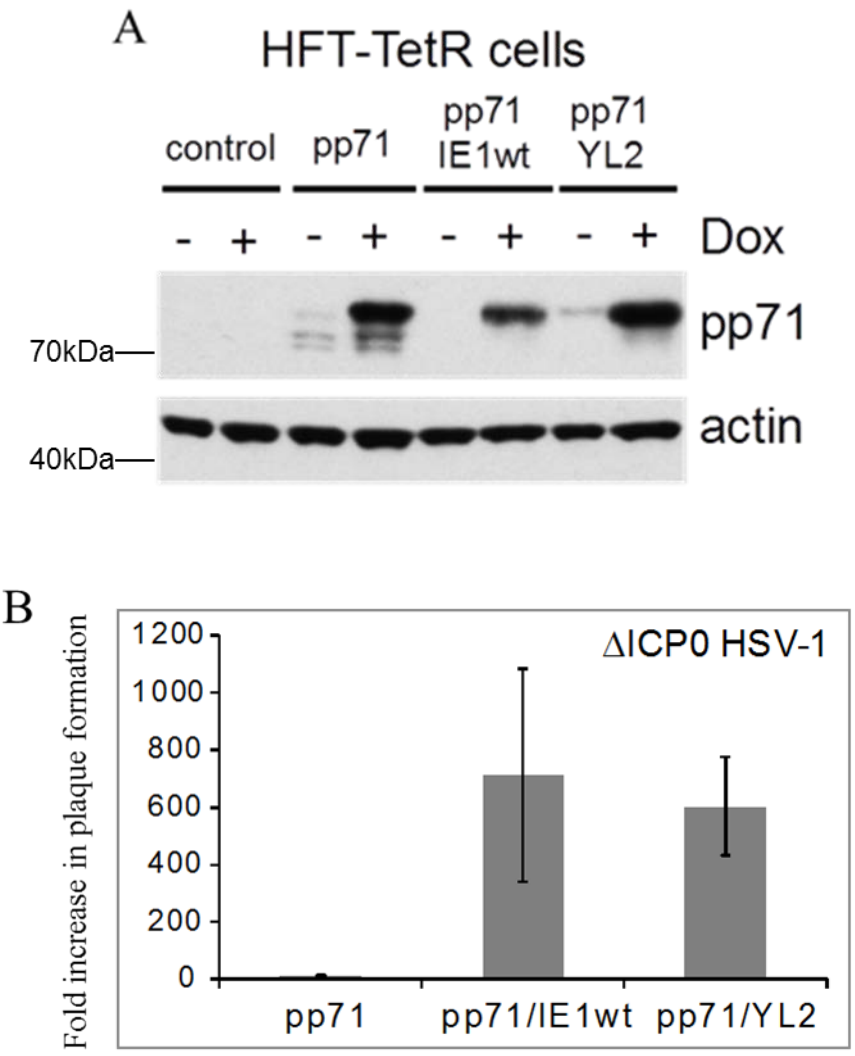

Figure 4.31 Analysis of IE1 wt and IE1 YL2 by co-expression with pp71 in HFT cells.

(A) Analysis of myc-pp71 expression in HFT.TetR.myc-pp71, HFT.TetR.myc-pp71.IE1 and HFT.TetR.myc-pp71.IE1 YL2 cell lines. Cells were induced for 24 h then the induced cell lysates were collected and probed by anti-pp71 mAb and anti-actin mAb as indicated. (B) Analysis of ΔICP0 HSV-1 complementation on HFT.TetR.myc-pp71, HFT.TetR.myc-pp71.IE1 and HFT.TetR.myc-pp71.IE1 YL2 cell lines. Cells were induced 24 h before infection. The induced cells were infected with a range of multiplicities of ΔICP0-HSV-1, then at 4 h after infection, the medium was changed to DMEM containing doxycycline and 1% human serum. At 24 h post infection, blue plaque assays were performed to collect the plaque formation efficiency data. The results are expressed as fold-increase in absolute titre (PFU per ml) in each cell type over that in HFT.TetR.mycpp71 cells. The data show the mean and range of the two values of duplicate experiments. The experiments in Figure 4.31 were performed by Anne Orr. The positions of molecular weight standards (in thousands) are indicated to the right of each panel.

4.8 ICP0 complements pp71 null mutant HCMV infection

Tegument protein pp71 is another ND10 interacting protein expressed by HCMV, which specifically interacts with hDaxx (Hofmann *et al.*, 2002) and disrupts the hDaxx/ATRX complex (Lukashchuk *et al.*, 2008). These functions are essential for pp71 to stimulate the HCMV MIEP and fulfil its function in immediate early infection stage. The shared property between ICP0 and pp71 is that although there is no evidence that ICP0 either interacts with or disrupts the hDaxx-ATRX complex (Lukashchuk & Everett, 2010), ICP0 disperses hDaxx and ATRX from ND10 and inhibits their recruitment to HSV-1 genomes (Lukashchuk & Everett, 2010). The repressive effects of hDaxx and the hDaxx/ATRX complex contribute to cell mediated restriction of infection by both HCMV and HSV-1 (Everett *et al.*, 2009; Hofmann *et al.*, 2002; Lukashchuk *et al.*, 2008; Saffert & Kalejta, 2006). In this section, HFT.ICP0 cells were used to investigate the possibility that arises from these observations that ICP0 might complement pp71 null mutant HCMV infection.

4.8.1 Analysis of complementation of pp71 null mutant HCMV infection by ICP0

A stock of the pp71 mutant ADsubUL82 (Δpp71 HCMV) (Bresnahan *et al.*, 2000; Bresnahan & Shenk, 2000) was titrated on HFT.TetR.myc-pp71 cells, then induced HFT.ICP0 cells were infected with Δpp71 HCMV at MOI 1. Within the next 4 days of infection, cell lysates were collected and analysed by WB (Figure 4.32).

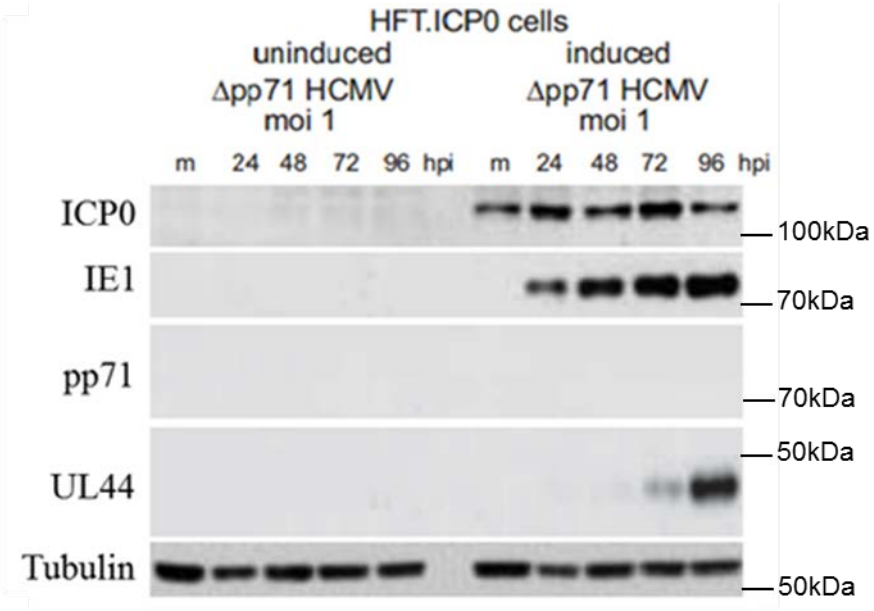

Figure 4.32 WB analysis of Δpp71 HCMV infection of induced and uninduced HFT.ICP0 cells.

Induced cells were treated with doxycycline for 24 h before infection. Induced and uninduced HFT.ICP0 cells were infected by Δpp71 HCMV at MOI 1, then at 4 h post infection, the cell medium was replaced with routine cell culture medium with 100 ng/ml doxycycline and 1% human serum. Cell lysates were collected at 24 h, 48 h, 72 h and 96 h post infection and probed by anti-ICP0 mAb 11060, anti-IE1 mAb, anti-pp71 mAb, anti-UL44 mAb and anti-Tubulin mAb as indicated. The secondary antibody was sheep anti-mouse IgG hrp conjugated antibody A4416. The positions of molecular weight standards (in thousands) are indicated to the right of each panel.

ICP0 stimulated Δpp71 HCMV infection, increasing the expression of both IE1 and UL44, while the absence of pp71 detection (even on a long exposure) confirmed the mutant virus phenotype (Figure 4.32; see also Figure 4.34 for a control for the pp71 antibody). The parallel negative control infection on uninduced HFT.ICP0 cells detected no HCMV protein expression.

To quantify the Δpp71 HCMV complementation assay on HFT.ICP0 cells, plaque assays were performed on HFT, HFT.TetR.myc-pp71 and HFT.ICP0 cell lines that were infected by Δpp71 HCMV at different MOIs. The complementation assay was performed as follows. HFT, HFT.TetR.myc-pp71 and HFT.ICP0 cells were seeded on 24-well plates at $1x10^5$cells/well. On the next day, cells were induced by treatment with 100 ng/ml doxycycline. The induced cells were infected by Δpp71 HCMV at sequential dilutions determined empirically to give countable numbers of plaques on each cell line. The same

experiment was performed three times to work out an average figure and standard deviation. The data are shown in Figure 4.33.

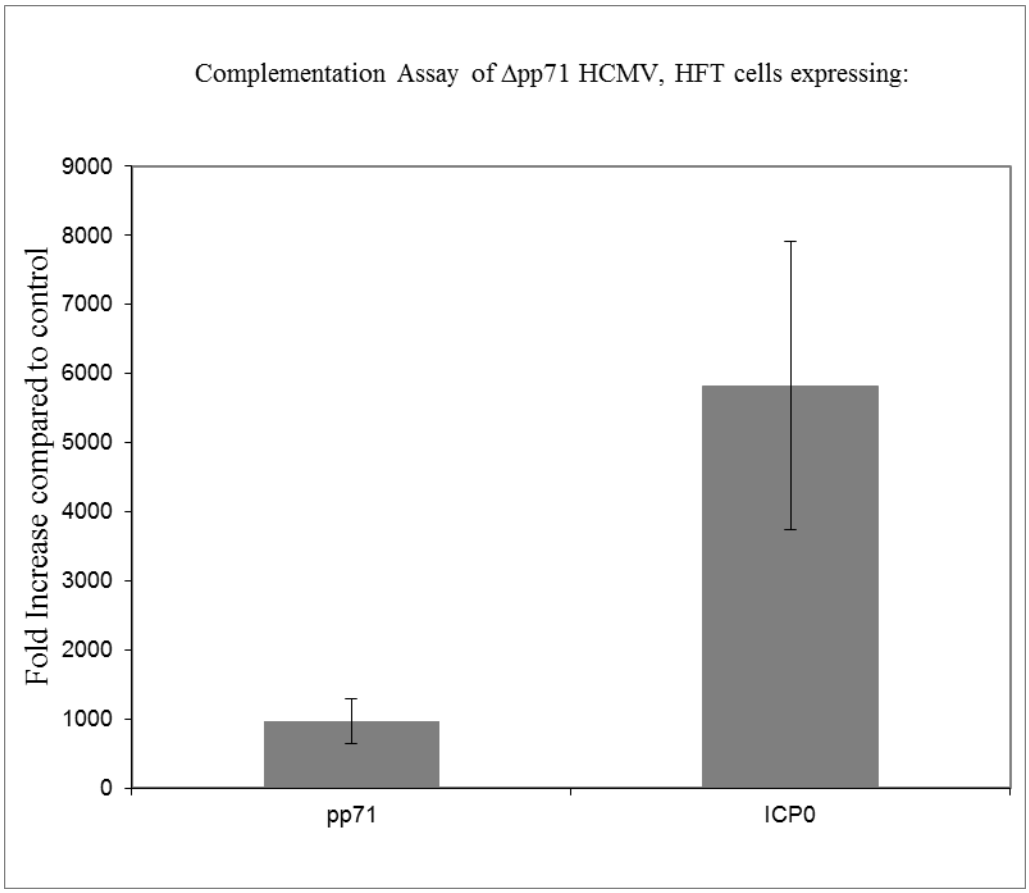

Figure 4.33 Complementation assay of Δpp71 HCMV on HFT.TetR.myc-pp71 and HFT.ICP0 cells.

HFT, HFT.TetR.myc-pp71 and HFT.ICP0 cells were induced by doxycycline treatment for 24 h before infection, then infected with Δpp71 HCMV at a series MOIs to give countable numbers of plaques on each cell line (titrated on HFT.TetR.myc-pp71 cells). At 4 h post infection, the cell medium was changed to DMEM with 100 ng/ml of doxycycline and 1% human serum. After 7 days of infection, the infected cells were fixed and permeabilized for anti-UL44 mAb staining. The results are expressed as fold-increase in absolute titre (PFU per ml) in each cell type over that in HFT cells.

The results showed that myc-pp71 expression in HFT cells complemented the Δpp71 mutant HCMV about 1000-fold over HFT cells, whereas ICP0 increased the mutant virus titre by about 6000-fold. This result of ICP0 complementation to a greater extent than pp71 is readily explained by the results in Section 4.4.2. In this scenario, ICP0 not only overcame the repression of the hDaxx-ATRX complex, but also provided a more convenient replication environment for Δpp71 HCMV by degrading PML and Sp100.

To compare the complementation of Δpp71 HCMV by ICP0 with wt HCMV infection, ADsubUL82 and the parental wt strain AD169 were titrated on HFT.ICP0 cells, as described in Section 2.2.5.5. ICP0 stimulated both wt HCMV and Δpp71 HCMV plaque formation, which enabled visible plaque formation more rapidly than pp71. Thus the incubation time for plaque formation in infected HFT-ICP0 cells could be reduced to 5-7 days. After calculating the virus titres, Δpp71 HCMV and AD169 were adjust to MOI 1 for the infection of HFT.ICP0 cells. The infected cells were collected as cell lysates at different time points and analysed by WB. The data are shown in Figure 4.34.

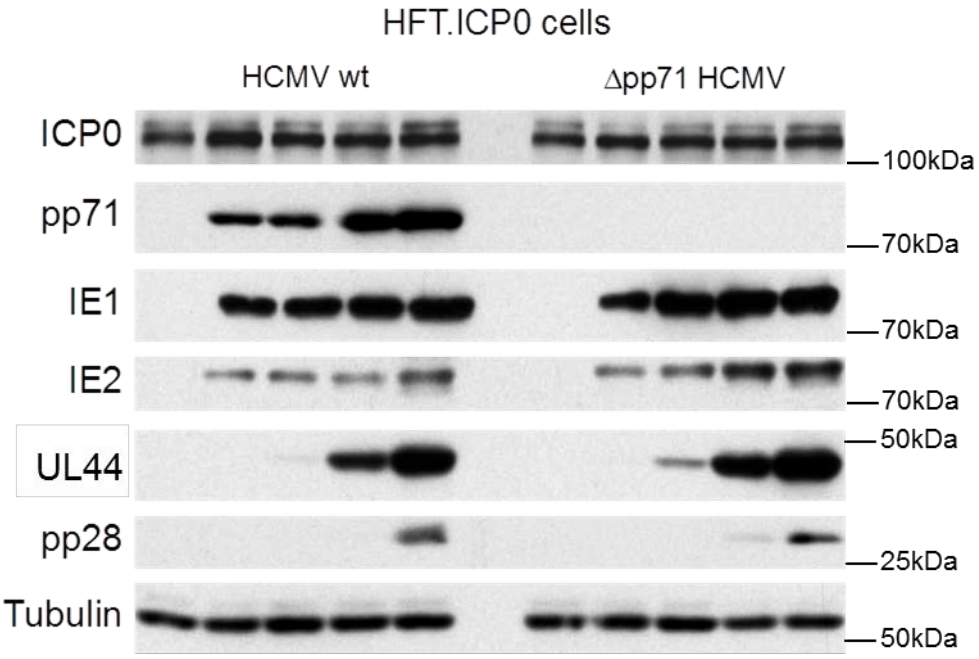

Figure 4.34 WB analysis of wt AD169 and Δpp71 HCMV infection of HFT.ICP0 cells.
HFT.ICP0 cells were seeded in 24-well plates. On the next day, the cells were induced for 24 h by treatment with DMEM with 100 ng/ml doxycycline. Induced cells were infected by AD169 and Δpp71 HCMV at MOI 1, then at 4 h post infection, the infection medium was replaced by routine cell culture medium with 100 ng/ml doxycycline and 1% human serum. Cell lysate were collected at 24 h, 48 h, 72 h and 96 h post infection and probed using anti-ICP0 mAb 11060, anti-IE1 mAb, anti-IE2 maAb, anti-pp71 mAb, anti-UL44 mAb, anti-pp28 mAb and anti-Tubulin mAb as indicated. The secondary antibody was sheep anti-mouse IgG hrp conjugated antibody A4416. The positions of molecular weight standards (in thousands) are indicated to the right of each panel.

As the MOI had been adjusted to 1, immediate early, early and late viral proteins were expressed in similar amounts in the AD169 and Δpp71 HCMV infections (Figure 4.34). This indicated the function of pp71 can be replaced by ICP0 in HCMV infection.

4.8.2 Prior expression of pp71 does not increase plaque formation by wt HCMV

In Section 4.4.2, IE1 was shown to increase wt HCMV plaque formation by about 20-fold over that in HFT cells. IE1 also stimulated the expression of other HCMV genes. Furthermore, the knock down of hDaxx has been demonstrated to increase wt HCMV (AD169) replication in previous publications (Glass & Everett, 2013; Tavalai *et al.*, 2008b). Thus, the question arose whether prior expression of pp71 could promote wt HCMV infection to levels in excess of those achieved by the pp71 provided in the tegument at the time of infection.

In this section, HFT.TetR.myc-pp71 cells were infected by AD169 to investigate whether the extra pp71 expressed in HFT cells could increase the HCMV plaque formation. The same experiment was performed three times to work out an average figure and standard deviation. The data are shown in Figure 4.35.

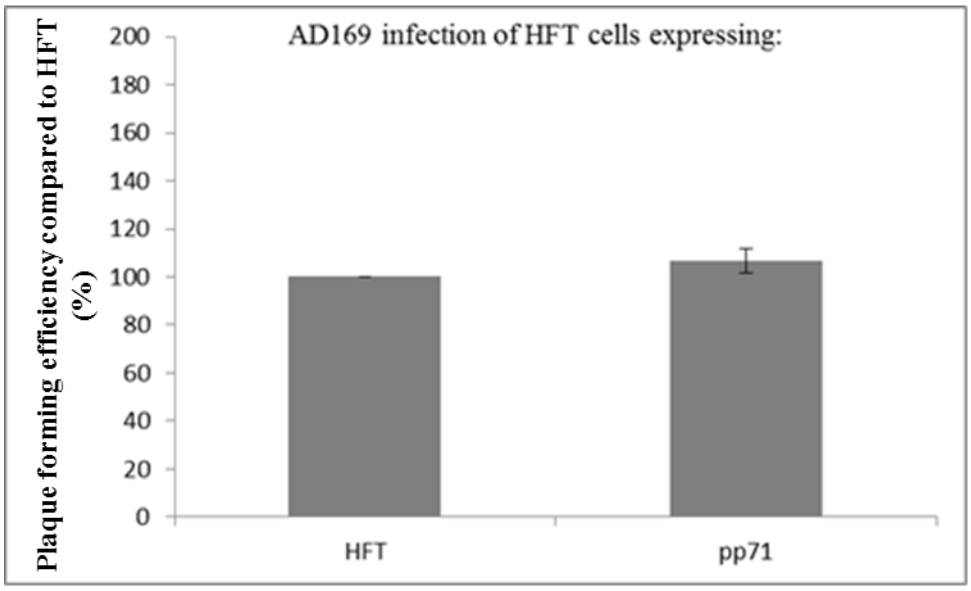

Figure 4.35 AD169 infections on HFT.TetR and HFT.TetR.myc-pp71 cells.
HFT.TetR and HFT.TetR.myc-pp71 cells were induced for 24 h before infection. Induced cells were infected by AD169 at a series MOIs determined empirically to give countable numbers of plaques on each cell line. After 10 days of incubation, the infected cells were fixed and permeabilized for anti-UL44 mAb staining. The results are expressed as percentage in each cell type over that in HFT cells.

Expression of myc-pp71 in HFT cells did not increase AD169 plaque formation, indicating that the pp71 in the AD169 particle is sufficient to overcome the hDaxx-ATRX repression

of the MIEP and the extra expressed pp71 in the host cells cannot further increase the infection.

4.9 Conclusion and discussion

Single inducible vectors expressed most viral genes efficiently in HFT cells. They provided a reliable and simple method for introducing modified genes into target cell lines. The inducible cell lines expressing relevant viral gene products were analysed by different biochemical and biological methods to investigate the protein properties.

Previous studies demonstrated that IE1 and pp71 can complement ICP0 null HSV-1 infection (Everett *et al.*, 2013a) and simultaneous expression of these HCMV proteins can recover 50% of the activity of ICP0. In this scenario the biochemical explanation of it was the antagonizing bioactivity of IE1 and pp71 on PML, Sp100 and hDaxx released the HSV-1 genome from the repression of ND10. ICP0 itself is more efficient on interacting with ND10 than IE1 or pp71 or both of them together. Considering the repression of ND10 on HCMV infection, it seemed highly possible that ICP0 could replace IE1 or pp71 in HCMV infection. To investigate this hypothesis, the HFT.ICP0 cell line was prepared in this chapter, and the control cell lines, HFT.IE1, HFT.TetR.myc-pp71 and HFT.TetR.myc-pp71.IE1, were also generated by the same methods.

HCMV protein expression cell lines were analysed for their effects on PML and the complementation of ICP0 null HSV-1 infection. IE1 expressed in HFT cells de-SUMO modified PML efficiently and co-localized with then dispersed PML. Even though the IE1 expressed in HFT cells complemented the ΔICP0 HSV-1 less efficiently than the similar infection on HA-TetR-IE1 cells, the co-expression with pp71 increased the ΔICP0 HSV-1 infection about 1500-fold, which was 50% of ICP0 complementation. pp71 expression complemented ΔICP0 HSV-1 at the same level as previously reported in HA-TetR-myc.pp71 cells. Thus, the difference between HFT and HepaRG-based cell lines didn't create significant variation on complementing ΔICP0 HSV-1 infection, except for the reduced effect of IE1 by itself.

IE1 was reported to be very important for HCMV infection on stimulating lytic infection and the mutant HCMV deleted of IE1 exon 4 was severely impaired at low MOI infection (Greaves & Mocarski, 1998). Even though the IE1 null HCMV infection and replication could be rescued at high MOI infection, it still doesn't represent the infection in *vivo*. To

rescue IE1 null HCMV infection at low MOI, the expression of IE1 in host cells is necessary (Greaves & Mocarski, 1998; Mocarski *et al.*, 1996). Alternatively, the revertant HCMV strains that insert IE1 exon 4 back into the HCMV genome could also rescue the mutant virus infection (Zalckvar *et al.*, 2013). In this chapter, HFT.IE1 cells successfully complemented TNdlIE1 and TBdlIE1 infection. The HFT.IE1 cells were also applied in TNdlIE1 cultivation to prepare virus stocks. Infection of HFT cells with TNdlIE1 that had been cultivated from HFT.IE1 cells demonstrated the mutant virus didn't insert IE1 genes from host cells into its genome, which confirmed that the rescue method of growing IE1 null HCMV is reliable.

In this chapter, both IE1 and ICP0 increased wt HCMV strain Towne infection by about 20-fold. ICP0 creates a nuclear environment favourable for lytic virus infection, part of which is similar to the effects of PML and Sp100 depletion. Depletion of ND10 components increased wt HCMV infection or IE gene expression in a number of previous studies (Adler *et al.*, 2011; Glass & Everett, 2013; Tavalai *et al.*, 2011; Tavalai *et al.*, 2008b). Thus, the increase caused by ICP0 was within expectation on the basis that ND10 have repressive effect on HCMV gene expression. Pre-expressing IE1 in HFT cells before HCMV infection had a similar effect on HCMV plaque formation as that in induced HFT.ICP0 cells, therefore also creating a more convenient nuclear environment for wt HCMV infection.

The HFT.ICP0 cell line was generated with the same inducible system used for HFT.IE1 cells. Furthermore, the effects of ICP0 onND10 are more efficient and widespread than those of IE1, but the infection of TNdlIE1 and TBdlIE1 on induced HFT.ICP0 cells wasn't complemented. The complementation results indicate that IE1 can specifically interact with the HCMV genome or HCMV gene products to stimulate viral replication. By analyzing HCMV gene expression, another immediate early gene product IE2 expression increase was noticed in HFT.ICP0 cells. It has been observed in previous reports that the deletion of IE1 specific sequence exon 4 completely abolished the IE1 expression but not IE2 (Greaves & Mocarski, 1998) and the deletion of ND10 components such as PML or hDaxx can increase IE2 expression (Tavalai *et al.*, 2008b). IE2 expression is driven by the MIEP (Baldick et al., 1997; Chau et al., 1999; Homer et al., 1999; Liu & Stinski, 1992), which is activated by pp71 (Bresnahan & Shenk, 2000; Cantrell & Bresnahan, 2006; Lukashchuk *et al.*, 2008). The presence of sumoylated PML is important for hDaxx recruitment to ND10 (Everett et al., 2013a; Lin et al., 2006), which represses IE2 expression. ICP0 expression in HFT cells efficiently degraded PML that created similar

infection environment as PML depletion and disturbed the hDaxx recruitment to viral genomes (Lukashchuk & Everett, 2010). Thus the increase of IE2 expression might be due to the indirect effect of ICP0 on hDaxx.

IE1 mutants introduced in chapter 3 were inserted into single inducible vectors in this chapter to prepare IE1 mutant expressing HFT cell lines. The IE1 mutants with reduced efficiency on complementing ICP0 null HSV-1 infection and those unable to be sumoylated were selected for further investigation in this chapter.

IE1 YL1 and YL2 were located in the first 85 amino acids that is shared by IE1 and IE2. IE1 YL1 is located in a region of the protein that includes the nucleus localization signal (Lee *et al.*, 2007). The IE1 null HCMV complementation assay demonstrated the amino acids located within IE1 YL1 were not important for IE1 bio-function or nuclear localisation in HFT-based cells. Furthermore, IF images of induced HA.TetR.IE1 YL1 cells also indicated this mutation was not essential for IE1 nuclear localization (Chapter 3).

Mutant IE1 YL2 expressed in HFT cells de-sumoylated PML almost as efficiently as IE1 wt and increased ICP0 null HSV-1 plaque formation in both HFT (this chapter) and HA-based cells (Chapter 3) (albeit less efficiently than IE1 wt). This evidence indicates that the amino acids located at IE1 YL2 are not essential for the IE1/PML interaction. In the presence of pp71, IE1 YL2 was almost as efficient as the wt protein in increasing ICP0 null mutant plaque formation. In contrast, IE1 YL2 was completely incapable of complementing ΔIE1 HCMV infection. Thus, the 52^{nd}, 54^{th} and 55^{th} amino acids in the IE1 sequence are not responsible for the interaction with PML or IE1 sumoylation, but are required for stimulating HCMV lytic infection in host cells. Thus the YL2 mutations define a motif of IE1 that is specifically required for HCMV infection, but are at least partially dispensable for other IE1 functions.

The sequences of the IE1 YL3 and YL4 mutations are located in the hydrophobic core of IE1 and both of these mutants are unable to interact with PML, be sumoylated or complement TNdlIE1 infection. This implies that the amino acid sequences located in IE1 YL3 and YL4 are essential to maintain IE1 3D structure and the integrity of the IE1 hydrophobic core is indispensable for IE1 bioactivity in HCMV infection and replication. Thus these mutants behave in a similar manner to the previously described L174P (Muller & Dejean, 1999; Xu *et al.*, 2001). IE1 mutant K450R was shown to have an attenuated growth kinetic in HCMV infection (Nevels *et al.*, 2004a). In this chapter using inducible

IE1 expression, the IE1 K450R mutant performed no differently from IE1 wt on complementing TNdlIE1 infection. Furthermore, HCMV gene expression in HFT.IE1 K450R cells was also similar as in HFT.IE1 wt cells. This raised the possibility that IE1 sumoylation is not essential for HCMV gene expression but important for the HCMV assembly process or viral particle release process. In the original study (Nevels *et al.*, 2004b), the growth defect of the IE1 K450R mutant viruses was attributed to a defect in IE2 expression although, consistent with the current study, UL44 expression was not affected.

The C-terminal domain of IE1 is important for the association of IE1 with PML and STAT2, but not for viral replication (Reinhardt *et al.*, 2005; Shin *et al.*, 2012). In Chapter 3, IE1 YL7 was shown unable to be sumoylated, but it performed similar to IE1 wt with regard to PML interaction and ΔICP0 HSV-1 complementation. In this chapter, IE1 K450R was investigated for complementation of ΔIE1 HCMV infection and again it performed with similar efficiency as IE1 wt. This was consistent with previous studies illustrating that the deletion of the 12 amino acids (Reinhardt *et al.*, 2005) or 16 amino acids (Shin *et al.*, 2012) in IE1 C terminal region has no negative effect on HCMV infection. In section 3.3.1 and section 4.7.1, the sumoylation of IE1 YL7 was abolished. Previous reports made the conclusion that the viral replication was not impaired by the C-terminal deletion (Reinhardt *et al.*, 2005; Shin *et al.*, 2012), but on the other hand it was reported sumoylation of IE1 contributes to viral replication (Nevels *et al.*, 2004a). It is possible that sumoylation and the CTD affect HCMV infection in vivo or during reactivation from latency in a manner that is not recapitulated during infection of cultured cells. Thus, further studies are still required on IE1 YL7 and the role of IE1 sumoylation during HCMV infection.

WB analysis of the IE1 mutant expressing HFT cell lines indicated that IE1 YL7 was incapable of being identified by the anti-IE1 1B12 antibody, indicating that the epitope recognised by this antibody is in the extreme C-terminus of the protein.

The re-activation assays performed in this chapter demonstrated the IE1 null HCMV can enter into host cells efficiently. By IE2 antibody staining at 4 days post infection, infected cells were identified to express a certain amount of IE2 which indicates low level expression of the viral genome in host cells. In this scenario, pp71 assembled in IE1 null HCMV interacted with hDaxx and released the MIEP from the repression of the hDaxx-ATRX complex. The MIEP then promoted IE2 expression, but not efficiently enough for stimulating viral infection into the lytic stage. Thus, in the first 4 days of ΔIE1 HCMV

quiescent infection, IE2 expression was maintained at a low level. The expression of IE1 enhanced the expression of IE2 and allowed activation of later classes of viral genes and thus stimulated the HCMV lytic infection.

IE2 is essential for HCMV infection which indicated by the study of IE2 deletion HCMV mutant which is severely impaired for viral infection and replication (White *et al.*, 2004). Even though there has been no evidence of a direct interaction between IE1 and IE2 in previous research reports, some research investigations demonstrated that IE1 and IE2 colocalize with ND10 (Ahn & Hayward, 1997; Korioth *et al.*, 1996; Wilkinson *et al.*, 1998) and immune-precipitation demonstrated a direct interaction between both IE1 and IE2 with HDAC3 (Nevels *et al.*, 2004b). Furthermore, the expression of IE1 can dramatically increase the IE2 expression as indicated in this study and others (Castillo & Kowalik, 2002). Thus, IE1 might perform as an enhancer on IE2 expression to fulfil the viral stimulation activity. Alternatively, it is also possible that an intermediate co-factor is responsible for IE1 and IE2 interaction, and thus explain why the region of IE1 identified by the YL2 mutation seems to be specifically required for efficient progression to later stages of HCMV infection.

5 Stimulation of ICP0-null HSV-1 and pp71 null HCMV infection by EBV proteins

5.1 Introduction

EBV is a member of the *Gammaherpesvirinae* family, which is one of the most common viruses which infect humans. As with HSV-1 and HCMV, EBV infection is separated into latent and lytic stages. Some components of ND10 have also been demonstrated to regulate or repress EBV infection in host cells (Echendu & Ling, 2008; Ling *et al.*, 2005; Sivachandran *et al.*, 2008; Tsai *et al.*, 2011). The proteins that EBV expresses that modulate and may counter the repression of ND10 are EBNA1, BNRF1 and EBNA-LP, which have been implicated in interactions with or effects on PML, hDaxx/ATRX and Sp100 respectively.

5.1.1 Similarities between EBV proteins and ICP0 from HSV-1

ICP0 is a very efficient protein in terms of interacting with and disrupting ND10 by affecting multiple components of these structures simultaneously. Previous data have demonstrated that at least some ICP0 functions can be mediated by the separate effects of two HCMV proteins, IE1 and pp71. The effects of IE1 on sumoylated forms of PML and Sp100 and the dispersion of the hDaxx-ATRX complex by pp71 rescued 50% of the activity of ICP0 in ICP0 null HSV-1 complementation assays. Thus, the ND10 interaction proteins from EBV were selected and investigated for their potential to complement or enhance ICP0 null HSV-1 infection.

EBV protein EBNA1 interacts with PML isoform IV then promotes the degradation of other PML isoforms (Sivachandran *et al.*, 2008). EBNA-LP interacts with Sp100 in ND10 and disperses it into the nucleoplasm (Echendu & Ling, 2008; Ling *et al.*, 2005). EBV tegument protein BNRF1 has been shown to interact with hDaxx, disrupt the ATRX-hDaxx complex and disperse hDaxx in the nucleus (Tsai *et al.*, 2011).

5.1.2 Similarities between BNRF-1 and pp71

Both BNRF-1 and pp71 are viral tegument proteins. BNRF1 is composed of 1318 amino acid residues, whereas pp71 has 559 amino acid residues. Both proteins are important for stimulating the immediate early stage of infection of EBV and HCMV, respectively. In host cells, BNRF-1 and pp71 share one interaction target in ND10 which is the hDaxx-

ATRX complex. They have been demonstrated to colocalize with hDaxx and then disperse the hDaxx-ATRX complex (Hofmann *et al.*, 2002; Lukashchuk *et al.*, 2008; Tsai *et al.*, 2011). Depletion of hDaxx allows greatly increased gene expression and replication by pp71 null mutant HCMV (Cantrell & Bresnahan, 2006; Kalejta & Shenk, 2003a; Lukashchuk *et al.*, 2008; Saffert & Kalejta, 2006; 2007).

5.2 Development of BNRF1, EBNA1 and EBNA-LP expression cell lines

The EBNA-LP coding sequence was obtained from Dr. Paul D. Ling and it was attached to a FLAG tag at the C-terminal end. The BNRF1 coding sequence, also attached to a FLAG tag, was a gift from Dr. Paul Lieberman. The EBNA1 coding sequence was a gift from Dr. Joanna Wilson. By PCR modification, a myc tag was attached at the 5' end of the EBNA1 sequence and restriction enzyme sites were also designed in the 5' PCR primer upstream of the myc-tag and also in the 3' primer downstream of the C-terminal end of the coding sequence. The molecular weight difference between EBNA-LP and BNRF-1 was about 90 kDa, which could be easily detected and separated by WB and therefore both proteins could be detected simultaneously with an anti-FLAG antibody when they were expressed in the same cell.

To express three EBV proteins in single cell line, four EBV protein lentiviral vectors were designed and prepared. The vector plasmid pLDT.myc-EBNA1 was prepared by two steps. The first step used PCR to attach the myc tag at the N-terminal end of the EBNA-1 coding sequence. The PCR product was separated by DNA gel electrophoresis and purified using a commercial DNA extraction kit. This myc tagged EBNA-1 sequence was digested by restriction enzymes to generate ligation sites, then after isolation by DNA gel electrophoresis and purification, the myc-EBNA1 sequence was inserted into the plasmid pLDT.TetR.IRES.P vector that has the puromycin resistance sequence. For BNRF1, a FLAG tagged vector plasmid with the pLDT inducible expression backbone and the puromycin resistance gene (provided by Anne Orr) was used to prepare a blasticidin resistant version by swapping the drug resistance marker with that from pLDTbla.mycpp71. The FLAG-tagged EBNA-LP sequence was inserted into a pLDT vector with neomycin resistance. Thus, the single expression cell lines could be generated from each vector by lentivirus infection of HFT.TetR cells, and double and triple EBV proteins expression cell lines could also be prepared through use of different antibiotic selections, coupled with other modifications as described below.

5.2.1 BNRF 1 expression cell lines

BNRF1 expressing cells were prepared by sequential transduction of HFT cells with pLKOneo.CMV.EGFPnlsTetR and pLDT.FLAG.BNRF1.puro vectors. HFT cells were firstly transduced with an EGFP-TetR expression vector with neomycin resistance. The resulting cells were transduced by pLDT.FLAG.BNRF1.puro vector and selected by puromycin. The doubly transduced cells were kept in DMEM with 500 µg/ml G418 and 1 µg/ml puromycin for selection. Expression of BNRF1 was detected by probing for the FLAG tag in WB and IF (Figure 5.1).

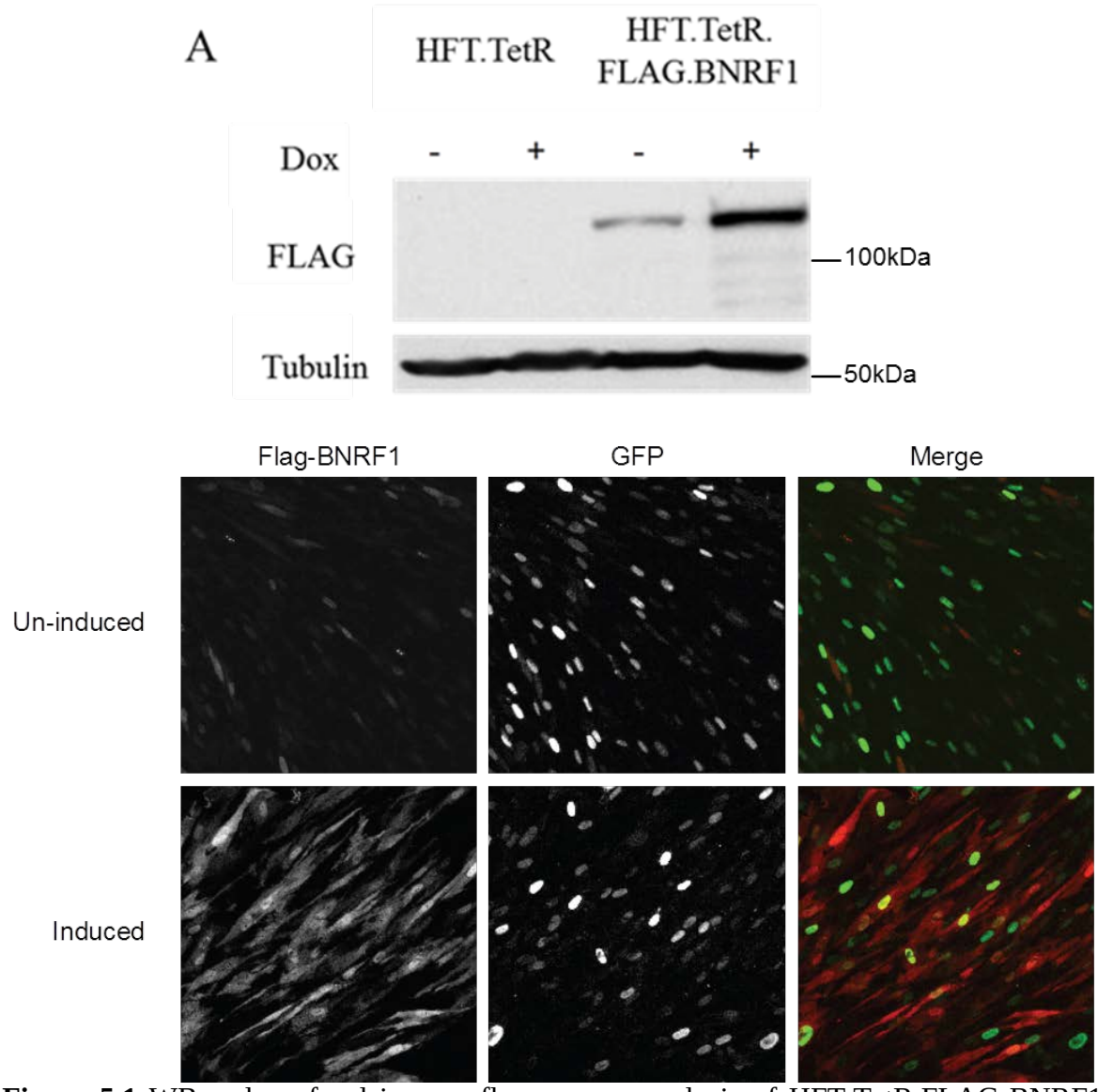

Figure 5.1 WB and confocal immunofluorescence analysis of HFT.TetR.FLAG-BNRF1 cells.

(A) WB analysis of the HFT.TetR.FLAG.BNRF1 cell line. Cells were induced by treatment with DMEM containing 100 ng/ml of doxycycline for 24 h, then the cell lysates were collected and probed by anti-FLAG mAb and anti-Tubulin mAb as indicated. (B) IF analysis of the HFT.TetR.FLAG.BNRF1 cell line. Cells were induced by treatment for 24

h with doxycycline, then the cells were fixed and permeabilised for anti-FLAG mAb staining. The secondary antibody was goat anti-mouse Alexa 555 conjugated antibody.

Figure 5.1 (A) shows that the HFT.TetR.FLAG.BNRF1 cells expressed FLAG-BNRF1 after the doxycycline induction, although some FLAG-BNRF1 leaky expression was detected in uninduced cells. The molecular weight of FLAG-BNRF1 was about 140 kDa. The IF analysis of HFT.TetR.FLAG.BNRF1 cells in Figure 5.1 (B) shows that, after a 24 h induction, the FLAG.BNRF1 protein was expressed in more than 80% of the cells, and the viral protein was spread in both nucleus and cytoplasm. The leaky expression of FLAG.BNRF1 was also observed in IF analysis as indicated by positive anti-FLAG mAb staining in a minority of uninduced cells.

5.2.2 EBNA1 expression cell lines

HFT.TetR.myc-EBNA1 cells that express myc-tagged EBNA1 by itself were generated by a similar protocol as HFT.TetR.FLAG-BNRF1 cells. The HFT.TetR cells were transduced by lentivirus made from the pLDT.myc.EBNA1 vector and selected with puromycin. The resulting cell line was grown in DMEM with 500 µg/ml G418 and 1 µg/ml puromycin, Then myc-EBNA1 expression was analysed by WB and IF (Figure 5.2 A, B). Meanwhile, any potential colocalization of EBNA1 with PML was also analysed by IF (Figure 5.2 C,D)

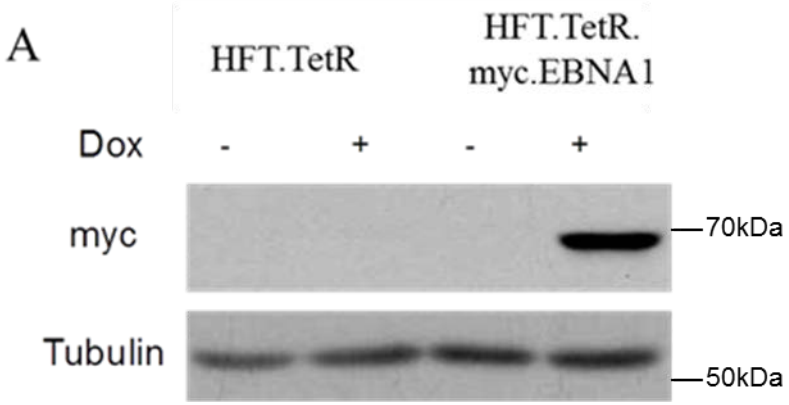

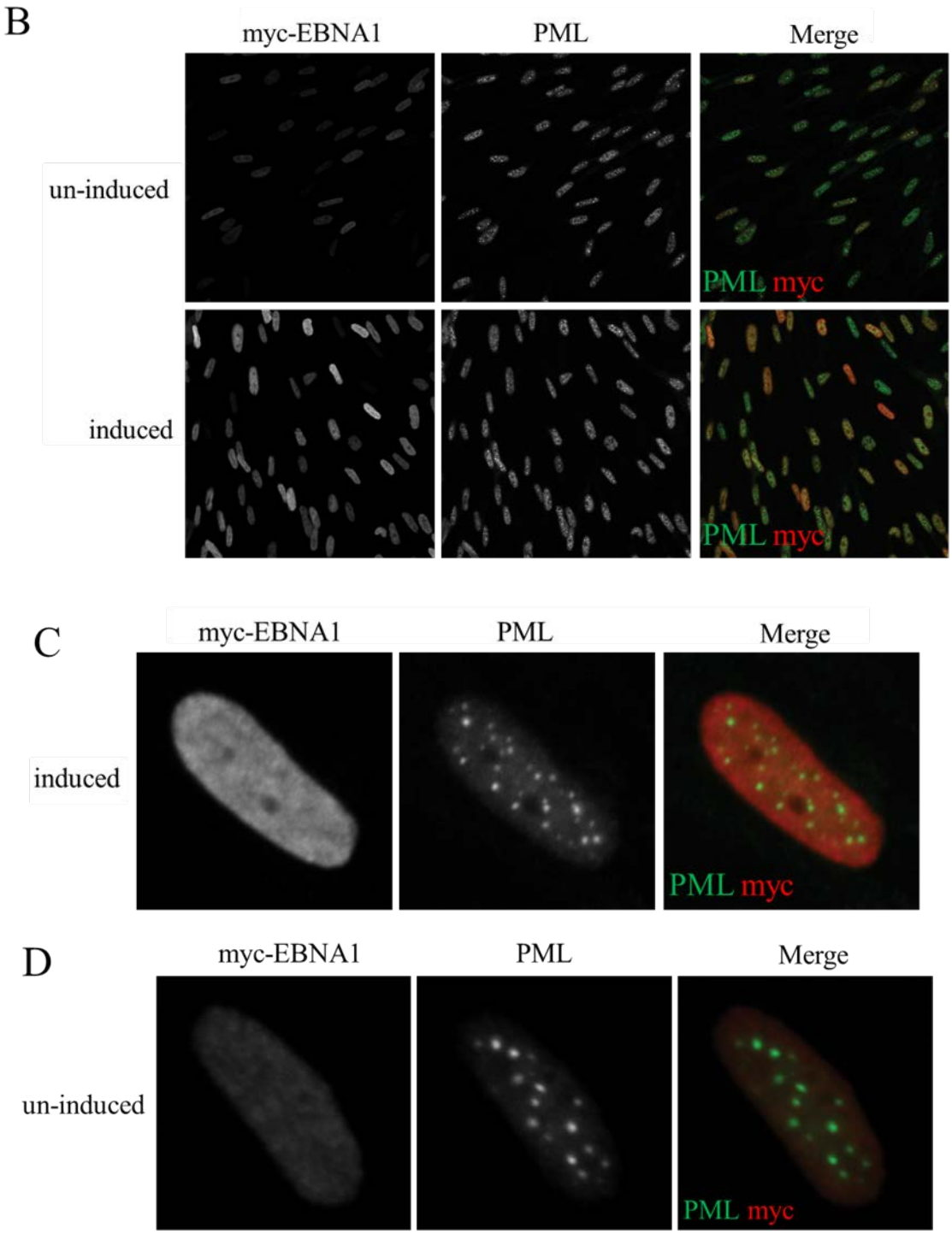

Figure 5.2 WB and IF analysis of HFT.TetR.myc-EBNA1 cells

(A) WB analysis of HFT.TetR.myc-EBNA1 cells. Cells were treated with DMEM containing 100 ng/ml of doxycycline for induction of myc.EBNA1 expression. After 24 h induction, cell lysates were collected and separated by SDS-PAGE using a 10% acrylamide gel. The proteins were transferred to a membrane which was probed using anti-myc and anti-Tubulin mAbs as indicated. (B) IF analysis of the myc-EBNA1 expression in HFT.TetR.myc-EBNA1 cells. Induced and uninduced cells were fixed and permeabilized after 24 h induction for anti-myc mAb and anti-PML rAb staining as indicated. (C) IF images of a single induced cell expressing myc-EBNA1. (D) IF images of a single uninduced cell expressing myc-EBNA1 at a low level. The positions of molecular weight standards (in thousands) are indicated to the right of each panel.

In Figure 5.2 (A), myc-EBNA1 expression was triggered by doxycycline induction. The IF analysis in Figure 5.2 (B) provided the information about the expression rate of myc-EBNA1. About 100% of the cells expressed myc-EBNA1 after treatment with doxycycline for 24 h. As with HFT.TetR.FLAG-BNRF1 cells, some expression of EBNA1 prior to induction was also observed by IF in this cell line, but this was not detectable by WB. It is possible that a longer exposure time for anti-myc mAb probing would show the leaky expression of the protein. The expression of myc-EBNA1 in uninduced cells was maintained at a much lower level compared with induced cells. Thus, this provided extra detail of any potential EBNA1 and PML interaction (Figure 5.2 C, D). Unlike the previous paper reported (Sivachandran *et al.*, 2010; Sivachandran *et al.*, 2008), co-localization of EBNA1 with PML was not observed in cells expressing either low or high amounts of the protein (Figure 5.2 C, D). Sivachandran *et al.* also observed dispersal of PML and/or a reduction in ND10 number in EBNA1 expression cells, which was also not observed in HFT.TetR.myc-EBNA1 cells. These discrepancies could have been caused by differences in cell type, expression method and expression level.

5.2.3 EBNA-LP expression cell lines

The expression of EBNA-LP by itself in HFT cells was achieved by a slightly different approach than that used for the previous cell lines. The selection marker of the pLDT.FLAG-EBNA-LP.neo vector is neomycin which had been used to select the HFT.TetR cells used for HFT.TetR.FLAG-BNRF1 and HFT.TetR.myc-EBNA1 preparation, and was therefore unavailable for this cell line. Vector pLDT.EYFP.TetR.IRES.P has puromycin resistance and expresses TetR together with inducible EYFP (see Materials and Methods). Previously, HFT.TetR.EYFP cells had been generated as a negative control for HCMV and HSV-1 infection experiments used in previous Chapters. In this chapter, HFT.TetR.EYFP cells were transduced by pLDT.FLAG-EBNA-LP.neo vector and the resulting cell line was selected by neomycin. HFT.TetR.FLAG-EBNA-LP cells were maintained in DMEM containing 500 µg/ml G418 and 1 µg/ml puromycin. WB and IF analyses of HFT.TetR.FLAG-EBNA-LP cells are shown in Figure 5.3 A, B. Furthermore, the interaction between EBNA-LP with ND10 was also studied by IF and the images are shown in Figure 5.4.

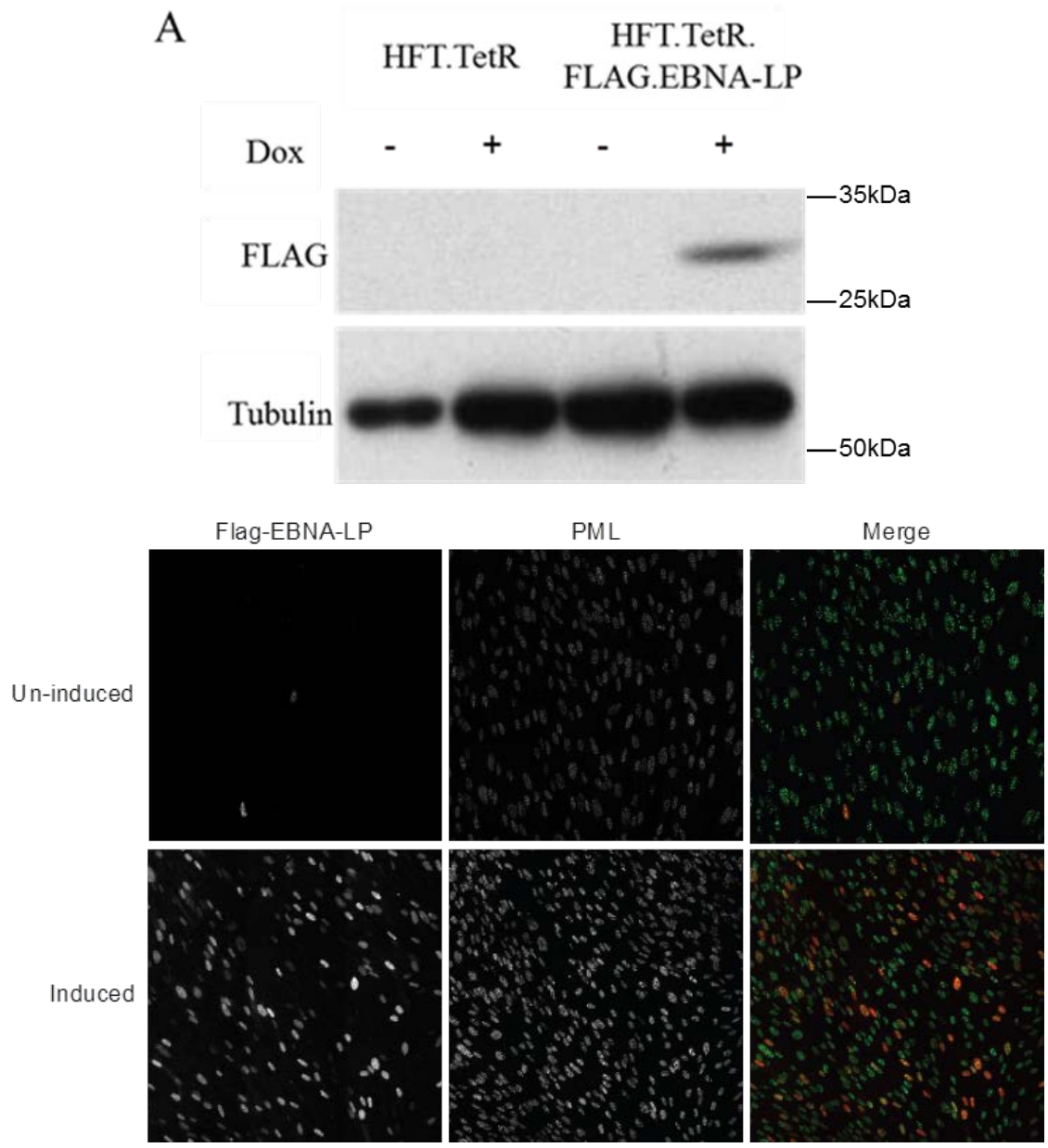

Figure 5.3 WB and IF analysis of HFT.TetR.FLAG-EBNA-LP cells

(A) WB analysis of HFT.TetR.FLAG-EBNA-LP cells. Induced cells were treated with DMEM containing 100 ng/ml doxycycline for 24 h. Then the cell lysates were collected and probed by anti-FLAG mAb and anti-Tubulin mAb as indicated. (B) IF analysis of induced and uninduced HFT.TetR.FLAG.EBNA-LP cells. Induced cells were treated by DMEM with 100 ng/ml doxycycline for 24 h. Then the induced and uninduced cells were fixed and permeabilized for anti-FLAG mAb and anti-PML rAb staining. The secondary antibodies were goat anti-mouse Alexa 555 conjugated antibody and goat anti-rabbit Alexa 633 conjugated antibody. The positions of molecular weight standards (in thousands) are indicated to the right of each panel.

As Figure 5.3 (A) shows, the expression of FLAG-EBNA-LP was relatively tightly regulated by the tetracycline inducible system that was constructed within the pLDT.EYFP.TetR.IRES.P vector. After induction, the expression of the viral protein was

as efficient as in the previous two EBV protein expression cell lines. This indicated that the TetR expressed by single inducible vector pLDT.EYFP.TetR.IRES.P was not only sufficient to control the EYFP expression but also efficient enough for FLAG-EBNA-LP expression. The IF analysis in Figure 3.52 (B) shows that about 70% of the cells expressed FLAG-EBNA-LP after 24 h induction with doxycycline, while in uninduced cells this was less than 1%. Furthermore, by observation of the low level expression of EBNA-LP in the small number of uninduced cells, and also the higher level of expression in the induced cells, the interaction between FLAG-EBNA-LP and ND10 was studied. (Figure 5.4 A,B)

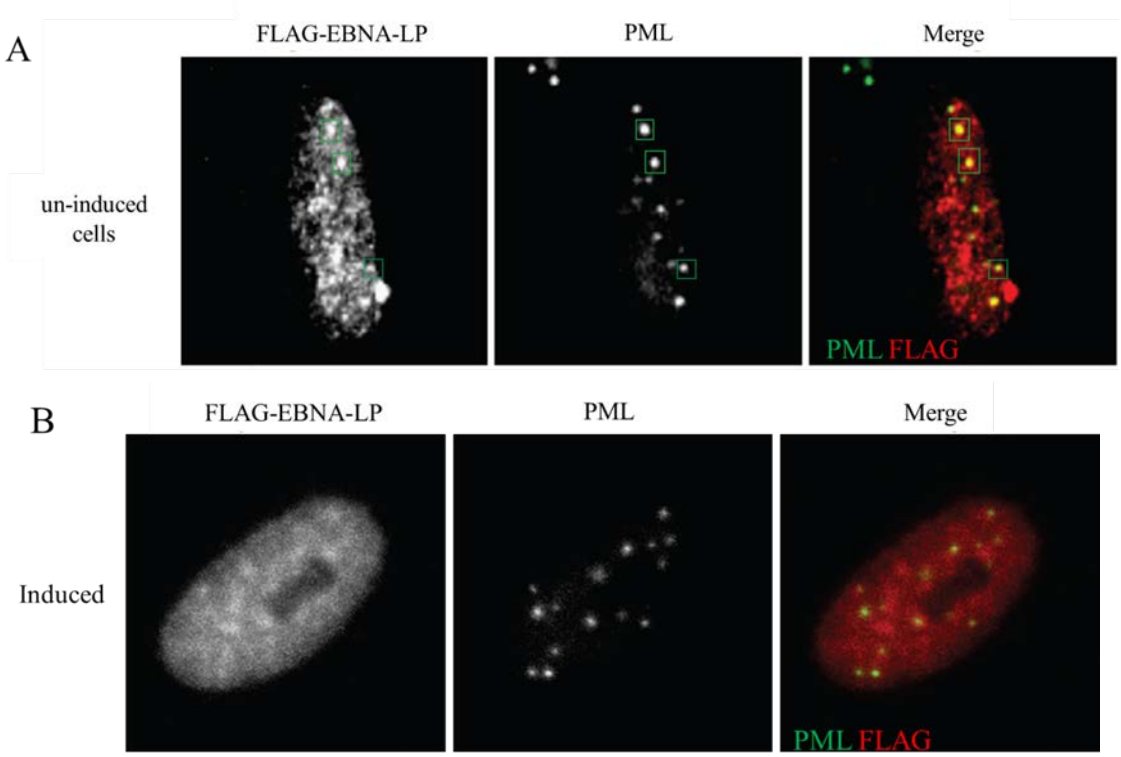

Figure 5.4 IF images of single cells expressing FLAG-EBNA-LP
(A) IF images of uninduced single cell expressing FLAG-EBNA-LP at low level. (B) IF images of induced single cell that expressing FLAG-EBNA-LP at high level.

The low level expression of EBNA-LP in HFT.TetR.FLAG.EBNA-LP cells provided detail of the interaction between EBNA-LP and ND10. Figure 5.4 (A) shows some evidence of co-localization between FLAG-EBNA-LP and PML when FLAG-EBNA-LP is expressed at a much lower level than in induced cells. A previous paper reported that EBNA-LP co-localizes with ND10 and disperses Sp100A in the nucleus (Ling *et al.*, 2005). The evidence of some co-localization between EBNA-LP and PML in Figure 5.4 A may represent the interaction between EBNA-LP and Sp100A. In Figure 5.4 (B), the expression of FLAG-EBNA-LP was induced by doxycycline for 24 h. In this case the

highly expressed EBNA-LP was more diffuse, which may reflect dispersal of Sp100A in the nucleus but there was insufficient time to test this possibility. Sp100A is dispensable for ND10 formation (Ishov *et al.*, 1999). Thus, high level EBNA-LP expression might disperse Sp100A without further damage to ND10 structure which would be consistent with the normal PML foci in Figure 5.4 B. However, it must be borne in mind that sustained expression of a viral protein in transduced diploid fibroblasts, as in this study, does not always give the same results in this type of assay as the more common approach of plasmid transfection of transformed laboratory cell lines. Therefore, as with the EBNA-1 and BNRF1 cell lines, a thorough IF analysis of all common ND10 proteins is required.

5.2.4 Double and triple viral protein expression cell lines

The TetR repressor expressed by the single inducible vector applied in HFT.TetR.EYFP cells had proved to be efficient for the control of the TetO sequence in another vector in the above experiments. The same method was used to prepare double and triple protein expression cell lines. HFT.BNRF1.EBNA-LP cells were prepared by sequential transduction of HFT.TetR.EYFP cells with pLDT.FLAG.EBNA-LP.neo and pLDT.FLAG.BNRF1.bla vectors. The resulting cell line was maintained in DMEM with 500 µg/ml G418, 1 µg/ml blasticidin and 1 µg/ml puromycin. HFT.EBNA1.EBNA-LP cells were generated by two sequential transductions of HFT cells, firstly with lentivirus made from pLDT.myc.EBNA1.TetR.IRES.P to generate HFT.myc.EBNA1 single inducible cell line. The resulting cells were selected by puromycin and transduced by the second vector, made from pLDT.FLAG.EBNA-LP.neo. Transduced cells were selected using neomycin and kept in DMEM with 500 µg/ml G418 and 1 µg/ml puromycin. HFT.EBNA1.BNRF1 cells were also prepared by two transductions. The HFT.myc.EBNA1 cells described previously were transduced by lentivirus produced from the pLDT.FLAG.BNRF1.bla vector to express FLAG-BNRF1. The resulting cells were selected by neomycin and kept in DMEM with 1 µg/ml blasticidin and 1 µg/ml puromycin. HFT cells expressing BNRF1, EBNA1 and EBNA-LP simultaneously were transduced three times by lentiviruses made from pLDT.myc.EBNA1.TetR.IRES.P, pLDT.FLAG.EBNA-LP.neo and pLDT.FLAG.BNRF1.bla vectors. The resulting cells were selected using puromycin, blasticidin and neomycin. The cell lines prepared above were analysed by WB as shown in Figure 5.5.

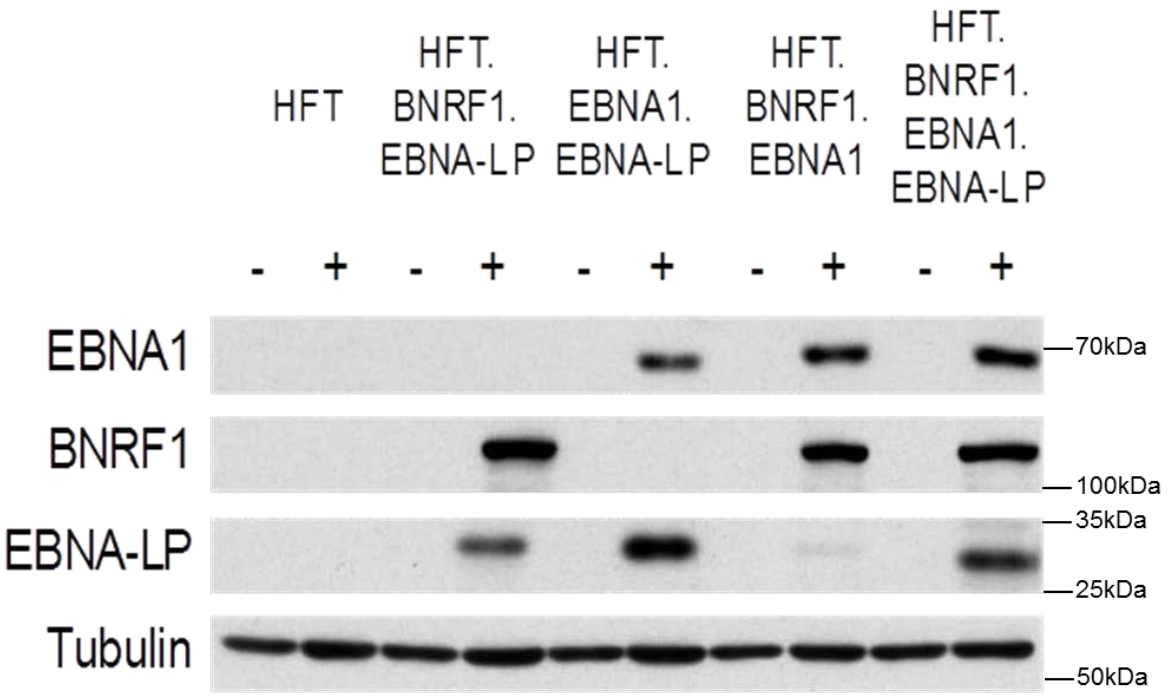

Figure 5.5 WB analyses of EBV protein expression cell lines.

HFT, HFT.BNRF1.EBNA-LP, HFT.EBNA1.EBNA-LP, HFT.BNRF1.EBNA1 and HFT.BNRF1.EBNA1.EBNA-LP cells were induced for 24 h by treatment with doxycycline. The uninduced cells were incubated within DMEM at the meantime. Cell lysates were collected and probed by anti-myc mAb, anti-FLAG mAb and anti-Tubulin mAb as indicated. The secondary antibody was sheep anti-mouse IgG hrp conjugated antibody A4416. The positions of molecular weight standards (in thousands) are indicated to the right of each panel.

The expression of myc-EBNA1 in HFT.EBNA1.EBNA-LP, HFT.EBNA1.BNRF1 and HFT.EBNA1.EBNA-LP.BNRF1 cells as indicated in Figure 5.5 was controlled by TetR protein expressed by the pLDT.myc.EBNA1.TetR.IRES.P vector. Furthermore, the TetR repressor also controlled FLAG-BNRF1 and FLAG-EBNA-LP expression in the above cell lines. These results indicate that the regulatory system provided by TetR expression from the pLDT.myc.EBNA1.TetR.IRES.P vector and the presence of TetO sequences in the additional vectors were efficient in controlling EBV protein expression.

BNRF1 of EBV and pp71 of HCMV are both tegument proteins and they share the ND10 hDaxx-ATRX complex interaction target. This raises the possibility that BNRF1 could replace pp71 in HCMV infection. To investigate the functional interchange between pp71 and BNRF1, HFT.EBNA1.EBNA-LP.pp71 and HFT.BNRF1.IE1 cell lines were generated. The HFT.EBNA1.EBNA-LP.pp71 cells were also used in comparison with HFT.EBNA1.EBNA-LP.BNRF1 cells in the ICP0 null HSV-1 complementation assay.

Meanwhile, HFT.BNRF1.IE1 cells were compared with HFT.ICP0 cells in the same complementation assay.

HFT.EBNA1.EBNA-LP.pp71 cells were prepared by transducing the HFT.EBNA1.EBNA-LP cells with lentivirus made from the pLDT.myc.pp71 vector which expresses blasticidin resistance for the resulting cell line selection. HFT.IE1 cells were transduced by pLDT.FLAG.BNRF1.bla to construct HFT.IE1.BNRF1 cells. WB analysis of protein expression in HFT.EBNA1.EBNA-LP.pp71 and HFT.BNRF1.IE1 cell lines is shown in Figure 5.6.

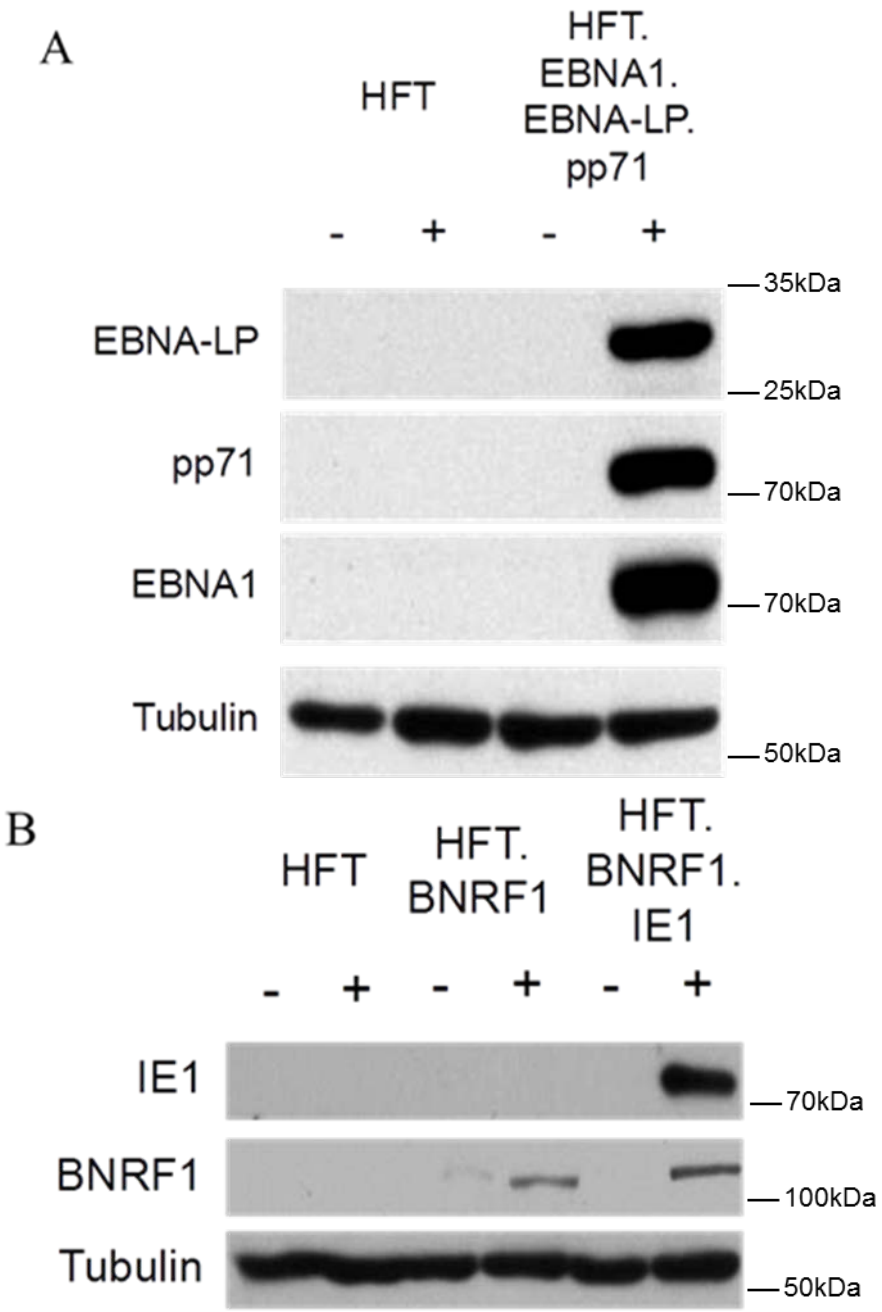

Figure 5.6 WB analyses of HFT.EBNA1.EBNA-LP.pp71 and HFT.BNRF1.IE1 cells

(A) WB analysis of HFT.EBNA1.EBNA-LP.pp71 cells. Induced cells were treated with DMEM containing 100 ng/ml doxycycline for 24 h and the uninduced cells were incubated in DMEM at the meantime. Cell lysates were collected and probed by anti-FLAG mAb, anti-myc mAb, anti-pp71 mAb and anti-Tubulin mAb as indicated. (B) WB analysis of HFT.BNRF1.IE1 cells. Cell lysates were probed by anti-FLAG mAb, anti-IE1 mAb and anti-Tubulin mAb as indicated. The secondary antibody was sheep anti-mouse IgG antibody A4416. The positions of molecular weight standards (in thousands) are indicated to the right of each panel.

Expression of pp71 in HFT.EBNA1.EBNA-LP.pp71 cells was triggered by doxycycline induction as indicated in Figure 5.6 A. The expression of IE1 in HFT.BNRF1.IE1 cells was

also efficient as shown in Figure 5.6 B. Those cell lines were investigated in the ICP0 null HSV-1 complementation assay to study the properties of the EBV proteins.

5.3 EBV proteins stimulate ICP0-null HSV-1 infection

The EBV proteins under study in this chapter have been reported to interact with ND10 components in the nucleus during latent and lytic infection. For example, EBNA1 disrupts ND10 and associates with PML through an interaction with PML IV (Sivachandran *et al.*, 2008), BNRF1 binds to hDaxx and disrupts the hDaxx-ATRX complex to stimulate early viral gene expression (Tsai *et al.*, 2011), and EBNA-LP interacts with and displaces Sp100 from ND10 in the nucleus (Ling *et al.*, 2005). These proteins therefore share some similarities to the functions of ICP0 in HSV-1, which degrades sumoylated PML and Sp100 and disperses hDaxx and ATRX complex in the nucleus (Everett *et al.*, 2009; Lukashchuk & Everett, 2010). The complementation assay of ΔICP0 HSV-1 by EBV protein expression in HFT cells was investigated in this section. The investigation was also extended to compare the abilities of pp71 and BNRF1 to complement ICP0 null HSV-1. Thus, HFT.EBNA-LP.EBNA1.pp71 cells were infected by ΔICP0 HSV-1 in parallel with HFT.EBNA-LP.EBNA1.BNRF1 in the same experiment.

This study was performed in a similar manner as the complementation assay of ΔICP0 HSV-1 in HFT.IE1 cells (Chapter 4.3). Briefly, HFT cells expressing the different EBV proteins were seeded in 24-well plates at $1x10^5$ cells/well and induced for 24 h to express viral proteins. The induced cells were infected with ΔICP0 HSV-1 and blue plaque assays were performed at 24 h post infection to collect the plaque formation efficiency data. The same experiments were performed three times to work out an average figure and standard deviation. The results are shown in Figure 5.7.

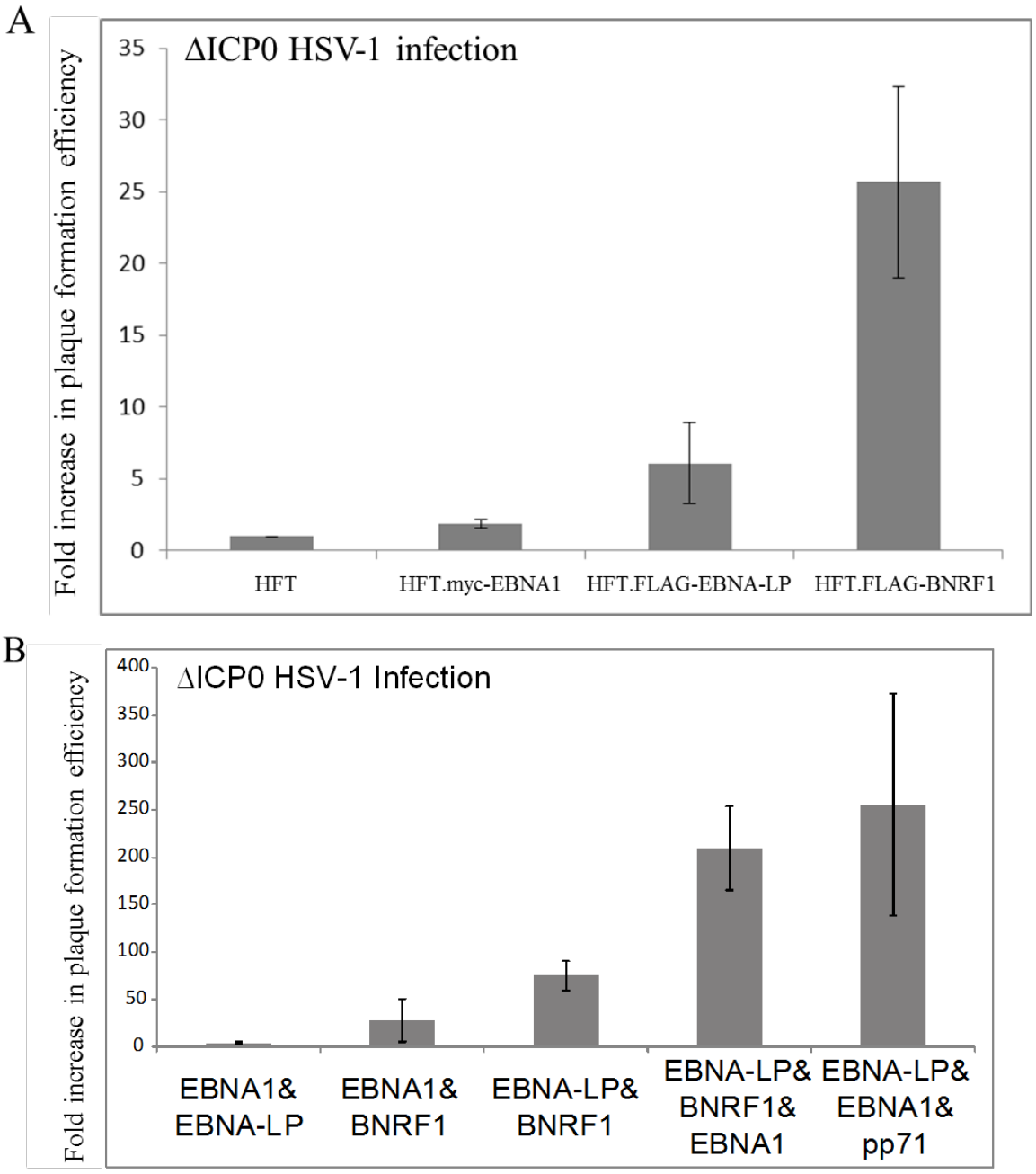

Figure 5.7 Complementation assay of ΔICP0 HSV-1 in EBV protein expression cell lines. (A) Complementation assay of ΔICP0 HSV-1 in HFT.myc.EBNA1, HFT.FLAG.BNRF1 and HFT.FLAG.EBNA-LP cells. Cells were induced by treatment with 100 ng/ml doxycycline for 24 h before infection. Induced cells were infected by ΔICP0 HSV-1 at different MOIs. After 4 h of infection, the cell medium was changed to DMEM with 100 ng/ml doxycycline and 1% human serum. At 24 h post infection, the infected cells were fixed and blue plaque assays were performed. Plaque formation efficiency data are expressed as fold-increase in absolute titre (PFU per ml) in each cell type over that in HFT cells. (B) Complementation assay of ΔICP0 HSV-1 in HFT.EBNA1.EBNA-LP, HFT.EBNA1.BNRF1, HFT.EBNA-LP.BNRF1, HFT.EBNA-LP.EBNA1.BNRF1 and HFT.EBNA-LP.EBNA1.pp71 cell lines. The infection protocols were as same as Figure 5.7 (A). The fold increases in plaque formation were measured against HFT cells.

Figure 5.7 (A) shows that expression of single EBV proteins stimulated ΔICP0 HSV-1 infection in each case. The mutant virus infections were only very slightly increased by expression of EBNA1 and to a greater but still relatively small degree by EBNA-LP. Meanwhile, BNRF1 increased the ΔICP0 HSV-1 infection about 25-fold. These data indicate that the expression of EBV proteins can complement ΔICP0 HSV-1 infection, but not as efficiently as ICP0. In Figure 5.7 (B), double EBV protein expression cell lines complemented ICP0 null HSV-1 infection to a greater degree. HFT.EBNA-LP.BNRF1 and HFT.EBNA1.BNRF1 cells complemented ΔICP0 HSV-1 infection about 50-fold whereas simultaneously expressing EBNA1 and EBNA-LP increased ΔICP0 HSV-1 infection only about 4-fold. Meanwhile, ΔICP0 HSV-1 infection was substantially increased in induced HFT.EBNA-LP.EBNA1.BNRF1 cells. These results indicate that EBNA1, EBNA-LP and BNRF1 can cooperatively release at least some of the repression of ΔICP0 HSV-1. These data are consistent with the hypothesis that the increased plaque formation of the ICP0 mutant are due to the combined effects of these EBV proteins on ND10 components, but further work is required to confirm that these proteins have the reported ND10-related functions in these cell lines.

The effect of substituting BNRF1 by pp71 was studied in the same complementation study. The HFT.EBNA-LP.EBNA1.pp71 cells increased the ΔICP0 HSV-1 infection by about 250-fold, which was very close to the 230-fold increase observed in HFT.EBNA-LP.BNRF1.EBNA1cells. This observation indicates the possibility of interchangeable activity between BNRF1 and pp71 and is consistent with the prediction in section 5.1.2.

Previously studies demonstrated the simultaneous expression of IE1 and pp71 in HFT cells can largely complement ΔICP0 HSV-1 infection (Figure 4.9). The data in Figure 5.7 B also indicate that BNRF1 can be replaced by pp71 in complementing ICP0 null HSV-1 infection. To further investigate the interchangeable role between pp71 and BNRF1, HFT.IE1.BNRF1 cells were constructed. The same complementation assay in Figure 5.7 was performed on HFT.IE1.BNRF1 and HFT.ICP0 cells, and the results are shown in Figure 5.8.

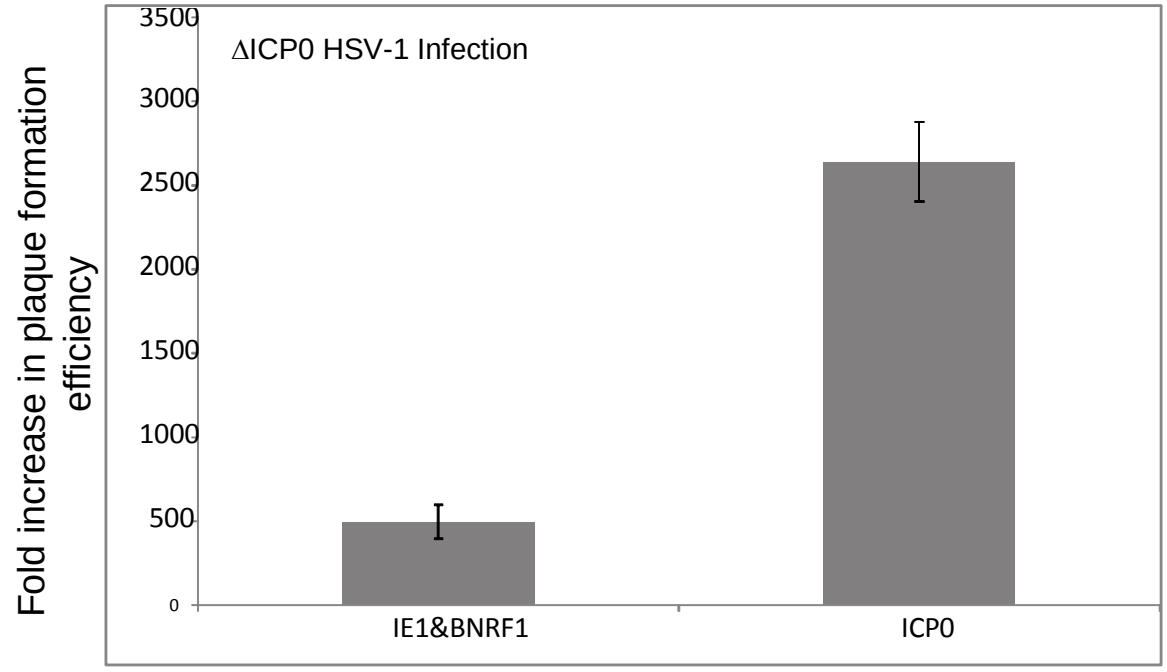

Figure 5.8 Complementation assay on HFT, HFT.IE1.BNRF1 and HFT.ICP0 cells.

Cells were treated with DMEM with 100 ng/ml doxycycline 24 h for induction. Induced cells were infected by ΔICP0 HSV-1 at sequential dilutions determined empirically to give countable numbers of plaques on each cell line. At 4 h post infection, cell medium was changed to DMEM with 100 ng/ml doxycycline and 1% human serum. After 24 h infection, the cells were fixed and blue plaque assays were performed for collecting the complementation efficiency data. This experiment was performed three times to obtain an average complementation data and standard deviation. The results are expressed as fold-increase in absolute titre (PFU per ml) in each cell type over that in HFT cells.

IE1 and BNRF1 together increased the ΔICP0 HSV-1 infection about 500-fold, which is about 20% of the activity of ICP0 in HFT.ICP0 cells. The previous data presented in section 4.3.3 showed that IE1 and pp71 together reached 50% of the activity of ICP0 in this assay. The above comparison analysis between pp71 and BNRF1 indicates the possibility that those two proteins might be interchangeable in HCMV infection. Thus, in the next section, BNRF1 expression cells were infected by pp71 null HCMV to further investigate the hypothesis in section 5.1.2.

5.4 BNRF-1 complements pp71 null HCMV infection

The hDaxx-ATRX complex represses the MIEP in the early stages of HCMV infection, and this repression can be overcome by HCMV tegument protein pp71 (Cantrell & Bresnahan, 2006; Lukashchuk *et al.*, 2008; Saffert & Kalejta, 2006). BNRF1, the most abundant tegument protein in EBV (Johannsen *et al.*, 2004), also interacts with hDaxx and disrupts the hDaxx-ATRX complex in the nucleus (Tsai *et al.*, 2011). The

complementation assay in section 5.3 indicated the interchangeable function between pp71 and BNRF1. Thus, it was interesting to investigate the potential of BNRF1 to substitute for the function of pp71 in HCMV infection to further compare these two tegument proteins.

A complementation assay of Δpp71 HCMV was performed on HFT, HFT.FLAG-BNRF1 and HFT.TetR.myc-pp71 cells. The infection protocols and methods were similar to those described in section 4.8. Briefly, HFT.TetR, HFT.FLAG-BNRF1 and HFT.TetR.myc-pp71 cells were induced and infected by pp71 null HCMV at different MOIs. The infected cells were incubated for 10 days to allow the formation of HCMV plaques. Then the HCMV plaque assay was performed using histochemical staining for UL44 and the plaque formation efficiency data were collected. The results are shown in Figure 5.9.

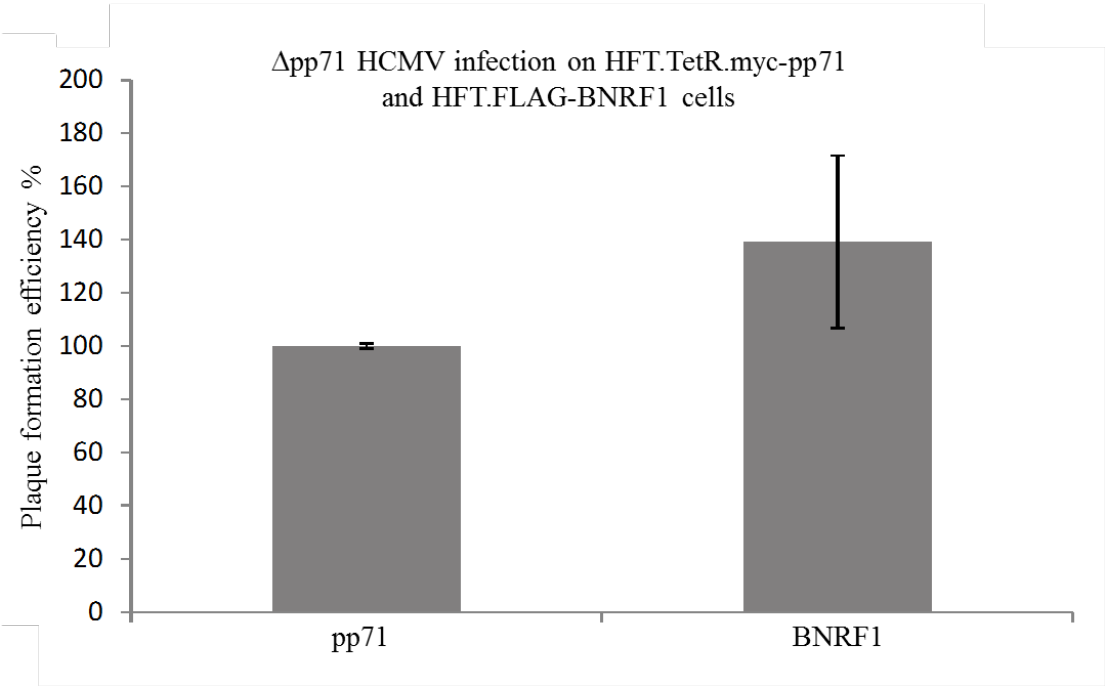

Figure 5.9 Complementation assay of Δpp71 HCMV on HFT.FLAG-BNRF1 and HFT.TetR.myc-pp71 cell lines.

Cells were induced with DMEM with 100 ng/ml doxycycline for 24 h before infection. Induced cells were infected at a series of MOIs. At 12 h post infection, the cell medium was changed to DMEM with 100 ng/ml doxycycline and 1% human serum. After 10 days of infection, the infected cells were fixed and permeabilized for HCMV plaque assays. The results were firstly calculated as fold-increases in absolute titre (PFU per ml) in each cell type over that in HFT cells. In this experiment, the plaque forming efficiency of the mutant virus was increased by about 200-fold in pp71-expressing cells compared to HFT cells. Complementation efficiency by myc-pp71 was set as 100% and the relative complementing efficiency of BNRF1 was worked out against myc-pp71. The same experiment was performed three times to calculate the average and standard deviation.

BNRF1 complemented the Δpp71 HCMV infection as efficiently as pp71 in Figure 5.9. The slightly increase of BNRF1 over that of pp71 might due to the different protein expression efficiency. The above complementation data was based on the plaque forming efficiency, which cannot provide direct information about HCMV gene expression. To investigate in more detail about the properties of BNRF1 in Δpp71 HCMV infection, infected cell lysates were analysed by WB (Figure 5.10).

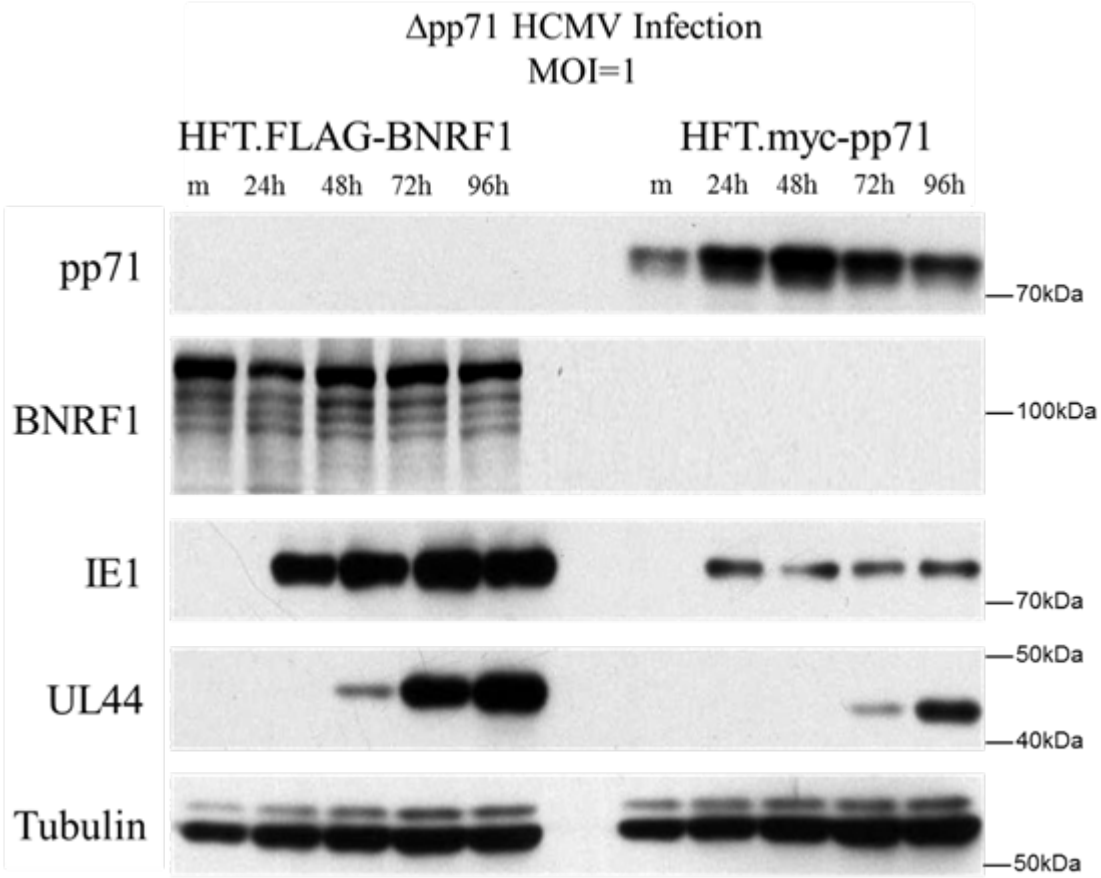

Figure 5.10 WB analysis of Δpp71 HCMV infection in HFT.FLAG-BNRF1 and HFT.TetR.myc-pp71 cell lines.

Cells were induced by doxycycline treatment for 24 h, then the induced cells were infected by Δpp71 HCMV at MOI 1 (titrated on HFT.TetR.myc-pp71 cells) for 12 h. Then the cell medium was changed to DMEM with 100 ng/ml doxycycline and 1% human serum. On consecutive days up to 4 days post infection, cell lysates were collected and probed by anti-pp71 mAb, anti-FLAG mAb, anti-IE1 mAb, anti-UL44 mAb and anti-Tubulin mAb as indicated. The positions of molecular weight standards (in thousands) are indicated to the right of each panel.

The WB analysis further confirmed that BNRF1 can complement Δpp71 HCMV infection in HFT cells. Consistent with the HCMV plaque assays, expression of both IE1 and UL44 in HFT.FLAG-BNRF1 cells was more efficient than in HFT.pp71 cells. The same

phenomenon was also noticed by observing the size of anti-UL44 mAb stained HCMV plaques that formed in pp71 and BNRF1 expression HFT cells (data not shown).

5.5 Conclusion and discussion

Previous data in chapter 3 found that expression of HCMV proteins IE1 and pp71 can recover about 50% of ICP0-null mutant HSV-1 infection, which indicates that β-herpes virus proteins can functionally replace an α-herpes virus protein. Chapter 4 investigated the properties of ICP0 in HCMV infection and demonstrated that ICP0 can complement pp71 null HCMV infection. Thus, ND10 interacting proteins from α-herpes virus and β-herpes virus can be functionally interchangeable. Then, an interesting question is whether γ-herpes virus proteins that interact with ND10 can replace their counterparts in HSV-1 and HCMV.

The study in this chapter demonstrated the possibility of using EBV proteins that interact with ND10 to replace HCMV proteins and partially rescue ICP0 null HSV-1 infection. Three EBV proteins investigated in this study performed different functions in viral infection. EBNA-LP and BNRF1 are relevant to EBV latent infection and expressed in lytic stage, further more BNRF1 is also demonstrated to be important for lytic infection (Feederle *et al.*, 2006; Finke *et al.*, 1987). EBNA1 is important during EBV infection and replication, but is also commonly expressed during latency to enable genome replication and partition of EBV genomes during cell division (Raab-Traub, 2002). Those EBV proteins expressed to interact with ND10 members increased ICP0 null HSV-1 infection at different levels. Single expression of EBNA1, EBNA-LP or BNRF1 complemented ΔICP0 HSV-1 less efficiently than double and triple proteins expression. Thus, it is possible that the EBV proteins cooperatively interact with ND10 for complementing ΔICP0 HSV-1 infection.

HFT.TetR.EBNA1 cells express EBNA1 efficiently but cannot disperse PML in this study. This was not consistent with a previous study that demonstrated that EBNA1 could degrade PML through an interaction with PML.IV (Sivachandran *et al.*, 2010; Sivachandran *et al.*, 2008). This might due to the difference between the expression cell lines that were used in these studies, or the expression of EBNA1 was insufficient for PML degradation in this study. Thus, that HFT cells expressing EBNA1 increased ΔICP0 HSV-1 infection only about 2-fold was within expectation. The other two EBV proteins, EBNA-LP and BNRF1, were investigated and demonstrated to interact with Sp100 and hDaxx

respectively (Echendu & Ling, 2008; Ling *et al.*, 2005; Tsai *et al.*, 2011). Single expression of EBNA-LP or BNRF1 achieved better complementation efficiency of ICP0 null HSV-1 than EBNA1. Co-expression of EBNA1 with EBNA-LP or BNRF1 increased ΔICP0 HSV-1 infection about 5- and 30-fold respectively, which are higher than each single EBV protein expression cell lines. Furthermore, simultaneous expression of EBNA-LP and BNRF1complemented ΔICP0 HSV-1 infection about 80-fold, which was the most efficient combination within the double EBV proteins expression cell lines. This might be related to the ND10 interaction efficiency of EBNA-LP and BNRF1, but due to the time limitation for these studies, further detail could not be provided at this stage. HFT cells expressing EBNA-LP, EBNA1 and BNRF1 complemented ICP0 null HSV-1 about 220-fold that was about 10% to the ICP0 complementation in Figure 5.8. The previous investigation of HFT.TetR.myc-EBNA1 cells indicating the expressed myc-EBNA1 was insufficient for PML degradation and dispersion, which might contribute less than EBNA-LP and BNRF1 in de-repression of ICP0 null HSV-1 infection. As introduced previously, more detail about the EBNA-LP and BNRF1 that was expressed in HFT.EBNA-LP.EBNA1.BNRF1 cells is required for making further conclusions from this complementation study. But, a brief conclusion that could be generated in this stage is that the EBV ND10 interacting proteins could enhance or complement ICP0 null HSV-1 infection by a considerable degree.

Previous studies demonstrated that HCMV proteins pp71 and IE1 together can largely complement ICP0 null HSV-1 infection (Everett *et al.*, 2013a). Therefore, to compare BNRF1 with pp71, the HCMV protein was co-expressed with EBV proteins in this study. The combinations examined were expression of BNRF1 with IE1, and EBNA1 and EBNA-LP with pp71. Due to the time limitations, there was no direct comparison performed between HFT.IE1.BNRF1 and HFT.IE1.pp71 in ΔICP0 HSV-1 complementation assays. HFT.EBNA-LP.EBNA1.pp71 cells were compared with HFT.EBNA-LP.EBNA1.BNRF1 cells directly on complementing ΔICP0 HSV-1 infection. Plaque formation efficiencies were similar in these triple proteins expression cell lines and the results demonstrated that pp71 and BNRF1 are interchangeable in complementing ΔICP0 HSV-1 infection. Furthermore, that HFT.IE1.BNRF1 cells rescued 20% activity of ICP0 in ΔICP0 HSV-1 complementation assays indicated the possibility of a similar cooperation mechanism between IE1/BNRF1 with IE1/pp71 to increase ΔICP0 HSV-1 infection.

A direct comparison assay was performed on HFT.FLAG-BNRF1 and HFT.myc-pp71 cells in the complementation of Δpp71 HCMV infection. The results demonstrated that the plaque formation efficiencies on HFT.FLAG-BNRF1 and HFT.myc-pp71 cells were similar. WB analysis of HCMV gene expression further confirmed the observation in the Δpp71 HCMV complementation study. Thus, with the data above, a brief conclusion that BNRF1 and pp71 are interchangeable could be made.

6 Summary, Discussion and Future Prospects

6.1 Summary

Intrinsic resistance of host cells to viral infection plays an important role in virus infection defence processes (Bieniasz, 2004). The studies presented in this thesis aimed to contribute more detail to the understanding of the intrinsic resistance mechanisms. By cross interchange of viral proteins from different herpes virus, the interchangeable role of ICP0, pp71, IE1, BNRF1, EBNA1 and EBNA-LP was partially demonstrated. Those viral proteins from different herpes viruses that belong to α, β and γ herpes virus families have all been demonstrated to interact with ND10 (Ahn *et al.*, 1998; Echendu & Ling, 2008; Everett *et al.*, 2006; Hofmann *et al.*, 2002; Sivachandran *et al.*, 2010; Tsai *et al.*, 2011). Previous work had indicated that IE1 and pp71 of HCMV can largely complement ΔICP0 HSV-1 infection (Everett *et al.*, 2013a). Thus, to extend this investigation, ICP0 was investigated in ΔIE1 HCMV and Δpp71 HCMV complementation assays. Furthermore, recent publications identified several EBV proteins that target ND10 during viral infection (Ling *et al.*, 2005; Sivachandran *et al.*, 2010; Tsai *et al.*, 2011). Those proteins were also introduced into the ΔIE1 HCMV and Δpp71 HCMV complementation assays to study the properties of EBV proteins in α and β herpes virus infections. With brief investigation, EBNA-LP, EBNA1 and BNRF1 were identified to stimulate ΔICP0 HSV-1 infection and BNRF1 was demonstrated to complement Δpp71 HCMV infection. These investigations indicated that herpes viruses could benefit from each other to de-repress gene expression, and in many cases it seems likely that this is related to their effects on ND10. This raises the possibility of developing a common anti-herpes virus treatment by interfering with the anti-ND10 functions of different herpes virus proteins.

6.2 Discussion

6.2.1 ND10 interacting proteins from different herpes virus families are Interchangeable

Previous work indicated that functions of ICP0 from HSV-1 that counteract ND10 can be viewed as being functionally separated into two proteins in HCMV, IE1 and pp71 (Everett *et al.*, 2013a). Tegument protein pp71 interacts with the hDaxx-ATRX complex and causes the degradation of hDaxx (Hwang & Kalejta, 2007; Saffert & Kalejta, 2006; 2007). Immediate early protein IE1 de-sumoylates and disperses PML and Sp100 during HCMV

infection and stimulates lytic infection (Ahn *et al.*, 1998; Greaves & Mocarski, 1998; Korioth *et al.*, 1996). The expression of IE1 and pp71 together rescued 50% of the activity of ICP0 in complementing ΔICP0 HSV-1 infection (Everett *et al.*, 2013a). In the reverse experiment, ICP0 was unable to complement ΔIE1 HCMV infection but successfully complemented Δpp71 HCMV infection in human fibroblast cells. The above investigation demonstrated that there are HCMV specific functions of IE1 for stimulating HCMV lytic infection. Meanwhile, it was demonstrated that pp71 can be replaced by ICP0 during HCMV infection. Furthermore, the results also predicted that in *vivo* infection, at least in principle, HCMV and HSV-1 might benefit from each other for stimulating lytic infection.

PML and Daxx depletion has been reported to improve IE1 null HCMV infection (Tavalai *et al.*, 2008b). This previous publication collected the complementation data by monitoring IE2 expression efficiency in infected cells (Tavalai *et al.*, 2008b). The paper suggested that ΔIE1 HCMV infection is repressed by PML and Daxx and the repression can be overcome by depletion of PML or Daxx or both of them. However, no further information about early or late viral gene expression and viral particle generation was provided to support the conclusion. Thus, the knock down of ND10 components may stimulate IE2 expression but not complete HCMV replication. The data presented in section 4.5 provided more detail about IE1 null HCMV early and late gene expression in infected human fibroblast cells. It was confirmed that the absence (degradation of PML and Sp100 in induced HFT.ICP0 cells) of PML and Sp100 increased IE2 expression but this was not sufficient for stimulation of abundant early and late gene expression. In other words, IE1 was still required for efficient HCMV infection and replication. Therefore, the IE1 must specifically interact with other HCMV proteins or genes to stimulate viral infection and this function is not replaceable by ICP0.

EBV tegument protein BNRF1 interacts with the hDaxx-ATRX complex to stimulate viral infection (Tsai *et al.*, 2011). It thus shares some of the same properties with pp71 such as interacting with the hDaxx-ATRX complex and being an abundant tegument protein in the viral structure (Hofmann *et al.*, 2002; Lukashchuk *et al.*, 2008; Tsai *et al.*, 2014; Tsai *et al.*, 2011). The complementation assay of Δpp71 HCMV indicated that BNRF1 can stimulate Δpp71 HCMV infection as efficiently as pp71, and the increases in Δpp71 HCMV gene expression stimulated by BNRF1 and pp71 were also in the same scale. This further confirmed the interchangeable role of BNRF1 and pp71. Thus, hDaxx-ATRX complex interacting viral proteins from different herpes viruses are interchangeable for each other.

6.2.2 The integrity of ND10 is important for HSV-1 infection resistance

Previous observations on ND10 interaction proteins from HCMV that stimulated ICP0 null HSV-1 infection (Everett *et al.*, 2013a) indicated that antagonizing the major components of ND10 can contribute to the de-repression of ΔICP0 HSV-1 infection. Chicken Adenovirus Gam1 protein was also reported to enhance ΔICP0 HSV-1 infection through ND10 disruption (Everett *et al.*, 2014), which further enhanced the notion that ND10 are important for resistance to HSV-1 infection at the cellular level. Thus, the ND10 interaction proteins from EBV were introduced into the ΔICP0 HSV-1 complementation assay to investigate the above notion and to study these EBV proteins' properties. EBNA1 was reported to interact with PML IV to disrupt ND10 and lower PML levels (Sivachandran *et al.*, 2008). EBNA-LP is responsible for Sp100 displacement from ND10 during EBV infection (Echendu & Ling, 2008). EBV tegument protein BNRF1 interacts with the hDaxx-ATRX complex to stimulate early gene expression (Tsai *et al.*, 2011). Those EBV proteins were all involved in de-stabilizing ND10 during EBV infection and contribute to EBV lytic infection. Therefore, EBV proteins were single, double and triple expressed in HFT cells. HFT.EBNA1.EBNA-LP.BNRF1 cells complemented ΔICP0 HSV-1 infection about 220-fold over HFT cells, which is the highest increase among the EBV protein expression cell lines prepared in this study. This observation further confirmed that the ND10 components cooperatively repress HSV-1 infection. Due to the time limitation, further investigation cannot be performed at this stage. Furthermore, the intrinsic resistance mechanism of ND10 on EBV is not yet well studied. Thus, it is still possible that more EBV proteins are involved in the interaction with ND10 and de-repress the viral genome expression by interfering with intrinsic resistance. Whether those potential candidates could contribute to HSV-1 infection still needs to be investigated.

6.2.3 IE1 and IE2 are essential for abundant HCMV gene expression

In this study, the investigation on ICP0 complementation and re-activation of IE1 null HCMV infection indicated that IE2 requires IE1 to initiate abundant HCMV early and late gene expression. Previous research work had observed a similar phenomenon indicating that IE1 cooperates with IE2 to synergistically activate many viral promoters (Klucher *et al.*, 1993; Malone *et al.*, 1990; Stenberg *et al.*, 1990). Other studies also indicated that neither IE1 nor IE2 are dispensable for efficient HCMV gene expression at low MOI

infection (Bresnahan & Shenk, 2000; Mocarski *et al.*, 1996; White & Spector, 2005). Furthermore, a study of quiescent infection of Δpp71 HCMV at low MOI on human fibroblast cells revealed expression of IE1 but not IE2 (Bresnahan & Shenk, 2000). The investigation of the YL series of IE1 mutants identified the amino acids located in the IE1 YL2 region as being specifically and absolutely required for IE1 functions in stimulating HCMV infection. Previous research reported by White and Spector introduced a HCMV mutant virus that deleted 48 amino acids in exon 3 and that was impaired at low and high MOI infection (White & Spector, 2005). These authors also applied IE1 expression human fibroblast cells to rescue this mutant virus infection but this failed to overcome the complete defect of the virus, which further enhanced the notion that both IE1 and IE2 are required for lytic infection, and that the same mutation within the IE2 sequence might also impair HCMV infection. Unlike the use of mutant viruses, the inducible cell line system allows the effects of such mutations on IE1 functions to be studied in the presence of wt IE2.

6.2.4 The mechanism by which herpes virus proteins that interact with the hDaxx-ATRX complex release viral gene expression

A previous paper reported that the HCMV IE1 protein stimulates viral gene expression by antagonizing histone deacetylation (HDAC) (Nevels *et al.*, 2004b). Tegument protein pp71 was reported to induce the degradation of hDaxx, which recruits HDAC enzymes to repress target gene repression (Hollenbach *et al.*, 2002; Li *et al.*, 2000), to stimulate HCMV gene expression (Saffert & Kalejta, 2006). This indicated that the invaded viral DNA becomes tightly wrapped by nucleosomes with repressive chromatin marks through the activity of histone deacetylase enzymes that repress viral gene expression. The presence of hDaxx-ATRX within ND10, and the observation that quiescent HSV-1 genomes are sequestered within ND10 (Everett *et al.*, 2007) suggests a linkage between ND10 sequestration and histone deacetylation of viral genomes. By adding TSA (histone deacetylase inhibitor) during the IE1 null HCMV infection, viral gene expression was increased and viral production was rescued to wt HCMV levels, but this treatment did not affect wt HCMV infection (Nevels *et al.*, 2004b). This phenomenon is consistent with the observation in section 4.8.2 that expressing pp71 in HFT cells prior to wt HCMV infection didn't further increase the infection. Thus, the intrinsic repression from HDACs could be efficiently antagonized by IE1 and pp71 expressed by wt HCMV, whereas additional inhibition of HDACs cannot contribute to further gene expression stimulation. In this study, expression of IE1 before infection created a more convenient host environment for

HCMV infection by targeting sumoylated PML and Sp100. How this might relate to inhibition of HDACs remains to be determined. In the scenario of IE1 null HCMV infected HFT.ICP0 cells, there is evidence that ICP0 also interacts with HDAC enzymes, although it did not apparently inhibit their activity (Lomonte *et al.*, 2004). There is considerable evidence that ICP0 promotes an open chromatin structure with acetylated histones (Ferenczy & DeLuca, 2009; 2011; Knipe & Cliffe, 2008), but it appears that TSA cannot substitute for ICP0 in the case of HSV-1 in HFs or HepaRG cells (Everett *et al.*, 2008; Preston & Nicholl, 2006), although it can have ICP0-like effects in Vero cells and neurones (Scherer *et al.*, 2014; Terry-Allison *et al.*, 2007).

One potential hypothesis that might explain some of these complex observations is to propose that stimulation by TSA can occur when repression is not complete. For example, in HFs and HepaRG cells, in absence of ICP0, HSV-1 genomes are highly repressed, but this is less true in Vero cells and neurones. Thus the chromatin structure might be more open in these, allowing TSA to work. In IE1 deficient HCMV, there is more IE gene expression than in ICP0 null HSV, so initial repression is not absolute (probably because of pp71). Thus TSA might stimulate IE1 deficient HCMV more efficiently than ICP0 null HSV-1. A testable prediction from this hypothesis is that TSA would increase ICP0 null HSV-1 infection more in pp71 expressing cells than in controls.

IE1 and pp71 were reported to interfere with HDAC function during the immediate early stage of viral infection (Nevels *et al.*, 2004b; Saffert & Kalejta, 2006). Furthermore hDaxx-ATRX complex interacting protein BNRF1 was reported to replace ATRX in ATRX-hDaxx-Histone H3.3 to facilitate EBV early infection (Tsai *et al.*, 2014). The above observations indicate that herpes virus genomes are wrapped into a repressive chromatin structure and the ATRX-hDaxx complex plays a role in this process in host cells. The mutant viruses that deleted IE1, pp71 or ICP0 are unable to proceed to lytic infection at low MOI infection, but the infection could be rescued at high MOI (Bresnahan & Shenk, 2000; Greaves & Mocarski, 1998; Stow & Stow, 1986). At low MOI infection, the viral genomes lack the proteins to open the viral genome into linear DNA for transcription and are sequestered within ND10. The expression of ND10 interacting proteins antagonizes the repression from ND10 and releases the viral genome into an open form for transcription. Whereas during high MOI infection, due to the large amount viral genomes released into nucleus, the cellular defence system that relies on ND10 is overloaded and some viral genomes overcome the intrinsic resistance of host cells to proceed to viral gene expression.

hDaxx co-localizes with PML by interaction with sumoylated PML via its SIM (Lin *et al.*, 2006). In IE1 expressing HepaRG cells, PML and Sp100 are desumoylated and dispersed and therefore negatively regulate hDaxx co-localization with ND10 (Everett *et al.*, 2013a). Thus, the question is whether hDaxx can recruit ATRX in the cells that PML and Sp100 are depleted or dispersed? If so, can this hDaxx-ATRX complex repress HCMV infection? A single experiment in this study answered part of the above questions. HFT.IE1 cells were infected with pp71 null HCMV in parallel with HFT.TetR.myc-pp71 cells. The HCMV plaque assay indicated that the induced HFT.IE1 cells cannot complement pp71-null HCMV infection (data not shown). A previous investigation from the Thomas Shenk lab found expression of both IE2 and IE1 is severely depressed in ADsubUL82 infected cells at low MOI infection (Bresnahan & Shenk, 2000). IE1 expression de-sumoylated and dispersed PML and Sp100 and dispersed hDaxx in induced HFT.IE1 cells before ADsubUL82 infection. But it appears that the dispersed hDaxx can still recruit ATRX and repress the MIEP during ADsubUL82 infection. Thus, the IE2 gene was still poorly expressed. As the investigation demonstrated in section 4.5 and section 4.6, IE2 requires IE1 to stimulate early and late gene expression at low MOI HCMV infection. Furthermore, pp71 null HCMV infected HFT.IE1 cells cannot de-repress the MIEP from hDaxx-ATRX complex without pp71. Thus the IE2 was not expressed in the absence of pp71 and IE1 was not capable of enhancing viral gene expression. From the above discussion, it indicates that IE1 and IE2 cooperatively stimulate HCMV gene expression and neither of them is dispensable for HCMV infection at low MOIs.

6.3 Future Prospects

6.3.1 Is the sequence located in IE1 YL2 important for IE2?

The previous discussion indicated the possibility that IE1 and IE2 might interact or in some way act in concert through intermediate co-factors (section 4.9). The data in section 4.7.3 identified the amino acids located at IE1 YL2 as essential for IE1 stimulating HCMV lytic infection but not important for IE1 sumoylation and desumoylating PML. Mutation sites of IE1 YL2 are also shared with IE2. Thus, the function of these amino acids in IE2 sequence is worth investigating.

The investigation in this thesis demonstrated that pp71 is replaceable by ICP0 and BNRF1. Other reports also indicated that the depletion of ATRX or hDaxx can improve Δpp71 HCMV infection (Cantrell & Bresnahan, 2006; Lukashchuk *et al.*, 2008; Tavalai *et al.*,

2008b). Therefore, the interaction with the hDaxx-ATRX complex is an important property for pp71 during HCMV infection. Previous research data observed low levels of IE1 expression during Δpp71 HCMV low MOI infection but no IE2 was expressed (Bresnahan & Shenk, 2000). The accumulating data has demonstrated that IE2 expression is enhanced by the MIEP which is repressed by the hDaxx-ATRX complex (Baldick *et al.*, 1997; Chau *et al.*, 1999; Homer *et al.*, 1999; Liu & Stinski, 1992). This repression could be released by pp71 (or ICP0 and BNRF1 in this study) through the interaction with hDaxx-ATRX complex, but not by IE1 in this study. Thus, expressing IE2 before Δpp71 HCMV infection may possibly rescue the mutant virus infection, as the co-expression of IE1 and IE2 could create a scenario for maintaining expression of the HCMV genome even in the absence of pp71, where viral genes could be stimulated for expression before being repressed by the hDaxx-ATRX complex.

6.3.2 ND10 interaction proteins from HSV-1 and HCMV are potentially interchangeable with their counterparts in EBV

Chapter 6 demonstrated that ND10 interacting proteins from EBV can increase ΔICP0 HSV-1 infection and complement Δpp71 HCMV infection. Furthermore, deletion of ND10 components contributes to increased HCMV infection (Cantrell & Bresnahan, 2006; Glass & Everett, 2013; Lukashchuk *et al.*, 2008; Tavalai *et al.*, 2008b) and ICP0 expression achieved a similar increase in this study. Therefore there is accumulating evidence indicating the importance of ND10 integrity for intrinsic resistance to HCMV infection. Therefore, introducing ND10 interacting proteins into cells prior to EBV infection is likely to enhance the lytic viral infection and reduce the proportion of cells entering latent infection.

BNRF1 was investigated in terms of replacing pp71 in HCMV infection in this study and this achieved very promising results. Both pp71 and BNRF1 are tegument proteins and interact with the hDaxx-ATRX complex. A recent publication indicates that BNRF1 replaces ATRX in the ATRX-hDaxx-Histone 3.3 complex to remodel the hDaxx-Histone 3.3 chaperone for stimulating EBV early infection (Tsai *et al.*, 2014). Investigations on the very early stages of HCMV infection found that pp71 colocalizes with the ATRX-hDaxx complex and disperses ATRX earlier than hDaxx from ND10 (Lukashchuk *et al.*, 2008). Thus, it is reasonable to predict similar interaction mechanisms between pp71 and BNRF1 and the ATRX-hDaxx complex. Thus pp71 might initially replace the ATRX in the ATRX-hDaxx complex at a very early time of HCMV infection and then disperse the

hDaxx later through forming pp71-hDaxx complex. Furthermore, these similar properties between pp71 and BNRF1 make it worthwhile to investigate whether pp71 can replace BNRF1 in EBV infection, and this result could contribute to future efforts to target their inhibitory effects on the ATRX-hDaxx complex for developing more efficient anti-herpes virus medicinal treatments.

6.3.3 Further analysis of the effects of EBV proteins on ND10

Due to time limitations, it was not possible to investigate thoroughly the potential effects of EBV protein expression on specific ND10 components to clarify whether their reported roles in this context are reproduced in the cell lines constructed here. It is also possible that these proteins might affect the response of ND10 components to herpesvirus infection and their recruitment to the viral genomes. These studies will be necessary to indicate whether their abilities to stimulate ICP0 null mutant HSV-1 infection, in cell expressing EBNA-1, EBNA-LP and BNRF1 simultaneously, for example, are connected to ND10 dynamics or to some other function.

6.3.4 A common anti-herpes virus infection target

ICP0 and pp71 were demonstrated to be interchangeable in the context of HCMV infection this thesis. Furthermore, BNRF1 was also confirmed to replace pp71 in complementing Δpp71 HCMV and increasing plaque formation by ΔICP0 HSV-1. These investigations indicate the possibility that HSV-1, HCMV and EBV are subject to the same cellular intrinsic resistance mechanisms caused by the hDaxx-ATRX complex and other ND10-related events. Despite the fact that the various viral proteins show no sequence similarity, they have nonetheless evolved to target the same group of cellular proteins. This suggests that interference with the mechanisms of targeting the hDaxx-ATRX could be a potential drug design target for developing new treatment for broad anti-herpes virus infections. On the same theme, the region identified in mutant YL2 forms a specific structural loop region on the IE1 surface (Scherer *et al.*, 2014) which the results presented here strongly suggest is essential for IE1 activity. Thus assays that screen for small molecules that interact with this loop region might provide leads towards a novel HCMV therapeutic approach.

7 References

Aapola, U., Kawasaki, K., Scott, H. S., Ollila, J., Vihinen, M., Heino, M., Shintani, A., Kawasaki, K., Minoshima, S., Krohn, K., Antonarakis, S. E., Shimizu, N., Kudoh, J. & Peterson, P. (2000). Isolation and initial characterization of a novel zinc finger gene, DNMT3L, on 21q22.3, related to the cytosine-5-methyltransferase 3 gene family. *Genomics* **65**, 293-298.

Abb, J. (1985). [Prevention and therapy of herpesvirus infections]. *Zentralbl Bakteriol Mikrobiol Hyg B* **180**, 107-120.

Adler, M., Tavalai, N., Muller, R. & Stamminger, T. (2011). Human cytomegalovirus immediate-early gene expression is restricted by the nuclear domain 10 component Sp100. *J Gen Virol* **92**, 1532-1538.

Ahn, J. H., Brignole, E. J., 3rd & Hayward, G. S. (1998). Disruption of PML subnuclear domains by the acidic IE1 protein of human cytomegalovirus is mediated through interaction with PML and may modulate a RING finger-dependent cryptic transactivator function of PML. *Mol Cell Biol* **18**, 4899-4913.

Ahn, J. H. & Hayward, G. S. (1997). The major immediate-early proteins IE1 and IE2 of human cytomegalovirus colocalize with and disrupt PML-associated nuclear bodies at very early times in infected permissive cells. *Journal of virology* **71**, 4599-4613.

Ahn, J. H. & Hayward, G. S. (2000). Disruption of PML-associated nuclear bodies by IE1 correlates with efficient early stages of viral gene expression and DNA replication in human cytomegalovirus infection. *Virology* **274**, 39-55.

Amon, W. & Farrell, P. J. (2005). Reactivation of Epstein-Barr virus from latency. *Rev Med Virol* **15**, 149-156.

Amon, W., White, R. E. & Farrell, P. J. (2006). Epstein-Barr virus origin of lytic replication mediates association of replicating episomes with promyelocytic leukaemia protein nuclear bodies and replication compartments. *J Gen Virol* **87**, 1133-1137.

Argentaro, A., Yang, J. C., Chapman, L., Kowalczyk, M. S., Gibbons, R. J., Higgs, D. R., Neuhaus, D. & Rhodes, D. (2007). Structural consequences of disease-causing mutations in the ATRX-DNMT3-DNMT3L (ADD) domain of the chromatin-associated protein ATRX. *Proc Natl Acad Sci U S A* **104**, 11939-11944.

Baker, L. A., Allis, C. D. & Wang, G. G. (2008). PHD fingers in human diseases: disorders arising from misinterpreting epigenetic marks. *Mutation research* **647**, 3-12.

Baldick, C. J., Jr., Marchini, A., Patterson, C. E. & Shenk, T. (1997). Human cytomegalovirus tegument protein pp71 (ppUL82) enhances the infectivity of viral DNA and accelerates the infectious cycle. *Journal of virology* **71**, 4400-4408.

Barlow, P. N., Luisi, B., Milner, A., Elliott, M. & Everett, R. (1994). Structure of the C3HC4 domain by 1H-nuclear magnetic resonance spectroscopy. A new structural class of zinc-finger. *Journal of molecular biology* **237**, 201-211.

Baumann, C., Schmidtmann, A., Muegge, K. & De La Fuente, R. (2008). Association of ATRX with pericentric heterochromatin and the Y chromosome of neonatal mouse spermatogonia. *BMC Mol Biol* **9**, 29.

Bell, P., Lieberman, P. M. & Maul, G. G. (2000). Lytic but not latent replication of epstein-barr virus is associated with PML and induces sequential release of nuclear domain 10 proteins. *Journal of virology* **74**, 11800-11810.

Bergink, S. & Jentsch, S. (2009). Principles of ubiquitin and SUMO modifications in DNA repair. *Nature* **458**, 461-467.

Bernardi, R. & Pandolfi, P. P. (2003). Role of PML and the PML-nuclear body in the control of programmed cell death. *Oncogene* **22**, 9048-9057.

Bernardi, R. & Pandolfi, P. P. (2007). Structure, dynamics and functions of promyelocytic leukaemia nuclear bodies. *Nat Rev Mol Cell Biol* **8**, 1006-1016.

Berube, N. G., Healy, J., Medina, C. F., Wu, S., Hodgson, T., Jagla, M. & Picketts, D. J. (2008). Patient mutations alter ATRX targeting to PML nuclear bodies. *Eur J Hum Genet* **16**, 192-201.

Bieniasz, P. D. (2004). Intrinsic immunity: a front-line defense against viral attack. *Nat Immunol* **5**, 1109-1115.

Biron, C. A., Nguyen, K. B., Pien, G. C., Cousens, L. P. & Salazar-Mather, T. P. (1999). Natural killer cells in antiviral defense: function and regulation by innate cytokines. *Annu Rev Immunol* **17**, 189-220.

Bischof, O., Kirsh, O., Pearson, M., Itahana, K., Pelicci, P. G. & Dejean, A. (2002). Deconstructing PML-induced premature senescence. *Embo J* **21**, 3358-3369.

Bloom, D. C. & Kwiatkowski, D. L. (2011). HSV-1 latency and the roles of LATs. In *Alphaherpesviruses Molecular Virology*, pp. 295-316. Edited by S. K. Weller. Norfolk, U.K.: Caister Academic Press.

Boddy, M. N., Howe, K., Etkin, L. D., Solomon, E. & Freemont, P. S. (1996). PIC 1, a novel ubiquitin-like protein which interacts with the PML component of a multiprotein complex that is disrupted in acute promyelocytic leukaemia. *Oncogene* **13**, 971-982.

Boisvert, F. M., Hendzel, M. J. & Bazett-Jones, D. P. (2000). Promyelocytic leukemia (PML) nuclear bodies are protein structures that do not accumulate RNA. *J Cell Biol* **148**, 283-292.

Borden, K. L. (2002). Pondering the promyelocytic leukemia protein (PML) puzzle: possible functions for PML nuclear bodies. *Mol Cell Biol* **22**, 5259-5269.

Boshart, M., Weber, F., Jahn, G., Dorsch-Hasler, K., Fleckenstein, B. & Schaffner, W. (1985). A very strong enhancer is located upstream of an immediate early gene of human cytomegalovirus. *Cell* **41**, 521-530.

Boshoff, C. & Weiss, R. (2002a). AIDS-related malignancies. *Nat Rev Cancer* **2**, 373-382.

Boshoff, C. & Weiss, R. (2002b). Aids-related malignancies. *Nature Reviews Cancer* **2**, 373-382.

Bostikova, V., Salavec, M., Smetana, J., Sleha, R., Coufalova, M., Splino, M. & Bostik, P. (2014). [Infections caused by human alpha herpes viruses.]. *Epidemiol Mikrobiol Imunol* **63**, 205-212.

Boutell, C., Cuchet-Lourenco, D., Vanni, E., Orr, A., Glass, M., McFarlane, S. & Everett, R. D. (2011). A viral ubiquitin ligase has substrate preferential SUMO targeted ubiquitin ligase activity that counteracts intrinsic antiviral defence. *PLoS Pathog* **7**, e1002245.

Boutell, C. & Everett, R. D. (2013). The regulation of alphaherpesvirus infections by the ICP0 family of proteins. *J Gen Virol* **94**, 465-481.

Boutell, C., Orr, A. & Everett, R. D. (2003). PML residue lysine 160 is required for the degradation of PML induced by herpes simplex virus type 1 regulatory protein ICP0. *Journal of virology* **77**, 8686-8694.

Boutell, C., Sadis, S. & Everett, R. D. (2002). Herpes simplex virus type 1 immediate-early protein ICP0 and is isolated RING finger domain act as ubiquitin E3 ligases in vitro. *Journal of virology* **76**, 841-850.

Brasch, K. & Ochs, R. L. (1992). Nuclear bodies (NBs): a newly "rediscovered" organelle. *Exp Cell Res* **202**, 211-223.

Brass, A. L., Dykxhoorn, D. M., Benita, Y., Yan, N., Engelman, A., Xavier, R. J., Lieberman, J. & Elledge, S. J. (2008). Identification of host proteins required for HIV infection through a functional genomic screen. *Science* **319**, 921-926.

Bresnahan, W. A., Hultman, G. E. & Shenk, T. (2000). Replication of wild-type and mutant human cytomegalovirus in life-extended human diploid fibroblasts. *Journal of virology* **74**, 10816-10818.

Bresnahan, W. A. & Shenk, T. E. (2000). UL82 virion protein activates expression of immediate early viral genes in human cytomegalovirus-infected cells. *Proceedings of the National Academy of Sciences of the United States of America* **97**, 14506-14511.

Cai, W. Z. & Schaffer, P. A. (1989). Herpes simplex virus type 1 ICP0 plays a critical role in the de novo synthesis of infectious virus following transfection of viral DNA. *Journal of virology* **63**, 4579-4589.

Cantrell, S. R. & Bresnahan, W. A. (2006). Human cytomegalovirus (HCMV) UL82 gene product (pp71) relieves hDaxx-mediated repression of HCMV replication. *Journal of virology* **80**, 6188-6191.

Capili, A. D. & Lima, C. D. (2007). Taking it step by step: mechanistic insights from structural studies of ubiquitin/ubiquitin-like protein modification pathways. *Curr Opin Struct Biol* **17**, 726-735.

Castillo, J. P. & Kowalik, T. F. (2002). Human cytomegalovirus immediate early proteins and cell growth control. *Gene* **290**, 19-34.

Cerboni, C., Mousavi-Jazi, M., Linde, A., Soderstrom, K., Brytting, M., Wahren, B., Karre, K. & Carbone, E. (2000). Human cytomegalovirus strain-dependent changes in NK cell recognition of infected fibroblasts. *J Immunol* **164**, 4775-4782.

Cesarman, E., Chang, Y., Moore, P. S., Said, J. W. & Knowles, D. M. (1995). Kaposi's sarcoma-associated herpesvirus-like DNA sequences in AIDS-related body-cavity-based lymphomas. *N Engl J Med* **332**, 1186-1191.

Cha, T. A., Tom, E., Kemble, G. W., Duke, G. M., Mocarski, E. S. & Spaete, R. R. (1996). Human cytomegalovirus clinical isolates carry at least 19 genes not found in laboratory strains. *Journal of virology* **70**, 78-83.

Chang, K. S., Fan, Y. H., Andreeff, M., Liu, J. & Mu, Z. M. (1995). The PML gene encodes a phosphoprotein associated with the nuclear matrix. *Blood* **85**, 3646-3653.

Chau, N. H., Vanson, C. D. & Kerry, J. A. (1999). Transcriptional regulation of the human cytomegalovirus US11 early gene. *Journal of virology* **73**, 863-870.

Chee, M. S., Bankier, A. T., Beck, S., Bohni, R., Brown, C. M., Cerny, R., Horsnell, T., Hutchison, C. A., 3rd, Kouzarides, T., Martignetti, J. A. & et al. (1990). Analysis of the protein-coding content of the sequence of human cytomegalovirus strain AD169. *Curr Top Microbiol Immunol* **154**, 125-169.

Chelbi-Alix, M. K. & de The, H. (1999). Herpes virus induced proteasome-dependent degradation of the nuclear bodies-associated PML and Sp100 proteins. *Oncogene* **18**, 935-941.

Chelbi-Alix, M. K., Pelicano, L., Quignon, F., Koken, M. H., Venturini, L., Stadler, M., Pavlovic, J., Degos, L. & de The, H. (1995). Induction of the PML protein by interferons in normal and APL cells. *Leukemia* **9**, 2027-2033.

Chelbi-Alix, M. K., Quignon, F., Pelicano, L., Koken, M. H. & de The, H. (1998). Resistance to virus infection conferred by the interferon-induced promyelocytic leukemia protein. *Journal of virology* **72**, 1043-1051.

Chi, J. H. & Wilson, D. W. (2000). ATP-Dependent localization of the herpes simplex virus capsid protein VP26 to sites of procapsid maturation. *Journal of virology* **74**, 1468-1476.

Compton, T. & Feire, A. (2007). Early events in human cytomegalovirus infection.

Condemine, W., Takahashi, Y., Zhu, J., Puvion-Dutilleul, F., Guegan, S., Janin, A. & de The, H. (2006). Characterization of endogenous human promyelocytic leukemia isoforms. *Cancer Res* **66**, 6192-6198.

Conway, J. F. & Homa, F. L. (2011). Nucleocapsid structure, assembly and DNA packaging of herpes simplex virus. In *Alphaherpesviruses Molecular Virology*, pp. 175-194. Edited by S. K. Weller. Norfolk, U.K.: Caister Academic Press.

Cuchet-Lourenco, D., Boutell, C., Lukashchuk, V., Grant, K., Sykes, A., Murray, J., Orr, A. & Everett, R. D. (2011). SUMO pathway dependent recruitment of

cellular repressors to herpes simplex virus type 1 genomes. *PLoS Pathog* **7**, e1002123.

Cuchet-Lourenco, D., Vanni, E., Glass, M., Orr, A. & Everett, R. D. (2012). Herpes simplex virus 1 ubiquitin ligase ICP0 interacts with PML isoform I and induces its SUMO-independent degradation. *Journal of virology* **86**, 11209-11222.

Cuchet, D., Sykes, A., Nicolas, A., Orr, A., Murray, J., Sirma, H., Heeren, J., Bartelt, A. & Everett, R. D. (2011). PML isoforms I and II participate in PML-dependent restriction of HSV-1 replication. *J Cell Sci* **124**, 280-291.

Daubeuf, S., Singh, D., Tan, Y., Liu, H., Federoff, H. J., Bowers, W. J. & Tolba, K. (2009). HSV ICP0 recruits USP7 to modulate TLR-mediated innate response. *Blood* **113**, 3264-3275.

Davis, M. G., Kenney, S. C., Kamine, J., Pagano, J. S. & Huang, E. S. (1987). Immediate-early gene region of human cytomegalovirus trans-activates the promoter of human immunodeficiency virus. *Proceedings of the National Academy of Sciences of the United States of America* **84**, 8642-8646.

Delboy, M. G., Siekavizza-Robles, C. R. & Nicola, A. V. (2010). Herpes simplex virus tegument ICP0 is capsid associated, and its E3 ubiquitin ligase domain is important for incorporation into virions. *Journal of virology* **84**, 1637-1640.

Dellaire, G. & Bazett-Jones, D. P. (2004). PML nuclear bodies: dynamic sensors of DNA damage and cellular stress. *Bioessays* **26**, 963-977.

DeLuca, N. A. (2011). Functions and mechanism of action of the herpes simplex virus regulatory protein, ICP4. In *Alphaherpesviruses Molecular Virology*, pp. 17-38. Edited by S. K. Weller. Norfolk, U.K.: Caister Academic Press.

Dent, A. L., Yewdell, J., Puvion-Dutilleul, F., Koken, M. H., de The, H. & Staudt, L. M. (1996). LYSP100-associated nuclear domains (LANDs): description of a new class of subnuclear structures and their relationship to PML nuclear bodies. *Blood* **88**, 1423-1426.

Deshaies, R. J. & Joazeiro, C. A. (2009). RING domain E3 ubiquitin ligases. *Annu Rev Biochem* **78**, 399-434.

Dimitropoulou, P., Caswell, R., McSharry, B. P., Greaves, R. F., Spandidos, D. A., Wilkinson, G. W. & Sourvinos, G. (2010). Differential relocation and stability of PML-body components during productive human cytomegalovirus infection: detailed characterization by live-cell imaging. *Eur J Cell Biol* **89**, 757-768.

Drane, P., Ouararhni, K., Depaux, A., Shuaib, M. & Hamiche, A. (2010). The death-associated protein DAXX is a novel histone chaperone involved in the replication-independent deposition of H3.3. *Genes Dev* **24**, 1253-1265.

DuBridge, R. B., Tang, P., Hsia, H. C., Leong, P. M., Miller, J. H. & Calos, M. P. (1987). Analysis of mutation in human cells by using an Epstein-Barr virus shuttle system. *Mol Cell Biol* **7**, 379-387.

Duprez, E., Saurin, A. J., Desterro, J. M., Lallemand-Breitenbach, V., Howe, K., Boddy, M. N., Solomon, E., de The, H., Hay, R. T. & Freemont, P. S. (1999). SUMO-1 modification of the acute promyelocytic leukaemia protein PML: implications for nuclear localisation. *J Cell Sci* **112**, 381-393.

Echendu, C. W. & Ling, P. D. (2008). Regulation of Sp100A subnuclear localization and transcriptional function by EBNA-LP and interferon. *J Interferon Cytokine Res* **28**, 667-678.

Efstathiou, S. & Preston, C. M. (2005). Towards an understanding of the molecular basis of herpes simplex virus latency. *Virus Res* **111**, 108-119.

Eisenberg, R. J., Heldwein, E. E., Cohen, G. H. & Krummenacher, C. (2011). Recent progress in understanding herpes simplex virus entry:relationship of structure to function. In *Alphaherpesviruses Molecular Virology*, pp. 131-152. Edited by S. K. Weller. Norfolk, U.K.: Caister Academic Press.

Eskiw, C. H. & Bazett-Jones, D. P. (2002). The promyelocytic leukemia nuclear body: sites of activity? *Biochem Cell Biol* **80**, 301-310.

Everett, R., O'Hare, P., O'Rourke, D., Barlow, P. & Orr, A. (1995). Point mutations in the herpes simplex virus type 1 Vmw110 RING finger helix affect activation of gene expression, viral growth, and interaction with PML-containing nuclear structures. *Journal of virology* **69**, 7339-7344.

Everett, R. D. (1984). Trans activation of transcription by herpes virus products: requirement for two HSV-1 immediate-early polypeptides for maximum activity. *EMBO J* **3**, 3135-3141.

Everett, R. D. (1987). A detailed mutational analysis of Vmw110, a trans-acting transcriptional activator encoded by herpes simplex virus type 1. *Embo J* **6**, 2069-2076.

Everett, R. D. (1988a). Analysis of the functional domains of herpes simplex virus type 1 immediate-early polypeptide Vmw110. *Journal of molecular biology* **202**, 87-96.

Everett, R. D. (1988b). Promoter sequence and cell type can dramatically affect the efficiency of transcriptional activation induced by herpes simplex virus type 1 and its immediate-early gene products Vmw175 and Vmw110. *Journal of molecular biology* **203**, 739-751.

Everett, R. D. (2000). ICP0, a regulator of herpes simplex virus during lytic and latent infection. *Bioessays* **22**, 761-770.

Everett, R. D. (2006a). Interactions between DNA viruses, ND10 and the DNA damage response. *Cell Microbiol* **8**, 365-374.

Everett, R. D. (2006b). The roles of ICP0 during HSV-1 infection. In *Alpha Herpesviruses Molecular and Cellular Biology*, pp. 39-64. Edited by R. M. Sandri-Goldin. Wymondham: Caister Academic Press.

Everett, R. D. (2011). The role of ICP0 in counteracting intrinsic cellular resistance to virus infection. In *Alphaherpesviruses: Molecular Virology*, pp. 51-72. Edited by S. K. Weller. Norfolk, U.K.: Caister Academic Press.

Everett, R. D. (2013). The spatial organization of DNA virus genomes in the nucleus. *PLoS Pathog* **9**, e1003386.

Everett, R. D., Bell, A. J., Lu, Y. & Orr, A. (2013a). The replication defect of ICP0-null mutant herpes simplex virus 1 can be largely complemented by the combined activities of human cytomegalovirus proteins IE1 and pp71. *Journal of virology* **87**, 978-990.

Everett, R. D., Boutell, C. & Hale, B. G. (2013b). Interplay between viruses and host sumoylation pathways. *Nat Rev Microbiol* **11**, 400-411.

Everett, R. D., Boutell, C., McNair, C., Grant, L. & Orr, A. (2010). Comparison of the biological and biochemical activities of several members of the alphaherpesvirus ICP0 family of proteins. *Journal of virology* **84**, 3476-3487.

Everett, R. D. & Chelbi-Alix, M. K. (2007). PML and PML nuclear bodies: implications in antiviral defence. *Biochimie* **89**, 819-830.

Everett, R. D., Chiocca, S. & Orr, A. (2014). The chicken adenovirus Gam1 protein, an inhibitor of the sumoylation pathway, partially complements ICP0-null mutant herpes simplex virus 1. *Journal of virology* **88**, 5873-5876.

Everett, R. D., Cross, A. & Orr, A. (1993). A truncated form of herpes simplex virus type 1 immediate-early protein Vmw110 is expressed in a cell type dependent manner. *Virology* **197**, 751-756.

Everett, R. D., Freemont, P., Saitoh, H., Dasso, M., Orr, A., Kathoria, M. & Parkinson, J. (1998). The disruption of ND10 during herpes simplex virus infection correlates with the Vmw110- and proteasome-dependent loss of several PML isoforms. *Journal of virology* **72**, 6581-6591.

Everett, R. D. & Maul, G. G. (1994). HSV-1 IE protein Vmw110 causes redistribution of PML. *EMBO J* **13**, 5062-5069.

Everett, R. D., Meredith, M., Orr, A., Cross, A., Kathoria, M. & Parkinson, J. (1997). A novel ubiquitin-specific protease is dynamically associated with the PML nuclear domain and binds to a herpesvirus regulatory protein. *Embo J* **16**, 1519-1530.

Everett, R. D. & Murray, J. (2005). ND10 components relocate to sites associated with herpes simplex virus type 1 nucleoprotein complexes during virus infection. *Journal of virology* **79**, 5078-5089.

Everett, R. D., Murray, J., Orr, A. & Preston, C. M. (2007). Herpes simplex virus type 1 genomes are associated with ND10 nuclear substructures in quiescently infected human fibroblasts. *Journal of virology* **81**, 10991-11004.

Everett, R. D., Parada, C., Gripon, P., Sirma, H. & Orr, A. (2008). Replication of ICP0-null mutant herpes simplex virus type 1 is restricted by both PML and Sp100. *Journal of virology* **82**, 2661-2672.

Everett, R. D., Parsy, M. L. & Orr, A. (2009). Analysis of the functions of herpes simplex virus type 1 regulatory protein ICP0 that are critical for lytic infection and derepression of quiescent viral genomes. *Journal of virology* **83**, 4963-4977.

Everett, R. D., Preston, C. M. & Stow, N. D. (1991). *Functional and genetic analysis of the role of Vmw110 in herpes simplex virus replication.* Boca Raton, Fla.: CRC Press, Inc.

Everett, R. D., Rechter, S., Papior, P., Tavalai, N., Stamminger, T. & Orr, A. (2006). PML contributes to a cellular mechanism of repression of herpes simplex virus type 1 infection that is inactivated by ICP0. *Journal of virology* **80**, 7995-8005.

Everett, R. D. & Zafiropoulos, A. (2004). Visualization by Live-Cell Microscopy of Disruption of ND10 during Herpes Simplex Virus Type 1 Infection. *Journal of virology* **78**, 11411-11415.

Feederle, R., Neuhierl, B., Baldwin, G., Bannert, H., Hub, B., Mautner, J., Behrends, U. & Delecluse, H. J. (2006). Epstein-Barr virus BNRF1 protein allows efficient transfer from the endosomal compartment to the nucleus of primary B lymphocytes. *Journal of virology* **80**, 9435-9443.

Ferenczy, M. W. & DeLuca, N. A. (2009). Epigenetic modulation of gene expression from quiescent herpes simplex virus genomes. *Journal of virology* **83**, 8514-8524.

Ferenczy, M. W. & DeLuca, N. A. (2011). Reversal of heterochromatic silencing of quiescent herpes simplex virus type 1 by ICP0. *Journal of virology* **85**, 3424-3435.

Ferenczy, M. W., Ranayhossaini, D. J. & Deluca, N. A. (2011). Activities of ICP0 involved in the reversal of silencing of quiescent herpes simplex virus 1. *Journal of virology* **85**, 4993-5002.

Finke, J., Rowe, M., Kallin, B., Ernberg, I., Rosen, A., Dillner, J. & Klein, G. (1987). Monoclonal and polyclonal antibodies against Epstein-Barr virus nuclear antigen 5 (EBNA-5) detect multiple protein species in Burkitt's lymphoma and lymphoblastoid cell lines. *Journal of virology* **61**, 3870-3878.

Fortunato, E. A. & Spector, D. H. (1999). Regulation of human cytomegalovirus gene expression. *Advances in virus research* **54**, 61-128.

Foster, K. M. & Jack, I. (1971). Binucleate DNA-synthesizing cells in cytomegalovirus infection after extracorporeal circulation. *Pathology* **3**, 9-12.

Fulop, T., Larbi, A. & Pawelec, G. (2013). Human T cell aging and the impact of persistent viral infections. *Front Immunol* **4**, 271.

Gareau, J. R. & Lima, C. D. (2010). The SUMO pathway: emerging mechanisms that shape specificity, conjugation and recognition. *Nat Rev Mol Cell Biol* **11**, 861-871.

Gawn, J. M. & Greaves, R. F. (2002). Absence of IE1 p72 protein function during low-multiplicity infection by human cytomegalovirus results in a broad block to viral delayed-early gene expression. *Journal of virology* **76**, 4441-4455.

Gibbons, R. J., Picketts, D. J., Villard, L. & Higgs, D. R. (1995). Mutations in a putative global transcriptional regulator cause X-linked mental retardation with alpha-thalassemia (ATR-X syndrome). *Cell* **80**, 837-845.

Gibson, W. (1996). Structure and assembly of the virion. *Intervirology* **39**, 389-400.

Gibson, W. & Roizman, B. (1972). Proteins specified by herpes simplex virus. 8. Characterization and composition of multiple capsid forms of subtypes 1 and 2. *Journal of virology* **10**, 1044-1052.

Glass, M. & Everett, R. D. (2013). Components of promyelocytic leukemia nuclear bodies (ND10) act cooperatively to repress herpesvirus infection. *Journal of virology* **87**, 2174-2185.

Gongora, C., David, G., Pintard, L., Tissot, C., Hua, T. D., Dejean, A. & Mechti, N. (1997). Molecular cloning of a new interferon-induced PML nuclear body-associated protein. *J Biol Chem* **272**, 19457-19463.

Gordon, Y. J., McKnight, J. L., Ostrove, J. M., Romanowski, E. & Araullo-Cruz, T. (1990). Host species and strain differences affect the ability of an HSV-1 ICP0 deletion mutant to establish latency and spontaneously reactivate in vivo. *Virology* **178**, 469-477.

Grant, K., Grant, L., Tong, L. & Boutell, C. (2012). Depletion of intracellular zinc inhibits the ubiquitin ligase activity of viral regulatory protein ICP0 and restricts herpes simplex virus 1 replication in cell culture. *Journal of virology* **86**, 4029-4033.

Greaves, R. F. & Mocarski, E. S. (1998). Defective growth correlates with reduced accumulation of a viral DNA replication protein after low-multiplicity infection by a human cytomegalovirus ie1 mutant. *Journal of virology* **72**, 366-379.

Gripon, P., Rumin, S., Urban, S., Le Seyec, J., Glaise, D., Cannie, I., Guyomard, C., Lucas, J., Trepo, C. & Guguen-Guillouzo, C. (2002). Infection of a human hepatoma cell line by hepatitis B virus. *Proceedings of the National Academy of Sciences of the United States of America* **99**, 15655-15660.

Guldner, H. H., Szostecki, C., Schroder, P., Matschl, U., Jensen, K., Luders, C., Will, H. & Sternsdorf, T. (1999). Splice variants of the nuclear dot-associated Sp100 protein contain homologies to HMG-1 and a human nuclear phosphoprotein-box motif. *J Cell Sci* **112 (Pt 5)**, 733-747.

Hancock, M. H., Cliffe, A. R., Knipe, D. M. & Smiley, J. R. (2010). Herpes simplex virus VP16, but not ICP0, is required to reduce histone occupancy and enhance histone acetylation on viral genomes in U2OS osteosarcoma cells. *Journal of virology* **84**, 1366-1375.

Harris, R. A., Everett, R. D., Zhu, X. X., Silverstein, S. & Preston, C. M. (1989). Herpes simplex virus type 1 immediate-early protein Vmw110 reactivates latent herpes simplex virus type 2 in an in vitro latency system. *Journal of virology* **63**, 3513-3515.

Harris, R. S., Bishop, K. N., Sheehy, A. M., Craig, H. M., Petersen-Mahrt, S. K., Watt, I. N., Neuberger, M. S. & Malim, M. H. (2003). DNA deamination mediates innate immunity to retroviral infection. *Cell* **113**, 803-809.

Hatziioannou, T., Perez-Caballero, D., Yang, A., Cowan, S. & Bieniasz, P. D. (2004). Retrovirus resistance factors Ref1 and Lv1 are species-specific variants of TRIM5alpha. *Proceedings of the National Academy of Sciences of the United States of America* **101**, 10774-10779.

Hay, R. T. (2005). SUMO: a history of modification. *Mol Cell* **18**, 1-12.

Hayhurst, G. P., Bryant, L. A., Caswell, R. C., Walker, S. M. & Sinclair, J. H. (1995). CCAAT box-dependent activation of the TATA-less human DNA polymerase alpha promoter by the human cytomegalovirus 72-kilodalton major immediate-early protein. *Journal of virology* **69**, 182-188.

Hermiston, T. W., Malone, C. L., Witte, P. R. & Stinski, M. F. (1987). Identification and characterization of the human cytomegalovirus immediate-early region 2 gene that stimulates gene expression from an inducible promoter. *Journal of virology* **61**, 3214-3221.

Heymann, J. B., Cheng, N., Newcomb, W. W., Trus, B. L., Brown, J. C. & Steven, A. C. (2003). Dynamics of herpes simplex virus capsid maturation visualized by time-lapse cryo-electron microscopy. *Nature structural biology* **10**, 334-341.

Hofmann, H., Sindre, H. & Stamminger, T. (2002). Functional interaction between the pp71 protein of human cytomegalovirus and the PML-interacting protein human Daxx. *Journal of virology* **76**, 5769-5783.

Hollenbach, A. D., McPherson, C. J., Mientjes, E. J., Iyengar, R. & Grosveld, G. (2002). Daxx and histone deacetylase II associate with chromatin through an interaction with core histones and the chromatin-associated protein Dek. *J Cell Sci* **115**, 3319-3330.

Holmes, S. J. (1996). Review of recommendations of the Advisory Committee on Immunization Practices, Centers for Disease Control and Prevention, on varicella vaccine. *J Infect Dis* **174 Suppl 3**, S342-344.

Holowaty, M. N., Zeghouf, M., Wu, H., Tellam, J., Athanasopoulos, V., Greenblatt, J. & Frappier, L. (2003). Protein profiling with Epstein-Barr nuclear antigen-1 reveals an interaction with the herpesvirus-associated ubiquitin-specific protease HAUSP/USP7. *J Biol Chem* **278**, 29987-29994.

Homer, E. G., Rinaldi, A., Nicholl, M. J. & Preston, C. M. (1999). Activation of herpesvirus gene expression by the human cytomegalovirus protein pp71. *Journal of virology* **73**, 8512-8518.

Huh, Y. H., Kim, Y. E., Kim, E. T., Park, J. J., Song, M. J., Zhu, H., Hayward, G. S. & Ahn, J. H. (2008). Binding STAT2 by the acidic domain of human cytomegalovirus IE1 promotes viral growth and is negatively regulated by SUMO. *Journal of virology* **82**, 10444-10454.

Hwang, J. & Kalejta, R. F. (2007). Proteasome-dependent, ubiquitin-independent degradation of Daxx by the viral pp71 protein in human cytomegalovirus-infected cells. *Virology* **367**, 334-338.

Irmiere, A. & Gibson, W. (1985). Isolation of human cytomegalovirus intranuclear capsids, characterization of their protein constituents, and demonstration that the B-capsid assembly protein is also abundant in noninfectious enveloped particles. *Journal of virology* **56**, 277-283.

Ishov, A. M. & Maul, G. G. (1996). The periphery of nuclear domain 10 (ND10) as site of DNA virus deposition. *J Cell Biol* **134**, 815-826.

Ishov, A. M., Sotnikov, A. G., Negorev, D., Vladimirova, O. V., Neff, N., Kamitani, T., Yeh, E. T., Strauss, J. F. & Maul, G. G. (1999). PML is critical for ND10 formation and recruits the PML-interacting protein daxx to this nuclear structure when modified by SUMO-1. *J Cell Biol* **147**, 221-234.

Ishov, A. M., Stenberg, R. M. & Maul, G. G. (1997). Human cytomegalovirus immediate early interaction with host nuclear structures: definition of an immediate transcript environment. *J Cell Biol* **138**, 5-16.

Ishov, A. M., Vladimirova, O. V. & Maul, G. G. (2002). Daxx-mediated accumulation of human cytomegalovirus tegument protein pp71 at ND10 facilitates initiation of viral infection at these nuclear domains. *Journal of virology* **76**, 7705-7712.

Ishov, A. M., Vladimirova, O. V. & Maul, G. G. (2004). Heterochromatin and ND10 are cell-cycle regulated and phosphorylation-dependent alternate nuclear sites of the transcription repressor Daxx and SWI/SNF protein ATRX. *J Cell Sci* **117**, 3807-3820.

Jamieson, D. R., Robinson, L. H., Daksis, J. I., Nicholl, M. J. & Preston, C. M. (1995a). Quiescent viral genomes in human fibroblasts after infection with herpes simplex virus type 1 Vmw65 mutants. *J Gen Virol* **76**, 1417-1431.

Jamieson, D. R. S., Robinson, L. H., Daksis, J. I., Nicholl, M. J. & Preston, C. M. (1995b). Quiescent viral genomes in human fibroblasts after infection with herpes simplex virus Vmw65 mutants. *Journal of General Virology* **76**, 1417-1431.

Jensen, K., Shiels, C. & Freemont, P. S. (2001). PML protein isoforms and the RBCC/TRIM motif. *Oncogene* **20**, 7223-7233.

Joazeiro, C. A. & Weissman, A. M. (2000). RING finger proteins: mediators of ubiquitin ligase activity. *Cell* **102**, 549-552.

Johannsen, E., Luftig, M., Chase, M. R., Weicksel, S., Cahir-McFarland, E., Illanes, D., Sarracino, D. & Kieff, E. (2004). Proteins of purified Epstein-Barr virus. *Proceedings of the National Academy of Sciences of the United States of America* **101**, 16286-16291.

Joung, J. K., Ramm, E. I. & Pabo, C. O. (2000). A bacterial two-hybrid selection system for studying protein-DNA and protein-protein interactions. *Proceedings of the National Academy of Sciences of the United States of America* **97**, 7382-7387.

Kalejta, R. F. (2008). Tegument proteins of human cytomegalovirus. *Microbiology and molecular biology reviews : MMBR* **72**, 249-265, table of contents.

Kalejta, R. F., Bechtel, J. T. & Shenk, T. (2003). Human cytomegalovirus pp71 stimulates cell cycle progression by inducing the proteasome-dependent degradation of the retinoblastoma family of tumor suppressors. *Mol Cell Biol* **23**, 1885-1895.

Kalejta, R. F. & Shenk, T. (2003a). The human cytomegalovirus UL82 gene product (pp71) accelerates progression through the G1 phase of the cell cycle. *Journal of virology* **77**, 3451-3459.

Kalejta, R. F. & Shenk, T. (2003b). Proteasome-dependent, ubiquitin-independent degradation of the Rb family of tumor suppressors by the human cytomegalovirus pp71 protein. *Proceedings of the National Academy of Sciences of the United States of America* **100**, 3263-3268.

Kamitani, T., Nguyen, H. P., Kito, K., Fukuda-Kamitani, T. & Yeh, E. T. (1998). Covalent modification of PML by the sentrin family of ubiquitin-like proteins. *J Biol Chem* **273**, 3117-3120.

Kamitani, T., Nguyen, H. P. & Yeh, E. T. (1997). Preferential modification of nuclear proteins by a novel ubiquitin-like molecule. *J Biol Chem* **272**, 14001-14004.

Kang, H., Kim, E. T., Lee, H. R., Park, J. J., Go, Y. Y., Choi, C. Y. & Ahn, J. H. (2006). Inhibition of SUMO-independent PML oligomerization by the human cytomegalovirus IE1 protein. *J Gen Virol* **87**, 2181-2190.

Keckesova, Z., Ylinen, L. M. & Towers, G. J. (2004). The human and African green monkey TRIM5alpha genes encode Ref1 and Lv1 retroviral restriction factor activities. *Proceedings of the National Academy of Sciences of the United States of America* **101**, 10780-10785.

Kempkes, B., Spitkovsky, D., Jansen-Durr, P., Ellwart, J. W., Kremmer, E., Delecluse, H. J., Rottenberger, C., Bornkamm, G. W. & Hammerschmidt, W. (1995). B-cell proliferation and induction of early G1-regulating proteins by Epstein-Barr virus mutants conditional for EBNA2. *EMBO J* **14**, 88-96.

Kerscher, O., Felberbaum, R. & Hochstrasser, M. (2006). Modification of proteins by ubiquitin and ubiquitin-like proteins. *Annu Rev Cell Dev Biol* **22**, 159-180.

Kim, Y. E., Lee, J. H., Kim, E. T., Shin, H. J., Gu, S. Y., Seol, H. S., Ling, P., Lee, C. H. & Ahn, J. H. (2011a). Human cytomegalovirus infection causes degradation of Sp100 proteins that suppress viral gene expression. *Journal of virology* **85**, 11928-11937.

Kim, Y. E., Lee, J. H., Kim, E. T., Shin, H. J., Gu, S. Y., Seol, H. S., Ling, P. D., Lee, C. H. & Ahn, J. H. (2011b). Human cytomegalovirus infection causes degradation of Sp100 proteins that suppress viral gene expression. *Journal of virology* **85**, 11928-11937.

Klucher, K. M., Sommer, M., Kadonaga, J. T. & Spector, D. H. (1993). In vivo and in vitro analysis of transcriptional activation mediated by the human cytomegalovirus major immediate-early proteins. *Molecular and cellular biology* **13**, 1238-1250.

Knipe, D. M. & Cliffe, A. (2008). Chromatin control of herpes simplex virus lytic and latent infection. *Nat Rev Microbiol* **6**, 211-221.

Knipe, D. M., Howley, P. M., Griffin, D. E., Lamb, R. A., Martin, M. A., Roizman, B. & Strauss, S. E. (2006). *Fields Virology*. Philadelphia: Lippincott Williams and Wilkins.

Knoblach, T., Grandel, B., Seiler, J., Nevels, M. & Paulus, C. (2011). Human cytomegalovirus IE1 protein elicits a type II interferon-like host cell response that depends on activated STAT1 but not interferon-gamma. *PLoS Pathog* **7**, e1002016.

Korioth, F., Maul, G. G., Plachter, B., Stamminger, T. & Frey, J. (1996). The nuclear domain 10 (ND10) is disrupted by the human cytomegalovirus gene product IE1. *Exp Cell Res* **229**, 155-158.

Krauss, S., Kaps, J., Czech, N., Paulus, C. & Nevels, M. (2009). Physical requirements and functional consequences of complex formation between the cytomegalovirus IE1 protein and human STAT2. *Journal of virology* **83**, 12854-12870.

Kutluay, S. B. & Triezenberg, S. J. (2009). Role of chromatin during herpesvirus infections. *Biochim Biophys Acta* **1790**, 456-466.

Kyratsous, C. A. & Silverstein, S. J. (2009). Components of nuclear domain 10 bodies regulate varicella-zoster virus replication. *Journal of virology* **83**, 4262-4274.

Lafemina, R. L., Pizzorno, M. C., Mosca, J. D. & Hayward, G. S. (1989). Expression of the acidic nuclear immediate-early protein (IE1) of human cytomegalovirus in stable cell lines and its preferential association with metaphase chromosomes. *Virology* **172**, 584-600.

Lavau, C., Marchio, A., Fagioli, M., Jansen, J., Falini, B., Lebon, P., Grosveld, F., Pandolfi, P. P., Pelicci, P. G. & Dejean, A. (1995). The acute promyelocytic leukaemia-associated PML gene is induced by interferon. *Oncogene* **11**, 871-876.

Lechner, M. S., Schultz, D. C., Negorev, D., Maul, G. G. & Rauscher, F. J., 3rd (2005). The mammalian heterochromatin protein 1 binds diverse nuclear proteins through a common motif that targets the chromoshadow domain. *Biochemical and biophysical research communications* **331**, 929-937.

Lecossier, D., Bouchonnet, F., Clavel, F. & Hance, A. J. (2003). Hypermutation of HIV-1 DNA in the absence of the Vif protein. *Science* **300**, 1112-1112.

Lee, H. R., Huh, Y. H., Kim, Y. E., Lee, K., Kim, S. & Ahn, J. H. (2007). N-terminal determinants of human cytomegalovirus IE1 protein in nuclear targeting and disrupting PML-associated subnuclear structures. *Biochem Biophys Res Commun* **356**, 499-504.

Lee, H. R., Kim, D. J., Lee, J. M., Choi, C. Y., Ahn, B. Y., Hayward, G. S. & Ahn, J. H. (2004). Ability of the human cytomegalovirus IE1 protein to modulate sumoylation of PML correlates with its functional activities in transcriptional regulation and infectivity in cultured fibroblast cells. *Journal of virology* **78**, 6527-6542.

Lewis, P. W., Elsaesser, S. J., Noh, K. M., Stadler, S. C. & Allis, C. D. (2010). Daxx is an H3.3-specific histone chaperone and cooperates with ATRX in replication-independent chromatin assembly at telomeres. *Proceedings of the National Academy of Sciences of the United States of America* **107**, 14075-14080.

Li, H., Leo, C., Zhu, J., Wu, X., O'Neil, J., Park, E. J. & Chen, J. D. (2000). Sequestration and inhibition of Daxx-mediated transcriptional repression by PML. *Mol Cell Biol* **20**, 1784-1796.

Li, X., Song, B., Xiang, S. H. & Sodroski, J. (2007). Functional interplay between the B-box 2 and the B30.2(SPRY) domains of TRIM5alpha. *Virology* **366**, 234-244.

Lilley, C. E., Chaurushiya, M. S., Boutell, C., Everett, R. D. & Weitzman, M. D. (2011). The intrinsic antiviral defense to incoming HSV-1 genomes includes specific DNA repair proteins and is counteracted by the viral protein ICP0. *PLoS Pathog* **7**, e1002084.

Lin, D. Y., Huang, Y. S., Jeng, J. C., Kuo, H. Y., Chang, C. C., Chao, T. T., Ho, C. C., Chen, Y. C., Lin, T. P., Fang, H. I., Hung, C. C., Suen, C. S., Hwang, M. J., Chang, K. S., Maul, G. G. & Shih, H. M. (2006). Role of SUMO-interacting motif in Daxx SUMO modification, subnuclear localization, and repression of sumoylated transcription factors. *Mol Cell* **24**, 341-354.

Ling, P. D., Peng, R. S., Nakajima, A., Yu, J. H., Tan, J., Moses, S. M., Yang, W. H., Zhao, B., Kieff, E., Bloch, K. D. & Bloch, D. B. (2005). Mediation of Epstein-Barr virus EBNA-LP transcriptional coactivation by Sp100. *EMBO J* **24**, 3565-3575.

Liu, B. & Stinski, M. F. (1992). Human cytomegalovirus contains a tegument protein that enhances transcription from promoters with upstream ATF and AP-1 cis-acting elements. *Journal of virology* **66**, 4434-4444.

Lium, E. K. & Silverstein, S. (1997). Mutational analysis of the herpes simplex virus type 1 ICP0 C3HC4 zinc ring finger reveals a requirement for ICP0 in the expression of the essential alpha27 gene. *Journal of virology* **71**, 8602-8614.

Lomonte, P., Thomas, J., Texier, P., Caron, C., Khochbin, S. & Epstein, A. L. (2004). Functional interaction between class II histone deacetylases and ICP0 of herpes simplex virus type 1. *Journal of virology* **78**, 6744-6757.

Loret, S., Guay, G. & Lippe, R. (2008). Comprehensive characterization of extracellular herpes simplex virus type 1 virions. *Journal of virology* **82**, 8605-8618.

Lukashchuk, V. & Everett, R. D. (2010). Regulation of ICP0-null mutant herpes simplex virus type 1 infection by ND10 components ATRX and hDaxx. *Journal of virology* **84**, 4026-4040.

Lukashchuk, V., McFarlane, S., Everett, R. D. & Preston, C. M. (2008). Human cytomegalovirus protein pp71 displaces the chromatin-associated factor ATRX from nuclear domain 10 at early stages of infection. *Journal of virology* **82**, 12543-12554.

Lukashchuk, V., Orr, A. & Everett, R. D. (2010). Regulation of ICP0 null mutant HSV-1 infection by ND10 components ATRX and hDaxx. *Journal of virology* **84**, 4026-4040.

Maeda, E., Akahane, M., Kiryu, S., Kato, N., Yoshikawa, T., Hayashi, N., Aoki, S., Minami, M., Uozaki, H., Fukayama, M. & Ohtomo, K. (2009). Spectrum of Epstein-Barr virus-related diseases: a pictorial review. *Jpn J Radiol* **27**, 4-19.

Mahajan, R., Delphin, C., Guan, T., Gerace, L. & Melchior, F. (1997). A small ubiquitin-related polypeptide involved in targeting RanGAP1 to nuclear pore complex protein RanBP2. *Cell* **88**, 97-107.

Malone, C. L., Vesole, D. H. & Stinski, M. F. (1990). Transactivation of a human cytomegalovirus early promoter by gene products from the immediate-early gene IE2 and augmentation by IE1: mutational analysis of the viral proteins. *Journal of virology* **64**, 1498-1506.

Marchini, A., Liu, H. & Zhu, H. (2001). Human cytomegalovirus with IE-2 (UL122) deleted fails to express early lytic genes. *Journal of virology* **75**, 1870-1878.

Matunis, M. J., Coutavas, E. & Blobel, G. (1996). A novel ubiquitin-like modification modulates the partitioning of the Ran-GTPase-activating protein RanGAP1 between the cytosol and the nuclear pore complex. *J Cell Biol* **135**, 1457-1470.

Maul, G. G. & Everett, R. D. (1994). The nuclear location of PML, a cellular member of the C3HC4 zinc- binding domain protein family, is rearranged during herpes simplex virus infection by the C3HC4 viral protein ICP0. *J Gen Virol* **75**, 1223-1233.

Maul, G. G., Guldner, H. H. & Spivack, J. G. (1993). Modification of discrete nuclear domains induced by herpes simplex virus type 1 immediate early gene 1 product (ICP0). *J Gen Virol* **74**, 2679-2690.

Maul, G. G., Ishov, A. M. & Everett, R. D. (1996). Nuclear domain 10 as preexisting potential replication start sites of herpes simplex virus type-1. *Virology* **217**, 67-75.

Maul, G. G., Negorev, D., Bell, P. & Ishov, A. M. (2000). Review: properties and assembly mechanisms of ND10, PML bodies, or PODs. *J Struct Biol* **129**, 278-287.

Maul, G. G., Yu, E., Ishov, A. M. & Epstein, A. L. (1995). Nuclear domain 10 (ND10) associated proteins are also present in nuclear bodies and redistribute to hundreds of nuclear sites after stress. *J Cell Biochem* **59**, 498-513.

Mazeron, M. C., Jahn, G. & Plachter, B. (1992). Monoclonal antibody E-13 (M-810) to human cytomegalovirus recognizes an epitope encoded by exon 2 of the major immediate early gene. *J Gen Virol* **73 (Pt 10)**, 2699-2703.

McFarlane, S. & Preston, C. M. (2011). Human cytomegalovirus immediate early gene expression in the osteosarcoma line U2OS is repressed by the cell protein ATRX. *Virus Res* **157**, 47-53.

Mehle, A., Goncalves, J., Santa-Marta, M., McPike, M. & Gabuzda, D. (2004). Phosphorylation of a novel SOCS-box regulates assembly of the HIV-1 Vif-Cul5 complex that promotes APOBEC3G degradation. *Genes Dev* **18**, 2861-2866.

Meroni, G. & Diez-Roux, G. (2005). TRIM/RBCC, a novel class of 'single protein RING finger' E3 ubiquitin ligases. *Bioessays* **27**, 1147-1157.

Michaelson, J. S. & Leder, P. (2003). RNAi reveals anti-apoptotic and transcriptionally repressive activities of DAXX. *J Cell Sci* **116**, 345-352.

Mische, C. C., Javanbakht, H., Song, B., Diaz-Griffero, F., Stremlau, M., Strack, B., Si, Z. & Sodroski, J. (2005). Retroviral restriction factor TRIM5alpha is a trimer. *Journal of virology* **79**, 14446-14450.

Mocarski, E. S., Kemble, G. W., Lyle, J. M. & Greaves, R. F. (1996). A deletion mutant in the human cytomegalovirus gene encoding IE1(491aa) is replication defective due to a failure in autoregulation. *Proceedings of the National Academy of Sciences of the United States of America* **93**, 11321-11326.

Morrison, E. E., Wang, Y. F. & Meredith, D. M. (1998). Phosphorylation of structural components promotes dissociation of the herpes simplex virus type 1 tegument. *Journal of virology* **72**, 7108-7114.

Muller, S. & Dejean, A. (1999). Viral immediate-early proteins abrogate the modification by SUMO-1 of PML and Sp100 proteins, correlating with nuclear body disruption. *Journal of virology* **73**, 5137-5143.

Muratani, M., Gerlich, D., Janicki, S. M., Gebhard, M., Eils, R. & Spector, D. L. (2002). Metabolic-energy-dependent movement of PML bodies within the mammalian cell nucleus. *Nat Cell Biol* **4**, 106-110.

Natarajan, R., Deshmane, S., Valyi-Nagy, T., Everett, R. & Fraser, N. W. (1991). A herpes simplex virus type 1 mutant lacking the ICP0 introns reactivates with normal efficiency. *Journal of virology* **65**, 5569-5573.

Negorev, D., Ishov, A. M. & Maul, G. G. (2001). Evidence for separate ND10-binding and homo-oligomerization domains of Sp100. *J Cell Sci* **114(Pt**, 59-68.

Negorev, D. & Maul, G. G. (2001). Cellular proteins localized at and interacting within ND10/PML nuclear bodies/PODs suggest functions of a nuclear depot. *Oncogene* **20**, 7234-7242.

Negorev, D. G., Vladimirova, O. V., Ivanov, A., Rauscher, F., 3rd & Maul, G. G. (2006). Differential role of Sp100 isoforms in interferon-mediated repression of herpes simplex virus type 1 immediate-early protein expression. *Journal of virology* **80**, 8019-8029.

Negorev, D. G., Vladimirova, O. V. & Maul, G. G. (2009). Differential functions of interferon-upregulated Sp100 isoforms: herpes simplex virus type 1 promoter-based immediate-early gene suppression and PML protection from ICP0-mediated degradation. *Journal of virology* **83**, 5168-5180.

Nevels, M., Brune, W. & Shenk, T. (2004a). SUMOylation of the human cytomegalovirus 72-kilodalton IE1 protein facilitates expression of the 86-kilodalton IE2 protein and promotes viral replication. *Journal of virology* **78**, 7803-7812.

Nevels, M., Nitzsche, A. & Paulus, C. (2011). How to control an infectious bead string: nucleosome-based regulation and targeting of herpesvirus chromatin. *Rev Med Virol* **21**, 154-180.

Nevels, M., Paulus, C. & Shenk, T. (2004b). Human cytomegalovirus immediate-early 1 protein facilitates viral replication by antagonizing histone deacetylation. *Proceedings of the National Academy of Sciences of the United States of America* **101**, 17234-17239.

Newhart, A., Negorev, D. G., Rafalska-Metcalf, I. U., Yang, T., Maul, G. G. & Janicki, S. M. (2013). Sp100A promotes chromatin decondensation at a cytomegalovirus-promoter-regulated transcription site. *Mol Biol Cell* **24**, 1454-1468.

Newhart, A., Rafalska-Metcalf, I. U., Yang, T., Negorev, D. G. & Janicki, S. M. (2012). Single-cell analysis of Daxx and ATRX-dependent transcriptional repression. *J Cell Sci* **125**, 5489-5501.

Nicoll, M. P., Proenca, J. T. & Efstathiou, S. (2012). The molecular basis of herpes simplex virus latency. *FEMS Microbiol Rev* **36**, 684-705.

Nisole, S., Stoye, J. P. & Saib, A. (2005). TRIM family proteins: retroviral restriction and antiviral defence. *Nat Rev Microbiol* **3**, 799-808.

O'Connor, C. M., Damania, B. & Kedes, D. H. (2003). De novo infection with rhesus monkey rhadinovirus leads to the accumulation of multiple intranuclear capsid species during lytic replication but favors the release of genome-containing virions. *Journal of virology* **77**, 13439-13447.

O'Rourke, D., Elliott, G., Papworth, M., Everett, R. & O'Hare, P. (1998). Examination of determinants for intranuclear localization and transactivation within the RING finger of herpes simplex virus type 1 IE110k protein. *J Gen Virol* **79**, 537-548.

Ozato, K., Shin, D. M., Chang, T. H. & Morse, H. C., 3rd (2008). TRIM family proteins and their emerging roles in innate immunity. *Nat Rev Immunol* **8**, 849-860.

Parkinson, J. & Everett, R. D. (2000). Alphaherpesvirus proteins related to herpes simplex virus type 1 ICP0 affect cellular structures and proteins. *Journal of virology* **74**, 10006-10017.

Paulus, C., Krauss, S. & Nevels, M. (2006). A human cytomegalovirus antagonist of type I IFN-dependent signal transducer and activator of transcription signaling. *Proceedings of the National Academy of Sciences of the United States of America* **103**, 3840-3845.

Perron, M. J., Stremlau, M., Song, B., Ulm, W., Mulligan, R. C. & Sodroski, J. (2004). TRIM5alpha mediates the postentry block to N-tropic murine leukemia viruses in human cells. *Proceedings of the National Academy of Sciences of the United States of America* **101**, 11827-11832.

Perry, L. J., Rixon, F. J., Everett, R. D., Frame, M. C. & McGeoch, D. J. (1986). Characterization of the IE110 gene of herpes simplex virus type 1. *J Gen Virol* **67**, 2365-2380.

Pertel, T., Hausmann, S., Morger, D., Zuger, S., Guerra, J., Lascano, J., Reinhard, C., Santoni, F. A., Uchil, P. D., Chatel, L., Bisiaux, A., Albert, M. L., Strambio-De-Castillia, C., Mothes, W., Pizzato, M., Grutter, M. G. & Luban, J. (2011). TRIM5 is an innate immune sensor for the retrovirus capsid lattice. *Nature* **472**, 361-365.

Perusina Lanfranca, M., Mostafa, H. H. & Davido, D. J. (2013). Two Overlapping Regions within the N-Terminal Half of the Herpes Simplex Virus 1 E3 Ubiquitin

Ligase ICP0 Facilitate the Degradation and Dissociation of PML and Dissociation of Sp100 from ND10. *Journal of virology* **87**, 13287-13296.

Pickart, C. M. & Eddins, M. J. (2004). Ubiquitin: structures, functions, mechanisms. *Biochim Biophys Acta* **1695**, 55-72.

Pluta, A. F., Earnshaw, W. C. & Goldberg, I. G. (1998). Interphase-specific association of intrinsic centromere protein CENP-C with HDaxx, a death domain-binding protein implicated in Fas-mediated cell death. *J Cell Sci* **111**, 2029-2041.

Preston, C. M. & Nicholl, M. J. (1997). Repression of gene expression upon infection of cells with herpes simplex virus type 1 mutants impaired for immediate-early protein synthesis. *Journal of virology* **71**, 7807-7813.

Preston, C. M. & Nicholl, M. J. (2005). Human cytomegalovirus tegument protein pp71 directs long-term gene expression from quiescent herpes simplex virus genomes. *Journal of virology* **79**, 525-535.

Preston, C. M. & Nicholl, M. J. (2006). Role of the cellular protein hDaxx in human cytomegalovirus immediate-early gene expression. *J Gen Virol* **87**, 1113-1121.

Raab-Traub, N. (2002). Epstein-Barr virus in the pathogenesis of NPC. *Semin Cancer Biol* **12**, 431-441.

Reddehase, M. J. (2013). *Cytomegaloviruses. From Molecular Pathogenesis to Intervention.* Norfolk, U.K.: Caister Academic Press.

Reeves, M., Woodhall, D., Compton, T. & Sinclair, J. (2010). Human cytomegalovirus IE72 protein interacts with the transcriptional repressor hDaxx to regulate LUNA gene expression during lytic infection. *Journal of virology* **84**, 7185-7194.

Regad, T. & Chelbi-Alix, M. K. (2001). Role and fate of PML nuclear bodies in response to interferon and viral infections. *Oncogene* **20**, 7274-7286.

Reichelt, M., Wang, L., Sommer, M., Perrino, J., Nour, A. M., Sen, N., Baiker, A., Zerboni, L. & Arvin, A. M. (2011). Entrapment of viral capsids in nuclear PML cages is an intrinsic antiviral host defense against varicella-zoster virus. *PLoS Pathog* **7**, e1001266.

Reinhardt, J., Smith, G. B., Himmelheber, C. T., Azizkhan-Clifford, J. & Mocarski, E. S. (2005). The carboxyl-terminal region of human cytomegalovirus IE1491aa contains an acidic domain that plays a regulatory role and a chromatin-tethering domain that is dispensable during viral replication. *Journal of virology* **79**, 225-233.

Reyda, S., Tenzer, S., Navarro, P., Gebauer, W., Saur, M., Krauter, S., Buscher, N. & Plachter, B. (2014). The tegument protein pp65 of human cytomegalovirus acts as an optional scaffold protein that optimizes protein uploading into viral particles. *Journal of virology* **88**, 9633-9646.

Rice, S. A., Long, M. C., Lam, V., Schaffer, P. A. & Spencer, C. A. (1995). Herpes simplex virus immediate-early protein ICP22 is required for viral modification of host RNA polymerase II and establishment of the normal viral transcription program. *Journal of virology* **69**, 5550-5559.

Ritchie, K., Seah, C., Moulin, J., Isaac, C., Dick, F. & Berube, N. G. (2008). Loss of ATRX leads to chromosome cohesion and congression defects. *J Cell Biol* **180**, 315-324.

Rivera-Molina, Y. A., Martinez, F. P. & Tang, Q. (2013). Nuclear domain 10 of the viral aspect. *World J Virol* **2**, 110-122.

Rixon, F. J. & McNab, D. (1999). Packaging-competent capsids of a herpes simplex virus temperature-sensitive mutant have properties similar to those of in vitro-assembled procapsids. *Journal of virology* **73**, 5714-5721.

Roizman, B., Knipe, D. M. & Whitley, R. J. (2006). Herpes Simplex Viruses. In *Fields Virology*, 5th edn, pp. 2501-2602. Philadelphia: Lippincott Williams and Wilkins.

Rowe, W. P., Hartley, J. W., Waterman, S., Turner, H. C. & Huebner, R. J. (1956). Cytopathogenic agent resembling human salivary gland virus recovered from tissue cultures of human adenoids. *Proc Soc Exp Biol Med* **92**, 418-424.

Russell, J., Stow, N. D., Stow, E. C. & Preston, C. M. (1987). Herpes simplex virus genes involved in latency in vitro. *J Gen Virol* **68**, 3009-3018.

Ryu, S. W., Chae, S. K. & Kim, E. (2000). Interaction of Daxx, a Fas binding protein, with sentrin and Ubc9. *Biochemical and biophysical research communications* **279**, 6-10.

Sacks, W. R. & Schaffer, P. A. (1987). Deletion mutants in the gene encoding the herpes simplex virus type 1 immediate-early protein ICP0 exhibit impaired growth in cell culture. *Journal of virology* **61**, 829-839.

Saffert, R. T. & Kalejta, R. F. (2006). Inactivating a cellular intrinsic immune defense mediated by Daxx is the mechanism through which the human cytomegalovirus pp71 protein stimulates viral immediate-early gene expression. *Journal of virology* **80**, 3863-3871.

Saffert, R. T. & Kalejta, R. F. (2007). Human cytomegalovirus gene expression is silenced by Daxx-mediated intrinsic immune defense in model latent infections established in vitro. *Journal of virology* **81**, 9109-9120.

Samaniego, L. A., Neiderhiser, L. & DeLuca, N. A. (1998). Persistence and expression of the herpes simplex virus genome in the absence of immediate-early proteins. *Journal of virology* **72**, 3307-3320.

Sanders, R. L., Clark, C. L., Morello, C. S. & Spector, D. H. (2008). Development of cell lines that provide tightly controlled temporal translation of the human cytomegalovirus IE2 proteins for complementation and functional analyses of growth-impaired and nonviable IE2 mutant viruses. *Journal of virology* **82**, 7059-7077.

Sandri-Goldin, R. M. (2011). The functions and activities of HSV-1 ICP27, a multifunctional regulator of gene expression. In *Alphaherpesviruses Molecular Virology*, pp. 39-50. Edited by S. K. Weller. Norfolk, U.K.: Caister Academic Press.

Scaglioni, P. P., Yung, T. M., Cai, L. F., Erdjument-Bromage, H., Kaufman, A. J., Singh, B., Teruya-Feldstein, J., Tempst, P. & Pandolfi, P. P. (2006). A CK2-dependent mechanism for degradation of the PML tumor suppressor. *Cell* **126**, 269-283.

Scherer, M., Klingl, S., Sevvana, M., Otto, V., Schilling, E. M., Stump, J. D., Muller, R., Reuter, N., Sticht, H., Muller, Y. A. & Stamminger, T. (2014). Crystal structure of cytomegalovirus IE1 protein reveals targeting of TRIM family member PML via coiled-coil interactions. *PLoS Pathog* **10**, e1004512.

Scherer, M. & Stamminger, T. (2014). The human cytomegalovirus IE1 protein: past and present developments. *Future Virology* **9**, 415-430.

Schreiner, S. & Wodrich, H. (2013). Virion factors that target Daxx to overcome intrinsic immunity. *Journal of virology* **87**, 10412-10422.

Seeler, J. S., Marchio, A., Sitterlin, D., Transy, C. & Dejean, A. (1998). Interaction of SP100 with HP1 proteins: a link between the promyelocytic leukemia-associated nuclear bodies and the chromatin compartment. *Proceedings of the National Academy of Sciences of the United States of America* **95**, 7316-7321.

Sheehy, A. M., Gaddis, N. C., Choi, J. D. & Malim, M. H. (2002). Isolation of a human gene that inhibits HIV-1 infection and is suppressed by the viral Vif protein. *Nature* **418**, 646-650.

Sheehy, A. M., Gaddis, N. C. & Malim, M. H. (2003). The antiretroviral enzyme APOBEC3G is degraded by the proteasome in response to HIV-1 Vif. *Nat Med* **9**, 1404-1407.

Shen, T. H., Lin, H. K., Scaglioni, P. P., Yung, T. M. & Pandolfi, P. P. (2006). The mechanisms of PML-nuclear body formation. *Mol Cell* **24**, 331-339.

Shen, Z., Pardington-Purtymun, P. E., Comeaux, J. C., Moyzis, R. K. & Chen, D. J. (1996). UBL1, a human ubiquitin-like protein associating with human RAD51/RAD52 proteins. *Genomics* **36**, 271-279.

Shih, H. M., Chang, C. C., Kuo, H. Y. & Lin, D. Y. (2007). Daxx mediates SUMO-dependent transcriptional control and subnuclear compartmentalization. *Biochem Soc Trans* **35**, 1397-1400.

Shin, H. J., Kim, Y. E., Kim, E. T. & Ahn, J. H. (2012). The chromatin-tethering domain of human cytomegalovirus immediate-early (IE) 1 mediates associations of IE1, PML and STAT2 with mitotic chromosomes, but is not essential for viral replication. *J Gen Virol* **93**, 716-721.

Sivachandran, N., Cao, J. Y. & Frappier, L. (2010). Epstein-Barr virus nuclear antigen 1 Hijacks the host kinase CK2 to disrupt PML nuclear bodies. *Journal of virology* **84**, 11113-11123.

Sivachandran, N., Sarkari, F. & Frappier, L. (2008). Epstein-Barr nuclear antigen 1 contributes to nasopharyngeal carcinoma through disruption of PML nuclear bodies. *PLoS Pathog* **4**, e1000170.

Smith, M. C., Boutell, C. & Davido, D. J. (2011). HSV-1 ICP0: paving the way for viral replication. *Future Virol* **6**, 421-429.

Smith, M. C., Goddard, E. T., Perusina Lanfranca, M. & Davido, D. J. (2013). hTERT extends the life of human fibroblasts without compromising type I interferon signaling. *PLoS ONE* **8**, e58233.

Sobol, P. T. & Mossman, K. L. (2011). Mechanisms of subversion of type 1 interferon responses by alphaherpesviruses. In *Alphaherpesviruses: Molecular Virology*, pp. 219-236. Edited by S. K. Weller. Norfolk, UK: Caister Academic Press.

Sokolskaja, E., Berthoux, L. & Luban, J. (2006). Cyclophilin A and TRIM5alpha independently regulate human immunodeficiency virus type 1 infectivity in human cells. *Journal of virology* **80**, 2855-2862.

Song, J., Durrin, L. K., Wilkinson, T. A., Krontiris, T. G. & Chen, Y. (2004). Identification of a SUMO-binding motif that recognizes SUMO-modified proteins. *Proceedings of the National Academy of Sciences of the United States of America* **101**, 14373-14378.

Spengler, M. L., Kurapatwinski, K., Black, A. R. & Azizkhan-Clifford, J. (2002). SUMO-1 modification of human cytomegalovirus IE1/IE72. *Journal of virology* **76**, 2990-2996.

Stenberg, R. M., Fortney, J., Barlow, S. W., Magrane, B. P., Nelson, J. A. & Ghazal, P. (1990). Promoter-specific trans activation and repression by human cytomegalovirus immediate-early proteins involves common and unique protein domains. *Journal of virology* **64**, 1556-1565.

Stenberg, R. M., Witte, P. R. & Stinski, M. F. (1985). Multiple spliced and unspliced transcripts from human cytomegalovirus immediate-early region 2 and evidence for a common initiation site within immediate-early region 1. *Journal of virology* **56**, 665-675.

Sternsdorf, T., Jensen, K. & Will, H. (1997). Evidence for covalent modification of the nuclear dot-associated proteins PML and Sp100 by PIC1/SUMO-1. *J Cell Biol* **139**, 1621-1634.

Stow, N. D. & Stow, E. C. (1986). Isolation and characterization of a herpes simplex virus type 1 mutant containing a deletion within the gene encoding the immediate early polypeptide Vmw110. *J Gen Virol* **67**, 2571-2585.

Straus, S. E., Cohen, J. I., Tosato, G. & Meier, J. (1993). NIH conference. Epstein-Barr virus infections: biology, pathogenesis, and management. *Ann Intern Med* **118**, 45-58.

Stremlau, M., Owens, C. M., Perron, M. J., Kiessling, M., Autissier, P. & Sodroski, J. (2004). The cytoplasmic body component TRIM5alpha restricts HIV-1 infection in Old World monkeys. *Nature* **427**, 848-853.

Stuurman, N., de Graaf, A., Floore, A., Josso, A., Humbel, B., de Jong, L. & van Driel, R. (1992). A monoclonal antibody recognizing nuclear matrix-associated nuclear bodies. *J Cell Sci* **101 (Pt 4)**, 773-784.

Sullivan, V., Talarico, C. L., Stanat, S. C., Davis, M., Coen, D. M. & Biron, K. K. (1992). A protein kinase homologue controls phosphorylation of ganciclovir in human cytomegalovirus-infected cells. *Nature* **358**, 162-164.

Szostecki, C., Guldner, H. H., Netter, H. J. & Will, H. (1990). Isolation and characterization of cDNA encoding a human nuclear antigen predominantly recognized by autoantibodies from patients with primary biliary cirrhosis. *J Immunol* **145**, 4338-4347.

Szostecki, C., Krippner, H., Penner, E. & Bautz, F. A. (1987). Autoimmune sera recognize a 100 kD nuclear protein antigen (sp-100). *Clin Exp Immunol* **68**, 108-116.

Tang, J., Wu, S., Liu, H., Stratt, R., Barak, O. G., Shiekhattar, R., Picketts, D. J. & Yang, X. (2004). A novel transcription regulatory complex containing death domain-associated protein and the ATR-X syndrome protein. *J Biol Chem* **279**, 20369-20377.

Tavalai, N., Adler, M., Scherer, M., Riedl, Y. & Stamminger, T. (2011). Evidence for a dual antiviral role of the major nuclear domain 10 component Sp100 during the immediate-early and late phases of the human cytomegalovirus replication cycle. *Journal of virology* **85**, 9447-9458.

Tavalai, N., Kraiger, M., Kaiser, N. & Stamminger, T. (2008a). Insertion of an EYFP-pp71 (UL82) coding sequence into the human cytomegalovirus genome results in a recombinant virus with enhanced viral growth. *Journal of virology* **82**, 10543-10555.

Tavalai, N., Papior, P., Rechter, S., Leis, M. & Stamminger, T. (2006). Evidence for a role of the cellular ND10 protein PML in mediating intrinsic immunity against human cytomegalovirus infections. *Journal of virology* **80**, 8006-8018.

Tavalai, N., Papior, P., Rechter, S. & Stamminger, T. (2008b). Nuclear domain 10 components promyelocytic leukemia protein and hDaxx independently contribute to an intrinsic antiviral defense against human cytomegalovirus infection. *Journal of virology* **82**, 126-137.

Tavalai, N. & Stamminger, T. (2008). New insights into the role of the subnuclear structure ND10 for viral infection. *Biochim Biophys Acta* **1783**, 2207-2221.

Tavalai, N. & Stamminger, T. (2009). Interplay between Herpesvirus Infection and Host Defense by PML Nuclear Bodies. *Viruses* **1**, 1240-1264.

Terry-Allison, T., Smith, C. A. & DeLuca, N. A. (2007). Relaxed repression of herpes simplex virus type 1 genomes in Murine trigeminal neurons. *Journal of virology* **81**, 12394-12405.

Torok, M. & Etkin, L. D. (2001). Two B or not two B? Overview of the rapidly expanding B-box family of proteins. *Differentiation* **67**, 63-71.

Trus, B. L., Booy, F. P., Newcomb, W. W., Brown, J. C., Homa, F. L., Thomsen, D. R. & Steven, A. C. (1996). The herpes simplex virus procapsid: structure, conformational changes upon maturation, and roles of the triplex proteins VP19c and VP23 in assembly. *Journal of molecular biology* **263**, 447-462.

Tsai, K., Chan, L., Gibeault, R., Conn, K., Dheekollu, J., Domsic, J., Marmorstein, R., Schang, L. M. & Lieberman, P. M. (2014). Viral Reprogramming of the Daxx-Histone H3.3 Chaperone During EBV Early Infection. *Journal of virology*.

Tsai, K., Thikmyanova, N., Wojcechowskyj, J. A., Delecluse, H. J. & Lieberman, P. M. (2011). EBV tegument protein BNRF1 disrupts DAXX-ATRX to activate viral early gene transcription. *PLoS Pathog* **7**, e1002376.

van Lint, A. L., Murawski, M. R., Goodbody, R. E., Severa, M., Fitzgerald, K. A., Finberg, R. W., Knipe, D. M. & Kurt-Jones, E. A. (2010). Herpes simplex virus immediate-early ICP0 protein inhibits Toll-like receptor 2-dependent inflammatory responses and NF-kappaB signaling. *Journal of virology* **84**, 10802-10811.

Vanni, E., Gatherer, D., Tong, L., Everett, R. D. & Boutell, C. (2012). Functional characterization of residues required for the herpes simplex virus 1 E3 ubiquitin ligase ICP0 to interact with the cellular E2 ubiquitin-conjugating enzyme UBE2D1 (UbcH5a). *Journal of virology* **86**, 6323-6333.

Wang, L., Oliver, S. L., Sommer, M., Rajamani, J., Reichelt, M. & Arvin, A. M. (2011). Disruption of PML Nuclear Bodies Is Mediated by ORF61 SUMO-Interacting Motifs and Required for Varicella-Zoster Virus Pathogenesis in Skin. *PLoS Pathog* **7**, e1002157.

Wang, X., Huong, S. M., Chiu, M. L., Raab-Traub, N. & Huang, E. S. (2003). Epidermal growth factor receptor is a cellular receptor for human cytomegalovirus. *Nature* **424**, 456-461.

Wang, Y. & Dasso, M. (2009). SUMOylation and deSUMOylation at a glance. *J Cell Sci* **122**, 4249-4252.

Weller, S. K. (2011). *Alphaherpesviruses. Molecular Virology.* Norfolk, U.K.: Caister Academic Press.

White, E. A., Clark, C. L., Sanchez, V. & Spector, D. H. (2004). Small internal deletions in the human cytomegalovirus IE2 gene result in nonviable recombinant viruses with differential defects in viral gene expression. *Journal of virology* **78**, 1817-1830.

White, E. A. & Spector, D. H. (2005). Exon 3 of the human cytomegalovirus major immediate-early region is required for efficient viral gene expression and for cellular cyclin modulation. *Journal of virology* **79**, 7438-7452.

Wilcox, C. L., Smith, R. L., Everett, R. D. & Mysofski, D. (1997). The herpes simplex virus type 1 immediate-early protein ICP0 is necessary for the efficient establishment of latent infection. *Journal of virology* **71**, 6777-6785.

Wilkinson, G. W., Kelly, C., Sinclair, J. H. & Rickards, C. (1998). Disruption of PML-associated nuclear bodies mediated by the human cytomegalovirus major immediate early gene product. *J Gen Virol* **79** 1233-1245.

Woodhall, D. L., Groves, I. J., Reeves, M. B., Wilkinson, G. & Sinclair, J. H. (2006). Human Daxx-mediated repression of human cytomegalovirus gene expression correlates with a repressive chromatin structure around the major immediate early promoter. *J Biol Chem* **281**, 37652-37660.

Xu, Y., Ahn, J. H., Cheng, M., apRhys, C. M., Chiou, C. J., Zong, J., Matunis, M. J. & Hayward, G. S. (2001). Proteasome-independent disruption of PML oncogenic domains (PODs), but not covalent modification by SUMO-1, is required for human cytomegalovirus immediate-early protein IE1 to inhibit PML-mediated transcriptional repression. *Journal of virology* **75**, 10683-10695.

Xue, Y., Gibbons, R., Yan, Z., Yang, D., McDowell, T. L., Sechi, S., Qin, J., Zhou, S., Higgs, D. & Wang, W. (2003). The ATRX syndrome protein forms a chromatin-remodeling complex with Daxx and localizes in promyelocytic leukemia nuclear bodies. *Proceedings of the National Academy of Sciences of the United States of America* **100**, 10635-10640.

Yan, N. & Chen, Z. J. (2012). Intrinsic antiviral immunity. *Nat Immunol* **13**, 214-222.

Yao, F. & Courtney, R. J. (1992). Association of ICP0 but not ICP27 with purified virions of herpes simplex virus type 1. *Journal of virology* **66**, 2709-2716.

Yap, M. W., Nisole, S., Lynch, C. & Stoye, J. P. (2004). Trim5α protein restricts both HIV-1 and murine leukemia virus. *Proceedings of the National Academy of Sciences of the United States of America* **101**, 10786-10791.

Yap, M. W., Nisole, S. & Stoye, J. P. (2005). A single amino acid change in the SPRY domain of human Trim5alpha leads to HIV-1 restriction. *Curr Biol* **15**, 73-78.

Yongxu Lu, R. D. E. (2014). Analysis of the functional interchange between the IE1 and pp71 proteins of HCMV and ICP0 of HSV-1. *Journal of virology*, 03480-03414.

Young, L. S. & Rickinson, A. B. (2004). Epstein-Barr virus: 40 years on. *Nature reviews Cancer* **4**, 757-768.

Yu, X., Trang, P., Shah, S., Atanasov, I., Kim, Y. H., Bai, Y., Zhou, Z. H. & Liu, F. (2005). Dissecting human cytomegalovirus gene function and capsid maturation by ribozyme targeting and electron cryomicroscopy. *Proceedings of the National Academy of Sciences of the United States of America* **102**, 7103-7108.

Yu, X., Yu, Y., Liu, B., Luo, K., Kong, W., Mao, P. & Yu, X. F. (2003a). Induction of APOBEC3G ubiquitination and degradation by an HIV-1 Vif-Cul5-SCF complex. *Science* **302**, 1056-1060.

Yu, X. K., O'Connor, C. M., Atanasov, I., Damania, B., Kedes, D. H. & Zhou, Z. H. (2003b). Three-dimensional structures of the A, B, and C capsids of rhesus monkey rhadinovirus: insights into gammaherpesvirus capsid assembly, maturation, and DNA packaging. *Journal of virology* **77**, 13182-13193.

Zalckvar, E., Paulus, C., Tillo, D., Asbach-Nitzsche, A., Lubling, Y., Winterling, C., Strieder, N., Mucke, K., Goodrum, F., Segal, E. & Nevels, M. (2013). Nucleosome maps of the human cytomegalovirus genome reveal a temporal switch in chromatin organization linked to a major IE protein. *Proceedings of the National Academy of Sciences of the United States of America* **110**, 13126-13131.

Zhong, S., Muller, S., Ronchetti, S., Freemont, P. S., Dejean, A. & Pandolfi, P. P. (2000a). Role of SUMO-1-modified PML in nuclear body formation. *Blood* **95**, 2748-2752.

Zhong, S., Salomoni, P. & Pandolfi, P. P. (2000b). The transcriptional role of PML and the nuclear body. *Nat Cell Biol* **2**, E85-90.

Zhong, S., Salomoni, P., Ronchetti, S., Guo, A., Ruggero, D. & Pandolfi, P. P. (2000c). Promyelocytic leukemia protein (PML) and Daxx participate in a novel nuclear pathway for apoptosis. *J Exp Med* **191**, 631-640.

Zhou, Z. H., Macnab, S. J., Jakana, J., Scott, L. R., Chiu, W. & Rixon, F. J. (1998). Identification of the sites of interaction between the scaffold and outer shell in herpes simplex virus-1 capsids by difference electron imaging. *Proceedings of the National Academy of Sciences of the United States of America* **95**, 2778-2783.

Zhu, H., Shen, Y. & Shenk, T. (1995). Human cytomegalovirus IE1 and IE2 proteins block apoptosis. *Journal of virology* **69**, 7960-7970.

Appendix for Figure 3.7

	TetR	IE1	IE1.YL1	IE1.YL2	IE1.YL3
Plaque No.	3716	688500	415181	118688	3465
	TetR	IE1.YL4	IE1.YL5	IE1.YL6	IE1.YL7
Plaque No.	4569	7140	166425	429000	387844
	TetR	IE1	IE1.K450R		
Plaque No.	2681	430875	484875		

Appendix for Figure 4.3

	HFT	HFT.EYFP	HFT.ICP0
Plaque No.	2473	2200	6306000

Appendix for Figure 4.7

	HFT	HFT.EYFP	HFT.IE1
Plaque No.	2473	2200	18375

Appendix for Figure 4.8

	HFT	EYFP	pp71
Plaque No.	1454	1325	10267

Appendix for Figure 4.9

	HFT	EYFP	pp71&IE1
Plaque No.	1454	1325	2313600

Appendix for Figure 4.11

	HFT	HFT.IE1	HFT.ICP0
Plaque No.	6738	219267	164673

Appendix for Figure 4.12

	HFT	HFT.IE1	HFT.ICP0
Plaque No.	50340	1690470	743580

Appendix for Figure 4.13

	HFT	HFT.IE1	HFT.ICP0
Plaque No.	29900	864000	264825

Appendix for Figure 4.26

	HFT	HFT.IE1	HFT.IE1 YL1	HFT.IE1 YL2	HFT.IE1 YL3	HFT.IE1 YL4	HFT.IE1 K450R	HFT.IE1 YL7
Plaque No.	0	4572.9	3569.4	0	0	0	5011.5	2455.5

Appendix for Figure 4.33

	HFT	HFT.pp71	HFT.ICP0
Plaque No.	350	360628	1032701

Appendix for Figure 4.35

	HFT	HFT.pp71
Plaque No.	6738	7152

Appendix for Figure 5.7A

	HFT	HFT.EBNA1	HFT.EBNA-LP	HFT.BNRF1
Plaque No.	2346	4374	14318	60282

Appendix for Figure 5.7B

	HFT	HFT.EBNA1 &EBNA-LP	HFT.EBNA1 &BNRF1	HFT.BNRF1 &EBNA-LP	HFT.EBNA1&BNRF1&EBNA-LP	HFT.EBNA1 &EBNA-LP&pp71
Plaque No.	2581	10442	72828	193684	540844	659580

Appendix for Figure 5.8

	HFT	HFT.IE1&BNRF1	HFT.ICP0
Plaque No.	2243	1001400	4896900

Appendix for Figure 5.9

	HFT	HFT.pp71	HFT.BNRF1
Plaque No.	72	9783	14812